KAISO PROMOTES INTESTINAL INFLAMMATION & TUMORIGENESIS

KAISO: A NOVEL MEDIATOR OF INTESTINAL INFLAMMATION AND TUMORIGENESIS

By

CHRISTINA COLETTE PIERRE, B.Sc.

A Thesis submitted to the School of Graduate Studies In Partial Fulfillment of the Requirements for the Degree Doctor of Philosophy

McMaster University

DOCTOR OF PHILOSOPHY (2015) McMaster University

(Biology) Hamilton, Ontario

TITLE: Kaiso: A novel mediator of intestinal inflammation and tumorigenesis

AUTHOR: Christina Colette Pierre, B.Sc. (University of Waterloo)

SUPERVISOR: Dr. Juliet M. Daniel

NUMBER OF PAGES: 213

ABSTRACT

Multiple studies have implicated the POZ-ZF and methyl-DNA-binding transcription factor, Kaiso, in the regulation of genes and pathways that are important for development and tumorigenesis. In *Xenopus* embryos and mammalian cultured cells, Kaiso has been implicated as a negative regulator of the canonical Wnt signaling pathway. Paradoxically however, Kaiso depletion extends lifespan and delays polyp onset in the $Apc^{Min/+}$ mouse model of intestinal tumorigenesis, where aberrant activation of Wnt signaling results in the development of neoplasias. These findings call into question Kaiso's role as a negative regulator of canonical Wnt signaling and led us to hypothesize that Kaiso promotes intestinal tumorigenesis by a mechanism independent of its role in canonical Wnt signaling.

To further delineate Kaiso's role in intestinal tumorigenesis and to determine Kaiso's role in regulating canonical Wnt signaling in the murine intestine, we generated a Kaiso transgenic mouse model expressing an intestine-specific murine Kaiso transgene. We then crossed our Kaiso transgenic mice with $Apc^{Min/+}$ mice and analyzed the resultant progeny. Unexpectedly, Kaiso transgenic mice exhibited intestinal inflammation, increased expression of Wnt target genes and deregulated progenitor cell differentiation, although ectopic expression of Kaiso was not sufficient to drive tumorigenesis in the intestine. In agreement with previous studies, ectopic Kaiso expression in $Apc^{Min/+}$ mice resulted in a significantly shortened lifespan and increased tumour burden. While we were unable to determine the precise mechanism by which Kaiso promotes intestinal tumour development, we found that Kaiso-induced inflammation is enhanced in the

Apc$^{Min/+}$ background and ectopic Kaiso expression further intensifies Wnt target gene expression in this model.

Collectively, these studies have identified novel roles for Kaiso in regulating inflammation and cell-fate determination in the intestine. Furthermore, our findings suggest that Kaiso may contribute to intestinal tumorigenesis by promoting inflammation, which has been shown to be a predisposing factor for colorectal cancer development. Lastly, we have demonstrated distinct tissue and organism-specific roles for Kaiso in regulating canonical Wnt signaling.

While, the aforementioned studies were the primary focus of this thesis, we also examined Kaiso's role in DNA methylation-dependent repression of two tumour-associated genes, *cyclinD1* and *HIF1A*. Our studies revealed that Kaiso binds and regulates the *cyclinD1* locus via both sequence-specific and methylation-dependent DNA binding, suggesting that these alternate modes by which Kaiso binds to DNA may not be mutually exclusive. Furthermore, we identified a previously unexplored role for Kaiso in regulating the expression of the master regulator of hypoxia, *HIF1A*, which implicates Kaiso in modulating hypoxia-driven tumorigenic processes.

ACKNOWLEDGEMENTS

The work outlined in this thesis could not be completed without sustained blessings from God almighty. Throughout difficult times and triumphs, He has guided me and endowed me with patience, grace and determination.

This thesis is as much my parents' accomplishment as it is my own. Without their unconditional and unwavering support and guidance, the success that I have achieved thus far would not be possible. Daddy, it is through your example that I learnt how to work hard, sacrifice, dream big and never give up. I can never fully thank you for the sacrifices that you have made to guide me to this point in my life and beyond. Thank you for your emotional and financial support and invaluable life and career counseling. Mummy, you are my best friend, my rock and my confidante. You have always been and continue to be strong for me when I feel like I cannot be. On days when I felt down or defeated, a few words from you were enough to brighten my day and at times make me burst into laughter. You are truly my light, my sunshine and my role model. Thank you for your unconditional love and constant covering through prayer. Mum and Dad, I have developed into the woman I am today because of you and I hope that I have made you and will continue to make you proud.

To my siblings, Maria, Amanda and Jayson, thank you for your love, support and encouragement. I realize that it is rare to have such a close bond between siblings and I treasure each of your roles in my life. Special thanks to Mufs, for calling or messaging daily to check up on me. Although at times it may have seemed like I didn't appreciate

your calls, messages or visits, you have no idea what a comfort it has been to know that you were always a phone call or a short trip away.

Ryan, thank you for your love and support over the past two years. This time has been particularly challenging for me, and I know that at times I have been difficult to deal with. Thank you for your patience and understanding, for keeping me company during my late nights at the lab and for doing my Bradford assays and scraping my cells even though you complained about how mundane lab work is while completing these tasks. Your presence has been a constant and much-needed source of relief and comfort and I could not imagine getting through the past two years without you.

Several Daniel Lab members, past and present, have contributed significantly to my Ph.D. work. I would like to thank Nickett, Kyster and Sonali for teaching me everything I needed to know about molecular cell biology when I first started in the lab. To my personal walking, talking encyclopedia, Nickett, thank you so much for everything you have taught me in the lab and about life in general. Your kindness, sense of humour and dances to Beyonce's "Single ladies" made my adjustment to graduate student life much easier. Sonali, coming to the lab everyday and seeing your friendly, smiling face truly made the lab an enjoyable place for me. Your joyful spirit is infectious and you have taught me how to take many things in stride and to not sweat the small stuff. Shaiya, Blessing and Roopali, I will miss our late night dancing and singing sessions dearly. Being around students of such high caliber has challenged me to be my best and I am sincerely grateful for your contributions to my work. To my roomie Shaiya, thank you for your reliability, sincerity, generosity and constant willingness to help me. Your support

has certainly not gone unnoticed. Our time living together, drinking wine and singing Whitney Houston songs were some of the best years of grad school for me and I hope that you know that “mi casa siempre es su casa”. Meaghan, Jose and Shivanie thank you for your hard work and dedication to my thesis project. You should all be very proud of your contributions to this work and know that I am very grateful for your input. You are all exceptionally gifted and I am confident that you will excel in your future careers. Snezana, it is rare to encounter people who will give so willingly of their time and effort and expect nothing in return, so I am especially grateful for your efforts towards my work and for your dedication to the Daniel Lab. Lloyd, you have earned special mention here for being my personal iPod, following me around the lab while I was completing experiments late at night singing to me with your beautiful voice.

Lastly, I would like to thank my supervisory thesis committee, Dr. Juliet Daniel, Dr. Andre Bedard and Dr. Brad Doble for their expert advice and guidance. Juliet, thank you for putting up with my moodiness and for your nurturing, loving support throughout my studies. You have been a great mentor, supervisor and role model and I sincerely appreciate the time, effort and dedication you invested in me over the years.

TABLE OF CONTENTS

LIST OF FIGURES

LIST OF TABLES

LIST OF ABBREVIATIONS*

**Abbreviations for common molecular biology reagents and techniques as well as those that were used sparingly have been omitted for brevity*

5-aza-dC	5-aza-2'-deoxycytidine
APC	Adenomatous polyposis coli
ATOH1	Atonal homolog 1
β-TrCP	Beta-transducin repeat containing protein
BTB	Broad complex, Tramtrak, Bric à brac
CAC	Colitis-associated cancer
CBD	Catenin binding domain
CBP	CREB binding protein
CD	Crohn's disease
CK1	Casein kinase I
coREST	REST corepressor
CRC	Colorectal cancer
CTCF	CCCTC-binding factor
Dkk1	Dickkopf-1
EGF	Epidermal growth factor
FAP	Familial adenomatous polyposis
Frz	Frizzled
GSEA	Gene set enrichment analysis
GM-CSF	Granulocyte macrophage colony-stimulating factor
GSK3	Glycogen synthase kinase-3
HDAC	Histone deacetylase
HES	Hairy and enhancer of split
HIF-1	Hypoxia inducible factor-1
HRE	Hypoxia response element
IBD	Inflammatory bowel disease
JMD	Juxtamembrane domain
***Kaiso*$^{Tg/+}$**	Kaiso transgenic
KBS	Kaiso binding site
LEF	Lymphoid enhancer-binding factor
LRP	Low density lipoprotein receptor-related protein
MBD	Methyl-CpG binding domain
MCP-1	Monocyte chemotactic protein-1
meCpG	Methylated CpG
Min	Multiple intestinal neoplasia
MPO	Myeloperoxidase
MTG-16	Myeloid translocation gene 16
NCoR	Nuclear receptor co-repressor-1
NICD	Notch intracellular domain
NF- κB	Nuclear factor kappa B
Non-Tg	Non-transgenic

$p120^{ctn}$	p120 catenin
PAS	Periodic Acid-Schiff
PBF	Phosphate-buffered formalin
PDK1	Pyruvate dehydrogenase kinase 1
PHD	Prolyl hydroxylase
POZ	Pox virus and zinc finger
REST	RE1-silencing transcription factor
SMRT	Silencing mediator of retinoic acid and thyroid-hormone receptors
TCF	T-cell factor
TLE	Transducin-like enhancer of split
TMA	Tissue microarray
TNF-α	Tumour necrosis factor-alpha
UC	Ulcerative colitis
VHL	Von Hippel-Lindau
ZBTB	Zinc finger- and BTB domain-containing protein
ZF	Zinc finger
Znf131	Zinc finger protein 131

CHAPTER 1

INTRODUCTION

1.1. Overview

Colo**r**ectal **c**ancer (CRC) is the 3rd most commonly diagnosed cancer and the second leading cause of cancer deaths worldwide (Bray *et al.* 2013). Improved screening protocols have facilitated earlier detection thereby significantly reducing CRC patient mortality; however 25% of CRC patients that present with early stage disease and 50% of those that present with advanced disease will develop local recurrence and or metastases (Bilchik *et al.* 2006; Manfredi *et al.* 2006). Although systemic therapies for CRC have resulted in improved overall survival, the overall response rate is only 60% in patients with late stage disease (Langan *et al.* 2013). Thus the identification of biomarkers associated with CRC progression and aggressiveness may significantly enhance early diagnosis, inform treatment regimens and serve as novel therapeutic targets (Langan *et al.* 2013).

CRC refers to cancers that arise in the colon and rectum, components of the large intestine, which together with the small intestine form the lower gastrointestinal tract. The intestine is a complex multifunctional organ that is important for digestion and nutrient absorption, and which also acts as a barrier against external pathogens (Gregorieff and Clevers 2005). To serve these diverse functions, the mammalian intestinal epithelium undergoes constant renewal, which is fueled by a population of resident intestinal stem cells and driven by several signal transduction pathways, including the canonical Wnt signaling pathway (hereafter Wnt pathway) (Gregorieff and Clevers 2005). The Wnt

pathway regulates intestinal stem cell proliferation and differentiation into the specialized cell types that mediate intestinal function. Consequently, the Wnt pathway is a key mediator of intestinal homeostasis (Gregorieff and Clevers 2005).

Interestingly, activating mutations in the Wnt pathway are often the initiating event in a large proportion of CRC patients (Fodde *et al.* 2001). Thus, proteins that modulate this pathway may be of therapeutic importance in CRC. One such protein is the POZ-ZF transcription factor Kaiso that was implicated as a negative regulator of canonical Wnt signaling in *Xenopus laevis* embryos and cultured cells (Park *et al.* 2005; Spring *et al.* 2005; Iioka *et al.* 2009; Donaldson *et al.* 2012). Kaiso's impact on Wnt signaling in mammalian intestines however, remains largely unknown, and it is in this context that studies were initiated to examine the role of Kaiso in intestinal Wnt signaling and tumorigenesis. The studies described in this thesis aim to characterize Kaiso's role in intestinal tumorigenesis.

1.2. Wnt signaling in the intestine: From homeostasis to tumorigenesis

1.2.1. The intestinal epithelium

The mammalian adult intestines are separated into the small and large intestine. The architecture of both the small and large intestine is organized in a manner that maximizes the surface area through which absorption occurs. The small intestine is organized into finger-like projections, known as villi, which are separated by invaginations known as the crypts of Lieberkühn that house a population of intestinal stem cells (Potten and Loeffler

1990). There are also crypts in the large intestine. However, layers of flattened surface epithelium rather than villi separate neighbouring crypts (Potten and Loeffler 1990).

The intestinal epithelium is one cell layer thick and lines the lumen of the entire intestinal tract. In the small intestine, the epithelium comprises four main differentiated cell lineages, namely absorptive enterocytes and three different secretory lineages: Paneth cells, enteroendocrine cells and goblet cells (Gregorieff and Clevers 2005). The composition of the epithelium in the large intestine is reminiscent of that observed in the small intestine, with the exception that Paneth cells are largely absent. Paneth cells and goblet cells serve to defend the intestine from food- and environmentally-derived microbes by secreting antimicrobial agents and mucous respectively (Gregorieff and Clevers 2005). Enteroendocrine cells secrete hormones that modulate the peristaltic movements of the intestine and aid in digestion (Gregorieff and Clevers 2005). In addition to these four main cell types, two additional minor mucosal cell populations, M cells and tuft cells, are also present. M cells transport antigens from the intestinal lumen to underlying Peyer's patches, which form part of the gut-associated lymphoid tissue, while the precise function of tuft cells is still being elucidated (Gerbe *et al.* 2011; de Lau *et al.* 2012).

In the first weeks after birth, intestinal stem cells proliferate and migrate up the crypt-villus axis to generate a population of progenitor cells known as transit-amplifying cells (Gregorieff and Clevers 2005). Transit-amplifying cells differentiate into the absorptive and secretory lineages, which, with the exception of Paneth cells that migrate towards the crypt base, continue to migrate up the villi towards the intestinal lumen. Once

at the top of the villi, the epithelial cells undergo apoptosis and are sloughed off into the intestinal lumen (Hall *et al.* 1994; Shibahara *et al.* 1995). Through the processes of proliferation, migration and sloughing off, the intestinal epithelium is renewed every 3-5 days. A number of cell signaling pathways coordinate the proliferation and differentiation of the intestinal stem and progenitor cell populations. One of the most studied pathways in this context is the Wnt pathway (Gregorieff and Clevers 2005).

1.2.2. The canonical Wnt/ß-catenin signaling pathway

The Wnt pathway is a highly conserved signal transduction pathway that has crucial roles in embryonic development and tissue regeneration (Klaus and Birchmeier 2008). The extracellular signaling molecules of this pathway, Wnt ligands, are a family of 19 cysteine-rich glycoproteins that are secreted into the extracellular space and bind to a transmembrane protein receptor complex containing **F**ri**z**zled (Fz) and **l**ow density lipoprotein **r**eceptor-related **p**rotein (LRP) (Bhanot *et al.* 1996; Pinson *et al.* 2000; Tamai *et al.* 2000; Wehrli *et al.* 2000) (Figure 1.1).

The key effector of the Wnt pathway is the Armadillo catenin, β-catenin. In the absence of Wnt ligand, β-catenin is degraded by a destruction complex consisting of the scaffolding proteins APC (**a**denomatous **p**olyposis **c**oli) and Axin1/Axin2, which sequester β-catenin and promote its phosphorylation on serine45 (S45) by **c**asein **k**inase **I** (CKI) (Amit *et al.* 2002). This phosphorylation event enables subsequent phosphorylation of additional serine and threonine residues N-terminal to S45 by **g**lycogen **s**ynthase **k**inase **3** (GSK3). Phosphorylated β-catenin is recognized by the F-box-containing E3 ubiquitin protein ligase, **beta**-**t**ransducin **r**epeat **c**ontaining **p**rotein (β-TrCP), which

ubiquitinates β-catenin and targets it for proteasomal degradation (Hart *et al.* 1998; Kitagawa *et al.* 1999) (Figure 1.1).

It is postulated that upon binding of Wnt to the Fz/LRP co-receptor, the cytoplasmic tail of LRP becomes phosphorylated by GSK3 and CK1γ, which allows docking of Axin to LRP and sequestration of the destruction complex at the membrane (Tamai *et al.* 2004; Li *et al.* 2012). At the membrane, the destruction complex continues to bind and phosphorylate β-catenin, however β-TrCP ubiquitination is inhibited (Li *et al.* 2012) (Figure 1.1). Subsequently, newly synthesized β-catenin accumulates and translocates to the nucleus where it associates with the DNA-binding proteins of the **l**ymphoid **e**nhancer-binding **f**actor/**T**-**c**ell **f**actor (LEF/TCF, hereafter TCF) family of transcription factors (Behrens *et al.* 1996) (Figure 1.1). In unstimulated cells, TCF proteins are associated with transcriptional repressors of the Groucho/**T**ransducin-**l**ike **e**nhancer of split (TLE) family and thus, the expression of Wnt-responsive genes is inhibited (Behrens *et al.* 1996). However, in stimulated cells, the Wnt-induced binding of β-catenin to TCF proteins displaces the Groucho/TLE repressors. β-catenin contains a transactivation domain, and the β-catenin/TCF complex activates transcription of Wnt target genes (Waterman 2004) (Figure 1.1). The phenotypic consequences of nuclear β-catenin accumulation include cell proliferation, migration and differentiation (Klaus and Birchmeier 2008). As alluded to, these diverse functions of Wnt signaling and the downstream implications of these functions in development and homeostasis are exemplified in the mammalian intestine (Gregorieff and Clevers 2005).

Figure 1.1: The canonical Wnt/β-catenin signaling pathway. The key downstream effector of Wnt signaling, β-catenin (β-cat), is regulated by a protein complex known as the destruction complex, which targets the protein for ubiquitin-mediated proteasomal degradation in the absence of a Wnt signal (left panel). The Wnt pathway is activated when Wnt ligands bind to the Frizzled/LRP co-receptor complex, resulting in sequestration of the destruction complex at the membrane (right panel). Destruction complex-associated β-catenin does not undergo ubiquitination (Ub) and degradation; consequently phosphorylated β-catenin saturates the destruction complex. This enables newly synthesized β-catenin to accumulate and translocate to the nucleus where it binds TCF/LEF transcription factors to activate Wnt target genes.

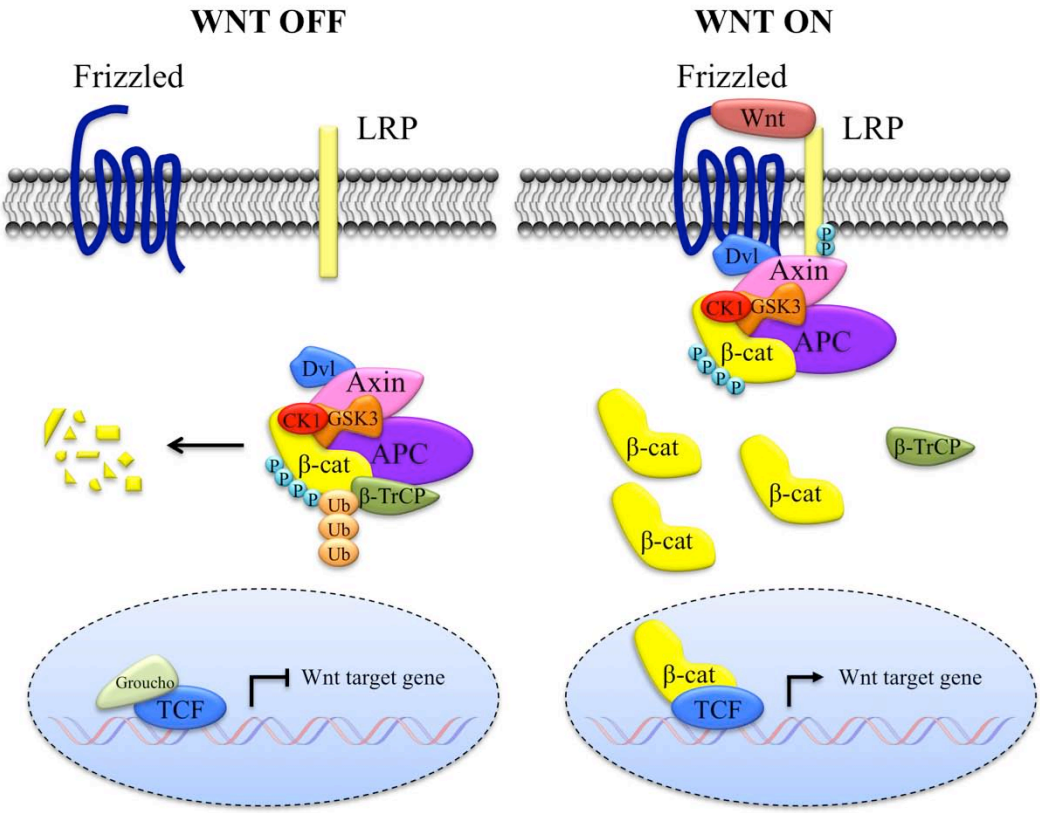
WNT OFF
WNT ON
Frizzled
LRP
Frizzled
Wnt
LRP
Dvl
Axin
CK1
GSK3
APC
β-cat
β-TrCP
Ub
Ub
Ub
P
P
P
P
Dvl
Axin
CK1
GSK3
APC
β-cat
P
P
P
P
P
P
β-cat
β-cat
β-cat
β-TrCP
Groucho
TCF
Wnt target gene
β-cat
TCF
Wnt target gene

1.2.3. Wnt signaling in intestinal homeostasis

Perhaps the first hint that Wnt signaling was involved in mediating intestinal homeostasis was the finding that loss-of-function mutations in the *Apc* gene result in intestinal neoplasia (Moser *et al.* 1990; Powell *et al.* 1992; Fodde *et al.* 1994). Subsequently, nuclear accumulation of β-catenin was observed in the proliferative cells at the bottom of crypts of the small and large intestine (Batlle *et al.* 2002; van de Wetering *et al.* 2002). Following these initial clues, multiple *in vivo* studies have garnered evidence supporting a role for Wnt signaling in the maintenance of stem cell proliferation and pluripotency, and consequently in intestinal homeostasis (Schepers and Clevers 2012).

In mice, homozygous disruption of the Tcf4 gene resulted in neonatal lethality, which was attributed to extensive stretching and tearing of the small intestinal epithelium (Korinek *et al.* 1998). Importantly, proliferative crypts were absent in the small intestines of *Tcf4*$^{-/-}$ mice, and there were decreased numbers of villi and a reduction in the epithelial cell population in the intervilli regions (Korinek *et al.* 1998). In another study, conditional deletion of Tcf4 in the intestine also abolished proliferative crypts coincident with a reduction in the expression of the Wnt target genes *CD44* and *Sox9* (van Es *et al.* 2012). Similar to Tcf4 loss, conditional depletion of β-catenin in the small intestine resulted in the loss of proliferative crypt compartments accompanied by a 50% reduction in villus length 4 days post β-catenin depletion (Fevr *et al.* 2007). β-catenin loss also elicited the forced differentiation of stem cells into the enterocytic lineage with an accompanying proliferation block, suggesting that in addition to promoting proliferation, Wnt signaling is necessary to maintain the pluripotency of intestinal stem cells (Fevr *et al.* 2007).

Evidence supporting a role for Wnt signaling in intestinal stem cell differentiation was garnered from several independent studies. Adenoviral expression of the Wnt antagonist **D**ic**kk**opf-**1** (Dkk1) resulted in the loss of crypt compartments and fewer villi two to four days after adenoviral administration, concomitant with reduced expression of the Wnt target genes *EphB2* and *CD44* (Kuhnert *et al.* 2004). Secretory cell lineages were largely absent from the intestines of transgenic mice harbouring an intestinal-specific *Dkk1* transgene, which was consistent with data obtained from β -catenin knockout mice that exhibit forced enterocytic differentiation (Pinto *et al.* 2003). Aberrant activation of the Wnt signaling pathway results in the rapid onset of crypt cell proliferation (Kim *et al.* 2005). Mice harbouring a transgene for the secreted Wnt agonist R-spondin exhibited diffuse thickening of the mucosa, crypt epithelial hyperplasia, and a greatly expanded zone of proliferating cells in the small intestine (Kim *et al.* 2005).

Collectively, these studies illustrate the two major functions of the Wnt pathway in intestinal stem cells: promoting proliferation and sustaining pluripotency. As unchecked proliferation is a fundamental trait of cancer cells (Hanahan and Weinberg 2011) it is not surprising that activating mutations in the Wnt pathway promote tumorigenesis in the intestine (Krausova and Korinek 2014).

1.2.4. Aberrant Wnt signaling in intestinal tumorigenesis

Massive parallel next-generation sequencing of matched human normal and tumour tissues revealed alterations of genes involved in Wnt signaling in 90% of CRCs. Specifically, inactivating mutations in *APC* or activating mutations in *β-catenin* were present in 80% of cases (Cancer Genome Atlas 2012). Loss-of-function mutations in *APC*

also underlie the etiology of **f**amilial **a**denomatous **p**olyposis (FAP), a heritable CRC syndrome that accounts for approximately 1% of hereditary CRCs (Half *et al.* 2009). FAP patients develop hundreds of polyps in the large intestine at an early age and eventually succumb to CRC (Fodde and Smits 2001). *APC* mutations follow Knudson's classical two-hit model of tumour suppressor inactivation: FAP patients inherit a germline mutation in one *APC* allele, but tumorigenesis only occurs in cells that somatically acquire a second hit or loss of heterozygosity of the *APC* allele (Lamlum *et al.* 1999; Goss and Groden 2000).

Several mouse models harbouring *Apc* mutations have been developed to facilitate the study of CRC. The first model to mimic the effect of *APC* mutation in humans was the $Apc^{Min/+}$ mouse, where Min stands for **m**ultiple **i**ntestinal **n**eoplasia. The $Apc^{Min/+}$ model was generated during an ethylnitrosourea mutagenesis program (Su *et al.* 1992). The mutant allele has a nonsense mutation in codon 850 of the *Apc* gene, which produces a truncated Apc polypeptide of ~ 95 kDa, as opposed to the full-length 312 kDa tumour suppressor protein (Figure 1.2.) (Fodde and Smits 2001). Heterozygous $Apc^{Min/+}$ mice develop more than 100 intestinal tumours primarily in the upper gastrointestinal tract (Fodde and Smits 2001). In contrast, most human CRC patients bearing *APC* mutations develop adenomas mainly in the colon and the rectum (Half *et al.* 2009). In line with findings in human CRC, most of the lesions that develop in $Apc^{Min/+}$mice have undergone a loss heterozygosity at the *Apc* locus or have completely lost chromosome 18 where the *Apc* gene resides (Fodde and Smits 2001).

Figure 1.2: Schematic representation of the APC protein. N-terminal heptad repeats of APC function as an oligimerization domain while the armadillo domain facilitates several other protein-protein interactions. The 15αα and 20αα repeats are necessary for β-catenin binding and degradation. Axin binds APC via the serine–alanine–methionine–proline (SAMP) repeats. The C-terminal of APC includes microtubule-, EB1-, and PDZ-binding domains.

\\

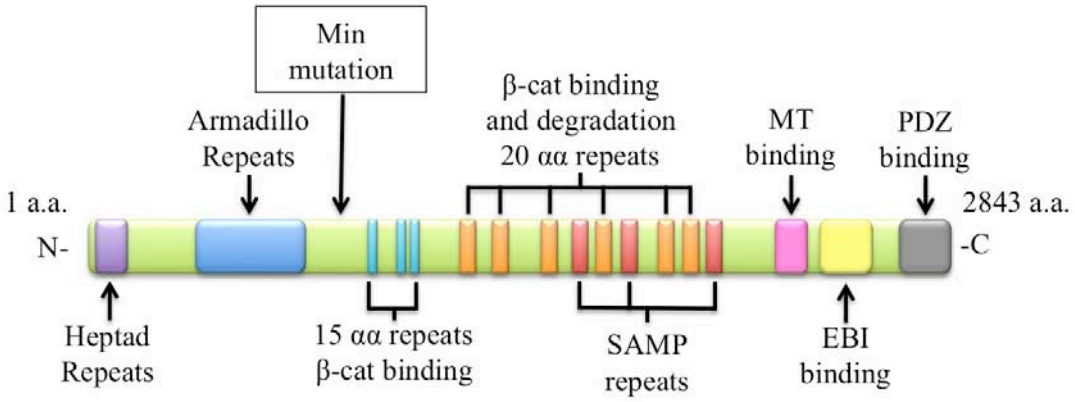
Min
mutation
Armadillo
Repeats
β-cat binding
and degradation
20 αα repeats
MT
binding
PDZ
binding
1 a.a.
N-
2843 a.a.
-C
Heptad
Repeats
15 αα repeats
β-cat binding
SAMP
repeats
EBI
binding

Although the *Apc*$^{Min/+}$ mouse is the best characterized intestinal neoplasia model to date, at least 20 other intestinal neoplasia models harbouring a number of different *Apc* mutations have been developed (Zeineldin and Neufeld 2013). Akin to human FAP patients, mutation of *Apc* at different sites results in variations in polyp multiplicity, polyp distribution and extraintestinal phenotypes among models, with some models more accurately recapitulating human FAP than the *Apc*$^{Min/+}$ model in terms of disease progression and polyp distribution (McCart *et al.* 2008; Zeineldin and Neufeld 2013). Nevertheless, the *Apc*$^{Min/+}$ model has been used extensively to determine genetic and epigenetic modifiers of CRC and to characterize the role of Wnt signaling in intestinal neoplasias (Clarke 2006).

1.2.5. An alternate role for the Wnt pathway effector, β-catenin

In addition to its role as the downstream effector of canonical Wnt signaling, β-catenin also localizes to the cell membrane where it exists in the multiprotein cadherin-catenin complex that mediates cell-cell adhesion (Vestweber and Kemler 1984; Ozawa *et al.* 1989). In these complexes, β-catenin functions in a structural capacity, which contrasts significantly with its function as the downstream effector and transcriptional coactivator of Wnt signaling. These alternate biological roles for β-catenin exemplify the diverse biology of a subfamily of Armadillo proteins known as the Armadillo catenins (McCrea and Gu 2010).

1.3. The multifunctional Armadillo catenins

The Armadillo catenin family of proteins possesses two key characteristics: they associate with cadherins in cadherin-catenin complexes and they possess a central Armadillo domain consisting of between nine and twelve 40-amino acid Armadillo repeats that function as binding interfaces (McCrea and Gu 2010). This Armadillo protein family has diverse biological roles, ranging from cell adhesion to gene regulation, and can be sub-classified into the β-catenin, plakophilin and p120 families on the basis of primary sequence homology. As a founding member of the Armadillo protein family and due to its key role as a Wnt pathway effector, β-catenin has been the most extensively studied. However since it's discovery and characterization, a plethora of roles for the non-classical catenin, p120 catenin (hereafter, $p120^{ctn}$) have emerged, highlighting the multifunctional nature of the Armadillo catenins (McCrea and Gu 2010). This section will focus on the various biological functions of $p120^{ctn}$ as they pertain to cadherin-mediated cell adhesion, signaling and disease.

1.3.1. The cadherin-catenin cell adhesion complex

The classical cadherins are a family of single-pass, transmembrane glycoproteins that mediate calcium-dependent cell-cell adhesion in animal tissues (Ivanov *et al.* 2001; Hiroki 2012). The type I classical cadherins (hereafter type I cadherins), namely E-(epithelial), N-(neural), P-(placental) and R-(retinal) cadherin, are the most abundant component of adherens junctions and are the most extensively studied cadherin family (Ivanov *et al.* 2001; Makrilia *et al.* 2009).

The stability of type I cadherin-mediated adhesions is aided, in part, through the indirect interaction of the cadherin cytoplasmic domain with the actin cytoskeleton via the Armadillo catenin proteins (Ivanov *et al.* 2001). Adhesion is mediated by the cadherin extracellular domain, which consists of five tandem repeats separated by linker regions featuring highly conserved amino acids that coordinate calcium ions in calcium-binding sites (Sotomayor *et al.* 2014). The extracellular domain extends from the cell surface to bind to type I cadherin molecules on adjacent cells via homotypic interactions (Gall and Frampton 2013) (Figure 1.3). The cadherin cytoplasmic domain features a **j**uxta**m**embrane **d**omain (JMD) and the **c**atenin-**b**inding **d**omain (CBD) (Gall and Frampton 2013) (Figure 1.3). $p120^{ctn}$ binds the cadherin JMD, while β-catenin and γ-catenin bind to the CBD (Gall and Frampton 2013) (Figure 1.3). The structurally unrelated catenin, α-catenin, binds either β-catenin or γ-catenin, consequently tethering the entire cadherin-catenin complex to the actin cytoskeleton (Ivanov *et al.* 2001; Makrilia *et al.* 2009). The functions of β- and γ-catenin in the cadherin-catenin complex are primarily structural. Indeed an E-cadherin-α-catenin fusion chimera and a mutant E-cadherin protein lacking the β-/γ-catenin binding domain were both capable of mediating cell adhesion that was at a minimum, comparable in strength to that mediated by wild type E-cadherin (Gottardi *et al.* 2001). In contrast, loss of function of $p120^{ctn}$ has considerably more deleterious effects on cell adhesion (Ireton *et al.* 2002; Davis *et al.* 2003; Kowalczyk and Reynolds 2004).

Figure 1.3: The Type I classical cadherin-catenin complex. The extracellular domains of cadherin dimers on neighbouring cells interact to stabilize basolateral cell-cell adhesions. Intracellularly, cadherins bind $p120^{ctn}$ at the JMD and regulate cadherin stability and turnover while β- and γ- catenin bind the CBD and tether the cadherin-catenin complex to the actin cytoskeleton via α-catenin dimers.

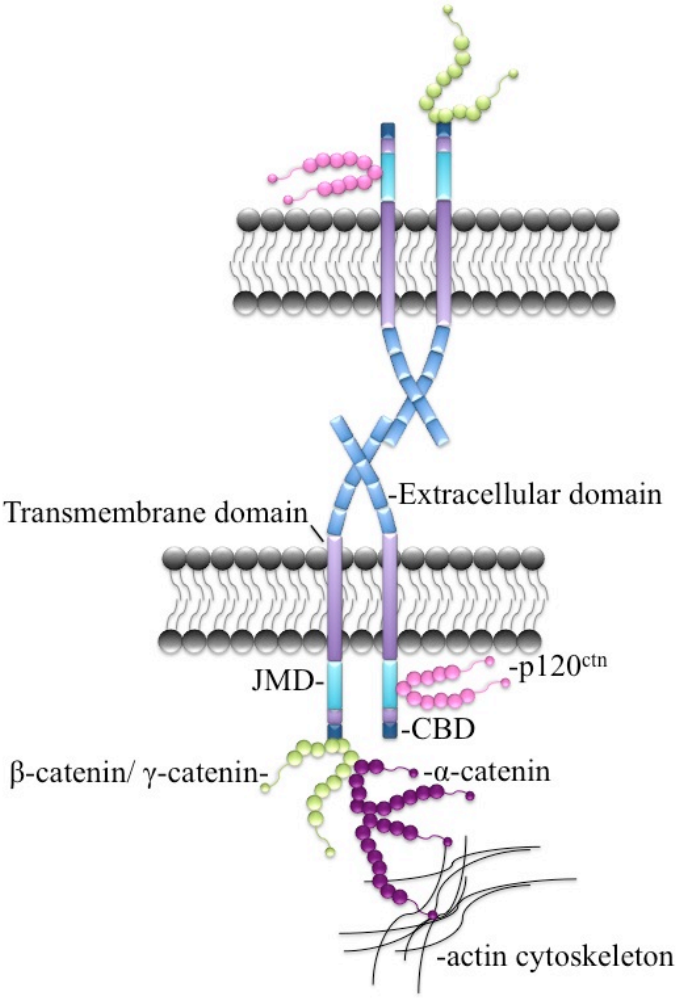
Transmembrane domain
-Extracellular domain
JMD-
-p120ctn
-CBD
β-catenin/ γ-catenin-
-α-catenin
-actin cytoskeleton

1.3.2. p120^{ctn} functions in adhesion and cell motility

p120^{ctn} was originally identified as one of eight prominent substrates for tyrosine phosphorylation by the Src oncoprotein in chicken cells expressing oncogenic variants of the avian *src* gene (Reynolds *et al.* 1989). It was subsequently demonstrated that tyrosine phosphorylation of p120^{ctn} also occurs in response to ligand-induced stimulation of receptor tyrosine kinases, including **e**pidermal **g**rowth **f**actor (EGF), colony stimulating factor and platelet-derived growth factor receptors (Downing and Reynolds 1991). These studies suggested that p120^{ctn} functioned as a downstream effector of receptor tyrosine kinase signaling, however analysis of p120^{ctn}'s predicted protein structure revealed none of the functional domains classically associated with mitogenic signaling (Downing and Reynolds 1991; Kanner *et al.* 1991; Reynolds *et al.* 1994).

Instead, p120^{ctn} was found to possess an Armadillo repeat domain similar to that previously identified in β-catenin and *Drosophila* Armadillo (Reynolds *et al.* 1994). At the time, the precise role of β- and γ-catenin in modulating cell adhesion had not been fully elucidated. However, both β- and γ-catenin interacted with the cytoplasmic tail of E-cadherin that is essential for cell adhesion, suggesting that these proteins participated in cell adhesion (Nagafuchi and Takeichi 1988; Ozawa *et al.* 1989). The presence of an Armadillo domain in p120^{ctn} hinted that it also bound to E-cadherin and consequently, participated in cell adhesion.

However unlike β- and γ-catenin, which function solely in a structural capacity in the cadherin-catenin complex, p120^{ctn} was found to regulate cadherin clustering, stability and turnover (Yap *et al.* 1998; Ireton *et al.* 2002; Davis *et al.* 2003; Kowalczyk and

Reynolds 2004). Indeed, deletion of the JMD inhibited lateral cadherin clustering and reduced cadherin adhesive strength (Yap *et al.* 1998). Evidence supporting a role for $p120^{ctn}$ in modulating cadherin stability was further gleaned from studies performed in SW48 colon carcinoma cells, which harbour a mutation in the $p120^{ctn}$ gene and have significantly reduced $p120^{ctn}$ expression (Ireton *et al.* 2002). These cells are incapable of forming a compact epithelial sheet and instead line up end to end in loosely organized arrays (Ireton *et al.* 2002). Exogenous expression of $p120^{ctn}$ in these cells results in increased E-cadherin expression and the formation of a more compact epithelial sheet (Ireton *et al.* 2002).

In a subsequent study, depletion of $p120^{ctn}$ in A431 human cervical carcinoma cells resulted in decreased E-cadherin expression at the membrane with a concomitant decrease in both α- and β-catenin (Davis *et al.* 2003). Strikingly, $p120^{ctn}$ depletion results in decreased expression of P-, VE-, and N-cadherins, suggesting that $p120^{ctn}$'s stabilizing function is not limited to E-cadherin (Davis *et al.* 2003). Using a combination of pulse-chase and biotin surface-labeling strategies, Davis *et al.* demonstrated that $p120^{ctn}$ depletion had no effect on E-cadherin synthesis but rather enhanced the rate at which E-cadherin is turned over at the membrane and subsequently targeted for proteasomal and/or lysozomal degradation (Davis *et al.* 2003). $p120^{ctn}$'s ability to stabilize E-cadherin was later attributed to the finding that $p120^{ctn}$'s binding to E-cadherin masks a di-leucine motif responsible for endocytosis of E-cadherin (Miyashita and Ozawa 2007).

In addition to modulating E-cadherin stability and consequently, cell-cell adhesion, $p120^{ctn}$ acts as a molecular switch between sessile and motile states (Yanagisawa *et al.*

2008). Up to 48 putative isoforms are generated through use of different translation start sites and alternative splicing of transcripts generated from the *CTNND1* gene that encodes $p120^{ctn}$ (Pieters *et al.* 2012). Although the functions of these different isoforms have not been fully elucidated, differentiated epithelial cells predominantly express shorter isoforms initiated by start codon three, known as $p120^{ctn}$ isoform 3 (Aono *et al.* 1999), whereas mesenchymal cells primarily express $p120^{ctn}$ isoform 1 (Yanagisawa *et al.* 2008). This differential expression of $p120^{ctn}$ isoforms in mesenchymal versus epithelial cells may be linked to the fact that $p120^{ctn}$ isoform 1 is capable of inhibiting the Rho-GTPase RhoA and activating the Rho-GTPases Rac and cdc42, which in turn results in increased cell motility and invasion (Anastasiadis *et al.* 2000; Anastasiadis and Reynolds 2001; Grosheva *et al.* 2001; Yanagisawa *et al.* 2008).

Combined, these studies outline a crucial role for $p120^{ctn}$ in stabilizing cadherin-mediated cell-cell adhesion and modulating cell motility, with the important implication that $p120^{ctn}$ dysfunction may lead to tumour metastasis, which is typically associated with E-cadherin loss/defective cell-cell adhesion. Indeed, loss, down-regulation or mislocalization of $p120^{ctn}$ is observed in many human cancers, and ablation of $p120^{ctn}$ in the murine salivary gland, skin epidermis, oral cavity, esophagus, squamous fore-stomach and intestines leads to neoplastic progression (Davis and Reynolds 2006; Perez-Moreno *et al.* 2006; Perez-Moreno *et al.* 2008; Smalley-Freed *et al.* 2011; Stairs *et al.* 2011; Peglion and Etienne-Manneville 2013). Notably, with the exception of the salivary gland, tumorigenesis in all of the aforementioned murine $p120^{ctn}$ knockout models was

invariably accompanied by inflammation, defining a novel role for p120^{ctn} as an anti-inflammatory mediator.

1.3.3. p120^{ctn}: a novel mediator of inflammation

Within the last decade, studies utilizing conditional p120^{ctn} knockout mice have amassed evidence supporting a role for p120^{ctn} in inflammation. Surprisingly, p120^{ctn}'s anti-inflammatory role is cell autonomous and can occur independently of its role in cell adhesion (Perez-Moreno *et al.* 2006; Perez-Moreno *et al.* 2008; Smalley-Freed *et al.* 2011; Stairs *et al.* 2011).

The first study to link p120^{ctn} loss to inflammation was conducted in mice with targeted knockout of p120^{ctn} in the skin (Perez-Moreno *et al.* 2006). In agreement with previous *in vitro* findings, p120^{ctn} knockout resulted in decreased cadherin and α- and β-catenin expression. Surprisingly, these defects had no effect on the number of adherens junctions per unit of membrane or on skin permeability. Another unexpected finding was skin hyperplasia in the p120^{ctn} knockout mice, which seemed largely unrelated to loss of the cadherin or catenin proteins. These mice also exhibited hair disintegration, wasting and enhanced vasculature, which combined with hyperplasia are classical features of chronic subcutaneous inflammation. Ultrastructural analysis of the underlying dermis in p120^{ctn} knockout mice revealed substantial immune cell infiltration that was attributed to increased activation of the pro-inflammatory molecule **n**uclear **f**actor-**κB** (NF-κB). Further analyses revealed that RhoA activity was increased on depletion of p120^{ctn}, which in turn activated NF-κB (Perez-Moreno *et al.* 2006). In a follow-up study by the same group, engraftment of skin from p120^{ctn} null mice onto nude mice resulted in neoplasia

and this was blocked when mice were treated with an NF-κB inhibitor (Perez-Moreno *et al.* 2008). These studies were the first to suggest that tumorigenesis originating from the loss of $p120^{ctn}$ may result from enhanced inflammation.

Tumorigenesis following $p120^{ctn}$ knockout in the squamous oral cavity, esophagus, and fore-stomach was also accompanied by inflammation (Stairs *et al.* 2011). As with $p120^{ctn}$ knockout in the skin, NF-κB induction was evident in the targeted tissues accompanied by increased secretion of **g**ranulocyte **m**acrophage **c**olony-**s**timulating **f**actor (GM-CSF), macrophage colony-stimulating factor (M-CSF), **m**onocyte **c**hemotactic **p**rotein-**1** (MCP-1), and tumour necrosis factor-α (TNF-α) (Stairs *et al.* 2011). Strikingly, myeloid cell lineages were more prevalent in cells cultured from tumour-bearing $p120^{ctn}$ knockout mice, which agrees with studies performed in the intestine-specific $p120^{ctn}$ knockout mice that displayed increased neutrophil recruitment in $p120^{ctn}$ knockout mice (Smalley-Freed *et al.* 2010; Smalley-Freed *et al.* 2011; Stairs *et al.* 2011).

Intestine-specific $p120^{ctn}$ knockout results in lethality at approximately 17 days postnatal due to major defects in cell-cell adhesion that produce severe intestinal barrier defects (Smalley-Freed *et al.* 2010). In this model, significant neutrophil infiltration was observed in the intestines, which was initially attributed to the compromised epithelial barrier. However, in co-cultures of $p120^{ctn}$-depleted HCA-7 colon carcinoma cells and neutrophils, neutrophil attachment to the HCA-7 cell monolayer was increased approximately 30-fold compared to wild-type cells (Smalley-Freed *et al.* 2010). These studies suggest that neutrophil accumulation in this model may not be fully attributed to a barrier defect, but may be a cell autonomous consequence of $p120^{ctn}$ knockout (Smalley-

Freed *et al.* 2010). To facilitate more long-term studies of the effect of p120^{ctn}-depletion in the intestine, a mosaic model was generated in which p120^{ctn} knockout was limited to approximately 10% of the intestine (Smalley-Freed *et al.* 2011). These mice also exhibited selective neutrophil accumulation in p120^{ctn} void regions and an intestinal barrier defect, albeit less severe than that observed in the complete knockout model. Approximately 50% of mosaic p120^{ctn} knockout mice developed tumours between 12-18 months of age, but these tumours were attributed to increased mutation rates resulting from intestinal inflammation, as tumours were not limited to p120^{ctn} void areas of the epithelium (Smalley-Freed *et al.* 2011). Importantly, p120^{ctn}-depleted HCA-7 cells secreted several neutrophil chemoattractants, confirming the results of the previous study showing increased neutrophil attachment to p120^{ctn}-depleted HCA-7 monolayers (Smalley-Freed *et al.* 2010; Smalley-Freed *et al.* 2011).

While p120^{ctn}'s anti-inflammatory function is still not fully understood, the widespread cellular effects resulting from p120^{ctn} loss supports the notion that like β-catenin, p120^{ctn} may modulate cell signaling pathways to influence changes in gene expression.

1.3.4 A nuclear role for p120^{ctn}

Similar to β-catenin, cytoplasmic and nuclear pools of p120^{ctn} have been observed, particularly in E-cadherin deficient carcinoma cells and in fibroblasts (van Hengel *et al.* 1999; Roczniak-Ferguson and Reynolds 2003). The cytoplasmic p120^{ctn} pool has been implicated in modulating cytoskeletal dynamics through regulation of Rho-GTPases to promote cell motility (Anastasiadis *et al.* 2000; Anastasiadis and Reynolds 2001;

Grosheva *et al.* 2001; Yanagisawa *et al.* 2008). However the role of the nuclear pool remains less characterized.

p120^{ctn}'s ability to translocate to the nucleus is attributed to Armadillo repeats 3 and 5 of its Armadillo domain (Roczniak-Ferguson and Reynolds 2003). Interestingly, Armadillo repeats 1-5 and 7 are required for p120^{ctn} binding to E-cadherin, suggesting that p120^{ctn}'s association with E-cadherin and p120^{ctn}'s nuclear translocation are mutually exclusive events (Ireton *et al.* 2002; Roczniak-Ferguson and Reynolds 2003).

Three nuclear binding partners for p120^{ctn} have been identified to date: the BTB/POZ (**B**road complex, **T**ramtrak, **B**ric à brac/ **Po**x virus and **z**inc finger) zinc finger (hereafter POZ-ZF) transcription factor Kaiso, the **RE**1-**S**ilencing **T**ranscription factor (REST), and the **REST** **co**repressor (coREST) (Daniel and Reynolds 1999; Lee *et al.* 2014). The interaction of p120^{ctn} with REST/coREST has only recently been unearthed, but the p120^{ctn}-coREST/REST interaction appears to promote differentiation of murine embryonic stem cells into a neuronal fate (Lee *et al.* 2014). However, our studies focus on characterizing the relationship between p120^{ctn} and Kaiso, which was the first nuclear binding partner identified for p120^{ctn} (Daniel and Reynolds 1999).

1.4 Structure and function of the POZ-ZF transcription factor Kaiso

1.4.1. Kaiso is a p120^{ctn}-specific interaction partner

In an attempt to gain insight into the role of p120^{ctn}, a yeast two-hybrid assay was performed using full-length p120^{ctn} as bait to identify novel p120^{ctn} binding partners (Daniel and Reynolds 1999). The most frequent clones identified corresponded to the C-

terminal zinc finger region of a novel transcription factor, Kaiso, also known as **z**inc finger- and **BTB** domain-containing protein-**33** (ZBTB33) (Daniel and Reynolds 1999). The Kaiso-p120^{ctn} interaction was mapped to Armadillo repeats 1-7 of p120^{ctn}, suggesting that Kaiso may interact with other members of the Armadillo catenin family. However Kaiso did not interact with any other component of the cadherin-catenin complex (Daniel and Reynolds 1999).

The first clue about the functional significance of Kaiso's interaction with p120^{ctn}, was the finding that p120^{ctn} inhibited Kaiso's ability to bind to DNA due to it's interaction with a region flanking Kaiso's DNA-binding domain (Daniel *et al.* 2002) (Figure 1.3). Indeed, several studies have demonstrated p120^{ctn}'s ability to alleviate Kaiso-mediated transcriptional repression (Kelly *et al.* 2004; Kim *et al.* 2004; Park *et al.* 2005; Spring *et al.* 2005; Jiang *et al.* 2012). Subsequent studies revealed an additional role for p120^{ctn} in modulating Kaiso function, by facilitating Kaiso's nuclear export (Zhang *et al.* 2011). In spite of the fact that Kaiso does not possess a *bona fide* nuclear export signal (Kelly *et al.* 2004), Kaiso exhibits dynamic subcellular localization in both cultured cells and tissues (Soubry *et al.* 2005; Jones *et al.* 2012). This dynamic localization may in part mirror p120^{ctn} localization since p120^{ctn} isoform 3 facilitates the nuclear export of Kaiso and results in increased cytoplasmic accumulation of Kaiso (Zhang *et al.* 2011).

Combined, these studies suggest an antagonistic relationship between Kaiso and p120^{ctn} whereby p120^{ctn} inhibits Kaiso function, either by blocking its interaction with

DNA or by shuttling it out of the nucleus. However, the functional consequence of the $p120^{ctn}$ -Kaiso interaction as it relates to human disease is still under investigation.

1.4.2. Kaiso is a dual-specificity DNA binding transcription factor

Isolation and characterization of full-length Kaiso led to its classification as a member of the POZ-ZF family of proteins that are implicated in vertebrate development and tumorigenesis (Daniel and Reynolds 1999). Shortly after its discovery, Kaiso was also classified as the first member of a novel group of proteins that bound methylated DNA (Prokhortchouk *et al.* 2001; Filion *et al.* 2006).

Like most BTB/POZ proteins, Kaiso possesses an N-terminal BTB/POZ domain that mediates protein-protein interactions (Daniel and Reynolds 1999) (Figure 1.4). It is via this domain that Kaiso homodimerizes (Kim *et al.* 2002) and heterodimerizes with other POZ-ZF proteins, e.g. **z**i**n**c **f**inger protein-**131** (Znf-131) (Donaldson *et al.* 2010), and recruits co-repressors including **n**uclear receptor **co-r**epressor-1 (NCoR) (Yoon *et al.* 2003) and **s**ilencing **m**ediator of **r**etinoic acid and **t**hyroid-hormone receptors (SMRT) (Raghav *et al.* 2012). Kaiso also possesses a C-terminal DNA-binding domain consisting of three Krüppel-like C_2H_2-type zinc fingers that recognizes and binds **me**thylated **CpG** (meCpG) dinucleotides and the consensus sequence (TC**CTGCNA**), where n is any nucleotide (core sequence bolded), known as the **K**aiso **b**inding **s**ite (KBS) (Daniel and Reynolds 1999; Prokhortchouk *et al.* 2001; Daniel *et al.* 2002) (Figure 1.3).

Given Kaiso's ability to recognize and bind meCpG dinucleotides, which are typically associated with inhibition of transcription (Klose and Bird 2006), it is not surprising that Kaiso functions as a transcriptional repressor. When bound to NCoR,

Kaiso mediates Class I **h**istone **de**a**c**etylase (HDAC)-dependent transcriptional repression at meCpG dinucleotide sites (Yoon *et al.* 2003). The mechanism by which Kaiso mediates repression when bound to the KBS or when in complex with SMRT is less characterized. However, Kaiso has been shown to recruit the scaffolding protein and co-repressor **m**yeloid **t**ranslocation **g**ene 16 (MTG-16) to the KBS, resulting in enhanced repression (Barrett *et al.* 2012). The MTG family of proteins recruit multiple co-repressor complexes with constituents such as NCoR, SMRT, mammalian Swi-independent 3a (msin3a) and HDACs to elicit transcriptional repression (Davis *et al.* 2003). Thus, Kaiso's interaction with MTG16 at KBS sites suggests that Kaiso-mediated repression via the KBS and meCpG sites may occur via similar mechanisms. Indeed, Kaiso interacts with both sites via similar mechanisms (Buck-Koehntop *et al.* 2012).

Although most evidence to date suggests that Kaiso functions primarily as a transcriptional repressor, three studies have suggested that Kaiso may also function as a transcriptional activator (Rodova *et al.* 2004; Defossez *et al.* 2005; Koh *et al.* 2014). One study examining the regulation of the neuromuscular gene *rapsyn* in congenital myasthenic syndromes found that a region of the *rapsyn* promoter containing a KBS was often mutated in affected individuals, suggesting that Kaiso may regulate *rapsyn* expression (Rodova *et al.* 2004). Indeed, Kaiso binds the *rapysn* promoter, but surprisingly Kaiso activated a minimal *rapysn* promoter-reporter construct (Rodova *et al.* 2004). Kaiso's regulation of the *rapysn* promoter is likely direct, since mutation of the KBS site attenuated Kaiso-mediated activation of the promoter-reporter construct (Rodova *et al.* 2004). Kaiso possesses two highly acidic regions (Figure 1.4) that are

Figure 1.4: Schematic representation of the POZ-ZF protein Kaiso. Kaiso possesses an N-terminal protein-protein interaction POZ domain as well as a C-terminal DNA-binding zinc finger (ZF) domain that is comprised of three C_2H_2-type zinc fingers. $p120^{ctn}$ binds to Kaiso's ZF domain and inhibits Kaiso's ability to regulate its target genes. Kaiso also possesses a nuclear localization signal (NLS) and two highly acidic regions that flank putative serine/threonine phosphorylation sites that are commonly associated with transcriptional activation.

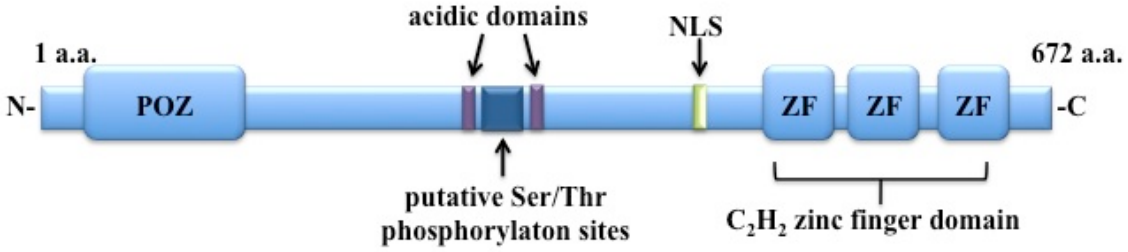
acidic domains
NLS
1 a.a.
672 a.a.
N-
POZ
ZF
ZF
ZF
-C
putative Ser/Thr
phosphorylaton sites
C_2H_2 zinc finger domain

characteristic of many transcriptional activators (Melcher 2000), and hence it is possible that Kaiso may utilize these regions to activate transcription of *rapsyn*. Another study demonstrated that Kaiso interacts with and inhibits the activity of the enhancer blocker CC**CTC**-binding **f**actor CTCF, and in so doing may activate transcription of promoters regulated by CTCF-bound insulators (Defossez *et al.* 2005). Finally, Kaiso was found to interact with the transcriptional co-activator p300 to promote acetylation of the p53 tumour suppressor, thereby enhancing p53's binding to apoptotic and cell cycle regulation genes (Koh *et al.* 2014).

Thus, although most studies to date have focused on Kaiso's ability to repress transcription, it is conceivable that Kaiso may function as both an activator and a repressor. Indeed, at least two other POZ-ZF proteins, namely Miz-1 and ZF-5, have also been shown to function as both transcriptional activators and repressors depending on the cofactors with which they interact (Kaplan and Calame 1997; Staller *et al.* 2001).

1.4.3. Kaiso's role as a DNA methylation-dependent transcriptional repressor

DNA methylation has long been recognized as a hallmark of a repressive chromatin state and inhibition of transcription (Klose and Bird 2006). Generally, DNA methylation inhibits gene expression in two ways: (i) Methylation of cytosine residues in CpG dinucleotides prevents DNA binding factors from recognizing their cognate binding sequences and (ii) Methyl-binding proteins that recognize and bind meCpG dinucleotides recruit co-repressor molecules that facilitate a repressive chromatin state (Klose and Bird 2006). There are three families of proteins that bind and repress methylated DNA, namely the **m**ethyl-CpG **b**inding **d**omain (MBD), **z**inc **f**inger (ZF), and SET and RING finger-

associated (SRA) domain proteins (Filion *et al.* 2006; Buck-Koehntop and Defossez 2013). Kaiso belongs to the ZF family of methyl-binding proteins and indeed it is the founding member of a subfamily comprised of the Kaiso-like proteins ZBTB4 and ZBTB38 (Filion *et al.* 2006).

Studies examining Kaiso's role as a methylation-dependent transcriptional repressor are complicated by the fact that Kaiso binds both the KBS and meCpG dinucleotides. Furthermore, the relative affinity of Kaiso for the KBS versus meCpG dinucleotides is still under active investigation. For instance, Kaiso has been shown to repress the proto-oncogene *CCND1*, which encodes the cell cycle regulator Cyclin D1 that is aberrantly expressed in several cancers and promotes tumour cell proliferation (Bates and Peters 1995; Donaldson *et al.* 2012; Jiang *et al.* 2012). Analysis of the *CCND1* promoter revealed a full KBS as well as a core KBS flanked by several CpG dinucleotides approximately 1,000 base pairs downstream of the full KBS**. We examined the relative importance of Kaiso binding to the KBS versus meCpG dinucleotides to regulate *cyclinD1* in MCF-7 breast carcinoma and HCT-116 CRC cell lines. Our findings indicate that in the context of the *cyclinD1* promoter Kaiso binds to both meCpG dinucleotides and a KBS site in the promoter, which suggests that Kaiso may utilize these two modes of binding simultaneously at a given locus (Chapter 5).**

The importance of proteins such as Kaiso that mediate methylation-dependent repression is becoming more evident, since alterations in global DNA methylation states are a common occurrence in tumours as well as during development (Das and Singal 2004). Regions with an elevated CpG content (CpG islands) exist throughout the genome

and overlap with the transcriptional start sites of approximately 60–70% of all human genes (Kulis *et al.* 2013). CpG islands are generally unmethylated whereas most regions with low CpG density are heavily methylated in normal tissues (Kulis *et al.* 2013). Interestingly, neoplastic transformation is associated with global and gene specific loss of DNA methylation with concurrent hypermethylation of CpG islands in promoters of tumour suppressor genes leading to tumour suppressor inactivation (Das and Singal 2004; Kulis *et al.* 2013; Li and Chen 2013). Kaiso may function to mediate gene expression in the context of neoplastic progression as it has been reported to bind and repress the methylated promoter regions of the *CDH1, CDKN2A*, *HIC1*, and *MGMT* tumour suppressor genes (Lopes *et al.* 2008; Jones *et al.* 2012; Jones *et al.* 2014).

Another putative Kaiso target gene, *HIF1A*, encodes the alpha subunit of the **h**ypoxia **i**nducible **f**actor **1** (HIF-1) transcription factor, which promotes the survival and aggressiveness of tumour cells exposed to commonly occurring hypoxic (low oxygen tension) microenvironments in tumours (Sullivan and Graham 2007). HIF-1α is oxygen labile, and hence functions as a molecular switch that enables the HIF-mediated transcriptional response in low oxygen tensions (Sullivan and Graham 2007) (Figure 1.5).

In normoxia (21% O_2), HIF-1α is negatively regulated by **p**rolyl **hy**droxylases (PHD), which hydroxylate proline residues in HIF-1α's oxygen-dependent degradation domain (Huang *et al.* 1996). Hydroxylation facilitates the recognition of HIF-1α by the **v**on **H**ippel-**L**indau (VHL) tumour suppressor protein, which binds and polyubiquitinates HIF-1α, targeting it for degradation in the 26S proteasome (Tanimoto *et al.* 2000) (Figure 1.5). However, in hypoxia, reduced oxygen availability limits HIF-1α hydroxylation so

Figure 1.5: Oxygen-dependent regulation of HIF-1. (A) In normoxia HIF-1α is hydroxylated by prolyl hydroxylases, which enables HIF-1α to be recognized by the VHL tumour suppressor protein. Subsequently, HIF-1α is polyubiquinated and targeted for proteasomal degradation. **(B)** In hypoxia, proline hydroxylation is inhibited and HIF-1α accumulates and translocates to the nucleus, where it dimerizes with HIF-1β and binds to HREs within the promoters of target genes. HIF-1 recruits transcriptional co-activators such as CBP (**C**REB **b**inding **p**rotein)/p300 for full transcriptional activity.

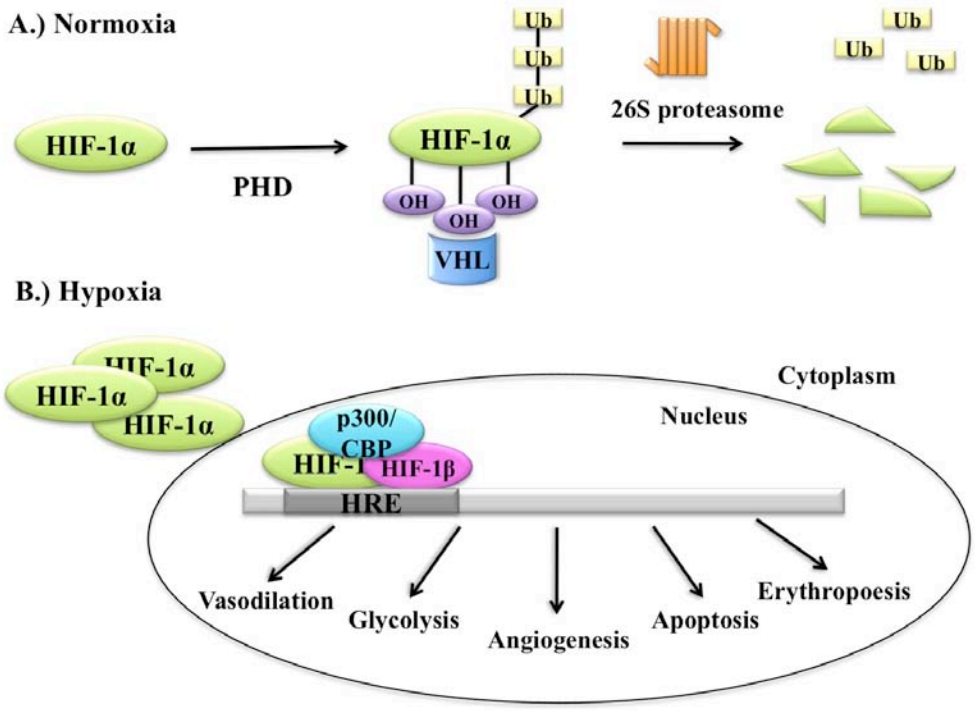
A.) Normoxia
Ub
Ub
Ub
HIF-1α
PHD
HIF-1α
OH
OH
OH
VHL
26S proteasome
Ub
Ub
Ub
B.) Hypoxia
HIF-1α
HIF-1α
HIF-1α
Cytoplasm
Nucleus
p300/
CBP
HIF-1β
HRE
Vasodilation
Glycolysis
Angiogenesis
Apoptosis
Erythropoesis

that it is stabilized and translocates to the nucleus where it dimerizes with the HIF-1β subunit to form a functional HIF-1 protein (Roberts and Ohh 2008). HIF-1 binds to the **h**ypoxia **r**esponse **e**lement (HRE) in the promoter of target genes and activates the expression of these genes in conjunction with co-activator proteins (Dames *et al.* 2002) (Figure 1.5).

In addition to the stabilization of HIF-1α protein that occurs in hypoxia, several other post-translational mechanisms regulate HIF-1α protein synthesis and degradation (Poon *et al.* 2009). The mechanisms regulating *HIF1A* transcription are less understood. However, a recent study demonstrated that *HIF1A* transcription is regulated via methylation of the *HIF1A* promoter (Koslowski *et al.* 2011). While performing studies focused on identifying genes that become selectively activated in cancer, Koslowski *et al.* noted that the expression of HIF-1α target genes is significantly enhanced in cells with a reduced CpG methylation state in hypoxia (Koslowski *et al.* 2011).

To further investigate the molecular bases of this effect, the authors treated HCT-116 and peripheral blood mononuclear cells, incubated in hypoxic conditions, with the demethylating agent **5**-**aza**-2'-**d**eoxy**c**ytidine (5-aza-dC). In agreement with their previous observations, treatment of cells with 5-aza-dC resulted in increased expression of *HIF1A* and HIF-1 target gene transcripts in hypoxia (Koslowski *et al.* 2011). Analysis of the *HIF1A* promoter revealed a CpG island spanning –271 to +96 base pairs and an HRE spanning –156 to − 152 base pairs relative to the transcription start site. Bisulphite sequencing of the promoter revealed heavy CpG methylation at positions –271 to −139, and treatment of cells with 5-aza-dC resulted in a progressive loss of CpG methylation in

this region (Koslowski *et al.* 2011). The HRE located within this CpG island was fully functional hinting at the existence of a positive feedback loop, whereby HIF-1 bound and activated the *HIF1A* promoter to augment HIF-1 expression during hypoxia. Importantly, methylation of the CpG within the HRE prevented HIF-1 binding to and activating the promoter (Koslowski *et al.* 2011).

We have explored a role for Kaiso in the methylation-dependent repression of the *HIF1A* gene based on our finding of increased expression of *HIF1A* transcripts in Kaiso depleted HCT-116 CRC cells. Our studies demonstrate that Kaiso binds and represses the *HIF1A* promoter in a methylation-dependent manner. Furthermore, Kaiso depletion results in increased expression of HIF-1α transcripts and protein. Kaiso's regulation of *HIF1A* expression occurs primarily during hypoxia, suggesting that Kaiso functions to fine-tune *HIF1A* expression during the hypoxic response (Chapter 6).

Collectively, these studies expand the repertoire of tumour-associated genes that are regulated by Kaiso in a methylation-dependent manner and provide insight into Kaiso's function at the molecular level.

1.5 Physiological roles for Kaiso in vertebrate development and tumorigenesis

1.5.1. Kaiso's role in development is organism-specific

Since the discovery of the first POZ-ZF proteins in *Drosophila*, several vertebrate POZ-ZF proteins have been cloned and characterized, and many are linked directly or indirectly to developmental and/or tumorigenic processes (Kelly and Daniel 2006). Like

most POZ-ZF proteins, Kaiso has also been implicated in vertebrate development; however, its function appears to be organism and/or tissue specific.

Most studies investigating Kaiso's role in development have been performed in *Xenopus laevis* embryos. Morpholino-mediated depletion of *xKaiso* resulted in defective mesodermal involution and incomplete blastopore closure. Consequently embryos transitioning into neurulation often exhibited exposed endoderm and incomplete axis formation and neural fold closure (Kim *et al.* 2004). Examination of cell behavior during gastrulation revealed that *xKaiso* depletion resulted in decreased convergent extension movements, which were attributed to increased expression of the non-canonical Wnt ligand *xWnt11* (Kim *et al.* 2004). Indeed, xKaiso bound to the *xWnt11* promoter and expression of dominant-negative *xWnt11* rescued gastrulation defects resulting from Kaiso depletion (Kim *et al.* 2004). In a subsequent study, a more widespread function for Kaiso in *Xenopus* development was proposed; *xKaiso* depletion triggered the premature activation of zygotic transcription suggesting that *xKaiso* is a genome-wide transcriptional repressor that is essential for appropriate onset of the mid-blastula transition (Ruzov *et al.* 2004). In addition to the gastrulation defects that were previously reported by Kim *et al.* (2004), Ruzov *et al.* (2004) observed developmental arrest and severe apoptosis in 90% of neurula-stage *xKaiso* depleted embryos. It was subsequently found that *xKaiso* depletion induces p53-mediated apoptosis (Ruzov *et al.* 2009).

Several lines of evidence gleaned from studies in *Xenopus* embryos have also hinted at a role for Kaiso as a negative regulator of the canonical Wnt signaling pathway (Park *et al.* 2005; Iioka *et al.* 2009; Ruzov *et al.* 2009). Indeed, Kaiso represses several

Wnt signaling targets including *siamois*, *c-Myc*, *c-Fos* and *cyclinD1* (Park *et al.* 2005) and consequently, Kaiso is able to rescue the double axis phenotype induced by constitutive Wnt signaling (Park *et al.* 2005). These early studies led to the hypothesis that the Kaiso-p120^{ctn} signaling trajectory converged on the canonical Wnt signaling pathway (Daniel 2007). However, deciphering Kaiso's role in regulating canonical Wnt signaling in *Xenopus* development has been complicated by a study that implicated Kaiso as a bimodal regulator of Wnt signaling (Iioka *et al.* 2009). In this study, both Kaiso depletion and overexpression inhibited Wnt signaling, while mild ectopic Kaiso expression potentiated Wnt signaling (Iioka *et al.* 2009). Kaiso's role as a negative regulator of Wnt signaling in *Xenopus* was solidified by a 2009 study that proposed a molecular mechanism for the interaction of xKaiso with xTcf3 (Ruzov *et al.* 2009). Ruzov *et al.* demonstrated that xKaiso interacted directly with xTcf3, leading to its dissociation from the promoters of Wnt target genes (Ruzov *et al.* 2009). Together these findings suggested that Kaiso may regulate canonical Wnt signaling by multiple mechanisms and indeed this idea is supported by another study that demonstrated that Kaiso binds a methylated region of the β -catenin promoter and represses β-catenin expression (Liu *et al.* 2014)

While most functional studies implicating Kaiso as a modulator of canonical Wnt signaling have been performed in the *Xenopus* model system, several studies utilizing cultured mammalian cells suggest that Kaiso may also regulate Wnt signaling in mammalian model systems. Our lab and others have reported that Kaiso represses a subset of Wnt target genes (*cyclinD1*, *MMP7*) in mammalian cultured cells (Spring *et al.*

2005; Donaldson *et al.* 2012; Jiang *et al.* 2012). Interestingly, activation of the Wnt signaling pathway was shown to inhibit Kaiso's repressive effects on Wnt target genes (Del Valle-Perez *et al.* 2011). Specifically, CK1ε phosphorylates $p120^{ctn}$ in response to Wnt stimulation, which promotes $p120^{ctn}$'s association with Kaiso. Since Kaiso's association with $p120^{ctn}$ is mutually exclusive from its association with TCF4, $p120^{ctn}$ binding to Kaiso causes Kaiso to disengage from TCF4 (Del Valle-Perez *et al.* 2011).

The aforementioned studies describing Kaiso's function in *Xenopus* development provided the rationale for subsequent studies examining the role of Kaiso in the context of other model organisms. Surprisingly, in contrast to the gross morphological defects seen in *xKaiso* depleted *Xenopus* embryos, Kaiso deficient mice exhibit no overt developmental phenotypes (Prokhortchouk *et al.* 2006). This, in part, may be attributed to the existence in mice of the Kaiso-like protein ZBTB4 for which there is no *Xenopus* homologue (Filion *et al.* 2006). ZBTB4 recognizes and binds methylated DNA and the KBS *in vitro*; thus, it is possible that it may function redundantly with Kaiso (Filion *et al.* 2006).

1.5.2. Roles for Kaiso in cancer

Using *in vitro* cell culture models, several studies have demonstrated roles for Kaiso in breast, lung, prostate and colorectal cancer (Lopes *et al.* 2008; Jiang *et al.* 2012; Jones *et al.* 2012; Jones *et al.* 2014). Furthermore, multiple studies have correlated Kaiso expression with malignant progression in prostate, breast and lung cancer tissues (Dai *et al.* 2009; Dai *et al.* 2010; Zhang *et al.* 2011; Jones *et al.* 2012; Vermeulen *et al.* 2012; Jones *et al.* 2014). In non-small cell lung cancer tissues, Kaiso expression was primarily

localized to the cytoplasm and positively correlated with advanced stage, poorer survival and metastatic progression. Two independent groups have examined Kaiso expression and localization in large cohorts of normal and tumour breast tissues (Vermeulen *et al.* 2012; Jones *et al.* 2014). In one study, nuclear Kaiso expression was positively correlated with advanced histological grade and the invasive basal/triple-negative breast cancer subtypes in a cohort of 477 invasive breast cancer patients (Vermeulen *et al.* 2012). In support of these findings, nuclear Kaiso was positively correlated with local invasion, lymph node metastases and overall poorer survival in a cohort of 100 patients with invasive ductal carcinoma (Jones *et al.* 2014). Nuclear Kaiso expression in prostate cancer tissues also positively correlates with increasing tumour grade and intense nuclear staining for Kaiso was observed in prostate cancer metastases (Jones *et al.* 2012). Collectively, these studies imply that Kaiso expression correlates with increased tumour aggressiveness.

Notwithstanding the importance of the aforementioned *in vitro* and correlational studies, these studies lack functional, *in vivo* evidence to support a role for Kaiso in tumorigenesis. The first study to examine the role of Kaiso in tumorigenesis using an *in vivo* model was conducted in 2005, when Prokhortchouk *et al.* examined the effect of Kaiso depletion on polyp formation in the $Apc^{Min/+}$ model of intestinal cancer (Prokhortchouk *et al.* 2006). Kaiso deficient $Apc^{Min/+}$ mice exhibited longer lifespan, delayed tumour onset and smaller tumours compared to their $Apc^{Min/+}$ counterparts suggesting that Kaiso functions in a pro-tumorigenic capacity in intestinal cancer (Prokhortchouk *et al.* 2006). This finding was surprising, given that tumorigenesis in this

model is driven by aberrant activation of the Wnt pathway and prior studies had characterized Kaiso as a repressor of canonical Wnt signaling (Park *et al.* 2005; Ruzov *et al.* 2009).

Notably, Kaiso's role in potentiating $Apc^{Min/+}$-mediated tumorigenesis may be independent of the Wnt signaling pathway, since Kaiso was found to bind to meCpG dinucleotides in the promoter regions of the *CDKN2A*, *HIC1*, and *MGMT* tumour suppressor genes in colon cancer cell lines resulting in silencing of these genes (Lopes *et al.* 2008). Furthermore, Kaiso depletion sensitized CRC cell lines to chemotherapy, proposing an alternate mechanism by which Kaiso may potentiate CRC.

As a first step towards clarifying Kaiso's role in modulating Wnt signaling and intestinal tumorigenesis, we generated and characterized a Kaiso transgenic ($Kaiso^{Tg/+}$) mouse expressing an N-terminal myc-tagged murine Kaiso transgene under the control of the intestinal-specific *villin* promoter. **Chapter 3 consists of the study describing the characterization of phenotypes resulting from intestinal-specific ectopic Kaiso expression.** To examine the role of Kaiso in Wnt signaling in the intestine and to determine the mechanism by which Kaiso induces intestinal tumorigenesis, we crossed our Kaiso transgenic mice with $Apc^{Min/+}$ mice. **The characterization of these phenotypes in $Kaiso^{Tg/+}$:$Apc^{Min/+}$ mice is outlined in Chapter 4.**

1.6. Summary of Intent

The multifunctional Armadillo catenins have emerged as important mediators of cell-adhesion and signal transduction. β-catenin, the most studied member of this family is the

key effector molecule of the canonical Wnt signaling pathway that is essential in maintaining intestinal homeostasis. While $p120^{ctn}$ has not been definitively linked to any specific signaling pathways, increasing evidence has implicated $p120^{ctn}$ and its binding partner Kaiso in canonical Wnt signaling in *Xenopus* and murine models (Park *et al.* 2005; Prokhortchouk *et al.* 2006; Iioka *et al.* 2009; Hong *et al.* 2010). To reiterate, in *Xenopus*, Kaiso is essential for embryonic development and Kaiso rescues the duplicate-axis phenotype caused by constitutive Wnt signaling (Ruzov *et al.* 2004; Park *et al.* 2005). In contrast, Kaiso depletion in a murine model had no deleterious effects on development, but Kaiso depletion resulted in delayed polyp onset and prolonged lifespan in $Apc^{Min/+}$ mice, suggesting that Kaiso may not inhibit Wnt signaling in the context of the murine intestine (Prokhortchouk *et al.* 2006). **We hypothesized that Kaiso drives intestinal tumorigenesis by a mechanism independent of its role in regulating Wnt signaling.**

To clarify and elucidate Kaiso's role in mammalian Wnt signaling and intestinal tumorigenesis we opted to use the well-characterized $Apc^{Min/+}$ mouse model, in which a mutation of the *Apc* gene results in constitutive activation of the Wnt signaling pathway. The objectives of this thesis were to: (**i) generate and characterize a Kaiso transgenic mouse (*Kaiso*$^{Tg/+}$) harbouring a myc-tagged murine Kaiso transgene under the control of the intestinal-specific *villin* promoter and (ii) cross *Kaiso*$^{Tg/+}$ mice with *Apc*$^{Min/+}$ mice to examine Kaiso's effect on Wnt-mediated intestinal tumorigenesis.**

I assisted in the generation and characterization of the $Kaiso^{Tg/+}$ mice, which exhibited intestinal inflammation and crypt hyperplasia accompanied by an increased abundance of secretory cell populations in the small intestine. Surprisingly, the small

intestines of *Kaiso*$^{Tg/+}$ mice also exhibited histological features consistent with chronic intestinal inflammation **(Chapter 3)**. Next, I generated and characterized *Kaiso*$^{Tg/+}$*:Apc*$^{Min/+}$ mice, which exhibited increased numbers of intestinal polyps, enhanced Wnt signaling in the intestine and significantly reduced lifespans compared to their *Apc*$^{Min/+}$ counterparts. Interestingly, the presence of the Min allele resulted in an accelerated onset of inflammation compared to *Kaiso*$^{Tg/+}$ mice **(Chapter 4).**

This thesis also describes studies examining Kaiso's function in methylation-dependent versus sequence-specific binding and repression of the *CCND1* gene which encodes cyclin D1. Kaiso has been characterized as a dual-specificity DNA binding transcription factor and we demonstrated that Kaiso binds the *CCND1* promoter in both a sequence-specific and methylation-dependent manner. We propose that Kaiso may simultaneously utilize both modes of DNA binding to regulate the expression of a given target gene **(Chapter 5)**.

Lastly, I examined Kaiso's role in methylation-dependent repression of the *HIF1A* gene. Kaiso bound to the *HIF1A* promoter and Kaiso depletion resulted in increased *HIF1A* transcript and protein expression. Kaiso's regulation of the *HIF1A* locus was methylation-dependent, since treatment of cells with 5-aza-dC abolished Kaiso's ability to bind to the *HIF1A* promoter and repress *HIF1A* expression. Intriguingly, Kaiso's regulation of the *HIF1A* promoter occurred primarily in hypoxia, which may be attributed to the finding that Kaiso protein is stabilized during hypoxia **(Chapter 6)**.

In summary, this thesis confirms that Kaiso overexpression promotes intestinal tumorigenesis and enhances our understanding of Kaiso's function in this process. We

also identified and characterized a novel Kaiso target gene, *HIF1A*, and gained insight into the mechanism via which Kaiso binds and regulates the cell cycle regulator *CCND1* whose misexpression is a key contributor to many human cancers. Combined, these findings expand our understanding of the increasingly diverse roles of Kaiso in mediating tumour-related processes.

CHAPTER 2

MATERIALS & METHODS

Mouse husbandry and mating

All mouse work was performed with the approval of the McMaster Animal Research Ethics Board (AREB) under Animal Utilization Protocol (AUP) #10-05-32. All mating was performed in a clean, vented-rack room at the McMaster University Central Animal Facility (CAF), Hamilton, ON. *Kaiso*$^{Tg/+}$ females were mated with *Apc*$^{Min/+}$ males (The Jackson Laboratory) to generate *Kaiso*$^{Tg/+}$*:Apc*$^{Min/+}$ mice. *Axin2*^{lacZ}*:Kaiso*$^{Tg/+}$ mice were generated by crossing *Axin2*^{lacZ} females with *Kaiso*$^{Tg/+}$ males. Pregnant females were fed a standard chow diet supplemented with transgenic dough once a week. 21 day-old pups were transferred to a Specific Pathogen Free (SPF) facility and fed a standard chow diet. For *Kaiso*$^{Tg/+}$*:Apc*$^{Min/+}$ and *Apc*$^{Min/+}$ mice, health monitoring was conducted daily and mice were weighed every 3 days until they exhibited signs of the experimental endpoint, which was defined as the point at which animals lost at least 15% of body weight and exhibited two or more of the following symptoms: poor body condition, profuse rectal bleeding, slow movement, pale extremities. All animals were euthanized by CO_2 asphyxiation, followed by cervical dislocation.

Mouse tissue harvest

Following euthanasia, spleen, liver, small intestine and large intestine tissues were immediately harvested. Intestinal tissues were flushed with cold 1xPBS, dissected longitudinally and either flash frozen or fixed in **p**hosphate-**b**uffered **f**ormalin (PBF) for

48 hours at room temperature. Spleen and liver tissues were rinsed in cold 1x PBS and fixed in PBF for 48 hours at room temperature. Tissues harvested for histological and immunohistochemistry (IHC) analyses were sectioned into 3 equal sections and rolled into "Swiss rolls" before fixation. Fixed tissues were paraffin-embedded, sectioned into 5 μm slices and mounted onto slides at the John Mayberry Histology Facility at McMaster University. Hematoxylin and eosin (H&E) stains were also performed by the John Mayberry Histology Facility.

Polyp measurements

Fixed intestinal tissues were stained for 30 seconds in a 0.05% methylene blue solution at room temperature. Tissues were washed repeatedly in 1xPBS until polyps became easily distinguishable from surrounding intestinal tissue. Polyps in stained intestinal sections were counted and polyp area (mm^2) was measured using ImageJ software. A students' T-test was performed to assess the statistical significance of any differences observed.

Immunohistochemistry

Paraffin was removed from tissue slides by incubating in xylenes at room temperature 3 times for 10 minutes before rehydration in an ethanol gradient. Tissue was permeabilized with TBS with 0.05% Tween-20 (TBS-T), and antigen retrieval was accomplished by boiling slides in a 10 mM sodium citrate solution (pH 6.0). Endogenous peroxidase was quenched with 3% hydrogen peroxide in TBS, after which tissues were incubated in a basal blocking solution consisting of 5% normal serum, 10% BSA in TBS-T, supplemented with avidin (Vector Labs) for 1 hour at room temperature. Primary antibodies were diluted in basal blocking solution supplemented with biotin (Vector

Labs). Tissues were incubated with primary antibodies at the following dilutions overnight at 4°C: rabbit anti-Kaiso pAb (1:1000), rat anti-MMP-7 mAb (Vanderbilt Antibody Resource) (1:200) and rabbit anti-cleaved caspase-3 mAb (Asp 175) (Cell Signaling, 1:200). BSA was excluded from the blocking solution for Ki67 staining, which was performed using rabbit anti-Ki67 mAb (Spring Biosciences) at a 1:150 dilution for 2 hours at room temperature. Tissues were washed 3 times for 2 minutes in TBS-T, once in TBS, and then incubated in biotinylated donkey anti-rabbit antibody at a 1:1000 dilution for 2 hours at room temperature. Slides were washed as before, and incubated for 30 minutes in an Elite ABC avidin-biotin horseradish peroxidase complex (Vector Labs). After a 3-minute wash in TBS, tissues were incubated in Vectastain DAB substrate (Vector Labs) for 3 minutes or until satisfactory colour development was achieved. Tissues were counterstained with Harris hematoxylin (Sigma), differentiated in acid ethanol (0.3% HCl in 70% ethanol), blued in Scott's tap water substitute, and dehydrated in an ethanol gradient. Tissues were dried by incubating in xylenes twice for 5 minutes and mounted in PolyMount (Polysciences Inc). CRC tissue microarrays were purchased from US Biomax (Catalogue #: CO951 and BC05115) and stained and scored for Kaiso as previously described (Jones *et al.* 2012). Briefly, tissues were assigned a score based on the intensity of Kaiso staining on a scale of 0 to +4.9, with 0 representing no staining and +4.9 representing intense staining. The percentage of cells at each staining intensity was estimated for each tissue section and to enable numeric analysis, the proportion of cells at each intensity was multiplied by that intensity. F4/80 staining for macrophages was conducted by the John Mayberry Histology Facility, McMaster University. All

images were acquired using the Aperio ScanScope and processed using ImageScope software.

β-galactosidase staining

For β-galactosidase staining, "Swiss-rolled" intestines were flash frozen in OCT (Tissue-Tek). Mounted tissues were fixed in 0.2% glutaraldehyde in 1x PBS for 10 minutes at 4°C then washed in detergent solution (0.02% NP-40, 0.01% sodium deoxycholate, 2 mM $MgCl_2$) for 10 minutes at room temperature. Tissues were stained in a 1 mg/mL X-gal solution (Sigma) for 24 hours at 37°C in the dark and washed 3 times in 1xPBS for 2 minutes each. Post-fixation was performed by incubating tissues in 4% paraformaldehyde for 10 minutes. Tissues were counterstained with Nuclear Fast Red (Sigma) for 3 minutes at room temperature and rinsed under running dH_2O for 5 min. Finally, tissues were dehydrated in an ethanol series and cleared with xylenes.

Myeloperoxidase (MPO) Assay

Flash frozen intestinal tissue was homogenized in a volume of HTAB buffer (0.5% hexadecyltrimethylammonium bromide in 50 mM phosphate buffer, pH 6.0) according to the formula V_{HTAB}= mg of tissue/50. Homogenates were cleared by centrifugation at 12,000 rpm for 5 minutes at 4°C. 200 µL of o-dianisidine dihydrochloride solution (16.8 mg/mL o-dianisidine dihydrocholide in 5 mM phosphate buffer, pH 6.0 with 50 µL of 1.2% H_2O_2) was mixed with 7 µL of tissue homogenate and absorbance at 450 nm was measured 3 times at 30 second intervals. The absorbance of each homogenate was measured in triplicate and the absorbances averaged to calculate MPO activity. MPO activity was calculated in units (U), where 1 U represents the amount of MPO required to

degrade 1 μmol of H_2O_2/minute at 25°C, which gives an absorbance of 1.13 X 10-2 nm/min. MPO activity in each sample was determined as the change in absorbance [ΔA(t2-t1)/Δmin]/(1.13 X 10^{-2}). MPO activity/mg of tissue was calculated by dividing MPO activity by 0.35 mg of tissue.

Multiplex Cytokine Assay

Approximately 50 mg of fresh tissue was homogenized in buffer containing 20 mM Tris HCl (pH 7.5), 0.5% Tween 20, 150 mM NaCl and cOmplete Ultratablets (Roche) (1 tablet per 25 mL of buffer). Tissue homogenates were diluted to contain equal amounts of total protein (>400 μg/mL) and sent to Eve Technologies Corporation (Calgary, Alberta) where cytokine content was measured in pg/mL using the Mouse 32-Plex Cytokine Panel. A students' T-test was performed to assess the statistical significance of any differences observed.

Protein Isolation and Immunoblot Analysis

100 mg of flash frozen mouse tissue was minced with a sterile blade and homogenized in 1 mL cold RIPA buffer (1% NP-40, 50 mM Tris, 150 mM NaCl, 0.5% sodium deoxycholate, 1% SDS, 0.5% Na_3VO_4 and cOmplete ULTRA Tablet (1 tablet/5 mL buffer) (Roche)) in a chilled tissue grinder (Kontes). Harvested lysates were poured into chilled microfuge tubes and further homogenized using a 21 gauge syringe. Lysates were incubated on ice for 30 minutes, followed by centrifugation at 13,000 rpm for 10 minutes at 4°C. The supernatants were transferred to new pre-chilled microfuge tubes.

Cultured cells were washed twice with 5 mL 1xPBS and incubated on ice for 10 minutes with 450 μL lysis buffer (0.5% NP-40, 50 mM Tris, 150 mM NaCl, 0.5%

Na_3VO_4 and Complete Mini Protease Inhibitor Cocktail Tablets (1 tablet/10 mL buffer) (Roche). Harvested lysates were transferred to pre-chilled microfuge tubes and centrifuged at 14,000 rpm for 5 minutes at 4°C. The supernatants were transferred to fresh pre-chilled microfuge tubes.

Total protein content was quantified in a Bradford assay. Volumes of supernatant representing at least 10 μg total protein were resuspended in Laemmli sample buffer, boiled for 5 minutes and subjected to electrophoresis in an SDS polyacrylamide gel. Proteins were transferred to a nitrocellulose membrane using a Hoeffer semi-dry transfer apparatus (Amersham Biosciences). To prevent non-specific antibody binding, the membranes were blocked with 3% skimmed milk/TBS (pH 7.4) and incubated at 4 °C overnight with primary antibodies diluted in 3% milk/TBS. For immunoblot analysis of mouse tissue homogenates featured in Chapters 3 and 4 the following antibodies were used: rabbit anti-Kaiso pAb (1:5,000), rabbit anti-Cyclin D1 pAb (US Biologicals, 1:5,000) and mouse anti-β-actin mAb (Sigma-Aldrich 1:30,000). For immunoblot analysis of whole cell lysates featured in Chapter 6, the following antibodies were used: rabbit anti-Kaiso pAb (1:10,000), mouse anti-HIF-1α mAb (BD Biosciences, 1:500), rabbit anti- PDK-1 mAb (ENZO Life Sciences, 1:1,000) and mouse anti-β-tubulin mAb (Sigma-Aldrich, 1:100,000). The membranes were washed 5 times for 5 minutes each with TBS and incubated at room temperature with HRP-conjugated donkey anti-mouse or goat anti-rabbit secondary antibody both at a dilution of 1:40,000 in 3% milk/TBS. Membranes were washed as previously described and processed with Enhanced Chemiluminescence (Amersham Biosciences) according to the manufacturer's protocol.

Cell culture

The HCT-116, MCF-7 and MDA-231 cells were purchased from ATCC. All cell lines were cultured in DMEM supplemented with 1% penicillin/streptomycin, 0.4% fungizone and 10% fetal bovine serum. All cells were cultured in a 5% CO_2, humidified incubator at 37°C. For hypoxia treatment, cells were incubated in a 5% CO_2, 1% O_2, humidified incubator at 37°C unless otherwise stated. For 5-aza-dC treatment, cells were treated daily with 10 μM 5-aza-dC (Sigma) in culture medium for at least 3 consecutive days before further analyses were performed. The Kaiso-depleted and control HCT-116 and MDA-MB-231 cell lines were generated by transfecting wild type cells with a retroviral vector containing a Kaiso-specific shRNA sequence (pRS-Kaiso), a retroviral vector containing a Kaiso-scrambled shRNA sequence (pRS-Kaiso scrambled) (control) and an empty retroviral vector (pRS-empty) (control) respectively. Stable pRS-Kaiso, pRS-Kaiso scrambled and pRS-empty cells were selected by culturing MDA-MB-231 cells in 0.8 μg/mL puromycin and HCT-116 cells in 2 μg/mL puromycin. The most efficient Kaiso-depleted clones were used for further analysis.

RNA isolation and microarray analysis

Stable HCT-116 pRS-Kaiso and HCT-116 control cells were suspended in culture medium and counted using the TC10 automated cell counter (Bio-Rad) according to the manufacturer's instructions. $3x10^6$ cells were centrifuged at 300g for 10 minutes at 4°C. The media was removed and the cells were washed by resuspending in 5 mL of 1x PBS, followed by centrifugation at 300g for 10 minutes at 4°C. RNA was extracted from the cell pellet using the RNeasy Mini Kit (Qiagen) according to the manufacturer's protocol.

Biological triplicates of RNA for both Kaiso-depleted and control cell lines were used for microarray analysis at the University Health Network Microarray Center (Toronto, Ontario) using Agilent's SurePrint G3 Human Exon 2x400K microarray.

Probes indicating significantly different relative transcript abundance between Kaiso-depleted and control cells were determined by Analysis of Variance (ANOVA) using MEV in the TM4 suite of microarray software (Saeed *et al.* 2003; Saeed *et al.* 2006). Data were first log transformed and values for each probe median centered. ANOVA was performed with a distribution based on 1000 permutations of the data, a significance value of $p<0.05$, and control of False Discovery Rate (FDR) at 5% (Benjamini *et al.* 2001).

Network analysis

Network analysis was implemented using the Cytoscape Reactome FI plug-in. Briefly, up-regulated genes (Fold change > 1.5, FDR<0.05) were mapped to unigene ID and subsequently mapped as nodes in Reactome (Wu *et al.* 2010). Nodes were subsequently clustered into network modules using Markov Clustering. This process identified 8 modules comprising at least 3 nodes.

Gene set enrichment analysis (GSEA)

GSEA was performed using gene expression profiles from control and Kaiso–depleted HCT-116 cells (described above), as previously described (Subramanian *et al.* 2005). Gene set permutation was used to estimate FDR.

Analysis of human tumour cohorts

All data was publicly available and downloaded from the gene expression omnibus (http://www.ncbi.nlm.nih.gov/geo/). The raw intensity files (.CEL) comprising each dataset were downloaded and normalized using the Robust Multichip Algorithm (RMA) to generate probe set intensities (Irizarry *et al.* 2003). The GSE41258 cohort was used for the analysis featured in Chapter 4 (n=123 primary colon cancer and n=25 normal patients). The GSE2034 (n=286) breast and GSE14333 (n=290) colon tumour cohorts were used for the analysis featured in Chapter 6. Briefly, probe sets were mapped to unigene IDs and in instances where multiple probes mapped to the same gene IDs only the probe set with the highest average expression was used. Pearson correlation was calculated between *Kaiso* and *HIF1A* expression within each cohort across all patients in Chapter 6.

Electrophoretic mobility shift assay

For the EMSA experiments in Chapter 5, double-stranded oligonucleotides (oligos) were created to span the +69 core KBS site of the *CCND1* promoter. Five mutated versions of the +69 oligo were generated to test the necessity of the core KBS and the various CpG dinucleotides for Kaiso binding. The oligos utilized in Chapter 5 are depicted in Table 2.1. For the EMSAs in Chapter 6, oligos were created to span the 3 KBS sites as well as a CpG rich region located in the *HIF1A* promoter (Table 2.2). A panel of GST-Kaiso fusion proteins were used to test Kaiso's binding to these DNA sites: KaisoΔPOZΔZF, which lacks both the POZ and ZF domains and serves as a negative control; KaisoΔPOZ, which lacks the POZ domain but possesses the ZF DNA-binding domain; KaisoZF, which consists of the ZF DNA-binding domain only. These GST fusion proteins were

bacterially expressed from the pGEX-5X-1 vector (Amersham) and the pGEX-5X-1 constructs expressing these proteins were generated by Abena Otchere.

Oligos were methylated by bacterial *SssI* CpG methyltransferase using the methyl donor S-adenosylmethionine (New England Biolabs). 500 ng of each oligo was incubated with 200U of *SssI* methyltransferase in a 250 µL reaction that contained 640 µM S-adenosyl methionine and 1xNEB buffer. The reactions were incubated at 37°C for 2 hours, after which the enzyme was inactivated at 65°C for 20 minutes. The methylated DNA samples were purified by standard phenol-chloroform extraction and ethanol precipitation.

The methylated and unmethylated oligos were radiolabelled in a reaction containing 1 µL [γ-^{32}P]-ATP, 1 µL polynucleotide kinase (PNK) and 1 µL PNK buffer in a 10 µL final volume reaction for 45 minutes at 37°C. The reaction was stopped with 25 mM EDTA and labeled probes were purified on a Chromaspin TE-10 column (Clontech). Labeled probes (50,000 c.p.m) were incubated with 200-400ng of GST-Kaiso fusion protein in a binding reaction (5 µL binding buffer, 5 µg BSA, 4.8% glycerol and 3 µg Poly dIdC) for 30 minutes on ice and then for 25 minutes at room temperature. The samples were run on a 4% acrylamide gel at 200V for 2 ½ hours after which the gel was dried at 80°C for 1 ½ hours before being exposed to XAR film at -80°C.

Chromatin Immunoprecipitation

Cells were grown to approximately 80% confluency at which time culture medium was aspirated and cells were washed twice with cold 1xPBS. 37% formaldehyde was diluted in serum-free DMEM (1.42% final concentration) and added to cells for 10 minutes at

room temperature with rocking in order to crosslink protein-DNA containing complexes. Cells were washed twice with cold 1xPBS and formaldehyde was quenched with 125 mM glycine for 5 minutes at room temperature. Cells were harvested from plates and centrifuged at 3,400 rpm for 5 minutes at 4°C. Cells were resuspended in 2 mL cell lysis buffer (5 mM PIPES pH 8.0, 85 mM KCl, 0.5% NP-40 and Complete Mini Protease Inhibitor Cocktail Tablets (1 tablet/10 mL buffer) (Roche)), dounced ten times and incubated on ice for 10 minutes. Lysed cells were centrifuged at 5,000 rpm for 5 minutes at 4°C, after which the nuclear pellets were resuspended in 250 µL nuclear lysis buffer (50 mM Tris-Cl pH 8.1, 10 mM EDTA, 1% SDS and Complete Mini Protease Inhibitor Cocktail Tablets (1 tablet/10 mL buffer) (Roche)) and incubated on ice for 10 minutes. The nuclear lysates were sonicated on ice for 5 rounds of 15 pulses each at 5% maximum power output and 90% duty cycle then centrifuged at 14,000 rpm for 10 minutes at 4°C to clear lysates. Lysates were pre-cleared using rabbit IgG (Abcam) and salmon sperm-blocked 50% Protein A Sepharose beads/lysis buffer (150 mM NaCl, 25 mM Tris pH 7.5, 5 mM EDTA, 1% Triton-X 100, 0.1% SDS and 0.5% deoxycholate).

At least 15 µg of sheared chromatin were incubated at 4°C overnight with 8 µg anti-Kaiso mouse monoclonal antibody, 4 µg Histone H3 rabbit polyclonal antibody (Abcam) and 4 µg mouse monoclonal negative control IgG antibody (Active Motif). The antibody-protein-DNA complexes were immunoprecipitated with 50 µL of 50% Protein A Sepharose beads/lysis buffer for 1 hour at 4°C. The beads were washed once with RIPA buffer (50 mM Tris pH 8.0, 150 mM NaCl, 0.1% SDS, 0.5% deoxycholate, 1% NP-40 and 1 mM EDTA) for 10 minutes, once with high salt buffer (50 mM Tris pH 8.0, 500

TABLE 2.1: Wild type and mutated oligos utilized in Chapter 5 spanning +69 KBS and proximal CpG dinucleotides in the *CCND1* promoter. (KBS red; CpG dinucleotides bolded; mutated sites underlined).

Oligo	Sense Strand Sequence (5'-3')
WT KBS	CTGT**CG**G**CG**CAGTAGCAG**CG**AGCAGCAGAG
KBS MUT	CTGT**CG**G**CG**CAGTAAAAT**CG**AGCAGCAGAG
CMUT1	CTGT**CG**G**CG**CAGTAGCAG**GG**AGCAGCAGAG
CMUT2	CTGT**GG**G**GG**CAGTAGCAG**CG**AGCAGCAGAG
CMUT3	CTGT**GG**G**GG**CAGTAGCAG**GG**AGCAGCAGAG
ALLMUT	CTGT**GG**G**GG**CAGTAAAAT**CG**AGCAGCAGAG

TABLE 2.2: Oligos utilized in Chapter 6 representing different potential binding sites for Kaiso in the *HIF1A* promoter (KBS red; CpG dinucleotides bolded; HRE in blue).

Oligo	*HIF1A* Promoter Region	Sense Strand Sequence (5'-3')
KBS-1	-690 to -655	GATTTTAAGATTTCCCTGCAACTTTATTTCCCTTGA
KBS-2	-455 to -417	GAAGGGCTTGCTGCCA**CG**AGG**CG**AAGTCTGCTTTTTTGAA
KBS-3	-162 to -127	A**CG**AGCA**CG**TGAG**CG**TCGCAGCC**CG**TCCCAGCTGTG
CpG	+45 to +80	CTCCCCTCCC**CGCGCG**CC**CG**AG**CGCG**CCTC**CG**CCCT

mM NaCl, 0.1% SDS, 0.5% deoxycholate, 1% NP-40 and 1 mM EDTA) for 10 minutes, once with lithium chloride wash (50 mM Tris pH 8.0, 1 mM EDTA, 250 mM LiCl, 1% NP-40 and 0.5% deoxycholate) for 5 minutes, and twice with TE buffer pH 8.0 (10 mM Tris, 1 mM EDTA) for 10 minutes each. Following treatment with RNase A (50 µg/mL) and proteinase K (250 µg/mL), crosslinks were reversed by incubating samples at 65°C overnight. Samples were subjected to 3 rounds of phenol chloroform extraction after which chromatin was precipitated by ethanol-salt precipitation.

For the ChIP experiments in Chapter 5, the recovered chromatin was suspended in RNase/DNase-free water, and then 2µL of recovered DNA was subjected to endpoint PCR. The PCR reaction contained 1X PCR buffer, 1.5 mM $MgCl_2$, 0.3 mM dNTPs, 0.4 mM forward and reverse primers, 0.5 µl of Taq polymerase (Life Technologies), and sterile water to a final volume of 25 µl. After completion of the PCR reaction, 10 µL of each reaction were loaded onto a 1.2% agarose gel with 0.5 µg/ml EtBr and electrophoresed at 120 V for 25 minutes in 1xTAE. Gels were imaged using an SRX-101A Medical Film Processor (Konica Minolta Medical Graphics Inc.). Primer sequences utilized in Chapter 5 along with their annealing temperatures are listed in Table 2.3.

For the ChIP experiments in Chapter 6, 5 µL of resuspended chromatin was subjected to qPCR using the PerfeCta SYBR Green SuperMix, ROX (Quanta BioSciences). Each reaction was performed in triplicate using the Applied BioSystems Prism 7900HT sequence detection system. Results were normalized to the IgG negative control and analyzed using the fold enrichment method. Sequences of primers utilized in Chapter 6 along with their annealing temperatures are listed in Table 2.4.

TABLE 2.3: *CCND1* promoter ChIP primer sequences and their respective annealing temperatures (utilized in Chapter 5).

Primer	Annealing Temperature (°C)	Sequence (5'-3')	
-1067 KBS	50.0	Fwd	TTTACATCTGCTTAAGTTTGCG
		Rvs	TTAGAATTTGCCCTGGGACT
+69 KBS	53.0	Fwd	CACACGGACTACAGGGGAGTT
		Rvs	CTCGGCTCTCGCTTCTGCTG
CpG5	53.6	Fwd	TTTGCATTTCTATGAAAACCGG
		Rvs	GCAACTTCAACAAAACTCCC
CpG8	58.0	Fwd	ACACGGACTACAGGGGAGTTTTG
		Rvs	ATTTCGAACCCCTGGGGAGG
Negative	58.0	Fwd	CCCTCGGTGTCCTACTTCAA
		Rvs	CACCACGGCAAACTTCAAAG

TABLE 2.4: *HIF1A* promoter ChIP primer sequences and their respective annealing temperatures (utilized in Chapter 6).

Primer	Annealing Temperature (°C)	Sequence (5'-3')	
KBS-3	60.0	Fwd	GGAGAAGGCGCAGAGTCC
		Rvs	AGGCGGGTTCCTCGAGAT
Negative	60.0	Fwd	AAGGGTCAATGGGGTCATTT
		Rvs	GGCACCAAATAGTATCCCCTAA

Luciferase assays

A portion of the *CCND1* promoter region (-1748 to +164) was PCR amplified and sub-cloned into the *Kpn1* and *BamH1* sites of the pGLuc (Gaussia luciferase) reporter vector (New England Biolabs). This *CCND1* promoter-luciferase construct was designated as the -1748*CD1* wild type reporter. Site-directed mutagenesis was used to mutate the KBS sequences located at positions -1067 (designated 1) and +69 (designated 2). The mutations were confirmed by sequencing and the resulting plasmid designated -1748*CD1* KBS (1, 2) mutant. Nickett Donaldson generated both the wild type and mutant -1748*CD1* plasmids, which were utilized for the luciferase experiments in Chapter 5. The plasmids were purified from $dam^{-/}dcm^{-}$ bacteria and then utilized as is or methylated as described for EMSA oligos prior to use in luciferase assays.

2.5×10^5 MCF-7 cells were seeded into 6-well dishes and transfected a minimum of 12 hours later with 0.6 μg of methylated or unmethylated luciferase plasmid (pGLuc-Basic, pGLuc-Basic wild type −1748*CD1* or pGLuc-Basic −1748*CD1* KBS (1,2) mutant), 0.5 μg of pRSV/β-galactosidase internal control and various amounts of effector plasmids (empty pCDNA3.1, pCDNA3.1-hKaiso-Kozak) and/or shRNA (pRS-Kaiso, pRS-Kaiso-scrambled). Cells were incubated with transfection complexes consisting of the aforementioned plasmids diluted in 150 mM NaCl with 10 equivalents (~17 μl) of ExGen-500 reagent (Fermentas) for 3 hours at 37°C in 5% CO_2. 24 hours post-transfection, 25 μL of the culture medium was assayed for luciferase activity with 50 μL of *Gaussia* luciferase substrate (New England Biolabs) on an LB Luminometer (Thermo Fisher). Luciferase activity was recorded as relative light units (RLU's) and normalized

for transfection efficiency using the internal control β-galactosidase activity for each experimental and control sample condition. Statistical significance was calculated using a one-way ANOVA and Tukey post-hoc test using measurements from at least three independent trials.

A pGLuc-*HIF1A* minimal promoter-luciferase plasmid was created by sub-cloning the region containing putative regulatory sequences spanning 919 bp upstream to 93 bp downstream of the *HIF1A* transcription start site from the pGL3-*HIF1A* vector (Promega) (34) into the EcoRV and HindIII sites of the pGLuc (Gaussia luciferase) reporter vector (New England Biolabs). Nickett Donaldson also generated this pGLuc-*HIF1A* plasmid, which was utilized for the luciferase experiments in Chapter 6.

For *HIF1A* promoter-luciferase assays, HCT-116 cells were seeded at 3.5×10^5 cells/well and MCF-7 cells were seeded at 2.5×10^5 cells/well into 6-well dishes. Reporter plasmids (pGLuc-basic or pGLuc-*HIF1A*), pRSV/β-galactosidase internal control plasmid and effector plasmids were utilized as described for *CCND1* promoter-luciferase assays. The same transfection and assay protocols performed for the *CCND1* promoter-reporter assays were also followed for the *HIF1A*-promoter luciferase assays.

Quantitative reverse transcription-PCR

For the qRT-PCR analysis in Chapter 4 total RNA was isolated from flash frozen tissues using the NucleoSpin RNA kit (Macherey-Nagel) according to the manufacturer's protocol. For the qRT-PCR analysis in Chapter 6, total RNA was isolated from cells at approximately 70% confluency using the RNeasy Mini Kit (Qiagen) according to the manufacturer's protocol. 1 μg of RNA from each sample was treated with DNase I

(Invitrogen) and reverse transcribed using the qScript cDNA SuperMix (Quanta BioSciences) according to the manufacturers' protocols. cDNA was amplified using the PerfeCta SYBR Green SuperMix, ROX (Quanta BioSciences). Each reaction was performed in triplicate using the Applied BioSystems Prism 7900HT sequence detection system. Primer sequences for the targets analyzed in Chapter 4 and their corresponding annealing temperatures are listed in Table 2.5, while those analyzed in Chapter 6 are listed in Table 2.6. The quantity of each target was determined using a standard curve and was normalized to GAPDH expression levels in Chapter 4 and β-actin expression levels in Chapter 6. The standard curve was constructed using 5-fold serial dilutions of cDNA reverse transcribed from a mixture of RNA from each experimental sample. Statistical analyses were conducted using GraphPad Prism software. Statistical significance was calculated using a Student's T test (unpaired, two-tailed) using measurements from at least three independent trials.

TABLE 2.5: Primer sequences used for qRT-PCR analysis in Chapter 4 and their respective annealing temperatures.

Target	Annealing Temperature (°C)	Sequence (5'-3')	
villin-Kaiso	55.0	Fwd	CAACTTCCTAAGATCTCCCAGGT
		Rvs	CAAGGAGTTCAGCAGACTGG
Gapdh	55.0	Fwd	ATGACCACAGTCCATGCCATC
		Rvs	CCTGCTTCACCACCTTCTTG
Axin2	*57.0*	Fwd	TGTGAGATCCACGGAAACAG
		Rvs	CTGCGATGCATCTCTCTCTG
Mmp7	57.0	Fwd	GCGGAGATGCTCACTTTGAC
		Rvs	GCATCTATCACAGCGTGTTC
EphB2	65.2	Fwd	CTGTGGTCGTCATTGCCATC
		Rvs	CATGCCTGGGGTCATGTGT
CD44	56.4	Fwd	AACGAGTGCAACTACAGCCT
		Rvs	CTCCGTACCAGGCATCTTCG
Lect2	61.8	Fwd	CGACTGTCTGGAAGAGGTTTTTG
		Rvs	GGTAAACTTTCTGCAGGGGC

TABLE 2.6: Primer sequences used for qRT-PCR analysis in Chapter 6 and their respective annealing temperatures.

Target	Annealing Temperature (°C)	Sequence (5'-3')	
HIF1A	60.8	Fwd	AGTGTACCCTAACTAGCCGAGGAA
		Rvs	TACCCACACTGAGGTTGGTTACTG
Kaiso	60.8	Fwd	AGAGGAAAGGGCATGGAGAGT
		Rvs	GGCCACGTTGCTCATTCAAG
PDK-1	60.8	Fwd	CGCAGTGCCTCTGGCTGGTTT
		Rvs	GCTGGGGACGCACCAGTCAT
β-actin	55.0	Fwd	CTCTTCCAGCCTTCCTTCCT
		Rvs	AGCACTGTGTTGGCGTACAG

CHAPTER 3

The POZ-ZF Transcription Factor Kaiso (ZBTB33) Induces Inflammation and Progenitor Cell Differentiation in the Murine Intestine

Preface:

This chapter consists of the published article entitled: ***"The POZ-ZF Transcription Factor Kaiso (ZBTB33) Induces Inflammation and Progenitor Cell Differentiation in the Murine Intestine"*** by Chaudhary R, Pierre CC, Nanan K, Wojtal D, Morone S, Pinelli C, Wood GA, Robine S, Daniel JM (PLoS One, 2013, Sep 5;8(9): e74160). This manuscript was reproduced in its original format and is an open-access article distributed under the terms of the Creative Commons Attribution License, which permits unrestricted use, distribution, and reproduction in any medium, provided the original author and source are credited.

This study describes the generation and characterization of an intestinal-specific Kaiso transgenic mouse model that was designed to examine the role of Kaiso in Wnt signaling, intestinal development and tumorigenesis. Kaiso transgenic mice exhibited no deleterious developmental defects, but unexpectedly developed chronic intestinal inflammation. Interestingly, $p120^{ctn}$ accumulates in the nucleus of intestinal epithelial cells expressing the Kaiso transgene and we postulated that the inflammation in this model might result from a loss of $p120^{ctn}$ anti-inflammatory function, although further studies are necessary to verify this hypothesis.

Contributions:

Roopali Chaudhary performed the experiments depicted in Figures 3.2, 3.3, 3.4, 3.5, 3.6A, 3.6B and 3.7. Christina Pierre wrote the manuscript and generated the data for Figures 3.1D, 3.6C and 3.8. Kyster Nanan generated the data for Figures 3.1A, 3.B and 3.C. Daria Wojtal performed the IHC for c-myc expression in Figure 3.2. Dr. Juliet Daniel provided significant intellectual input and guidance throughout the execution of this work and edited the manuscript text. All other authors contributed to the interpretation of data, edited the manuscript text or generated/assisted in the generation of reagents or optimization of experimental protocols for the manuscript.

OPEN ACCESS Freely available online PLOS ONE

The POZ-ZF Transcription Factor Kaiso (ZBTB33) Induces Inflammation and Progenitor Cell Differentiation in the Murine Intestine

Roopali Chaudhary[1☯], Christina C. Pierre[1☯], Kyster Nanan[2], Daria Wojtal[1], Simona Morone[3], Christopher Pinelli[4], Geoffrey A. Wood[4], Sylvie Robine[5], Juliet M. Daniel[1]*

1 Department of Biology, McMaster University, Hamilton, Ontario, Canada, **2** Department of Pathology & Molecular Medicine, Queen's University, Kingston, Ontario, Canada, **3** Department of Medical Sciences, University of Torino, Torino, Italy, **4** Department of Pathobiology, University of Guelph, Guelph, Ontario, Canada, **5** Department of Morphogenesis and Intracellular Signalling, Institut Curie-CNRS, Paris, France

Abstract

Since its discovery, several studies have implicated the POZ-ZF protein Kaiso in both developmental and tumorigenic processes. However, most of the information regarding Kaiso's function to date has been gleaned from studies in *Xenopus laevis* embryos and mammalian cultured cells. To examine Kaiso's role in a relevant, mammalian organ-specific context, we generated and characterized a Kaiso transgenic mouse expressing a murine Kaiso transgene under the control of the intestine-specific *villin* promoter. Kaiso transgenic mice were viable and fertile but pathological examination of the small intestine revealed distinct morphological changes. Kaiso transgenics ($Kaiso^{Tg/+}$) exhibited a crypt expansion phenotype that was accompanied by increased differentiation of epithelial progenitor cells into secretory cell lineages; this was evidenced by increased cell populations expressing Goblet, Paneth and enteroendocrine markers. Paradoxically however, enhanced differentiation in $Kaiso^{Tg/+}$ was accompanied by reduced proliferation, a phenotype reminiscent of Notch inhibition. Indeed, expression of the Notch signalling target HES-1 was decreased in $Kaiso^{Tg/+}$ animals. Finally, our Kaiso transgenics exhibited several hallmarks of inflammation, including increased neutrophil infiltration and activation, villi fusion and crypt hyperplasia. Interestingly, the Kaiso binding partner and emerging anti-inflammatory mediator $p120^{ctn}$ is recruited to the nucleus in $Kaiso^{Tg/+}$ mice intestinal cells suggesting that Kaiso may elicit inflammation by antagonizing $p120^{ctn}$ function.

Citation: Chaudhary R, Pierre CC, Nanan K, Wojtal D, Morone S, et al. (2013) The POZ-ZF Transcription Factor Kaiso (ZBTB33) Induces Inflammation and Progenitor Cell Differentiation in the Murine Intestine. PLoS ONE 8(9): e74160. doi:10.1371/journal.pone.0074160

Editor: Pierre-Antoine Defossez, Université Paris-Diderot, France

Received April 10, 2013; **Accepted** July 26, 2013; **Published** September 5, 2013

Funding: This work was supported by CIHR grant (MOP-84320) to Juliet Daniel. R. Chaudhary was the recipient of an Ontario Graduate Scholarship and C. Pierre was the recipient of a McMaster Prestige Award. The funders had no role in study design, data collection and analysis, decision to publish, or preparation of the manuscript.

Competing Interests: The authors have declared that no competing interests exist.

* E-mail: danielj@mcmaster.ca

☯ These authors contributed equally to this work.

Introduction

Since its discovery as a binding partner for the Src kinase substrate and cell adhesion protein $p120^{ctn}$, mounting evidence suggests that the POZ-ZF transcription factor Kaiso functions in vertebrate development and tumorigenesis [1,2,3,4,5,6,7,8]. To date however, Kaiso's role in these processes in mammalian systems remains unclear, and much controversy surrounds several aspects of Kaiso's function; this includes the mechanism by which it binds DNA [9,10,11,12,13,14,15,16,17] and its function in regulating the canonical Wnt signalling pathway that plays a key role in vertebrate development and tumorigenesis [8,11,14,18,19].

One study investigated the effect of Kaiso depletion on murine development and found that Kaiso null mice exhibited no overt developmental phenotypes [8]. This unexpected lack of a developmental phenotype may be attributed to the existence of two Kaiso-like proteins in mammals, ZBTB4 and ZBTB38, that may function redundantly with Kaiso [16,20], and highlights what may be an important consideration in deciphering Kaiso's role in mammalian systems. Surprisingly however, Kaiso depletion extended the lifespan, and delayed tumour onset in the $Apc^{Min/+}$ model of intestinal tumorigenesis [8]. This observation implicated Kaiso as an oncogene and is consistent with the report that Kaiso binds and represses methylated tumour suppressor and DNA repair genes in colon cancer cells [7]. Given that constitutive Wnt signalling resulting from mutation of *APC* functions as the first "hit" in $Apc^{Min/+}$-mediated tumorigenesis, the *Kaiso*-null/$Apc^{Min/+}$ phenotype suggests that Kaiso is a positive regulator of Wnt signalling. This result is surprising, since Kaiso has been implicated as a negative regulator of canonical Wnt signalling in *Xenopus laevis* embryos and in mammalian cultured cells [19,21,22,23]. However it remains possible that Kaiso may potentiate intestinal tumorigenesis in the $Apc^{Min/+}$ model via a non-Wnt related mechanism.

Consistent with this possibility, studies to elucidate the role of the Kaiso binding partner $p120^{ctn}$ in the intestine hinted at a non-cell autonomous mechanism for $p120^{ctn}$-mediated tumorigenesis [24,25]. Smalley Freed *et al.* found that mice with limited ablation of $p120^{ctn}$ developed adenomas in addition to an intestinal barrier defect and chronic inflammation [25]. Surprisingly, conditional

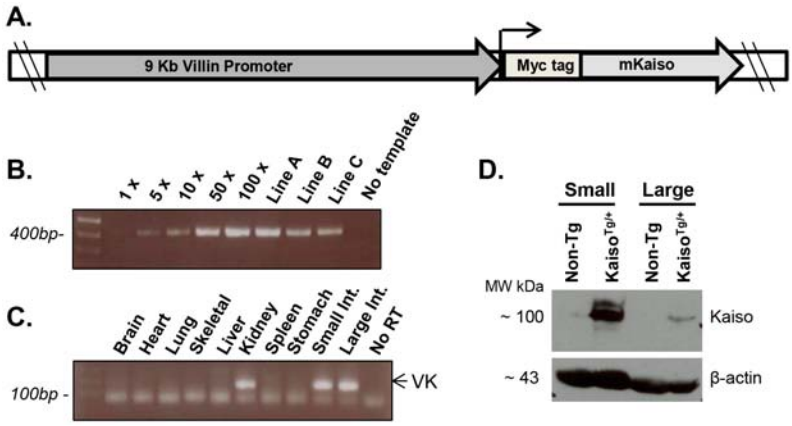

Figure 1. Generation of transgenic mouse lines ectopically expressing *villin*-Kaiso. (**A**) Myc-tagged murine *Kaiso* cDNA was cloned downstream of the 9 kb *villin* promoter sequence. (**B**) The transgene copy number in each transgenic line was evaluated via PCR. Line A transgenic animals have the greatest copy number. (**C**) RT-PCR confirmed expression of the Kaiso transgene in *villin*-expressing tissues of transgenic mice, *i.e.* the small intestine, large intestine, and kidneys. (**D**) Immunoblot analysis shows increased Kaiso expression in both small and large intestines in Kaiso transgenic ($Kaiso^{Tg/+}$) Line A mice compared to non-transgenic (Non-Tg) siblings.
doi:10.1371/journal.pone.0074160.g001

depletion of $p120^{ctn}$ in the murine intestine resulted in severe **i**nflammatory **b**owel **di**sease (IBD) and lethality [24,25]. Thus it was postulated that the adenomas arising in mice with limited $p120^{ctn}$ ablation was a result of chronic inflammation, which is considered a risk factor for colorectal cancer [26].

Since studies have implicated Kaiso in intestinal cancer development and progression [7,8], we generated an intestinal-specific Kaiso overexpression mouse model to clarify Kaiso's role in the context of murine intestinal epithelium development. We generated multiple Kaiso transgenic ($Kaiso^{Tg/+}$) founder lines, each with varying copy numbers of the transgene. $Kaiso^{Tg/+}$ mice were viable and fertile with no deleterious developmental phenotypes. However we noticed several phenotypes in the intestines of $Kaiso^{Tg/+}$ mice that were reminiscent of Notch inhibition. $Kaiso^{Tg/+}$ mice exhibited increased differentiation of intestinal epithelial progenitor cells into secretory cell lineages (Paneth, Goblet, enteroendocrine) accompanied by reduced proliferation, a phenotype consistent with Notch inhibition [27,28,29]. Indeed, expression of the Notch signalling target HES-1 was also reduced in $Kaiso^{Tg/+}$ mice. Interestingly, $p120^{ctn}$ localized mainly to the nucleus in the small intestine in $Kaiso^{Tg/+}$ mice, and this was accompanied by increased infiltration of inflammatory cells and myeloperoxidase activity (a surrogate marker for inflammation) suggesting that $Kaiso^{Tg/+}$ mice are more susceptible to inflammation. Together these data suggest that Kaiso functions in a pro-inflammatory role in the murine intestine by antagonizing the anti-inflammatory functions of $p120^{ctn}$.

Materials and Methods

Ethics Statement

All mouse work was conducted according to the guidelines of the McMaster University Animal Research Ethics Board (AREB). Protocols for mouse husbandry, breeding, genotyping and euthanasia were approved by AREB under Animal Utilization Protocol (AUP) 10-05-32. Euthanasia was achieved via CO_2 asphyxiation followed by cervical dislocation.

Generation of Villin-Kaiso Transgenic Mice

Kaiso transgenic mice were created at the London Regional Transgenic Facility, University of Western Ontario. Myc-tagged murine *Kaiso* (*mKaiso-MT*) was cloned downstream of the murine 9 Kb intestinal-specific *villin* promoter fragment in the pBluescript II vector provided by Dr. Sylvie Robine (Institut Curie, Paris, France) [30]. The *villin-mKaiso-MT* fragment was excised from the plasmid by restriction enzyme digest with *SalI*. The isolated fragment was microinjected into 1-cell C57BL6/CBA hybrid mouse embryos *in vitro*, which were then implanted into pseudo-pregnant foster mothers to produce transgenic founders. Transgenic pups were identified by **p**olymerase **c**hain **r**eaction (PCR) analysis of DNA from tail biopsies using primer pairs corresponding to sequences in the Myc tag and murine Kaiso (forward *5′-ATC ATC AAA GCC GGG TGG GCA-3′* and reverse *5′-TTT TCT ACT CTC CAT TTC ATT CAA GTC CTC-3′*). The transgenic lines were backcrossed with C57BL/6N mice (Taconic) for a minimum of 8 generations to obtain stable transgenic offspring, which initially produced three transgenic founder lines, followed by an additional four transgenic founder lines. All transgenic offspring were genotyped by PCR using DNA obtained from ear snips upon weaning. Mice were fed a standard mouse chow diet and breeders were housed in the disease-free barrier facility, while post-genotyping pups were housed in a specific pathogen free (SPF) room with 12 h/12 h light/dark cycle in accordance with McMaster Central Animal Facility's (CAF) Standard Operating Procedures (SOPs).

Transgene Copy Number

Copy number standards were prepared by spiking wild-type tail DNA with specified amounts of purified transgenic DNA. PCR was performed using standard DNA and transgenic DNA from each founder line using the primers described above. The intensity of the band amplified in each of the transgenic animals was compared to that of the standards to estimate transgene copy number.

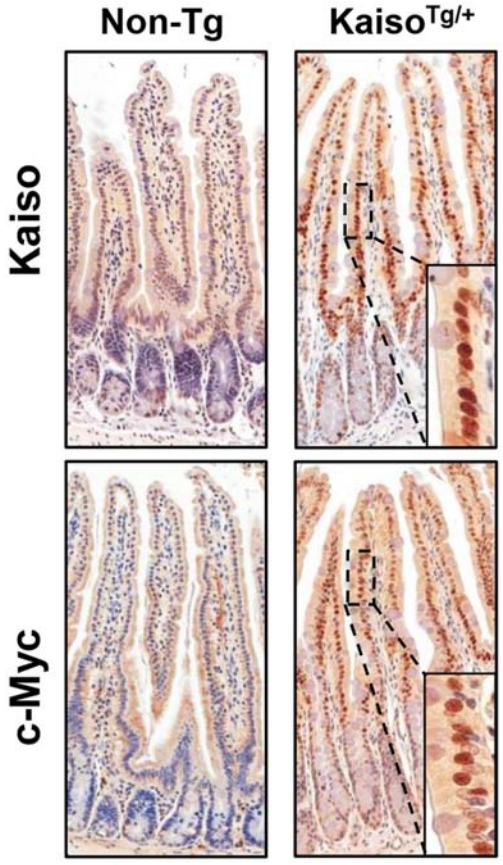

Figure 2. Subcellular localization and expression of ectopic Kaiso in Line A *Kaiso*$^{Tg/+}$ small intestines. *Kaiso*$^{Tg/+}$ mice display strong nuclear Kaiso in the villi and crypt cells, compared to non-transgenic mice (Non-Tg), which mainly display weak Kaiso staining in the cytoplasm. Additionally, *Kaiso*$^{Tg/+}$ mice display strong nuclear c-Myc staining corresponding to ectopic myc-tagged Kaiso expression, while Non-Tg mice display cytoplasmic c-Myc expression.
doi:10.1371/journal.pone.0074160.g002

Mouse Tissue Harvest

Mice were sacrificed via CO_2 asphyxiation according to the McMaster CAF SOPs. Small and large intestines were immediately removed from the sacrificed animals and flushed with cold **p**hosphate-**b**uffered **s**aline (PBS) on ice. Tissues were either flash frozen in liquid nitrogen for long term storage or rolled into "Swiss rolls" for fixation in 10% neutral-buffered formalin for 48 hours, followed by 70% ethanol dehydration at room temperature. The small intestine was divided into four equal sections for formalin fixation. Fixed tissues were sent to McMaster Core Histology Research Services for paraffin-embedding and sectioning at 5 μm within one week of tissue harvest, and placed onto glass slides for **i**mmuno**h**isto**c**hemical (IHC) analysis as outlined below.

Morphological Analysis

Crypt depth and villi length were evaluated using **h**aematoxylin and **e**osin (H&E) stained slides from both transgenic lines (n = 3 mice per genotype/founder line). Paneth cells were counted as eosin-filled cells at the base of the crypts. **P**eriodic **A**cid-**S**chiff (PAS) stain for Goblet cells was performed by the McMaster Core Histology Research Services according to standard protocols. All images were collected using the Aperio ScanScope system, and ImageScope software was used for all measurements. For each small intestine, 800 open crypts and 80 complete villi were assessed per mouse by two independent blind observers. Student's T-test was used to compare any observed differences for statistical significance using GraphPad Prism.

Immunohistochemistry

Tissue slides were incubated in xylenes at room temperature for 10 min (2 washes) to remove paraffin, followed by rehydration in an ethanol gradient. Tissue was permeabilized with **T**ris-**b**uffered **s**aline with 0.05% **T**ween-20 (TBS-T), and antigen retrieval was accomplished by boiling samples in 10 mM sodium citrate buffer (pH 6.0). Endogenous peroxidase activity was quenched with 3% hydrogen peroxide in TBS. Slides were incubated in 5% normal goat serum (NGS), 10% bovine serum albumin (BSA) in TBS-T with avidin blocking solution (Vector Laboratories) for 1 hour at room temperature. For Lysozyme staining (Pierce), antigen retrieval was performed by treating tissues with 200 μg/mL of Proteinase K (Roche) solution in 50 mM Tris, pH 7.4 for 5 minutes, and blocked in 10% NDS in PBS with avidin blocking solution for 1 hour at room temperature. The slides were then incubated with biotin blocking solution (Vector Laboratories) and primary antibodies: rabbit anti-Kaiso polyclonal (gift from Dr. Albert Reynolds) at 1:1000 dilution, and mouse anti-c-Myc (Santa Cruz) at 1:60, rabbit anti-Lysozyme (Peirce) 1:50 at 4°C overnight. For rat anti-Ki67 (DAKO at 1:20 dilution), mouse anti-Synaptophysin (DAKO at 1:20 dilution), rabbit anti-HES-1 (Santa Cruz at 1:75 dilution) and rabbit anti-Cyclin D1 (US Biological at a 1:100 dilution) staining, antigen retrieval was accomplished by boiling samples at 95°C in Target Retrieval Solution Citrate pH 6.0 (DAKO). Slides were blocked in 5% **n**ormal **d**onkey **s**erum (NDS) in TBS-T for Ki67 and Cyclin D1, in 5% NDS, 10% BSA in PBS for HES-1, and in 10% NGS, 10% BSA in PBS for Synaptophysin. Primary antibody incubation was performed for 2 hours at room temperature. After three 2-min washes in TBS-T, and one in TBS, slides were incubated in secondary antibodies (biotinylated donkey anti-rabbit [Vector Laboratories] at a 1:1000 dilution, biotinylated goat anti-mouse [Vector Laboratories] at a 1:1000 dilution, or biotinylated rabbit anti-rat [DAKO] at a 1:200 dilution) for 2 hours at room temperature. Slides were washed as before, and incubated for 30 min in an avidin-biotin horseradish peroxidase complex, Elite ABC (Vector Laboratories). After a brief wash in TBS, Vectastain DAB substrate (Vector Laboratories) was applied for 3 minutes for satisfactory colour development. Ki67 and Cyclin D1 staining required a DAB time of 7 minutes. Tissues were counterstained with Harris hematoxylin (Sigma), differentiated in acid ethanol (0.3% HCl in 70% ethanol), blued in Scott's tap water substitute, and dehydrated in a gradient of ethanol. Slides were then dried in xylenes and mounted using PolyMount (Polysciences Inc). Images were acquired using the Aperio ScanScope, and processed using ImageScope.

Immunofluorescence

Tissue slides were incubated in xylenes at room temperature for 10 min (2 washes) to remove paraffin, followed by rehydration in

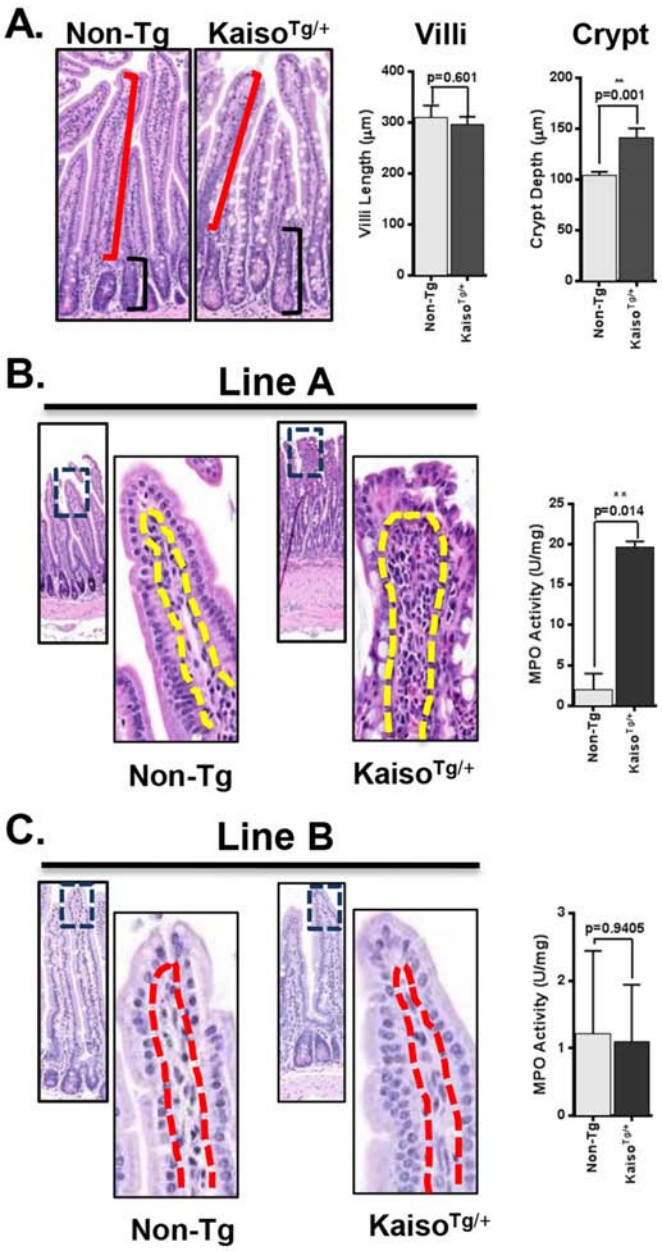

Figure 3. Kaiso transgenic mice exhibit inflammation of the intestinal mucosa. (**A**) **H**ematoxylin and **e**osin (H&E) stained sections were used to measure villi length (red bracket; ~80 villi/mouse) and crypt depth (black bracket; ~800 open crypts/mouse). *Kaiso*$^{Tg/+}$ display increased crypt depth compared to their Non-Tg siblings, p = 0.001. (**B**) *Kaiso*$^{Tg/+}$ mice exhibit increased immune cell infiltration of the lamina propria (yellow demarcated area) accompanied by increased MPO activity compared to their Non-Tg siblings, p = 0.014. (**C**) Line B mice do not exhibit immune cell infiltration or enhanced MPO activity compared to Non-Tg siblings. ** represents significance.
doi:10.1371/journal.pone.0074160.g003

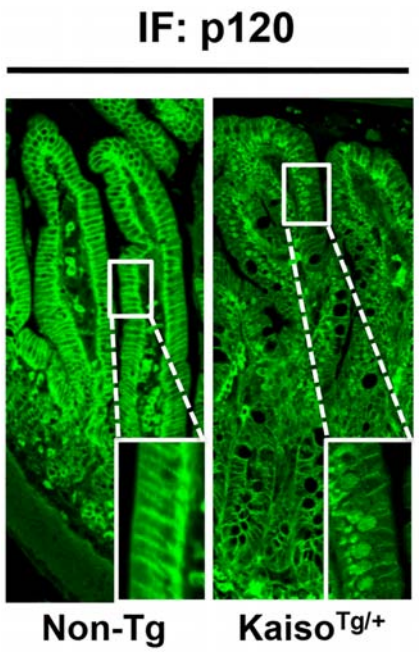

Figure 4. *Kaiso*$^{Tg/+}$ mice display nuclear p120^{ctn} in villi of the small intestine. Immunofluorescence staining for p120^{ctn} showed nuclear localization of p120^{ctn} in epithelial cells of villi overexpressing Kaiso (*Kaiso*$^{Tg/+}$), while Non-Tg mice displayed membrane localized p120^{ctn}.
doi:10.1371/journal.pone.0074160.g004

an ethanol gradient as described above. Tissue was permeabilized with 0.05% TBS-T, and antigen retrieval was accomplished by boiling samples in 10 mM sodium citrate buffer (pH 6.0). Tissues were incubated in 5% normal goat serum, 10% bovine serum albumin in TBS-T for 1 hour at room temperature. The slides were then incubated with mouse monoclonal anti-p120 (BD Biosciences) at a dilution of 1:500 at 4°C overnight. After three 10 min washes in TBS-T, and one in TBS, slides were incubated in secondary antibodies (Alexa-488 goat anti-mouse [Invitrogen], at a dilution of 1:500) for 2 hours in the dark at room temperature. Slides were washed as before, and incubated for 30 min in the dark with TOTO-3 dye (Invitrogen; 1:1000) to stain the nuclei. Slides were mounted in ProLong Gold (Invitrogen) overnight in the dark and stored at −20°C until imaging. Images were captured and processed using a Leica Confocal Microscope.

Protein Isolation and Immunoblot

50 mg of flash frozen mouse tissue was minced with a sterile blade and homogenized in 1 mL cold RIPA buffer (1% NP-40, 50 mM Tris, 150 mM NaCl, 0.5% sodium deoxycholate, 1% SDS, 0.5% Na_3VO_4 and cOmplete ULTRA Tablet (1 tablet/ 5 mL buffer) [Roche]) in a chilled tissue grinder (Kontes). Harvested lysates were poured into chilled microfuge tubes followed by further homogenization using a 21 Gauge syringe. Lysates were incubated on ice for 30 minutes, followed by centrifugation at 13,000 RPM for 10 min at 4°C. The supernatants were transferred to new pre-chilled microfuge tubes. Total protein content was quantified by Bradford assay, and 25 μg of protein was resuspended in Laemmli sample buffer, boiled for 5 minutes and subjected to electrophoresis in an SDS polyacrylamide gel. Proteins were transferred to a nitrocellulose membrane using a Hoeffer semi-dry transfer apparatus (Amersham Biosciences). To prevent non-specific antibody binding, the membranes were blocked with 3% skimmed milk/TBS (pH 7.4) and incubated at 4°C overnight with antibody diluted in 3% milk/TBS. Antibodies used were as follows: anti-Kaiso rabbit polyclonal antibody at a 1:30,000 dilution, anti-Cyclin D1 rabbit polyclonal antibody (US Biological) at a 1:5,000 dilution, anti-β-actin mouse monoclonal antibody (Sigma Aldrich) at a 1:30,000 dilution. The membranes were washed 5×5 minutes each with TBS and incubated at room temperature with HRP-conjugated donkey anti-mouse or goat anti-rabbit secondary antibody both at a dilution of 1:40,000 in 3% milk/TBS. Membranes were washed as previously described and processed with Enhanced Chemiluminescence (Amersham Biosciences) according to the manufacturer's protocol.

RNA Isolation

Mouse tissue was homogenized and total RNA purified using the RNeasy Kit (Qiagen). Briefly, ~20 mg frozen tissues were chopped finely with a clean blade, resuspended in 600 μl Qiagen Buffer RLT, and homogenized on ice in a glass tissue grinder. Lysates were further homogenized using a 21 Gauge needle and syringe on ice. Total RNA was then purified from the homogenized lysate using the RNeasy kit according to manufacturer's instructions.

RT-PCR

Reverse **t**ranscriptase PCR (RT-PCR) analysis was performed using SuperScriptII One-Step RT-PCR with Platinum Taq (Invitrogen). Briefly, 1 μg of RNA was DNaseI treated (Invitrogen) to remove any genomic DNA contamination. 100 ng total RNA was used for each reaction with primers specific to the *villin-mKaiso* transcript and transcription factor II D (TFIID) as a loading control. The primer pairs used were as follows*: villin-mKaiso*: forward *5′-CAA CTT CCT AAG ATC TCC CAG GT-3′* and reverse *5′-CAA GGA GTT CAG CAG ACT GG -3′*; *TFIID*: forward *5′-CCA CGG ACA ACT GCG TTG AT-3′* and reverse *5′-GGC TCA TAG CTA CTG AAC TG-3′*. The RT-PCR program included one round of cDNA synthesis at 50°C for 30 minutes, followed by denaturation at 95°C for 2 minutes. Twenty five cycles of DNA amplification was performed as follows: denaturation at 95° for 30 sec, annealing at 56°C for 30 sec, and extension at 72°C. Final extension occurred at 72°C for 10 mins.

Quantitative RT-PCR

Total RNA was purified from ~ 20 mg of small intestinal tissue as described above. 1 μg of RNA was DNaseI treated (Invitrogen) to remove any genomic DNA contamination, and cDNA synthesis was accomplished using the SuperScript III First-Strand Synthesis System (Invitrogen). RNA abundance was compared using PerfeCTa SYBR Green SuperMix Reaction Mixes (Quanta Biosciences). The standard curve method was used to calculate relative expression of HES1 and Kaiso following normalization to the housekeeping gene, GAPDH, and then normalizing to the non-Tg tissue level. Primer sequences used are as follows: *villin-mKaiso* as stated above; *mHES1*: forward *5′-AAA ATT CCT CCT CCC CGG TG-3′* and reverse *5′-TTT GGT TTG TCC GGT GTC G-3′*; and *mGAPDH: forward 5′–ATG ACC ACA GTC CAT GCC ATC–3′* and reverse *5′-CCT GCT TCA CCA CCT TCT TG-3′*.

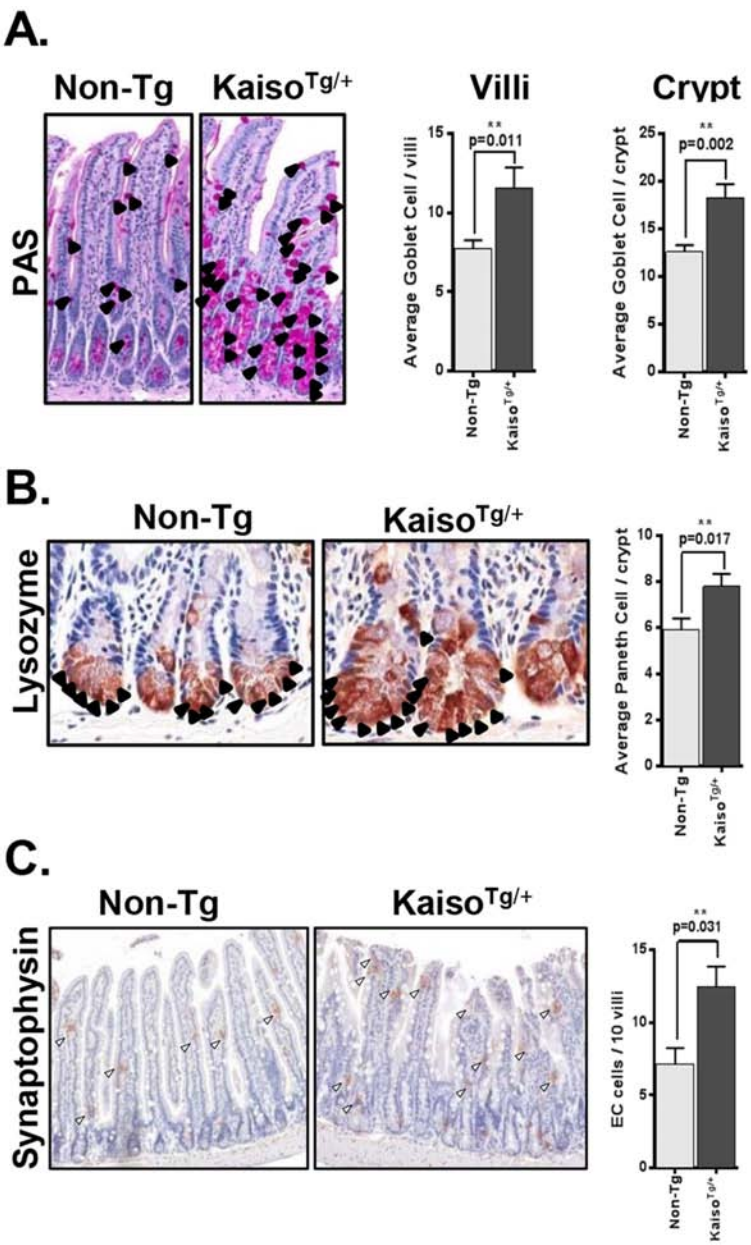

Figure 5. Secretory cell lineages are expanded in the intestines of *Kaiso*$^{Tg/+}$ mice. (**A**) PAS stain for Goblet cells (black arrowheads) revealed increased numbers of Goblet cells in both the villi and crypts of *Kaiso*$^{Tg/+}$ intestines, p = 0.011 & 0.002. (**B**) Lysozyme staining revealed increased Paneth cell numbers in *Kaiso*$^{Tg/+}$ mice, p = 0.017. (**C**) Synaptophysin positive enteroendocrine cells (arrowheads) are increased in *Kaiso*$^{Tg/+}$ mice, p = 0.031. n = 3 mice/genotype; measurements performed by two independent blind observers; T-test used for p-value. ** represents significance.
doi:10.1371/journal.pone.0074160.g005

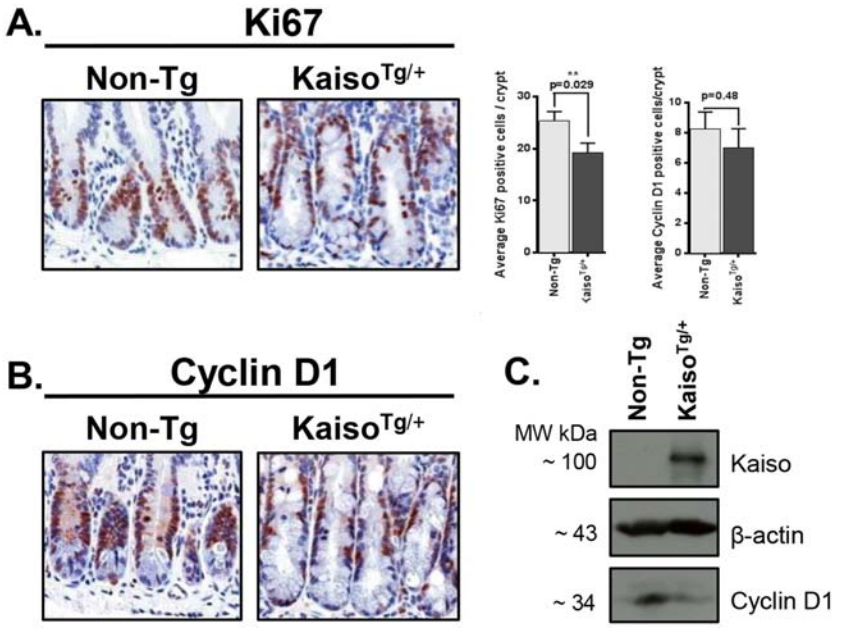

Figure 6. Cell proliferation is decreased in *Kaiso*$^{Tg/+}$ mice. Cell proliferation was evaluated by Ki67 (**A**) and Cyclin D1 (**B**) staining. Both markers exhibited reduced staining in *Kaiso*$^{Tg/+}$ mice compared to their Non-Tg siblings. Reduced CyclinD1 expression was also confirmed by immunoblot analysis of 3 different mice intestines (**C**). ** represents significance.
doi:10.1371/journal.pone.0074160.g006

Student's T-test was used to determine significance using GraphPad Prism.

Myeloperoxidase (MPO) Assay

Approximately 50 mg of flash frozen ileum and colon were homogenized in 50 mg/mL of 0.5% HTAB buffer (0.5% hexadecyltrimethylammonium bromide in 50 mM phosphate buffer, pH 6.0) via sonication at 30 Hz for 4 minutes. Homogenates were cleared by centrifugation at 12,000 rpm for 15 minutes at 4°C. MPO Assay was carried by adding 200 µL of o-dianisidine dihydrochloride solution (16.8 mg/mL o-dianisidine dihydrochloride in 5 mM phosphate buffer, pH 6.0 with 50 µL of 1.2% H_2O_2) to 96-well plates. Samples (7 µL) were added to each well of the 96-well plate in triplicate, and absorbance measured at 450 nm every 30 sec (3 readings). The MPO activity was measured in units (U), where 1 U represents the amount of MPO needed to degrade 1 µmoL of H_2O_2/minute at 25°C, which gives an absorbance of 1.13×10^{-2} nm/min. MPO activity in each sample was determined as the change in absorbance $[\Delta A(t_2\text{-}t_1)]/\Delta\text{min}]/(1.13\times10^{-2})$. MPO activity/mg of tissue was calculated by dividing MPO U by 0.35 mg of tissue (7 µL homogenate×50 mg/mL buffer). Student's T-test was used to compare any observed differences for statistical significance using GraphPad Prism.

Results

Generation of *villin-Kaiso* Transgenic Mice

Kaiso transgenic (*Kaiso*$^{Tg/+}$) mice were generated by cloning the sequence encoding N-terminal myc-tagged murine *Kaiso* downstream of a 9 Kb regulatory promoter region of the mouse *villin* gene (Figure 1A). The *villin-Kaiso* construct was injected into fertilized C57BL6/CBA embryos that were subsequently transferred to pseudopregnant foster mothers and resulted in four transgenic founder mice (Line A, B, C, D). Upon backcrossing with C57BL/6N mice, only lines A, B and C transmitted the transgene to their progeny at rates of 15%, 32% and 57%, respectively. Since pronuclear injections result in random genome integration, transgene copy number was estimated by PCR (Figure 1B). The three founders possessed varying copy numbers of the Kaiso transgene, with line A having the highest copy number and line C having the lowest copy number. Unfortunately, Line C died prior to being established and thus Lines A and B were used for further analysis. Upon founder line establishment (8 generations of backcrossing), Lines A and B transmitted the transgene at rates of 33.8% and 35.9% respectively, which is lower than the expected Mendelian rate of 50%.

To confirm tissue-specific expression of the *Kaiso* transgene, RT-PCR was performed with transgene-specific primers. As expected, the transgene was detected in all 3 villin-positive tissues: kidneys, small intestine and large intestine (Figure 1C). Kaiso protein expression was confirmed by Western blot analysis of protein harvested from small and large intestine (Figure 1D). Consistent with the transgene copy number observed via PCR, higher Kaiso protein expression was detected in Line A transgenics compared to Line B, with the lowest protein expression in Line C (data not shown).

To further evaluate and confirm Kaiso expression and localization in *Kaiso*$^{Tg/+}$ and Non-Tg tissues, IHC was performed on tissues harvested from small and large intestines of Line A and Line B mice using a Kaiso-specific antibody. Line A *Kaiso*$^{Tg/+}$ mice

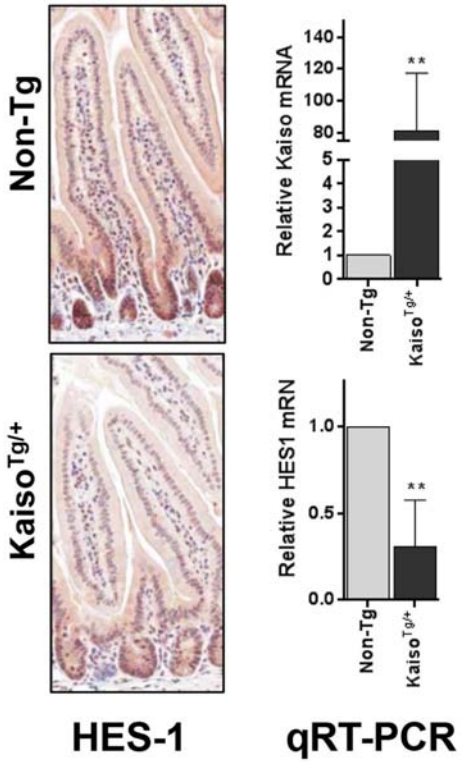

Figure 7. *Kaiso*$^{Tg/+}$ mice display decreased HES-1 expression in the small intestine. Both Non-Tg and *Kaiso*$^{Tg/+}$ tissues displayed nuclear HES-1 expression in the crypts of the small intestine, however *Kaiso*$^{Tg/+}$ tissue displays significantly decreased HES-1 expression in the villi. Quantitative RT-PCR showed a significant decrease in HES-1 expression in *Kaiso*$^{Tg/+}$ mice. Values were first normalized to the GAPDH housekeeping gene, followed by normalizing to non-Tg HES-1 expression (** represents $p<0.05$).
doi:10.1371/journal.pone.0074160.g007

exhibited stronger nuclear Kaiso expression in the villi and increased nuclear expression in the crypts of the small intestine compared to their Non-Tg siblings (Figure 2). However, Line B *Kaiso*$^{Tg/+}$, which overexpressed less Kaiso than Line A, exhibited predominantly cytoplasmic localized Kaiso (Figure S1A). In the large intestine, both transgenic lines exhibited stronger Kaiso nuclear staining than their Non-Tg siblings (Figure S1B). Furthermore, strong nuclear Kaiso expression was observed in the epithelial cells near the top of the crypts, with lower expression at the bottom of the crypts (Figure 2). To confirm that increased Kaiso expression in *Kaiso*$^{Tg/+}$ mice was due to the transgene rather than an enhancement of endogenous *Kaiso* gene expression, we evaluated c-Myc expression in Line A small intestines. Indeed, *Kaiso*$^{Tg/+}$ mice exhibited stronger staining in comparison to Non-Tg mice, consistent with the expression of myc-tagged Kaiso (Figure 2). All subsequent analyses were performed on Line A *Kaiso*$^{Tg/+}$ (unless noted otherwise).

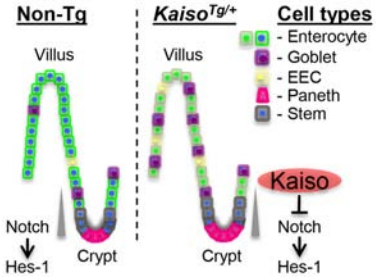

Figure 8. Schematic model of Kaiso's postulated effects in the intestine. Notch signalling in the crypts modulates differentiation of progenitor cells into the various epithelial cell lineages: enterocytes, Goblet, Paneth and **e**ntero**e**ndo**c**rine (EEC) cells. The gradient of Notch signaling is indicated by the grey triangle. HES-1 is necessary for the proper specification of these cell types. p120^{ctn} localizes to the membrane in the enterocytes of Non-Tg mice (green-membraned cells), but is recruited to the nucleus in *Kaiso*$^{Tg/+}$ mice (green nucleated cells), which inhibits Notch signaling and Hes-1 expression, thus inducing inflammation.
doi:10.1371/journal.pone.0074160.g008

Kaiso Transgenic Mice Exhibit Symptoms of Inflammation in the Intestinal Mucosa

After establishing that Kaiso was robustly expressed in the intestine via our transgene we next sought to determine the effect of ectopic Kaiso on intestinal morphology and function. Examination of H&E stained sections from small and large intestinal tissues of 1-year old Line A mice revealed longer crypts with no difference in villi length in the small intestine (Figure 3A), although this phenotype was not observed in Line B mice. We also noticed that several villi were fused and blunted in our Line A *Kaiso*$^{Tg/+}$ mice in comparison to the characteristic elongated, finger-like appearance of villi in Non-Tg mice (Figure 3). To rule out the possibility that this phenotype was an artefact resulting from the transgene insertion site, we examined H&E sections from additional *Kaiso*$^{Tg/+}$ lines that had been backcrossed for only 3 generations (Lines D, E, F & G). Two of these lines, Lines E and F, exhibited even more robust Kaiso expression than Line A mice, concomitant with extensive villi fusion and blunting (Figure S2).

Crypt hyperplasia accompanied by fused, blunted villi has been previously reported in both humans and mice exhibiting chronic inflammation of the intestinal mucosa [31,32,33,34], suggesting that ectopic Kaiso expression may cause intestinal inflammation. Indeed, closer examination of *Kaiso*$^{Tg/+}$ intestines (Line A, E and F) revealed increased immune cell infiltration of the lamina propria compared to their Non-Tg siblings (Figure 3B and Figure S2); however no such phenotype was observed in Line B mice with low ectopic Kaiso expression (Figure 3C). We also measured the levels of **m**yelo**p**er**o**xidase (MPO), which is a surrogate marker for inflammation, in *Kaiso*$^{Tg/+}$ and Non-Tg intestinal tissues. MPO activity was increased in the distal small intestine (ileum) of Lines A, E and F *Kaiso*$^{Tg/+}$ mice compared to their age-matched Non-Tg siblings (Figure 3B and Figure S2), while no change in MPO activity was detected in Line B mice (Figure 3C). Interestingly, the proximal colon of Lines E and F also exhibited increased MPO activity while mice from Lines A and B exhibited no such change (data not shown). These data suggest that ectopic Kaiso expression may predispose the murine intestine to inflammation, but this effect may be dose-dependent.

Ectopic Kaiso Overexpression Results in Nuclear Accumulation of p120^{ctn}

Given that *Kaiso*$^{Tg/+}$ mice exhibited an inflammatory response similar to that elicited by limited p120^{ctn} depletion [24], albeit less severe, we examined p120^{ctn} expression in the small intestines of our *Kaiso*$^{Tg/+}$ mice. Interestingly, in *Kaiso*$^{Tg/+}$ mice we observed nuclear localization of p120^{ctn} and reduced p120^{ctn} staining at the membrane in the distal small intestine (Figure 4). However in Non-Tg siblings, p120^{ctn} was largely membrane bound (Figure 4). Taken together this data suggests that Kaiso overexpression results in nuclear accumulation of p120^{ctn}, and decreased membrane-bound p120^{ctn}, which phenocopies the consequences of p120^{ctn} depletion [25].

Kaiso$^{Tg/+}$ Mice Exhibit Enhanced Differentiation of Progenitor Cells into Secretory Cell Fates

While characterizing the effect of ectopic Kaiso expression on intestinal morphology, we noted a significant expansion of Goblet cells in both the small and large intestine of Line A *Kaiso*$^{Tg/+}$ mice. Thus, we performed PAS staining for the Goblet cell-specific marker, Mucin, and quantification of Mucin positive (+) cells confirmed a significant increase in the Goblet cell population in both the small and large intestines of Line A mice compared to Line B and Non-Tg mice (Figure 5A & Figure S3). Interestingly, staining for the Paneth and enteroendocrine markers, lysozyme and synaptophysin respectively, revealed that these cell populations were also expanded in the small and large intestine of Line A *Kaiso*$^{Tg/+}$ mice but not in Line B or Non-Tg mice (Figure 5B, C & Figure S3).

The expansion of secretory cell lineages in our *Kaiso*$^{Tg/+}$ mice led us to hypothesize that Kaiso may be driving progenitor cell differentiation. However, since we also observed crypt expansion in *Kaiso*$^{Tg/+}$ mice, we questioned whether the increase in secretory cells was indicative of increased progenitor cell proliferation. Hence we examined the expression of the cell proliferation marker Ki67. Surprisingly, Ki67 expression was decreased in Line A mice and Ki67 positive cells were localized more apical to the normal crypt/villus boundary (Figure 6A). We next evaluated the expression of the Kaiso target gene *cyclin D1* [4,21] that has been shown to drive proliferation in the intestinal epithelium and is frequently overexpressed in colon cancer [35]. Similar to Ki67, Cyclin D1 expression was also decreased in Line A *Kaiso*$^{Tg/+}$ mice but surprisingly the apparent decreased numbers of Cyclin D1 positive (+) cells in *Kaiso*$^{Tg/+}$ intestines was not statistically significant (Figure 6B, C).

Previous studies have reported an expansion of secretory cell lineages and a reduction in the number of proliferating columnar base cells upon inhibition of the Notch signalling pathway in the intestine [28,29,36,37]. Specifically, depletion of the Notch target gene *Hes-1* resulted in increased expression of secretory cell markers in the intestine of *Hes-1* null mice, suggesting that Hes-1 is necessary for specification of secretory cells in the intestine [37]. This prompted us to examine the expression of Hes-1 in our *Kaiso*$^{Tg/+}$ mice. Line A *Kaiso*$^{Tg/+}$ mice exhibited decreased Hes-1 staining and reduced expression of *Hes-1* mRNA compared to Non-Tg littermates (Figure 7). Together our data demonstrate that ectopic Kaiso elicits enhanced differentiation of progenitor cells into secretory lineages, perhaps through the down-regulation of the Notch target *Hes-1*.

Discussion

Since Kaiso's discovery over a decade ago, several studies have utilized *Xenopus laevis* and cultured cells as models to elucidate Kaiso's biological roles [1,2,8,15,38,39,40,41]. Here we describe the first study to examine the role of Kaiso in a relevant organ-specific context, the murine intestine. Using the murine *villin* promoter we were able to successfully drive intestinal-specific expression of the *Kaiso* transgene. In all founder lines, Kaiso was expressed along the entire crypt-villus axis with the most robust expression in the villi, which is consistent with the normal expression pattern of villin [30].

A previous report examining the effect of Kaiso depletion on *Apc*$^{Min/+}$-mediated tumorigenesis found that Kaiso depletion resulted in fewer tumours [8], suggesting that Kaiso functions as an oncogene. However ectopic Kaiso expression was not sufficient to drive spontaneous tumour formation in our mouse model. Nonetheless, our Kaiso$^{Tg/+}$ Line A, mice exhibited enlarged crypts accompanied by fused, blunted villi, increased immune cell infiltration and increased MPO activity (indicative of neutrophil accumulation and inflammation) suggesting that *Kaiso*$^{Tg/+}$ mice have greater susceptibility to inflammation. Indeed, preliminary cytokine analysis of *Kaiso*$^{Tg/+}$ intestinal tissue revealed increased activity of the pro-inflammatory cytokine TNF-α compared to Non-Tg intestines (data not shown). Analysis of additional Kaiso transgenic lines (Lines E and F) revealed a similar intestinal phenotype to Line A, with concomitant increased neutrophil activation as measured by MPO activity. Increased MPO activity is often correlated with **u**lcerative **c**olitis (UC), a form of IBD and patients with IBD are at a higher risk of colon cancer [26,42,43,44]. Thus in accordance with Knudson's multiple hit theory of tumorigenesis, it is possible that Kaiso's full oncogenic potential may only be unmasked in the presence of a second oncogenic insult such as *Apc* mutation or p53 loss of function. Intriguingly, preliminary analysis of intestinal tissues from a **d**extran **s**odium **s**ulfate (DSS)-induced model of colitis (kind gift of Dr. Elena Verdú), revealed increased expression of Kaiso compared to non-DSS treated mice (Figure S4), further supporting the notion that Kaiso overexpression plays a role in intestinal inflammation.

The enhanced inflammation observed in *Kaiso*$^{Tg/+}$ mice may be linked to altered p120^{ctn} function. Kaiso overexpression resulted in the nuclear localization of p120^{ctn}, suggesting that Kaiso may somehow recruit or sequester p120^{ctn} to the nucleus. Given that p120^{ctn} was mainly localized to the cytoplasm and the cell membrane in non-transgenic mice, this change in localization may be indicative of altered or reduced p120^{ctn} function that may phenocopy p120^{ctn} loss observed by Smally Freed *et al.* [25]. Future studies are needed to determine whether p120^{ctn} directly contributes to the Kaiso overexpression phenotype.

Interestingly, the phenotypes observed in Lines A, E and F mice were not observed in Line B mice which express significantly lower levels of ectopic Kaiso; this suggests that a threshold level of Kaiso expression is necessary for the observed inflammatory phenotype. Additionally, no change in MPO activity was seen in Line B mice, further supporting our hypothesis of threshold effects of Kaiso expression. This is not surprising since varying amounts of Kaiso were shown to have completely opposite effects in *Xenopus laevis* embryos [18]. Hence in Line B mice, it is likely that Kaiso expression is below the threshold at which it elicits inflammation and leads to expanded crypts.

Finally, *Kaiso*$^{Tg/+}$ mice exhibited increased populations of Goblet, Paneth and enteroendocrine cells. This expansion of secretory cell populations accompanied by decreased cell proliferation is consistent with the phenotype observed upon pharmacological inhibition of Notch signalling [28] and in Hes-1^{null} mice [37]. One study found that Notch signalling is activated in intestinal epithelium in response to inflammation and is required

for proper regeneration of the intestinal epithelium following colitis induced damage [45]. It should be noted that 90-day old *Kaiso*$^{Tg/+}$ mice exhibit increased Goblet cells but do not exhibit any overt signs of inflammation or myeloperoxidase activity (data not shown). This suggests that inflammation in these mice develops over time although Notch inhibition is present at a very early age. Thus it is possible that the intestinal epithelium in our *Kaiso*$^{Tg/+}$ mice is incapable of regeneration following bacterial or physical insult and consequently develops chronic inflammation over time.

In summary, Kaiso overexpression promotes inflammation and inhibits Notch signalling in the murine intestine. These findings support a model in which *Kaiso*$^{Tg/+}$ mice develop inflammation, possibly by altering p120^{ctn} localization and consequently function (Figure 8). Kaiso's inhibition of the Notch pathway may hinder the ability of these mice to repair and regenerate the epithelium in response to inflammation, resulting in chronic inflammation that increases in severity over time, thus making the mice more susceptible to inflammation-induced tumorigenesis.

Supporting Information

Figure S1 Ectopic Kaiso expression in the intestine of *Kaiso*$^{Tg/+}$ mice. (A) Line B *Kaiso*$^{Tg/+}$ mice display sporadic nuclear expression and strong cytoplasmic Kaiso expression in the epithelial cells of the villi but lack Kaiso expression in the crypts, compared to Non-Tg mice. **(B)** In the colon, Non-Tg mice display low nuclear Kaiso expression in the crypts, while Line A and B *Kaiso*$^{Tg/+}$ show strong nuclear Kaiso expression, with the apical epithelial cells displaying the most Kaiso expression. Line A colons show greater Kaiso expression than Line B colons.
(TIF)

Figure S2 Ectopic Kaiso expression in the small intestine of multiple Kaiso transgenic lines induces inflammatory cell infiltration. *Kaiso*$^{Tg/+}$ mice display strong nuclear Kaiso expression in the villi and crypt cells, however Non-Tg mice display weak Kaiso expression with most Kaiso localizing to the cytoplasm. Line E and F (generation 3) show strong Kaiso expression from the base of the crypts to the top of the villi. Interestingly, in all three *Kaiso*$^{Tg/+}$ lines analysed, ectopic Kaiso expression also appears to induce villi fusion (black arrows). Histological analysis showed increased neutrophil infiltration into the villi of Lines A, E and F *Kaiso*$^{Tg/+}$ mice (yellow demarcated area). An MPO assay of Line A, E and F ileums show increased MPO activity when compared to age-matched Non-Tg. Immunofluorescence revealed nuclear p120^{ctn} in both Line E and F in the villi.
(TIF)

Figure S3 Line A *Kaiso*$^{Tg/+}$ mice display increased numbers of differentiated cells in the colon. *Kaiso*$^{Tg/+}$ mice display a significant increase in Goblet (PAS stain), and enteroendocrine cells (synaptophysin) in the large intestine (colon) compared to their Non-Tg littermates.
(TIF)

Figure S4 Kaiso expression is increased in DSS-treated murine colon tissues. Preliminary analysis of DSS-induced murine colitis model intestinal tissues revealed increased Kaiso nuclear expression in DSS-treated colon tissues whereas non-treated mice show low cytoplasmic Kaiso expression.
(TIF)

Acknowledgments

We would like to thank Dr. Albert Reynolds (Vanderbilt University) for the anti-Kaiso rabbit polyclonal antibody and Dr. Sylvie Robine (Institute Curie, Paris, France) for the villin construct. Additionally, we would like to thank Christina Hayes and Dr. Elena Verdú (McMaster University) for their assistance with the MPO Assay.

Author Contributions

Conceived and designed the experiments: RC CCP KN JMD. Performed the experiments: RC CCP KN DW SM. Analyzed the data: RC CCP GW CP JMD. Contributed reagents/materials/analysis tools: SR. Wrote the paper: RC CCP JMD.

References

1. Cofre J, Menezes JR, Pizzatti L, Abdelhay E (2012) Knock-down of Kaiso induces proliferation and blocks granulocytic differentiation in blast crisis of chronic myeloid leukemia. Cancer Cell Int 12: 28.
2. Vermeulen JF, van de Ven RA, Ercan C, van der Groep P, van der Wall E, et al. (2012) Nuclear Kaiso expression is associated with high grade and triple-negative invasive breast cancer. PLoS One 7: e37864.
3. Wang Y, Li L, Li Q, Xie C, Wang E (2012) Expression of P120 catenin, Kaiso, and metastasis tumor antigen-2 in thymomas. Tumour Biol.
4. Jiang G, Wang Y, Dai S, Liu Y, Stoecker M, et al. (2012) P120-catenin isoforms 1 and 3 regulate proliferation and cell cycle of lung cancer cells via beta-catenin and Kaiso respectively. PLoS One 7: e30303.
5. Dai SD, Wang Y, Jiang GY, Zhang PX, Dong XJ, et al. (2010) Kaiso is expressed in lung cancer: its expression and localization is affected by p120ctn. Lung Cancer 67: 205–215.
6. Dai SD, Wang Y, Miao Y, Zhao Y, Zhang Y, et al. (2009) Cytoplasmic Kaiso is associated with poor prognosis in non-small cell lung cancer. BMC Cancer 9: 178.
7. Lopes EC, Valls E, Figueroa ME, Mazur A, Meng FG, et al. (2008) Kaiso contributes to DNA methylation-dependent silencing of tumor suppressor genes in colon cancer cell lines. Cancer Res 68: 7258–7263.
8. Prokhortchouk A, Sansom O, Selfridge J, Caballero IM, Salozhin S, et al. (2006) Kaiso-deficient mice show resistance to intestinal cancer. Mol Cell Biol 26: 199–208.
9. Blattler A, Yao L, Wang Y, Ye Z, Jin VX, et al. (2013) ZBTB33 binds unmethylated regions of the genome associated with actively expressed genes. Epigenetics Chromatin 6: 13.
10. Daniel JM, Spring CM, Crawford HC, Reynolds AB, Baig A (2002) The p120(ctn)-binding partner Kaiso is a bi-modal DNA-binding protein that recognizes both a sequence-specific consensus and methylated CpG dinucleotides. Nucleic Acids Res 30: 2911–2919.
11. Donaldson NS, Pierre CC, Anstey MI, Robinson SC, Weerawardane SM, et al. (2012) Kaiso Represses the Cell Cycle Gene cyclin D1 via Sequence-Specific and Methyl-CpG-Dependent Mechanisms. PLoS One 7: e50398.
12. Prokhortchouk A, Hendrich B, Jorgensen H, Ruzov A, Wilm M, et al. (2001) The p120 catenin partner Kaiso is a DNA methylation-dependent transcriptional repressor. Genes Dev 15: 1613–1618.
13. Ruzov A, Dunican DS, Prokhortchouk A, Pennings S, Stancheva I, et al. (2004) Kaiso is a genome-wide repressor of transcription that is essential for amphibian development. Development 131: 6185–6194.
14. Ruzov A, Hackett JA, Prokhortchouk A, Reddington JP, Madej MJ, et al. (2009) The interaction of xKaiso with xTcf3: a revised model for integration of epigenetic and Wnt signalling pathways. Development 136: 723–727.
15. Ruzov A, Savitskaya E, Hackett JA, Reddington JP, Prokhortchouk A, et al. (2009) The non-methylated DNA-binding function of Kaiso is not required in early Xenopus laevis development. Development 136: 729–738.
16. Sasai N, Nakao M, Defossez PA (2010) Sequence-specific recognition of methylated DNA by human zinc-finger proteins. Nucleic Acids Res 38: 5015–5022.
17. Yoon HG, Chan DW, Reynolds AB, Qin J, Wong J (2003) N-CoR mediates DNA methylation-dependent repression through a methyl CpG binding protein Kaiso. Mol Cell 12: 723–734.
18. Iioka H, Doerner SK, Tamai K (2009) Kaiso is a bimodal modulator for Wnt/beta-catenin signaling. FEBS Lett 583: 627–632.
19. Park JI, Kim SW, Lyons JP, Ji H, Nguyen TT, et al. (2005) Kaiso/p120-catenin and TCF/beta-catenin complexes coordinately regulate canonical Wnt gene targets. Dev Cell 8: 843–854.
20. Filion GJ, Zhenilo S, Salozhin S, Yamada D, Prokhortchouk E, et al. (2006) A family of human zinc finger proteins that bind methylated DNA and repress transcription. Mol Cell Biol 26: 169–181.
21. Donaldson NS, Pierre CC, Anstey MI, Robinson SC, Weerawardane SM, et al. (2012) Kaiso represses the cell cycle gene cyclin D1 via sequence-specific and methyl-CpG-dependent mechanisms. PLoS One In Press.

22. Park JI, Ji H, Jun S, Gu D, Hikasa H, et al. (2006) Frodo links Dishevelled to the p120-catenin/Kaiso pathway: distinct catenin subfamilies promote Wnt signals. Dev Cell 11: 683–695.
23. Spring CM, Kelly KF, O'Kelly I, Graham M, Crawford HC, et al. (2005) The catenin p120ctn inhibits Kaiso-mediated transcriptional repression of the beta-catenin/TCF target gene matrilysin. Exp Cell Res 305: 253–265.
24. Smalley-Freed WG, Efimov A, Burnett PE, Short SP, Davis MA, et al. (2010) p120-catenin is essential for maintenance of barrier function and intestinal homeostasis in mice. J Clin Invest 120: 1824–1835.
25. Smalley-Freed WG, Efimov A, Short SP, Jia P, Zhao Z, et al. (2011) Adenoma formation following limited ablation of p120-catenin in the mouse intestine. PLoS One 6: e19880.
26. Terzic J, Grivennikov S, Karin E, Karin M (2010) Inflammation and colon cancer. Gastroenterology 138: 2101–2114 e2105.
27. Ogaki S, Shiraki N, Kume K, Kume S (2013) Wnt and notch signals guide embryonic stem cell differentiation into the intestinal lineages. Stem Cells 31: 1086–1096.
28. VanDussen KL, Carulli AJ, Keeley TM, Patel SR, Puthoff BJ, et al. (2012) Notch signaling modulates proliferation and differentiation of intestinal crypt base columnar stem cells. Development 139: 488–497.
29. Zecchini V, Domaschenz R, Winton D, Jones P (2005) Notch signaling regulates the differentiation of post-mitotic intestinal epithelial cells. Genes Dev 19: 1686–1691.
30. Pinto D, Robine S, Jaisser F, El Marjou FE, Louvard D (1999) Regulatory sequences of the mouse villin gene that efficiently drive transgenic expression in immature and differentiated epithelial cells of small and large intestines. J Biol Chem 274: 6476–6482.
31. Ostanin DV, Pavlick KP, Bharwani S, D'Souza D, Furr KL, et al. (2006) T cell-induced inflammation of the small and large intestine in immunodeficient mice. Am J Physiol Gastrointest Liver Physiol 290: G109–119.
32. Kuhnert F, Davis CR, Wang HT, Chu P, Lee M, et al. (2004) Essential requirement for Wnt signaling in proliferation of adult small intestine and colon revealed by adenoviral expression of Dickkopf-1. Proc Natl Acad Sci U S A 101: 266–271.
33. Jacques P, Elewaut D (2008) Joint expedition: linking gut inflammation to arthritis. Mucosal Immunol 1: 364–371.
34. Goldstein NS (2006) Isolated ileal erosions in patients with mildly altered bowel habits. A follow-up study of 28 patients. Am J Clin Pathol 125: 838–846.
35. Yang R, Bie W, Haegebarth A, Tyner AL (2006) Differential regulation of D-type cyclins in the mouse intestine. Cell Cycle 5: 180–183.
36. Milano J, McKay J, Dagenais C, Foster-Brown L, Pognan F, et al. (2004) Modulation of notch processing by gamma-secretase inhibitors causes intestinal goblet cell metaplasia and induction of genes known to specify gut secretory lineage differentiation. Toxicol Sci 82: 341–358.
37. Jensen J, Pedersen EE, Galante P, Hald J, Heller RS, et al. (2000) Control of endodermal endocrine development by Hes-1. Nat Genet 24: 36–44.
38. van Roy FM, McCrea PD (2005) A role for Kaiso-p120ctn complexes in cancer? Nat Rev Cancer 5: 956–964.
39. Daniel JM (2007) Dancing in and out of the nucleus: p120(ctn) and the transcription factor Kaiso. Biochim Biophys Acta 1773: 59–68.
40. Martin Caballero I, Hansen J, Leaford D, Pollard S, Hendrich BD (2009) The methyl-CpG binding proteins Mecp2, Mbd2 and Kaiso are dispensable for mouse embryogenesis, but play a redundant function in neural differentiation. PLoS One 4: e4315.
41. Jones J, Wang H, Zhou J, Hardy S, Turner T, et al. (2012) Nuclear Kaiso indicates aggressive prostate cancers and promotes migration and invasiveness of prostate cancer cells. Am J Pathol 181: 1836–1846.
42. Rubin DC, Shaker A, Levin MS (2012) Chronic intestinal inflammation: inflammatory bowel disease and colitis-associated colon cancer. Front Immunol 3: 107.
43. Saleh M, Trinchieri G (2011) Innate immune mechanisms of colitis and colitis-associated colorectal cancer. Nat Rev Immunol 11: 9–20.
44. Xavier RJ, Podolsky DK (2007) Unravelling the pathogenesis of inflammatory bowel disease. Nature 448: 427–434.
45. Okamoto R, Tsuchiya K, Nemoto Y, Akiyama J, Nakamura T, et al. (2009) Requirement of Notch activation during regeneration of the intestinal epithelia. Am J Physiol Gastrointest Liver Physiol 296: G23–35.

CHAPTER 4

Kaiso overexpression promotes intestinal inflammation and potentiates intestinal tumorigenesis in $Apc^{Min/+}$ mice

Preface:

This chapter consists of the manuscript in preparation entitled: ***"Kaiso overexpression promotes intestinal inflammation and potentiates intestinal tumorigenesis in $Apc^{Min/+}$ mice"*** by Christina C. Pierre, Joseph Longo, Meaghan Mavor, Snezana Milosavljevic, Roopali Chaudhary, Ebony Gilbreath, Clayton Yates and Juliet M. Daniel. Revisions were made to maintain formatting consistency with other chapters. Significant revisions include elimination of methods section (details in Chapter 2), removal of reference list (included in combined thesis list), and re-numbering of figures in order of appearance in the text.

This study aimed to examine the effect of Kaiso overexpression on intestinal Wnt signaling and CRC progression. In brief, ectopic expression of Kaiso in the $Apc^{Min/+}$ model accelerated polyp formation and resulted in significantly diminished lifespan. Kaiso's repressive effects on canonical Wnt signaling as demonstrated in *Xenopus* embryos and mammalian cultured cells, is not maintained in the murine intestine. Instead, Kaiso overexpression results in activation of Wnt signaling, which may contribute to tumour burden in $Kaiso^{Tg/+}$:$Apc^{Min/+}$ mice. Another potential mechanism by which Kaiso may promote intestinal tumorigenesis is by inducing inflammation in the intestinal mucosa, since $Kaiso^{Tg/+}$:$Apc^{Min/+}$ mice exhibit hallmarks of intestinal inflammation, a phenotype known to accelerate tumour formation. Kaiso expression positively correlates

with neoplastic progression in human intestinal tissue, supporting a role for Kaiso in CRC progression.

Contributions:

Christina Pierre wrote the manuscript and performed experiments for Figure 4.1A, 4.1C, 4.1D, 4.2, 4.3, 4.4A, 4.6C & D and 4.7. Joseph Longo quantified the Ki67 positive cells in Figure 4.5B, generated the data for Figure 4.5C, 4.6A and 4.6B and assisted with tissue harvest and health monitoring. Meaghan Mavor generated the data in Figure 4.4B, 4.5A, the IHC in Figure 4.5B and assisted with tissue harvest and health monitoring. Roopali Chaudhary assisted with the experiments in Figure 4.7D. Dr. Clayton Yates (Tuskeegee University, Tuskeegee, AL) performed Kaiso tissue microarray staining and Dr. Ebony Gilbreath (Tuskeegee University, Tuskeegee, AL) scored the human tissue microarrays depicted in Figure 4.1B. Dr. Juliet Daniel provided significant intellectual input and guidance throughout the execution of this work and edited the manuscript.

ABSTRACT

Constitutive Wnt/β-catenin signaling is a key contributor to colorectal cancer. Although inactivation of the tumour suppressor adenomatous polyposis coli is recognized as an early event in CRC development, the accumulation of multiple subsequent oncogenic insults facilitates malignant transformation. One potential contributor to colorectal carcinogenesis is the POZ-ZF transcription factor Kaiso, whose deletion extends lifespan and delays polyp onset in the widely used $Apc^{Min/+}$ mouse model of intestinal cancer. These findings suggested that Kaiso potentiates intestinal tumorigenesis, but this was paradoxical as Kaiso was previously implicated as a negative regulator of Wnt/β-catenin signaling. To resolve Kaiso's role in intestinal tumorigenesis and canonical Wnt signaling, we generated a transgenic mouse model ($Kaiso^{Tg/+}$) expressing an intestinal-specific myc-tagged Kaiso transgene. We then mated $Kaiso^{Tg/+}$ and $Apc^{Min/+}$ mice to generate $Kaiso^{Tg/+}$:$Apc^{Min/+}$ mice for further characterization. $Kaiso^{Tg/+}$:$Apc^{Min/+}$ mice exhibited reduced lifespan and increased polyp multiplicity compared to $Apc^{Min/+}$ mice. Consistent with this murine phenotype, we found that Kaiso expression positively correlates with human CRC progression, supporting a role for Kaiso in human CRC. Interestingly, Wnt target gene expression was increased in $Kaiso^{Tg/+}$:$Apc^{Min/+}$ mice, suggesting that Kaiso's function as a negative regulator of canonical Wnt signaling, as seen in *Xenopus*, is not maintained in this context. Notably, $Kaiso^{Tg/+}$:$Apc^{Min/+}$ mice exhibited increased neutrophil activation and cytokine production compared to their $Apc^{Min/+}$ counterparts. This phenotype was consistent with our previous report that $Kaiso^{Tg/+}$ mice exhibit

chronic intestinal inflammation. Together our findings highlight a role for Kaiso in promoting Wnt signaling, inflammation and tumorigenesis in the mammalian intestine.

INTRODUCTION

Uncontrolled Wnt signaling is a key contributor to CRC and identifying proteins or molecules that modulate this pathway have great potential for drug development for CRC treatment. In the past decade several new Wnt/β-catenin regulators and pathways that negatively or positively modulate Wnt signaling have been discovered but a thorough understanding of their roles in CRC remains unknown (Rosenbluh *et al.* 2014). One novel Wnt/β-catenin regulator is the POZ-ZF transcription factor Kaiso that was first identified as a binding partner for the Armadillo catenin and cell adhesion cofactor $p120^{ctn}$ (Daniel and Reynolds 1999). Kaiso is a unique dual-specificity POZ-ZF transcription factor that binds DNA at methylated CpG dinucleotides or a specific sequence known as the Kaiso Binding Site (Daniel and Reynolds 1999; Prokhortchouk *et al.* 2001; Daniel *et al.* 2002). Although few *bona fide* Kaiso target genes have been characterized to date, evidence from *Xenopus* embryos and mammalian cultured cells implicate Kaiso as a negative regulator of Wnt signaling, possibly via its interaction with members of the Tcf family of transcription factors and repression of Wnt target genes (Park *et al.* 2005; Spring *et al.* 2005; Del Valle-Perez *et al.* 2011; Donaldson *et al.* 2012). Surprisingly, Kaiso depletion results in delayed polyp onset and prolonged lifespan in the $Apc^{Min/+}$ mouse model of intestinal neoplasia (Prokhortchouk *et al.* 2006). $Apc^{Min/+}$ mice carry a nonsense mutation in codon 850 of the *Apc* gene, leading to a truncated and non-functional Apc polypeptide, nuclear accumulation of β-catenin and constitutive activation of Wnt target genes (Fodde *et al.* 2001). Given that Kaiso has been implicated as a negative regulator of the Wnt pathway, the unexpected delayed polyp onset in Kaiso-null $Apc^{Min/+}$ mice may be

independent of Kaiso's function in Wnt signaling. Indeed, Kaiso has been implicated in colorectal cancer progression via Wnt-unrelated mechanisms (Lopes *et al.* 2008), but no study has examined the effects of Kaiso overexpression on CRC development in mouse models.

Previously, we found that intestinal-specific *Kaiso*$^{Tg/+}$ mice exhibited several phenotypic abnormalities including hyperplasia, villi fusion and crypt expansion (Chaudhary *et al.* 2013). Interestingly, *Kaiso*$^{Tg/+}$ mice also exhibited increased leukocyte infiltration of the lamina propria and neutrophil activation, hinting that Kaiso may drive inflammation in the intestine (Chaudhary *et al.* 2013). This idea is further supported by the finding that mice with limited ablation of p120^{ctn} (*i.e.* unregulated Kaiso function) in the intestine developed chronic inflammation and adenomas (Chaudhary *et al.* 2013). Approximately 20% of all colorectal cancers can be attributed to genetic and familial syndromes, while the remainder are due to sporadic mutations influenced by environmental factors (Fodde and Smits 2001; Grivennikov 2013). Colitis-associated cancer (CAC) is a CRC subtype that results from the occurrence of clinically detectable, chronic intestinal inflammation in patients with inflammatory bowel disease (IBD) (Feagins *et al.* 2009; Saleh and Trinchieri 2011; Rubin *et al.* 2012). IBD is characterized as the overactive immune response to intestinal microbiota and other environmental stimuli in genetically predisposed individuals, and increasing evidence indicates that IBD increases the risk of CRC by up to 20% (Eaden *et al.* 2001; Canavan *et al.* 2006; Jess *et al.* 2012). Our findings in *Kaiso*$^{Tg/+}$ mice, combined with previous studies implicating Kaiso in CRC (Prokhortchouk *et al.* 2006; Lopes *et al.* 2008), led us to hypothesize that Kaiso

may potentiate $Apc^{Min/+}$ tumorigenesis by predisposing the intestinal epithelium to inflammation through a mechanism akin to CAC.

In this study, we mated our $Kaiso^{Tg/+}$ mice with $Apc^{Min/+}$ mice to generate $Kaiso^{Tg/+}$: $Apc^{Min/+}$ mice. Ectopic Kaiso expression significantly shortened the lifespan of $Apc^{Min/+}$ mice and resulted in approximately 3-fold more polyps. $Kaiso^{Tg/+}$:$Apc^{Min/+}$ mice also presented with extensive regions of atypical hyperplasia, increased mitoses and focal crypt abscesses, which were largely absent or present at a lower frequency in age-matched $Apc^{Min/+}$ mice. Examination of Wnt target gene expression in $Kaiso^{Tg/+}$ mice revealed that ectopic Kaiso expression increases the expression of Wnt target genes, and this effect is further amplified in $Kaiso^{Tg/+}$:$Apc^{Min/+}$ mice. Lastly, $Kaiso^{Tg/+}$:$Apc^{Min/+}$ mice exhibited increased neutrophil activation and pro-inflammatory cytokine production. Together, our data suggest that Kaiso expression may induce intestinal inflammation, which then predisposes mice to intestinal tumorigenesis.

RESULTS

Kaiso expression is increased in human colorectal tumour tissues and $Apc^{Min/+}$ polyps

To date, most studies implicating Kaiso in intestinal tumorigenesis have utilized murine models and cultured CRC cell lines (Prokhortchouk *et al.* 2006; Lopes *et al.* 2008). However, given that no study has examined the expression of Kaiso in a large cohort of CRC patient tissues, we sought to examine Kaiso expression in human normal and tumorous colorectal tissues. We analyzed *Kaiso* expression in a gene expression data set consisting of 74 normal colon tissues, 49 colonic polyp tissues, 186 primary

Figure 4.1: Kaiso expression is increased in CRC patient biopsies and in *Apc*$^{Min/+}$ polyps. (A) Comparison of Kaiso mRNA expression in normal colon tissues, polyps, primary tumours and metastases. **(B)** IHC analysis and quantification of Kaiso protein expression in human primary colorectal tumours and metastases compared to normal colon biopsies. **(C)** Kaiso expression and localization in *Apc*$^{Min/+}$ polyps and adjacent villi. (**D)** Western blot comparing Kaiso expression in Non-Tg versus *Apc*$^{Min/+}$ intestinal tissues. (**** represents $p<0.0001$. Error bars indicate standard error of the mean)

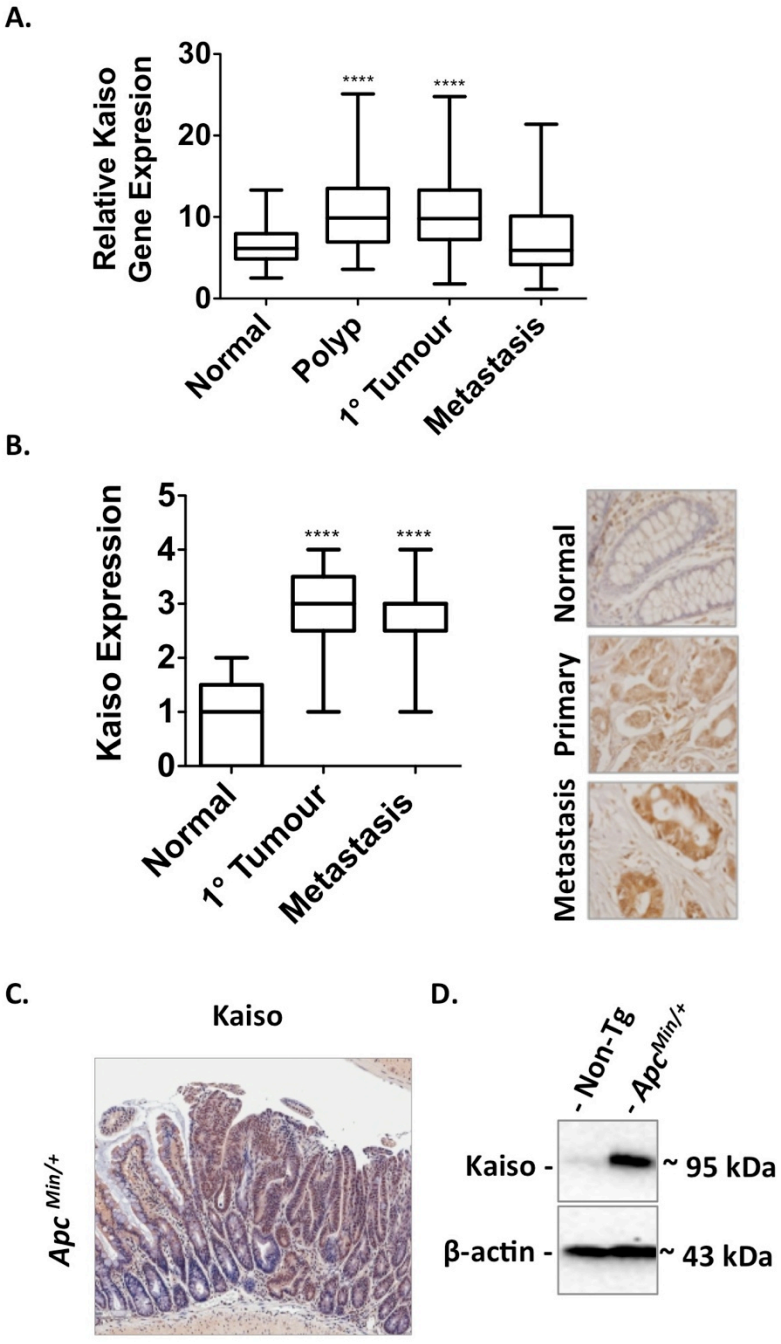
A.
Relative Kaiso Gene Expresion
30
20
10
0
****
****
Normal
Polyp
1° Tumour
Metastasis
B.
Kaiso Expression
5
4
3
2
1
0
****
****
Normal
1° Tumour
Metastasis
Normal
Primary
Metastasis
C.
Kaiso
Apc Min/+
D.
- Non-Tg
- ApcMin/+
Kaiso -
~ 95 kDa
β-actin -
~ 43 kDa

colorectal tumour tissues and 69 metastases (Higgins *et al.* 2003). *Kaiso* expression was significantly increased in polyps and primary tumours compared to normal tissues ($p<0.0001$ and $p<0.0001$, respectively) (Figure 4.1A). Kaiso expression was also increased in metastases, although this increase was not significant (Figure 4.1A). To complement our bioinformatics studies, we examined Kaiso expression in two colorectal cancer **t**issue **m**icro**a**rrays (TMAs) that consisted of 17 normal colon tissues, 60 primary tumour tissues and 40 metastases (US Biomax, MD, USA). In agreement with our bioinformatics analysis, Kaiso expression was largely absent or low in normal colon biopsies compared to primary tumour biopsies ($p< 0.0001$) where robust Kaiso staining was observed (Figure 4.1B). We also noted significantly increased Kaiso expression in metastases ($p< 0.0001$) (Figure 4.1B), suggesting that post-transcriptional mechanisms may further increase Kaiso expression in the context of metastatic CRC. No difference was observed in Kaiso expression between primary and metastatic tissues (Figure 4.1B).

We next examined Kaiso expression in $Apc^{Min/+}$ mice compared to non-transgenic (Non-Tg) mice. Since $Apc^{Min/+}$ mice develop polyps primarily in the small intestine (Fodde *et al.* 2001), we focused our studies on the small intestine unless otherwise stated. In agreement with our findings in human CRC tissues, nuclear Kaiso expression was increased in polyps relative to the surrounding intestinal epithelium (Figure 4.1C) and relative to that of Non-Tg mice (data not shown). Immunoblot analysis also confirmed increased expression of Kaiso in $Apc^{Min/+}$ intestinal homogenates compared to Non-Tg mice (Figure 4.1D). Combined, these findings suggest that Kaiso expression positively correlates with malignant progression in CRC.

Kaiso overexpression significantly attenuates the lifespan of $Apc^{Min/+}$ mice

Previous studies investigating the effect of Kaiso depletion on murine development demonstrated that *Kaiso*-null mice exhibited no deleterious developmental defects (Prokhortchouk *et al.* 2006). However, when *Kaiso*-null mice were mated with $Apc^{Min/+}$ mice the resultant progeny exhibited prolonged lifespan and decreased polyp size, although no change in polyp number was observed (Prokhortchouk *et al.* 2006).

To complement and extend the studies of Prokhortchouk *et al.*, we generated and characterized a mouse model expressing an intestinal-specific, murine myc-tagged Kaiso transgene (Chaudhary *et al.* 2013). We opted for a transgenic approach to overcome the potential effects of functional redundancy between Kaiso and the Kaiso-like proteins ZBTB4 and ZBTB38 that may have precluded effective resolution of Kaiso's role in the Kaiso knockout model. Up to 12 months of age, $Kaiso^{Tg/+}$ mice did not develop polyps, but they displayed crypt hyperplasia and dysplasia of varying severities (Chaudhary *et al.* 2013). To facilitate our investigation of Kaiso's role in intestinal tumorigenesis, we utilized the $Apc^{Min/+}$ model of colon cancer as a sensitized background and mated these mice with two independently generated $Kaiso^{Tg/+}$ lines to generate $Kaiso^{Tg/+}$:$Apc^{Min/+}$ mice. $Kaiso^{Tg/+}$ Line E mice express more ectopic Kaiso than $Kaiso^{Tg/+}$ Line A mice, indicative of a higher transgene copy number (Chaudhary *et al.* 2013). As expected, $Kaiso^{Tg/+}$:$Apc^{Min/+}$ mice exhibited robust nuclear Kaiso staining in both the polyps and the intestinal epithelium (Figure 4.2). However, Kaiso expression in $Kaiso^{Tg/+}$:$Apc^{Min/+}$ polyps was heterogeneous, with some cells expressing more Kaiso than others (Figure 4.2). Additionally, although Kaiso expression was increased in the crypts of

Figure 4.2: Kaiso is highly expressed in the villi and crypts of *Kaiso$^{Tg/+}$:Apc$^{Min/+}$* mice.

IHC analysis reveals high Kaiso expression in polyps, villi and crypts of *Apc$^{Min/+}$* and *Kaiso$^{Tg/+}$:Apc$^{Min/+}$* mice.

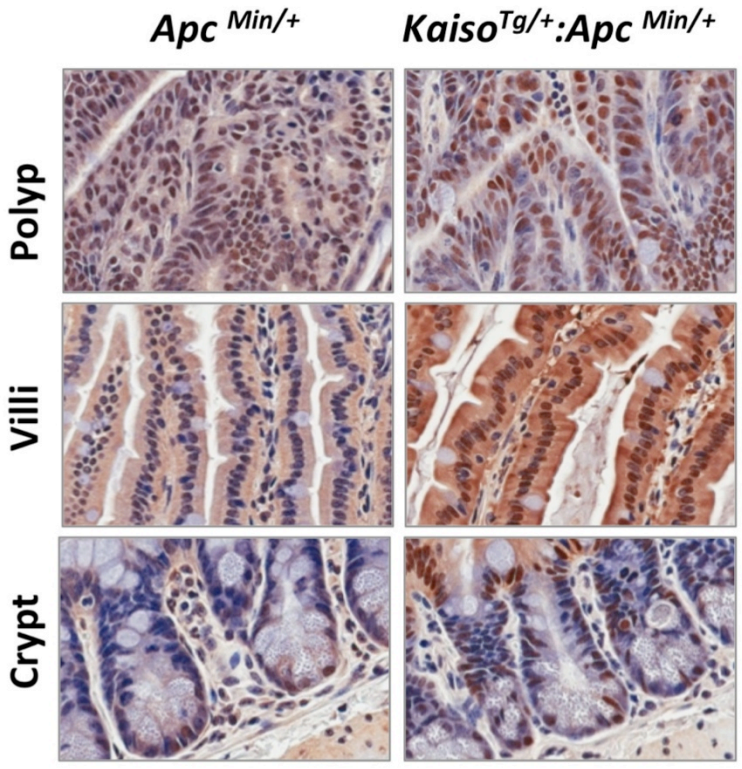
Apc Min/+
Kaiso Tg/+:Apc Min/+
Polyp
Villi
Crypt

Kaiso$^{Tg/+}$*:Apc*$^{Min/+}$ mice compared to *Apc*$^{Min/+}$ mice, crypt staining was not as pronounced as that observed in the villi, where both nuclear and cytoplasmic Kaiso was evident.

We recently reported that *Kaiso*$^{Tg/+}$ mice exhibited normal lifespan and that no intestinal polyps were detected in *Kaiso*$^{Tg/+}$ Line A mice up to one year of age although the mice exhibited crypt hyperplasia (Chaudhary *et al.* 2013). However, *Kaiso*$^{Tg/+}$*:Apc*$^{Min/+}$ mice exhibited significantly reduced lifespan compared to *Apc*$^{Min/+}$ mice ($p<0.0001$) in a dose-dependent manner, *i.e.* *Kaiso*$^{Tg/+}$*:Apc*$^{Min/+}$ Line E mice (high Kaiso expression) exhibited significantly reduced lifespan compared to *Kaiso*$^{Tg/+}$*:Apc*$^{Min/+}$ Line A mice (moderate Kaiso expression) ($p<0.05$), suggesting that increased transgene dosage resulted in a more severe phenotype (Figure 4.3A). Overall health, as indicated by weight and liver pigmentation, were also assessed in age-matched 90 day-old *Kaiso*$^{Tg/+}$*:Apc*$^{Min/+}$ and *Apc*$^{Min/+}$ mice, since loss of 15% of body mass and anemia are often used as endpoint indicators in *Apc*$^{Min/+}$ mice. At 90 days of age, both *Kaiso*$^{Tg/+}$*:Apc*$^{Min/+}$ Line A and Line E mice weighed less than their *Apc*$^{Min/+}$ counterparts (Figure 4.3B). No significant difference in weight between *Kaiso*$^{Tg/+}$*:Apc*$^{Min/+}$ Line A and Line E mice was observed, although the significantly diminished lifespan of *Kaiso*$^{Tg/+}$*:Apc*$^{Min/+}$ Line E mice precluded weight measurement of a larger sample size. Notably, *Kaiso*$^{Tg/+}$ Line E mice also weighed significantly less than their Non-Tg counterparts (Figure 4.3B), suggesting that ectopic Kaiso expression results in decreased weight even in the absence of the Min mutation. At 90 days of age, *Kaiso*$^{Tg/+}$*:Apc*$^{Min/+}$ mice exhibited decreased liver pigmentation, while *Apc*$^{Min/+}$ mice livers showed little to no loss of pigment (Figure 4.3C, Top Panel). We also noted that *Kaiso*$^{Tg/+}$*:Apc*$^{Min/+}$ mice

Figure 4.3: Lifespan of *Apc*$^{Min/+}$ mice is attenuated by ectopic Kaiso expression. (A) Kaplan-Meier survival curve comparing survival of *Apc*$^{Min/+}$ and *Kaiso*$^{Tg/+}$*:Apc*$^{Min/+}$ mice (Median survival *Apc*$^{Min/+}$= 161.5 days vs. *Kaiso*$^{Tg/+/}$*:Apc*$^{Min/+}$ Line A= 112.5 & Line E= 88.5 days; n≥8, Log rank test p<0.0001). **(B)** *Kaiso*$^{Tg/+}$*:Apc*$^{Min/+}$ Line A and Line E mice weigh significantly less than their *Apc*$^{Min/+}$ counterparts at 90 days of age. *Kaiso*$^{Tg/+}$ Line A and Line E mice also weigh less than their Non-Tg littermates at this age (n≥5). **(C)** Anemia and splenomegaly are enhanced in *Kaiso*$^{Tg/+}$*:Apc*$^{Min/+}$ mice as indicated by loss of liver pigment (top panel) and enlarged spleen (bottom panel). (**D)** Spleen weight is significantly increased in 90 day-old *Kaiso*$^{Tg/+}$*:Apc*$^{Min/+}$ mice. (* represents p≤0.05; ** represents p≤0.01; **** represents p<0.0001. Error bars indicate standard error of the mean)

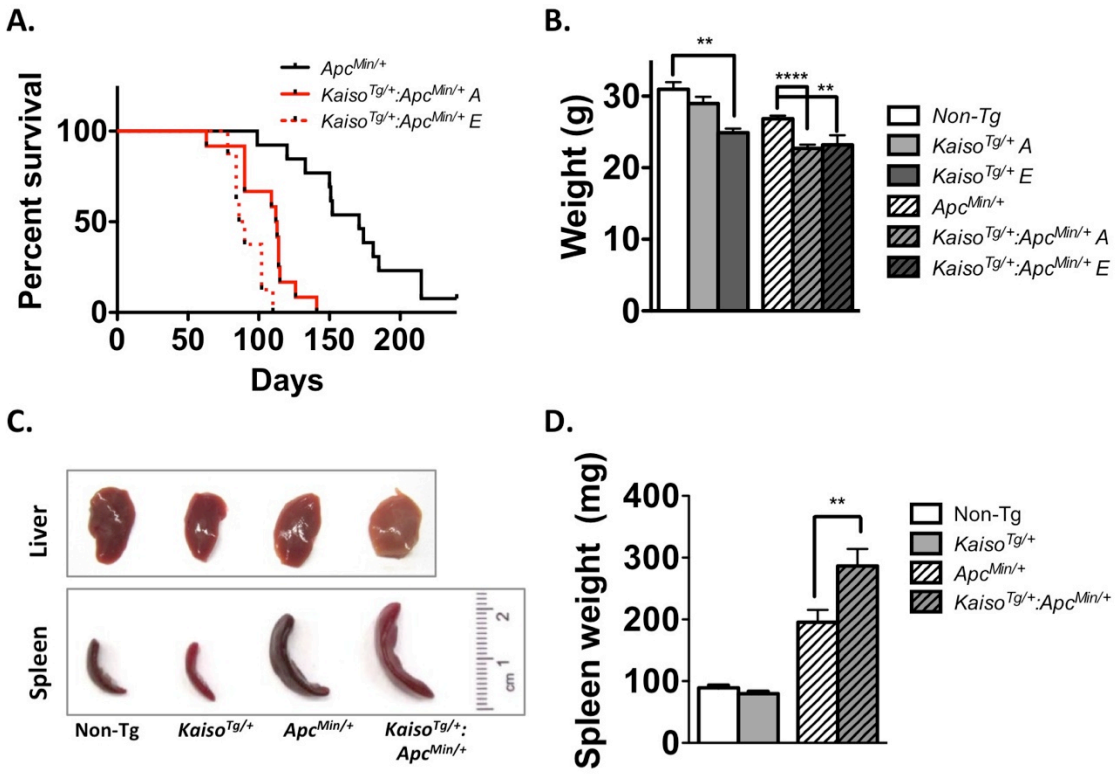
A.
Percent survival
100
50
0
0 50 100 150 200
Days
Apc^Min/+
Kaiso^Tg/+:Apc^Min/+ A
Kaiso^Tg/+:Apc^Min/+ E
B.
Weight (g)
30
20
10
0
**
****
**
Non-Tg
Kaiso^Tg/+ A
Kaiso^Tg/+ E
Apc^Min/+
Kaiso^Tg/+:Apc^Min/+ A
Kaiso^Tg/+:Apc^Min/+ E
C.
Liver
Spleen
cm 1 2
Non-Tg
Kaiso^Tg/+
Apc^Min/+
Kaiso^Tg/+: Apc^Min/+
D.
Spleen weight (mg)
400
300
200
100
0
**
Non-Tg
Kaiso^Tg/+
Apc^Min/+
Kaiso^Tg/+:Apc^Min/+

had grossly enlarged spleens, which weighed significantly more than spleens isolated from *Apc*$^{Min/+}$ mice (Figure 4.3C, Bottom Panel, Figure 4.3D). However the relevance, if any, of these enlarged spleens to the phenotype of *Kaiso*$^{Tg/+}$*:Apc*$^{Min/+}$ mice or CRC is unknown.

Polyp burden is increased in Kaiso$^{Tg/+}$:Apc$^{Min/+}$ mice

We next examined the polyp burden in *Kaiso*$^{Tg/+}$*:Apc*$^{Min/+}$ mice. Gross histological examination of the small intestines from *Kaiso*$^{Tg/+}$*:Apc*$^{Min/+}$ mice revealed extensive regions of focal atypical hyperplasia (Figure 4.4A, Panel i) and increased mitoses. Regions of atypical hyperplasia were also evident in *Apc*$^{Min/+}$ mice, albeit at a much lower frequency (Figure 4.4A, Panel ii). *Kaiso*$^{Tg/+}$*:Apc*$^{Min/+}$ mice also exhibited increased numbers of early adenomas and numerous formed adenomas, which were largely absent in *Apc*$^{Min/+}$ mice (Figure 4.4A, Panels i & ii). More importantly, *Kaiso*$^{Tg/+}$*:Apc*$^{Min/+}$ Line A mice exhibited ~2.5-fold more and Line E mice ~5-fold more polyps at death than *Apc*$^{Min/+}$ mice. At 90 days of age, *Kaiso*$^{Tg/+}$*:Apc*$^{Min/+}$ Line A mice exhibited ~3-fold more polyps than age-matched *Apc*$^{Min/+}$ mice, suggesting that increased Kaiso expression accelerates polyp onset (Figure 4.4B).

Kaiso$^{Tg/+}$*:Apc*$^{Min/+}$ polyps were significantly smaller than those of *Apc*$^{Min/+}$ mice at both 90 days of age and at death (~110 days), although this difference was more apparent at death (Figure 4.5A, Panel i). We postulated that the decreased polyp size in *Kaiso*$^{Tg/+}$*:Apc*$^{Min/+}$ mice may be attributed to the significantly shortened lifespan of these mice compared to their *Apc*$^{Min/+}$ counterparts. Indeed, the size distribution of polyps in

Figure 4.4: Ectopic Kaiso enhances polyp formation in *Apc*$^{Min/+}$ mice. (A) *Kaiso*$^{Tg/+}$*:Apc*$^{Min/+}$ mice exhibit extensive regions of focal atypical hyperplasia (i, ii, red arrowheads) and formed adenomas (i, white arrowhead) compared to their *Apc*$^{Min/+}$ counterparts (i), which exhibit mostly focal early adenomas (black arrowheads). **(B)** *Kaiso*$^{Tg/+}$*:Apc*$^{Min/+}$ mice exhibit significantly more polyps than *Apc*$^{Min/+}$ mice ($n \geq 6$). (** represents $p \leq 0.01$; **** represents $p < 0.0001$. Error bars indicate standard error of the mean)

A.

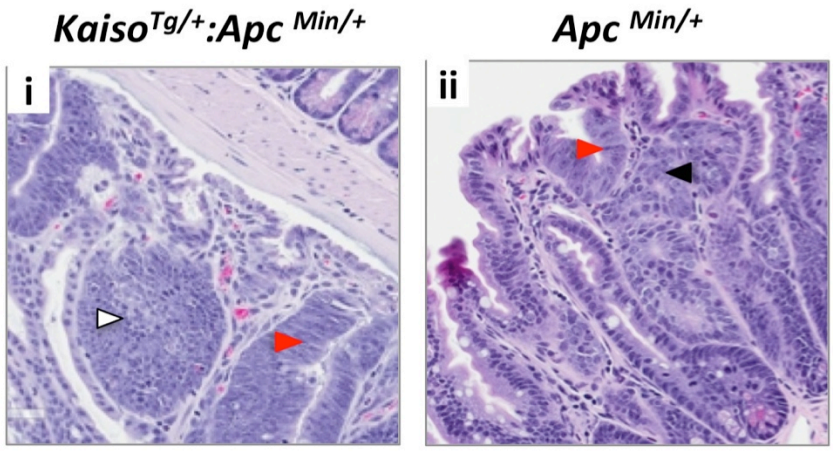
Kaiso Tg/+:Apc Min/+
Apc Min/+
i
ii

B.

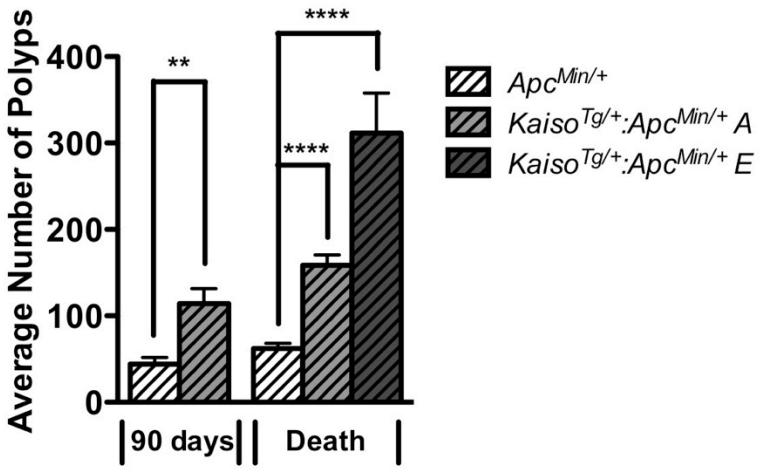
Average Number of Polyps
400
300
200
100
0
**
****
****
90 days
Death
Apc Min/+
Kaiso Tg/+:Apc Min/+ A
Kaiso Tg/+:Apc Min/+ E

Figure 4.5: *Kaiso*$^{Tg/+}$*:Apc*$^{Min/+}$ mice have smaller polyps than *Apc*$^{Min/+}$ mice at death. **(A)** Intestinal polyps of Line A and Line E *Kaiso*$^{Tg/+}$*:Apc*$^{Min/+}$ mice are significantly smaller than those of *Apc*$^{Min/+}$ mice (n≥292) (left panel). Age-matched *Apc*$^{Min/+}$ and *Kaiso*$^{Tg/+}$*:Apc*$^{Min/+}$ mice exhibit no difference in size distribution of polyps at 90 days of age (middle panel) but exhibit fewer polyps greater than 3 mm^2 at death (right panel). (**B)** Staining for the proliferation marker Ki67 revealed no change in proliferation in the crypts of *Apc*$^{Min/+}$ and *Kaiso*$^{Tg/+}$*:Apc*$^{Min/+}$ mice. (**C)** The percentage of apoptotic cells per polyp is greater in *Kaiso*$^{Tg/+}$*:Apc*$^{Min/+}$ mice. (* represents p≤0.05; ** represents p≤0.01; **** represents p<0.0001. Error bars indicate standard error of the mean)

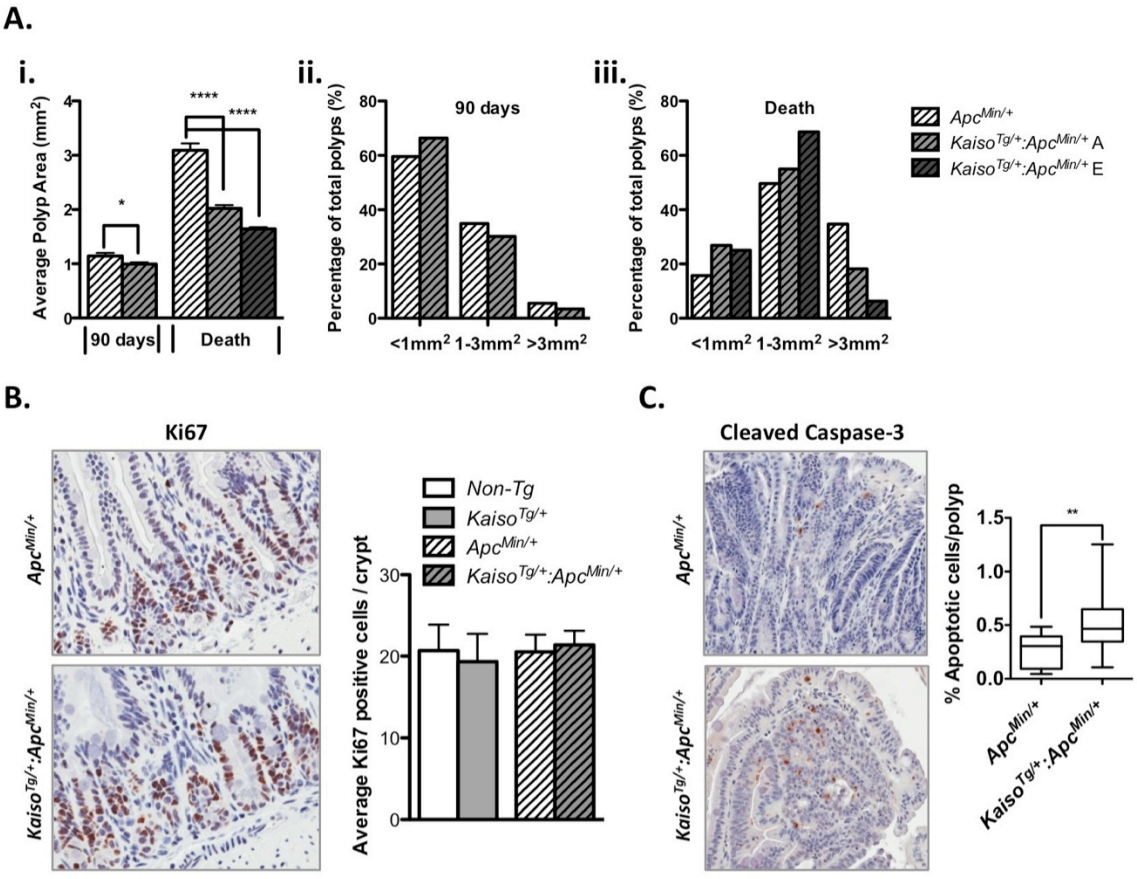
A.
i.
Average Polyp Area (mm²)
90 days
Death
ii.
Percentage of total polyps (%)
90 days
<1mm² 1-3mm² >3mm²
iii.
Percentage of total polyps (%)
Death
<1mm² 1-3mm² >3mm²
Apc^Min/+
Kaiso^Tg/+:Apc^Min/+ A
Kaiso^Tg/+:Apc^Min/+ E
B.
Ki67
Apc^Min/+
Kaiso^Tg/+:Apc^Min/+
Non-Tg
Kaiso^Tg/+
Apc^Min/+
Kaiso^Tg/+:Apc^Min/+
Average Ki67 positive cells / crypt
C.
Cleaved Caspase-3
Apc^Min/+
Kaiso^Tg/+:Apc^Min/+
% Apoptotic cells/polyp
Apc^Min/+
Kaiso^Tg/+:Apc^Min/+

Kaiso$^{Tg/+}$*:Apc*$^{Min/+}$ mice at 90 days of age was similar to that of *Apc*$^{Min/+}$ mice (Figure 4.5A, Panel ii). However, at death, *Kaiso*$^{Tg/+}$*:Apc*$^{Min/+}$ mice exhibited fewer polyps of 3 mm^2 or larger, but a greater proportion of polyps less than 1 mm^2 and 1-3 mm^2 compared to their *Apc*$^{Min/+}$ counterparts (Figure 4.5A, Panel iii).

Although the reduced polyp size in *Kaiso*$^{Tg/+}$*:Apc*$^{Min/+}$ mice could be attributed to their shortened lifespan, it remained possible that the reduced polyp size could also be attributed to decreased proliferation or increased apoptosis. Staining for the proliferation marker Ki67 revealed no difference in the proliferation rates of normal or polyp tissue between *Apc*$^{Min/+}$ and *Kaiso*$^{Tg/+}$*:Apc*$^{Min/+}$ mice at 90 days of age (Figure 4.5B). To measure apoptosis, intestinal sections were stained for cleaved caspase-3 (Gunther *et al.* 2013) and the percentage of apoptotic cells/polyp determined. *Kaiso*$^{Tg/+}$*:Apc*$^{Min/+}$ mice exhibited more cleaved caspase-3-positive cells than *Apc*$^{Min/+}$ *mice*, suggesting that ectopic Kaiso expression increases apoptosis in intestinal polyps resulting in the decreased polyp size seen in *Kaiso*$^{Tg/+}$*:Apc*$^{Min/+}$ mice (Figure 4.5C).

Wnt signaling is up-regulated upon ectopic expression of Kaiso

Our finding that ectopic Kaiso expression increases polyp burden while Kaiso loss delays polyp onset in the *Kaiso*$^{Tg/+}$*:Apc*$^{Min/+}$ mice model (Prokhortchouk *et al.* 2006) is paradoxical in light of previous studies where Kaiso has been implicated as a negative regulator of canonical Wnt signaling (Park *et al.* 2005; Ruzov *et al.* 2009). Our findings in the *Kaiso*$^{Tg/+}$*:Apc*$^{Min/+}$ mice model raised the possibility that Kaiso's role as a negative regulator of Wnt signaling may be context dependent. To clarify Kaiso's function in regulating Wnt signaling in the intestine we examined the effect of ectopic Kaiso

expression on Wnt target gene expression. *Kaiso*$^{Tg/+}$ mice were crossed with heterozygous *Axin2*^{lacZ} mice, a Wnt reporter line in which the DNA sequence encoding a nuclear-localized β-galactosidase (NLS-*lacZ*) is inserted in-frame into exon 2 of the endogenous *Axin2* gene (Lustig *et al.* 2002). Surprisingly, *Axin2*^{lacZ}*:Kaiso*$^{Tg/+}$ mice exhibited increased expression of β-galactosidase compared to *Axin2*^{lacZ} mice (Figure 4.6A). Consistent with this finding, *Kaiso*$^{Tg/+}$ mice and *Kaiso*$^{Tg/+}$*:Apc*$^{Min/+}$ mice exhibited increased staining for the Wnt target gene MMP-7 compared to control mice (Figure 4.6B). To confirm that Kaiso was positively regulating Wnt/β-catenin target gene expression in murine intestines, we examined the mRNA expression of four established Wnt target genes (*MMP7*, *Axin2, CD44* and *EphB2)* in the intestine by using qRT-PCR. The expression of all four target genes was significantly increased in *Kaiso*$^{Tg/+}$*:Apc*$^{Min/+}$ mice relative to control mice, ($p < 0.05$) (Figure 4.6C). *Kaiso*$^{Tg/+}$ mice also exhibited increased expression of all four target genes, although these changes were not significant (Figure 4.6C). Expression of β-catenin was mildly elevated in *Kaiso*$^{Tg/+}$ and *Kaiso*$^{Tg/+}$*:Apc*$^{Min/+}$ mice (Appendix Figure 1), and expression of the Wnt pathway antagonist *Lect2* was significantly decreased in *Kaiso*$^{Tg/+}$ mice relative to Non-Tg mice (Figure 4.6D). Collectively, these data suggest that Kaiso's transcriptional repression effects on Wnt signaling are context-dependent and are not maintained in the *Apc*$^{Min/+}$ model.

Kaiso induces inflammation in Apc$^{Min/+}$ mice

Previously, we found that 12 month-old *Kaiso*$^{Tg/+}$ mice exhibited signs of chronic intestinal inflammation, *i.e.* villi blunting, leukocyte infiltration and neutrophil activation (Chaudhary *et al.* 2013) but it was unclear whether the Kaiso-induced inflammation

Figure 4.6: Kaiso potentiates Wnt signaling in the intestine: (A) *Axin2*^{lacZ}:*Kaiso*$^{Tg/+}$ mice exhibit increased Wnt reporter activity. (**B)** MMP7 expression is increased in *Kaiso*$^{Tg/+}$ and *Kaiso*$^{Tg/+}$*:Apc*$^{Min/+}$ mice relative to their respective controls (non-transgenic or *Apc*$^{Min/+}$). (**C)** mRNA expression of Wnt target genes in *Kaiso*$^{Tg/+}$, *Kaiso*$^{Tg/+}$*:Apc*$^{Min/+}$ and control mice. (**D)** Expression of the Wnt antagonist Lect2 is reduced in *Kaiso*$^{Tg/+}$ mice. (* represents $p \leq 0.05$; *** represents $p \leq 0.001$; **** represents $p < 0.0001$. Error bars indicate standard error of the mean)

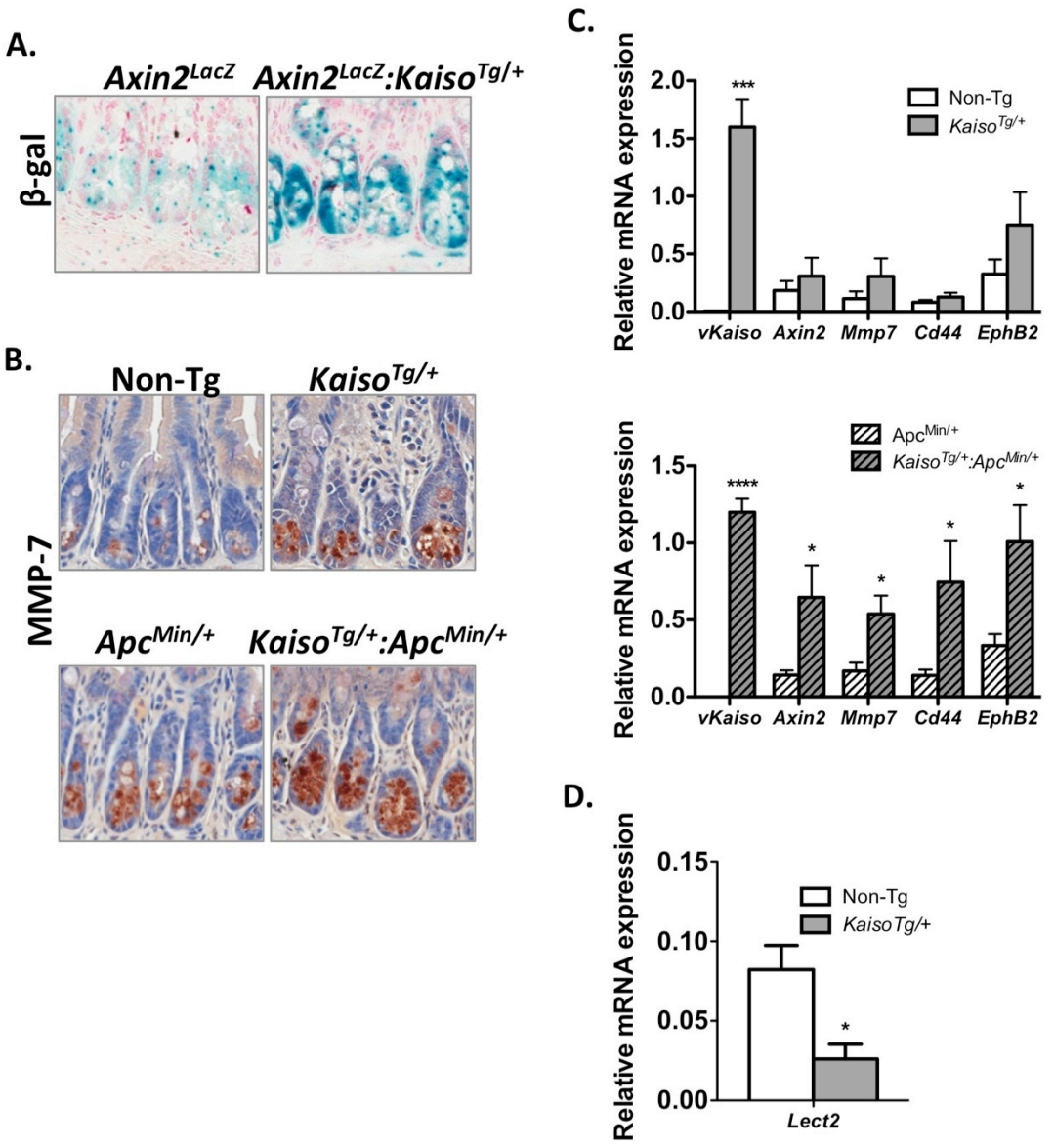
A.
Axin2LacZ
Axin2LacZ:KaisoTg/+
β-gal
B.
Non-Tg
KaisoTg/+
MMP-7
ApcMin/+
KaisoTg/+:ApcMin/+
C.
Relative mRNA expression
2.0
1.5
1.0
0.5
0.0
***
Non-Tg
KaisoTg/+
vKaiso
Axin2
Mmp7
Cd44
EphB2
ApcMin/+
KaisoTg/+:ApcMin/+
****
*
D.
0.15
0.10
0.05
0.00
Non-Tg
KaisoTg/+
Lect2

occurred at younger ages. When we examined the ileum of 90 day-old Line A *Kaiso*$^{Tg/+}$ mice (when intestinal polyps are already well-developed in *Kaiso*$^{Tg/+}$*:Apc*$^{Min/+}$ mice), an intestinal inflammation phenotype was evident, albeit at a lower frequency than that observed in older mice (Figure 4.7A). Extensive macrophage recruitment was also evident in inflamed epithelia overlying Peyer's patches in the ileum of Line A *Kaiso*$^{Tg/+}$ mice as measured by F4/80 staining (Figure 4.7B). We also noticed several crypt abscesses in our *Kaiso*$^{Tg/+}$*:Apc*$^{Min/+}$ mice (Figure 4.7C), reminiscent of those frequently observed in the colon of patients with IBD. However, abscesses were completely absent in both Line A *Kaiso*$^{Tg/+}$ and *Apc*$^{Min/+}$ mice.

We next performed an MPO assay on intestinal homogenates to assess neutrophil activation as a surrogate marker for inflammation. No significant change in MPO activity was observed in 90 day-old *Kaiso*$^{Tg/+}$ mice relative to Non-Tg mice (data not shown), but a 6-fold increase in activity was observed in 90 day-old *Kaiso*$^{Tg/+}$*:Apc*$^{Min/+}$ mice relative to *Apc*$^{Min/+}$ mice (Figure 4.7D). Several pro-inflammatory cytokines and chemokines associated with innate immunity were also enriched in *Kaiso*$^{Tg/+}$*:Apc*$^{Min/+}$ intestinal homogenates, namely granulocyte stimulating factors GM-CSF and G-CSF, eotaxin, IL-3, IL-7, LIF, MCP-1 and MIP1B (Figure 4.7E). Collectively these data suggest that the increased polyp burden in *Kaiso*$^{Tg/+}$*:Apc*$^{Min/+}$ mice may in part be due to Kaiso-induced intestinal inflammation.

Figure 4.7: *Kaiso*$^{Tg/+}$*:Apc*$^{Min/+}$ mice exhibit intestinal inflammation. (A) H&E image showing villi blunting (black arrowhead), villi fusion (red arrow head) and immune cell infiltration of the lamina propria (red dotted line) in 90 day-old *Kaiso*$^{Tg/+}$mice, phenotypes that are absent in age-matched Non-Tg mice. (**B)** F4/80 staining for macrophages and activated monocytes show recruitment of these immune cells to a Peyer's patch in an inflamed region in the ileum of 90 day-old *Kaiso*$^{Tg/+}$. (**C)** H&E image of crypt abscesses observed in *Kaiso*$^{Tg/+}$*:Apc*$^{Min/+}$ mice. (**D)** MPO activity is increased in small and large intestines (SI & LI) of *Kaiso*$^{Tg/+}$*:Apc*$^{Min/+}$ mice. (**E)** Pro-inflammatory cytokines are upregulated in *Kaiso*$^{Tg/+}$*:Apc*$^{Min/+}$ mice. (* represents $p \leq 0.05$; ** represents $p \leq 0.01$; *** represents $p \leq 0.001$; **** represents $p < 0.0001$. Error bars indicate standard error of the mean)

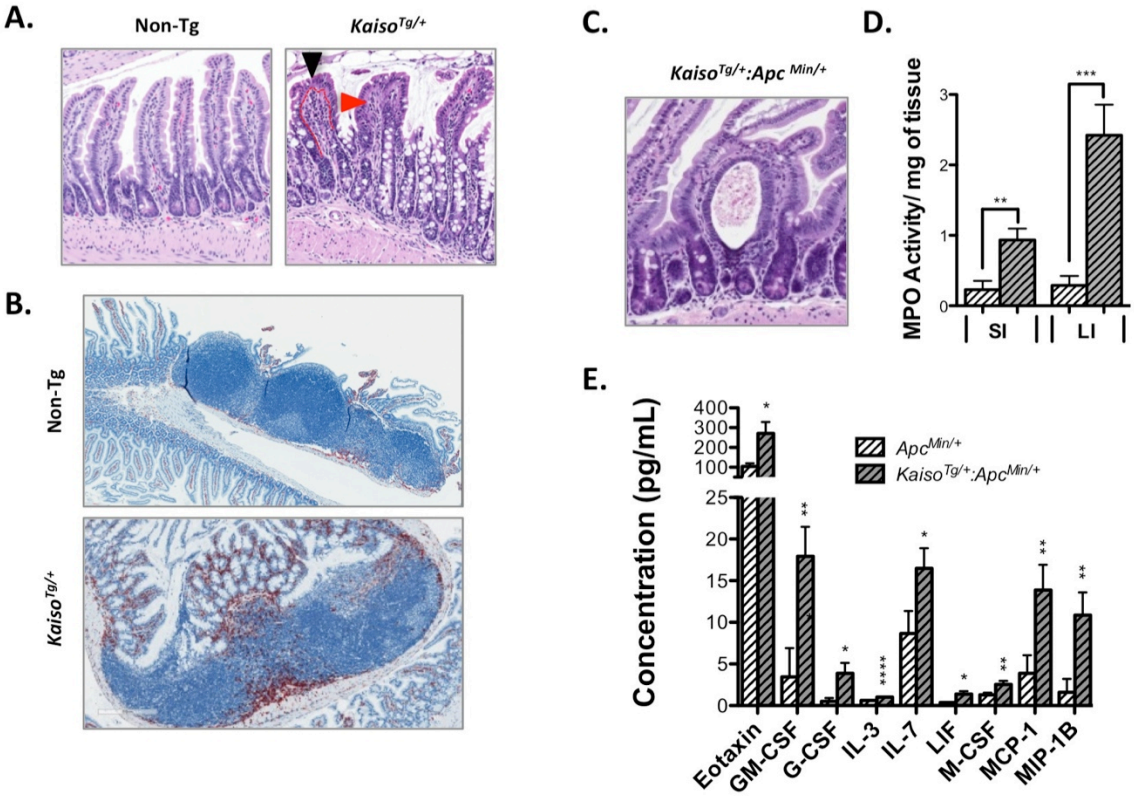
A.
Non-Tg
Kaiso Tg/+
B.
Non-Tg
Kaiso Tg/+
C.
Kaiso Tg/+:Apc Min/+
D.
MPO Activity/ mg of tissue
SI
LI
E.
Concentration (pg/mL)
Apc Min/+
Kaiso Tg/+:Apc Min/+
Eotaxin
GM-CSF
G-CSF
IL-3
IL-7
LIF
M-CSF
MCP-1
MIP-1B

DISCUSSION

Kaiso has been implicated in the development and progression of several human cancers, including colorectal cancer (Soubry *et al.* 2005; van Roy and McCrea 2005; Prokhortchouk *et al.* 2006; Lopes *et al.* 2008; Dai *et al.* 2009; Dai *et al.* 2010; Zhang *et al.* 2011; Cofre *et al.* 2012; Donaldson *et al.* 2012; Jones *et al.* 2012; Vermeulen *et al.* 2012). To date however, most cancer-related studies examining Kaiso's role have been largely correlative (Soubry *et al.* 2005; Prokhortchouk *et al.* 2006; Dai *et al.* 2009; Dai *et al.* 2010; Vermeulen *et al.* 2012), while studies offering mechanistic insights have been performed primarily in mammalian cultured cells (van Roy and McCrea 2005; Lopes *et al.* 2008; Zhang *et al.* 2011; Cofre *et al.* 2012; Jones *et al.* 2012). Here, we describe the first study to examine a potential mechanistic role of Kaiso in colorectal cancer using the $Apc^{Min/+}$ mouse model of intestinal cancer.

As previously reported, Kaiso deletion extends the lifespan of $Apc^{Min/+}$ mice (Prokhortchouk *et al.* 2006). Therefore, our finding that ectopic Kaiso expression decreases the lifespan of $Apc^{Min/+}$ mice was not surprising. However, unlike the Prokhortchouk *et al.* study, which reported no difference in the number of polyps between *Kaiso*-null $Apc^{Min/+}$ and $Apc^{Min/+}$ mice (Prokhortchouk *et al.* 2006), we found increased polyp multiplicity in $Kaiso^{Tg/+}$:$Apc^{Min/+}$ compared to $Apc^{Min/+}$ mice. Notwithstanding the disadvantages associated with the use of transgenic mouse models, our study highlights one advantage of the $Kaiso^{Tg/+}$ model; namely that certain effects arising from Kaiso depletion models may be masked due to the existence of the Kaiso-like proteins (ZBTB4 and ZBTB38) or other methyl-DNA-binding proteins that may function redundantly with

Kaiso (Sasai *et al.* 2010). Indeed, this may explain why *Kaiso*$^{Tg/+}$*:Apc*$^{Min/+}$ mice exhibited more polyps than *Apc*$^{Min/+}$ mice, while *Kaiso*-null *Apc*$^{Min/+}$ mice did not exhibit the opposite effect (*i.e.* less polyps) (Prokhortchouk *et al.* 2006). The finding that ectopic Kaiso expression increases polyp number but decreases polyp size was surprising, since typically polyp number and size are positively correlated. *Kaiso*$^{Tg/+}$*:Apc*$^{Min/+}$ mice exhibit histologically more advanced tumours than age-matched *Apc*$^{Min/+}$ mice, although there was no difference in tumour proliferation rate, suggesting that *Kaiso*$^{Tg/+}$*:Apc*$^{Min/+}$ mice tumours form earlier. Although the significantly shortened lifespan of *Kaiso*$^{Tg/+}$*:Apc*$^{Min/+}$ mice may account for the smaller tumour size, the recent report that Kaiso promotes p53-dependent apoptosis (Koh *et al.* 2014), coupled with our observation of increased apoptotic cells in *Kaiso*$^{Tg/+}$*:Apc*$^{Min/+}$ polyps, suggests that the smaller polyps observed in *Kaiso*$^{Tg/+}$*:Apc*$^{Min/+}$ mice may be due, at least in part, to an increase in apoptosis.

Consistent with our previous findings that *Kaiso*$^{Tg/+}$ mice exhibited intestinal inflammation, *Kaiso*$^{Tg/+}$*:Apc*$^{Min/+}$ mice likewise exhibited enhanced intestinal inflammation. The onset of inflammation seems to be accelerated in the presence of the *Min* allele, consistent with reports that polyp formation is accompanied by increased inflammation in *Apc*$^{Min/+}$ mice (McClellan *et al.* 2012). Although a thorough investigation of the mechanism by which Kaiso promotes inflammation is beyond the scope of this study, it is possible that Kaiso's role in inflammation may be linked to its binding partner p120^{ctn}. Recent studies have characterized p120^{ctn} as an anti-inflammatory mediator in several tissues, including the intestine (Perez-Moreno *et al.* 2006; Smalley-Freed *et al.* 2010; Smalley-Freed *et al.* 2011; Stairs *et al.* 2011; Hu 2012). Conditional depletion of

p120^{ctn} in the murine intestine results in acute inflammation and lethality at less than 21 days of age (Smalley-Freed *et al.* 2010), while limited p120^{ctn} ablation (~15% of the intestinal epithelium) results in chronic inflammation and adenoma formation (Smalley-Freed *et al.* 2011). While the cause of inflammation following p120^{ctn} depletion in the intestine is not fully understood, significant barrier defects due to decreased E-cadherin expression may be a contributing factor (Smalley-Freed *et al.* 2011). Remarkably, *Kaiso*$^{Tg/+}$ mice also exhibit a barrier defect, but there was no apparent decrease in p120^{ctn} or E-cadherin expression, suggesting that the barrier defect in *Kaiso*$^{Tg/+}$ mice may be a consequence rather than a cause of inflammation (our unpublished data). Ongoing studies are focused on characterizing the interplay between Kaiso and p120^{ctn} in regulating inflammation in the intestine.

One major goal of this study was to clarify whether Kaiso's function as a negative regulator of the Wnt signaling pathway is maintained in the murine intestine. We found that contrary to findings in *Xenopus* embryos and mammalian cultured cells (Park *et al.* 2005; Ruzov *et al.* 2009; Del Valle-Perez *et al.* 2011), ectopic Kaiso expression increased Wnt target gene expression. While this was initially surprising and unexpected, such an outcome could be explained by the fact that Kaiso has both transcriptional repression and activation roles (Rodova *et al.* 2004; Kelly and Daniel 2006). Alternately, the active Wnt signaling in mammalian intestines may be promoting p120^{ctn}'s interaction with Kaiso and relieving Kaiso's inhibition of β-catenin/TCF transcriptional activation, as recently observed by del Valle-Perez *et al.* (Del Valle-Perez *et al.* 2011). Such a possibility is also consistent with the *Xenopus* models proposed by Ruzov *et al.* (Ruzov *et al.* 2009), who

suggest that the interaction between Kaiso and Tcf results in their mutual disengagement from Wnt target genes. Since Wnt signaling is most active in the intestinal crypts where it regulates the proliferation and differentiation of intestinal stem cells (Gregorieff and Clevers 2005), it is conceivable that the active Wnt signaling in intestinal crypts promotes Kaiso's dissociation from Tcf4, thereby inhibiting Kaiso's repressive effects on Wnt target genes. However, since the majority of polyps in $Apc^{Min/+}$ mice have undergone a loss of heterozygosity at the *Apc* locus (Fodde and Smits 2001), the increased Wnt target gene expression observed in $Kaiso^{Tg/+}$:$Apc^{Min/+}$ mice may be also partially attributed to the significantly higher polyp burden.

An additional explanation for Kaiso's potentiation of Wnt signaling in the murine intestine may involve Kaiso's role in epigenetic or methylation-dependent gene silencing (Prokhortchouk and Hendrich 2002; Filion *et al.* 2006). Multiple Wnt antagonists including SFRPs and DKK1 are downregulated through promoter hypermethylation in colorectal cancer (Sato *et al.* 2007; Phesse *et al.* 2008; Samuel *et al.* 2009; Zhang *et al.* 2014). Intriguingly, the methylated DNA binding protein MBD2 binds and regulates the modestly characterized Wnt pathway repressor *Lect2,* which functions to repress Wnt target gene expression at or below the level of TCF (Phesse *et al.* 2008). Our detection of decreased *Lect2* mRNA expression in $Kaiso^{Tg/+}$ mice suggests that Kaiso's stimulatory effect on Wnt signaling may be attributed to Kaiso-mediated methylation-dependent silencing of Wnt pathway antagonists.

In conclusion, the correlation between increased Kaiso expression and neoplastic progression in human colorectal cancer tissues, coupled with our findings that Kaiso

overexpression potentiates Wnt-mediated polyp formation, Wnt target gene expression and inflammation in $Apc^{Min/+}$ mice, suggest that Kaiso may function in several distinct oncogenic capacities in colorectal cancer pathogenesis.

ACKNOWLEDGEMENTS

We would like to thank Dr. Albert Reynolds (Vanderbilt University) for supplying us with Kaiso rabbit polyclonal antibody, Dr. Balasubramanyam Karanam (Tuskeegee University) for staining the CRC tissue microarrays and Mr. Kyster Nanan for generating the $Kaiso^{Tg/+}$ Line A mice.

CHAPTER 5

Kaiso represses the cell cycle gene cyclinD1 via sequence-specific and methyl-CpG-dependent mechanisms.

Preface:

This chapter consists of the following article in its originally published format: ***"Kaiso represses the cell cycle gene cyclinD1 via sequence-specific and methyl-CpG-dependent mechanisms"***, by Donaldson NS, Pierre CC, Anstey MI, Robinson SC, Weerawardane SM, Daniel JM. (PLoS One. 2012;7(11):e50398). This is an open-access article distributed under the terms of the Creative Commons Attribution License, which permits unrestricted use, distribution, and reproduction in any medium, provided the original author and source are credited.

In this study, we characterized *cyclinD1* as a Kaiso target gene and examined the mechanism via which Kaiso binds to the *cyclinD1* promoter. We found that Kaiso associates with the *cyclinD1* promoter by binding to both a KBS and methylated CpG dinucleotides located in the promoter region. Importantly, Kaiso depletion in HCT-116 colon carcinoma cells resulted in increased *cyclinD1* expression and increased proliferation, validating *cyclinD1* as a Kaiso target gene.

Contributions:

Dr. Nickett Donaldson wrote the manuscript and performed experiments featured in Figures 5.1D, 5.2C, 5.3, 5.5 and 5.6. Christina Pierre performed the EMSA experiment in Figure 5.4, and assisted with experiments depicted in Figures 5.1D, 5.2C, 5.3B, 5.5 and 5.6. Michelle Anstey performed the EMSA experiments in Figures 5.1A and 5.2B. Shaiya

Robinson performed the western blot in Figure 5.7A and Sonali Weerawardane performed the MTT cell proliferation assay in Figure 5.7B. Dr. Juliet Daniel provided significant intellectual input and guidance throughout the execution of this work and edited the manuscript.

OPEN ACCESS Freely available online PLOS ONE

Kaiso Represses the Cell Cycle Gene *cyclin D1* via Sequence-Specific and Methyl-CpG-Dependent Mechanisms

Nickett S. Donaldson[☽], Christina C. Pierre[☽], Michelle I. Anstey, Shaiya C. Robinson, Sonali M. Weerawardane, Juliet M. Daniel*

Department of Biology, McMaster University, Hamilton, Ontario, Canada

Abstract

Kaiso is the first member of the POZ family of zinc finger transcription factors reported to bind DNA with dual-specificity in both a sequence- and methyl-CpG-specific manner. Here, we report that Kaiso associates with and regulates the *cyclin D1* promoter via the consensus **K**aiso **b**inding **s**ite (KBS), and also via methylated CpG-dinucleotides. The methyl-CpG sites appear critical for Kaiso binding to the *cyclin D1* promoter, while a core KBS in close proximity to the methyl-CpGs appears to stabilize Kaiso DNA binding. Kaiso's binding to both sites was demonstrated *in vitro* using **e**lectrophoretic **m**obility **s**hift **a**ssays (EMSA) and *in vivo* using **Ch**romatin **i**mmuno**p**recipitation (ChIP). To elucidate the functional relevance of Kaiso's binding to the *cyclin D1* promoter, we assessed Kaiso overexpression effects on a minimal *cyclin D1* promoter-reporter that contains both KBS and CpG sites. Kaiso repressed this minimal *cyclin D1* promoter-reporter in a dose-dependent manner and transcriptional repression occurred in a KBS-specific and methyl-CpG-dependent manner. Collectively our data validates *cyclin D1* as a Kaiso target gene and demonstrates a mechanism for Kaiso binding and regulation of the *cyclin D1* promoter. Our data also provides a mechanistic basis for how Kaiso may regulate other target genes whose promoters possess both KBS and methyl-CpG sites.

Citation: Donaldson NS, Pierre CC, Anstey MI, Robinson SC, Weerawardane SM, et al. (2012) Kaiso Represses the Cell Cycle Gene *cyclin D1* via Sequence-Specific and Methyl-CpG-Dependent Mechanisms. PLoS ONE 7(11): e50398. doi:10.1371/journal.pone.0050398

Editor: Pierre-Antoine Defossez, Université Paris-Diderot, France

Received June 14, 2012; **Accepted** October 19, 2012; **Published** November 30, 2012

Funding: This work was funded by Canadian Institutes of Health Research (CIHR) Grant # MOP-84320 to Dr. Juliet Daniel. Dr. Nickett S. Donaldson was a recipient of an Ontario Graduate Fellowship, an Ontario Graduate Scholarship in Science and Technology and an Ontario Graduate Scholarship. Michelle Anstey was the recipient of a DOD Breast Cancer Predoctoral Scholarship. The funders had no role in study design, data collection and analysis, decision to publish, or preparation of the manuscript.

Competing Interests: The authors have declared that no competing interests exist.

* E-mail: danielj@mcmaster.ca

☽ These authors contributed equally to this work.

Introduction

In the past decade, increasing evidence has revealed an important role for epigenetic modifications such as DNA methylation in the regulation of gene expression, reviewed in [1,2]. Specifically, the methylation of cytosine bases in CpG-dinucleotides within gene promoters plays a key role in transcriptional repression of various target genes that are implicated in many human diseases including cancer [1,2,3]. These promoter-associated methylated CpG-dinucleotides are recognized and bound by proteins that can distinguish between methylated and non-methylated CpG sites [4]. Until recently, the vast majority of methyl-DNA binding proteins were characterized by the presence of a **m**ethyl-DNA **b**inding **d**omain (MBD) [4]. However, several recent studies revealed that other protein families also possess methyl-DNA binding abilities, reviewed in [4,5]. For example, the novel **Po**x virus and **z**inc **f**inger (POZ-ZF) transcription factor Kaiso and its Kaiso-like relatives, ZBTB4 and ZBTB38, recognize and bind methylated CpG-dinucleotides and repress transcription via these methylated-CpG sites [5,6,7]. However Kaiso, ZBTB4 and ZBTB38 all lack an MBD [6,7]. Interestingly, Kaiso and ZBTB4 also bind DNA in a sequence-specific manner via the consensus **K**aiso **b**inding **s**ite (KBS; TCCTGCNA, where N is any nucleotide) and this distinguishes them as unique dual-specificity transcription factors [6,8]. Of these three proteins, Kaiso is the best characterized and represses target genes that are causally linked to vertebrate development and tumorigenesis [5,9,10,11,12,13,14].

Kaiso was originally discovered as a binding partner for the Src kinase substrate and cell adhesion catenin cofactor $p120^{ctn}$ [15]. This interaction was reminiscent of the β-catenin-TCF interaction that plays a crucial role in canonical WNT signaling [16,17]; indeed, we and others found that Kaiso represses a subset of Wnt target genes while $p120^{ctn}$'s interaction with Kaiso relieves Kaiso-mediated transcriptional repression [9,10,12]. Kaiso is a member of the POZ-ZF family of transcription factors that play important roles in vertebrate development and tumorigenesis [18]. Structurally, Kaiso possesses the characteristic protein-protein interaction POZ domain at its N-terminus and three C_2H_2-type DNA-binding zinc fingers at its C-terminus [15]. It is through these zinc fingers that Kaiso binds DNA with dual-specificity via the sequence-specific KBS or methylated CpG-dinucleotides to exert its gene regulatory effects [11,12,14,19]. For example, Kaiso represses *Wnt 11* [9] and the matrix metalloprotease gene *matrilysin* in a sequence-

specific manner [12], whereas it represses the *metastasis-associated gene 2* (*MTA2*) in a methyl CpG-dependent manner [14]. The importance of the methylation-dependent versus sequence-specific transcriptional regulation by Kaiso remains controversial. Thus, we initiated studies to characterize the Wnt signaling target and cell cycle regulator gene *cyclin D1* as a putative Kaiso target gene, because its promoter possessed both sequence-specific KBS's and CpG-dinucleotide rich regions. Although previous studies in *Xenopus* and human lung tumor cells have implicated *cyclin D1* as a putative Kaiso target gene [10,20], the direct mechanism(s) by which Kaiso binds and negatively regulates *cyclin D1* expression remain unknown.

Here we demonstrate that Kaiso binds directly to the *cyclin D1* promoter in a KBS sequence-specific or methyl-CpG-dependent manner. ChIP assays confirmed an endogenous association between Kaiso and the *cyclin D1* promoter, and our minimal promoter-reporter assays demonstrate that Kaiso represses *cyclin D1* promoter-driven luciferase activity. Importantly, Kaiso's ability to repress the minimal *cyclin D1* promoter-reporter was abolished upon mutation of the KBS and in the absence of CpG methylation. Collectively, our data demonstrate that Kaiso transcriptionally represses the cell cycle regulator *cyclin D1*, and suggest that *cyclin D1* is a *bona fide* Kaiso target gene regulated by Kaiso's dual-specificity mechanisms. Our study also shows that Kaiso's sequence-specific and methylation-dependent DNA binding and transcriptional regulation may not be mutually exclusive events but instead may function to fine-tune gene expression and/or expand the repertoire of genes regulated by Kaiso.

Materials and Methods

Cell Culture

Human MCF7 (breast carcinoma) and HCT 116 (colon carcinoma) cells were purchased from ATCC (Manassas, VA) and grown in Dulbecco's Modified Eagles medium (DMEM) (Hyclone) supplemented with 4 mM L-glutamine, 100 U/ml penicillin, 100 μg/ml streptomycin (Invitrogen, Life Technologies, Grand Island, NY), 10% fetal bovine serum (Hyclone) and 0.5 μg/ml fungizone (Invitrogen/Life Technologies). The cells were grown at 37°C and 5% CO_2 in a humidified incubator. For 5-azacytidine treatment, cells were incubated in 5 μM 5-azacytidine (Sigma Aldrich) in serum supplemented DMEM for 72 hours. Due to the short half-life of 5-azacytidine in solution, fresh serum supplemented DMEM with 5-azacytidine to a final concentration of 5 μM was replenished every 24 hours during the 72-hour incubation period.

Electrophoretic Mobility Shift Assay (EMSA)

Double-stranded oligonucleotides spanning the appropriate KBS or CpG sites in the *cyclin D1* promoter were annealed, radiolabelled and purified as previously described [21]. The -1067 KBS probe (5′ TTATGC**CG**GC*TCCTGCCA*GCCCCCT-CA**CG**C 3′) contained the consensus Kaiso binding site (*TCCTGCNA*, underlined and italicized) and two CpG-dinucleotides (**bold**) while the +69 KBS probe (5′ CTGT**CG**G**CG**CAG-*TAGCAG***CG**AGCAGCAGAG 3′) contained the core KBS (*CTGCNA*) and three CpG-dinucleotides (**bold**). The *cyclin D1* promoter-derived CpG oligonucleotide sequences used in this study are listed in Table 1. In brief, the CpG and +69 KBS oligonucleotides were methylated using *Sss1* methyltransferase according to the manufacturer's protocol (New England Biolabs - NEB, Ipswich, MA). The oligonucleotides were end-labeled at 37°C for 45 minutes with [γ-^{32}P] ATP using polynucleotide kinase (NEB). Both un-methylated and methylated radiolabelled oligonucleotides were purified on a TE-10 column (Clontech, Mountain View, CA) and radioactivity was quantitated on a Tri-Carb 2900TR scintillation analyzer (Perkin Elmer). 30,000 cpm of each labeled probe was incubated with the specified bacterially-expressed GST-Kaiso fusion proteins in 1X binding buffer (25 mM HEPES, 100 mM KCl, 1 mM EDTA, 10 mM $MgCl_2$, 0.1% NP40, 5% glycerol & 1 mM DTT) on ice for 30 minutes followed by incubation at room temperature for 30 minutes. Each reaction was loaded onto a 4% polyacrylamide gel in 0.5X TBE (45 mM Tris Borate, 1 mM EDTA) and electrophoresed for 2.5 hours at 200 V. The gel was dried at 80°C for 1.5 hours and exposed to XAR film at −80°C overnight.

cyclin D1 Promoter Sub-cloning and *in vitro* Methylation

The minimal *cyclin D1* promoter region (−1748 to +164) was PCR amplified and sub-cloned upstream of the *Gaussia* luciferase gene in the pGLuc Basic vector (NEB) using *Kpn1* and *BamH1* sites. This *cyclin D1* promoter-reporter luciferase construct was designated as the −1748*CD1* wild type reporter, and contained the −1067 and +69 core KBSs in addition to multiple CpG sites. The KBS sequences located at positions −1067 (designated 1) and +69 (designated 2) were mutated via site-directed mutagenesis. The mutations were confirmed by sequencing (Mobix Facility, McMaster University) and the resulting plasmid called −1748*CD1* KBS (1, 2) mutant. The reporter plasmids were purified from $dam^{-/}dcm^{-}$ bacteria and then methylated by treating with the methyl donor S-adenosylmethionine (NEB) in the presence of bacterial *Sss1* CpG methyltransferase (NEB). Briefly, 50 μg of each plasmid DNA was incubated with 200U of *Sss1* methyltransferase in a 250 μL reaction that contained 640 μM S-adenosyl methionine and 1X NEB buffer. The reactions were incubated at 37°C for 2 hours, after which the enzyme was inactivated at 65°C for 20 minutes. The methylated DNA samples were purified by standard phenol-chloroform extraction and ethanol precipitation. CpG-methylated plasmids were digested with the methylation-resistant restriction enzyme *HpaII* to confirm complete methylation. The pGluc-Basic vector was used as a negative control while the pGluc-1748*CD1* wild type and mutated reporters were used to assess Kaiso's regulation of the *cyclin D1* promoter via the KBS and methylated CpG sites.

Table 1. *cyclin D1*-derived oligonucleotides used in EMSA to assess Kaiso binding.

Probe Name	Oligonucleotide Sequence	# CpGs
−1067 KBS	TTATGC**CG**GC*TCCTGCCA*GCCCCCTCA**CG**C	2
+69 KBS	CTGT**CG**G**CG**CAG*TAGCAG***CG**AGCAGCAGAG	3
CpG1	G**CG**GGGGAGGGGG**CGCG**GGAGGAATTCACC	2
CpG2	**CG**TTCTTGGAAATG**CG**CCCATTCTGC**CG**GC	3
CpG3	TATGGGGTGT**CG**C**CGCG**CCCCAGTCACCCC	2
CpG4	GC**CG**CAGGGCAGG**CGCG**G**CG**CCTCAGGGAT	3
CpG5	CC**CG**G**CG**TTTGG**CG**CC**CGCG**CCCCCTCCCC	4
CpG6	GCCCCCTCCCCCTG**CG**CC**CG**CCCCC**CG**CCCC	3
CpG7	CAGAGGGCTGT**CG**G**CG**CAG*TAGCAG***CG**AGC	3
CpG8	GAGGGGCAGAAGAG**CGCG**AGGGAG**CGCG**GG	2

Ten oligonucleotides were synthesized from different regions of the *cyclin D1* promoter and used in EMSA experiments to elucidate Kaiso binding. The CpGs are bolded while the KBSs are bolded and italicized (i.e. −1067KBS, +69KBS and CpG7).

doi:10.1371/journal.pone.0050398.t001

Transient Transfection and Luciferase Assays

MCF7 cells were seeded at 2.5×10^5 cells/mL into 6-well dishes and incubated for at least 12 hrs until the cells were approximately 50–60% confluent. Each well was transfected with 600 ng of reporter DNA plasmid (pGLuc-Basic, pGLuc-Basic wild type −1748*CD1* or pGLuc-Basic −1748*CD1* KBS (1,2) mutant), 500 ng of pRSV/β-galactosidase internal control and various amounts of effector plasmids (pcDNA3 empty, pcDNA3 human Kaiso, or pRS-Kaiso) by diluting the DNA in 150 mM NaCl and mixing gently before adding 10 equivalents (~17 µl) of ExGen-500 reagent (Fermentas, Burlington, ON). The mixture was gently vortexed, and incubated without disturbing at RT for 15 minutes to allow transfection complex formation. The complexes were then added drop-wise to the cells in fresh serum-supplemented DMEM medium before incubating the cells for 3 hours at 37°C with 5% CO_2, after which the reagent was aspirated and replaced with 2 mL of fresh DMEM. 24 hours post-transfection, 25 µL of the culture medium was assayed for luciferase activity with 50 µL of *Gaussia* luciferase substrate (NEB) on an LB luminometer (Thermo Fisher). Luciferase activity was recorded as relative light units (RLU's) and normalized for transfection efficiency using the internal control β-galactosidase activity for each experimental and control sample condition.

Chromatin Immunoprecipitation (ChIP)

MCF7 and HCT 116 cells were grown to ~80% confluency and cross-linked with 1% formaldehyde in DMEM medium. The cells were placed on a belly dancer and gently shaken for 10 minutes at room temperature. Formaldehyde fixation was stopped by adding 1 M glycine to a final concentration of 125 mM and the cells rocked for 5 minutes at room temperature. The cells were washed twice with 5 mL of ice-cold 1X PBS, and harvested by scraping in 1 mL PBS containing complete Mini Protease Inhibitor Cocktail Tablet (Roche, Mannheim, Germany). The cells were collected in 15 mL conical tubes and pelleted by centrifugation at 4°C for 5 minutes at 2,000 rpm and the supernatants aspirated. Cell pellets were re-suspended in 2 mL of ice-cold ChIP lysis buffer (5 mM PIPES pH 8.0, 85 mM KCL, 0.5% NP-40, with protease inhibitors) and dounced ten times with a homogenizer, before incubating on ice for 15 minutes. The lysates were centrifuged at 5,000 rpm for 5 minutes at 4°C and the nuclear pellet resuspended in 250 µL of Nuclear lysis buffer (50 mM Tris-Cl pH 8.1, 10 mM EDTA, 1% SDS, with protease inhibitors). After incubating on ice for 10 minutes, the nuclear pellets were sonicated at 90% duty, 5% power for 5 rounds of 15-second pulses to achieve sheared chromatin fragment lengths of ~100–1000 base pairs. The lysates were cleared by centrifugation at 14,000 rpm for 10 minutes at 4°C and the supernatant transferred to new microfuge tubes. 7.5 µg of chromatin was pre-cleared by incubating end-over-end for 1 hour at 4°C with 5 µL of rabbit IgG (Abcam, Cambridge, MA) in a 500 µL reaction. Fifty µL of salmon sperm-blocked Protein A beads was added to the pre-cleared lysate and rotated as above before centrifuging at 5,000 rpm for 3 minutes. The supernatant was subjected to immunoprecipitation with 4 µg Kaiso 6F monoclonal antibody [22], 2 µg Histone H3 polyclonal antibody (Abcam) or negative control mouse IgG antibody (Active Motif, Carlsbad, CA) at 4°C and rotated end-over-end overnight. The immunoprecipitated samples were centrifuged at 13,000 rpm for 2 minutes at 4°C before 50 µL of Protein-A rabbit-anti-mouse bridge or Protein-A beads (depending on antibody isotype used for IP) was added to each immunoprecipitated supernatant sample. Samples were rotated end-over-end at 4°C for 1 hour and the precipitated samples washed six times (1X with 1 mL of RIPA buffer for 10 minutes at 4°C, 1X with high salt buffer for 10 mins, 1X with LiCl buffer for 5 minutes and 2X with TE buffer for 10 minutes each). After removing the supernatant, 300 µL of 1X TE buffer and 1.5 µL of RNase A (10 mg/mL) was added to the immunoprecipitate and 10% input samples before incubating for 30 minutes at 37°C. 15 µL of 10% SDS and 3.75 µL of proteinase K (20 mg/mL) were added and the samples incubated at 37°C for a minimum of 4 hours. The samples were then reversed cross-linked overnight at 65°C and DNA purified using standard phenol-chloroform extraction and ethanol precipitation. The DNA was resuspended in 50 µL of sterile dH_2O and used for PCR amplification.

PCR Amplification

Two microliters of recovered DNA from each chromatin immunoprecipitated sample was used in a PCR reaction that contained 1X PCR buffer, 1.5 mM $MgCl_2$, 0.3 mM dNTPs, 0.4 mM forward and reverse primers (-1067 KBS-Forward: 5′-TTTACATCTGCTTAAGTTTGCG-3′ & -1067 KBS-Reverse 5′-TTAGAATTTGCCCTGGGACT-3′, +69 KBS-Forward: 5′-CACACGGACTACAGGGGAGTT-3′ & +69 KBS-Reverse: 5′-CTCGGCTCTCGCTTCTGCTG-3′, CpG5-Forward: 5′-TTTGCATTTCTATGAAAACCGG-3′, & CpG5-Reverse 5′-GCAACTTCAACAAAACTCCC-3′, and CpG8-Forward: 5′-ACACGGACTACAGGGGAGTTTTG-3′ & CpG8-Reverse: 5′-ATTTCGAACCCCTGGGGAGG-3′ and negative control-Forward: 5′-CCCTCGGTGTCCTACTTCAA-3′ & negative control-Reverse 5′-CACCACGGCAAACTTCAAAG-3′), 0.5 µl of Taq polymerase (Invitrogen/Life Technologies), and sterile water to a final volume of 25 µl. The PCR conditions were as follows: initial denaturation at 95°C for 5 minutes, followed by 36 cycles of denaturation at 95°C for 1 minute, annealing at 50°C for 1 minute (for the -1067 KBS), 53°C for 1 minute (for the +69 core KBS), 53.6°C for 45 seconds (for CpG5) or 58°C for 45 seconds (for CpG8) with extension at 72°C for 30 seconds, and a final extension at 72°C for 45 seconds. 10 µL of each PCR reaction were loaded onto a 1.2% agarose gel with 0.5 µg/ml EtBr, electrophoresed at 120 V for 25 minutes in 1X TAE solution and the gel imaged.

Western Blot

HCT116 and MCF7 cells were washed twice with 5 mL of cold 1XPBS and lysed with 500 µL lysis buffer containing 0.5% NP-40, 0.5% Na_3VO_4 and complete mini protease inhibitor cocktail tablet (Roche). Lysates were centrifuged at 13,000 RPM for 15 minutes at 4°C and the pellet discarded. 10 µg of total protein was denatured in 2X **L**aemmli **s**ample **b**uffer (LSB) by boiling for 5 minutes. Equal amounts of protein were separated by SDS-**p**oly**a**crylamide **g**el **e**lectrophoresis (PAGE) and transferred onto nitrocellulose membrane. Membranes were blocked for 1 hour at room temperature with 3% skim milk in 1X **T**ris **B**uffered **S**aline (TBS; pH 7.4). The membranes were then incubated overnight at 4°C with primary antibodies at the following dilutions: anti-Kaiso rabbit polyclonal antibody (1:30,000); anti-Cyclin D1 rabbit monoclonal antibody (Cell Signaling; 1:1000); anti-β-actin mouse monoclonal antibody (Sigma Aldrich; 1:5000). Membranes were washed once for 30 minutes and then 4 times for 5 minutes with 1XTBS, pH 7.4, followed by incubation with either donkey anti-mouse or goat anti-rabbit **h**orse**r**adish **p**eroxidase (HRP)-conjugated secondary antibodies (1:40 000) for 2 hours at room temperature with rocking. Membranes were washed as described, and then processed and visualized using the Enhanced Chemiluminescent System (Amersham Biosciences) according to the manufacturer's protocol.

MTT Cell Proliferation Assay

Cells were seeded in 96-well plates in triplicate in 100 µL of serum-supplemented media. 24 hours after seeding, 20 µL thiazolyl blue tetrazolium bromide (Sigma Aldrich) in dH_2O was added to the media in each well to a final concentration of 0.5 mg/mL. Cells were incubated for 4 hours in a 5% CO_2, humidified incubator. Following incubation, media was aspirated from wells (without disturbing purple crystals at bottom) and 100 µL per well DMSO was added to cells to solubilize formazan crystal product. Crystals were allowed to dissolve for 5–10 minutes and absorbance read at 570 nm using a spectrophotometer. Growth of HCT 116 pRS-empty and HCT 116 pRS-Kaiso was plotted relative to the HCT 116 parental cell line.

Results

Kaiso Binds the *cyclin D1* -1067 Promoter Region in a KBS-specific Manner

Cyclin D1 was first postulated to be a potential Kaiso target gene after elevated *cyclin D1* mRNA levels were detected in *Xenopus laevis* embryos following *xKaiso* depletion [10]. More recently studies in lung cancer cell lines have also implicated *cyclin D1* as a Kaiso target gene [20]. However, *cyclin D1* was never validated as a *bona fide* Kaiso target gene and it was unknown whether the changes in *cyclin D1* mRNA and protein levels were a direct or indirect effect of transcriptional regulation by Kaiso. Our lab has identified numerous CpG dinucleotide-rich regions and three KBSs (at positions −2336, −1067 and +69 in the *cyclin D1* promoter, ID#:6842 from the Transcriptional Regulatory Element Database) relative to the transcriptional start site (Figure 1A). As a first step towards validating *cyclin D1* as a Kaiso target gene and determining the mechanism by which it is regulated, we examined Kaiso's ability to bind the human *cyclin D1* promoter *in vitro*. We performed EMSA studies using various bacterially-expressed and purified GST-Kaiso fusion proteins and nine oligonucleotides that individually corresponded to the KBS found at position -1067 and various CpG rich regions of the *cyclin D1* promoter (Figures 1, 2 & S1). The −1067 KBS oligonucleotide used in Figure 1 possessed the full KBS (TCCTGCNA) and two CpG sites while one of the CpG oligonucleotides (CpG7) used in Figure 2 contained a core KBS (CTGCNA) and three CpG sites (see Figure 2).

We employed GST-Kaiso fusion proteins lacking the Kaiso POZ domain for our EMSA studies, since we and others have found that the presence of the POZ domain in most full-length POZ-ZF proteins resulted in weak or no association with DNA *in vitro*, [23] and our unpublished data. In repeated experiments, we found that GST-Kaiso-ΔPOZ (lacking the N-terminal POZ domain) and GST-Kaiso-ZF domain could bind the −1067 KBS region of the *cyclin D1* promoter (Figure 1C, lanes 3 & 4). As expected, no binding was observed with the GST alone or GST-Kaiso-ΔPOZΔZF negative controls (Figure 1C, lanes 1 & 2). To confirm that Kaiso was binding the −1067 region in a KBS-specific manner, three point mutations were introduced into the core KBS (CTGCNA to **A**T**TA**CA) sequence. When this mutated oligonucleotide (−1067 mut.) was tested in EMSA, Kaiso DNA binding was completely abolished (Figure 1C, lanes 7 & 8). This confirmed that Kaiso was binding directly to the −1067 *cyclin D1* promoter region in a KBS-specific manner.

To confirm that Kaiso bound the −1067 KBS region of the *cyclin D1* promoter endogenously, we next performed ChIP experiments using chromatin isolated from MCF7 and HCT 116 cells, which express moderate to high levels of Kaiso respectively, and immunoprecipitated the DNA-protein complexes with the Kaiso-specific monoclonal antibody 6F [22]. PCR was performed with primers that flanked the −1067 KBS region in the *cyclin D1* promoter and we repeatedly amplified fragments of ~170 bp from MCF7 and HCT 116 chromatin samples (Figure 1D). This fragment was also present in the 5% input and Histone-H3 positive control lanes but absent in the IgG negative control and no template lanes. Interestingly, treatment of MCF7 cells with 5′-azacytidine for 3 days did not affect Kaiso's ability to associate with the −1067 KBS region (Figure 1D). Our findings confirm that Kaiso associates with the *cyclin D1* promoter endogenously via the −1067 KBS region and suggest that this interaction may be methylation independent.

Kaiso Binds *cyclin D1* Promoter Regions Possessing Multiple Methyl-CpG Sites

Since Kaiso is a dual-specificity DNA-binding transcription factor that also binds methylated CpG-dinucleotides [7,19,21] and the *cyclin D1* promoter possesses many CpG sites, we performed studies to determine whether Kaiso could bind and regulate *cyclin D1* expression via some of these CpG sites. Thus, we synthesized eight oligonucleotides corresponding to eight different CpG regions of the *cyclin D1* promoter (spanning −1504 to +102 relative to the transcriptional start site, Figure 1A). Each oligonucleotide possessed CpG-dinucleotides but some contained three single CpG-dinucleotides (*e.g.* CpG-2, -6, -7) while others possessed a combination of single and consecutive CpG-dinucleotides, (*e.g.* CpG-1, -3, -4, -5, -8) (Figure 2A). All oligonucleotide probes were methylated *in vitro* with *Sss1* methyltransferase and then individually tested for Kaiso's ability to bind them. Using GST-Kaiso-ZF fusion proteins, we found that Kaiso bound all eight oligonucleotides with varying efficiency in a methylation-specific manner (Figure 2B). Interestingly, Kaiso bound most efficiently to probes containing two consecutive CpG and three single CpG-dinucleotides (CpG5) or two sets of consecutive CpG-dinucleotides (CpG8) (Figure 2B, lanes 10 and 16). Surprisingly, Kaiso did not bind the non-methylated CpG7 probe that possessed a core KBS and this suggested that in the context of the *cyclin D1*+69KBS region, Kaiso has a higher affinity for methyl-CpG-dinucleotides than for the KBS.

As before, we confirmed the Kaiso–methyl-CpG interaction *in vivo* using ChIP experiments with chromatin isolated from HCT 116 cells, which express high levels of Kaiso, and the Kaiso-specific monoclonal antibody 6F (Figure 2C). PCR was performed with primers that flanked the two CpG sites that showed the highest levels of Kaiso binding in EMSA (CpG5 and CpG8). We repeatedly amplified fragments of ~233 bp and ~197 bp corresponding to the *cyclin D1* CpG5 and CpG8 regions respectively (Figure 2C). These fragments were absent in the IgG negative control and no template lanes. Hence, our data indicate that Kaiso also associates specifically with the *cyclin D1* promoter endogenously via the CpG5 and CpG8 regions.

Kaiso Binds Specifically to the +69 core KBS Region in a Methyl-CpG Dependent Manner

Since Kaiso bound to the methylated CpG7 but not to the non-methylated CpG7 which possessed a core KBS (CTGCNA) and three single CpG dinucleotides (Figure 2B, compare lanes 13 & 14), we sought to determine the relevance of this core KBS in the *cyclin D1* promoter and whether it contributed to Kaiso's binding to this probe. EMSA experiments were performed with an oligonucleotide named "+69 core KBS" that encompassed most of the CpG7 probe and seven additional nucleotides at the 3′ end. We included the full-length GST-Kaiso fusion protein in these EMSA experiments after determining that full-length Kaiso can

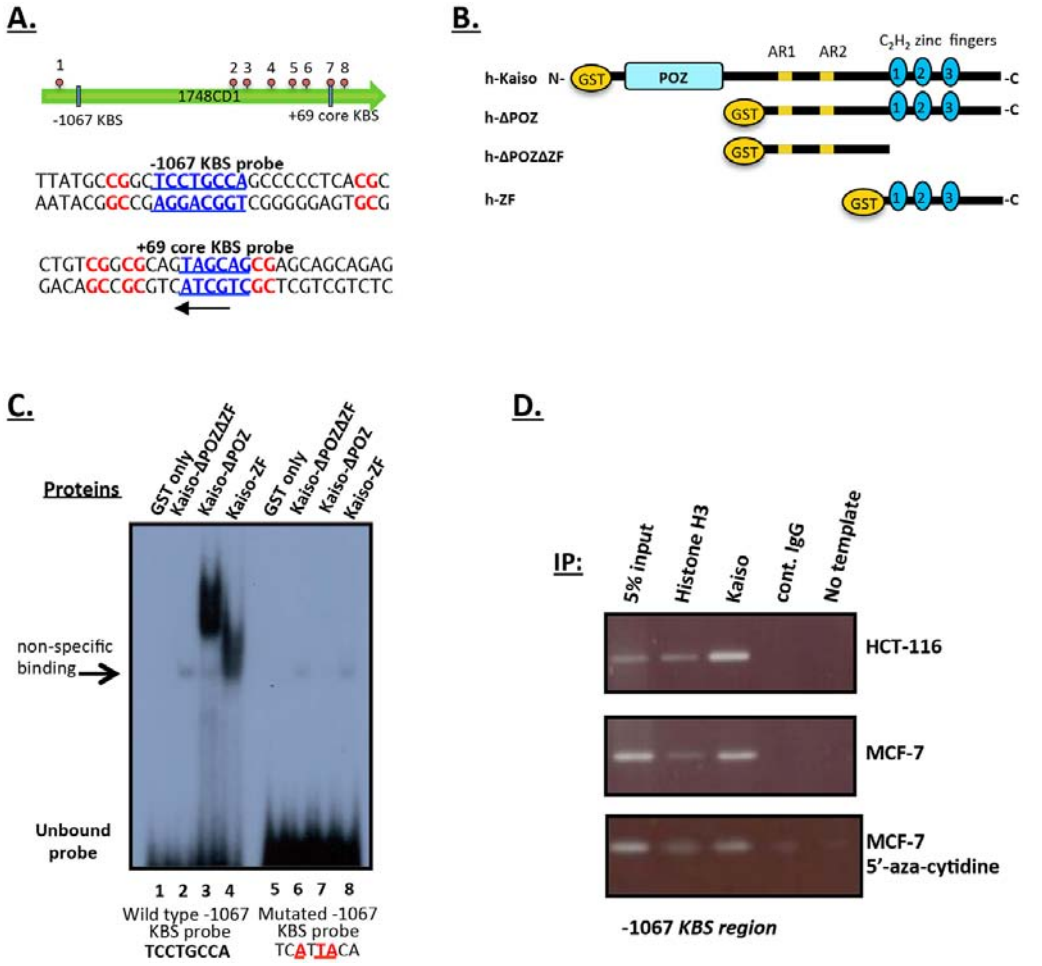

Figure 1. Kaiso binds specifically to the −1067 KBS site of the *cyclin D1* promoter *in vitro* and *in vivo*. (**A**) Schematic representation of the ~1748 *cyclin D1* promoter fragment showing the −1067 KBS, the +69 core KBS (in blue and underlined) and some of the CpG sites in red. Red circles represent CpG sites analyzed in this study. (**B**) Schematic of GST-Kaiso fusion proteins used in this study. The various GST-Kaiso fusion proteins were expressed in bacteria before purification using GST beads. The N-terminal GST-moiety, the Kaiso-POZ domain and three zinc fingers are indicated. (**C**) GST-Kaiso proteins bound the wild type radiolabelled −1067 oligonucleotide probe in a KBS-specific manner. The negative controls, GST alone and GST-KaisoΔPOZΔZF, lacking the POZ and ZF domain did not bind the probe. None of the GST-Kaiso fusion proteins bound the −1067 probe when the KBS was mutated. (**D**) ChIP analysis of the *cyclin D1* promoter in HCT 116 and MCF7 cells revealed that Kaiso specifically associates with the *cyclin D1* promoter −1067 KBS region.
doi:10.1371/journal.pone.0050398.g001

bind the *cyclin D1* promoter-derived oligonucleotides, albeit weaker than the GST-Kaiso deletion mutants lacking the POZ domain. Consistent with our earlier findings, all the GST-Kaiso fusion proteins possessing the zinc finger domain bound the +69 core KBS oligonucleotide in a methylation-dependent manner but none bound the un-methylated oligonucleotide despite the presence of the core KBS sequence (Figure 3A, compare lanes 8–10 to lanes 3–5). Indeed, when the +69 core KBS "CTGCNA" was mutated to "**A**T**TT**NA" the GST-Kaiso fusion proteins still bound the methylated mutated probe (Figure 3A, lanes 19 & 20) albeit with a lower affinity than the wild type probe. This suggested that methylation is necessary and sufficient for Kaiso binding to the +69 region. However, although the core KBS does not appear to the essential for Kaiso binding to the +69 KBS region, the presence of the core KBS seems to stabilize or increase the affinity for Kaiso binding to this site (compare Figure 3A lanes 19 & 20 to lanes 9 & 10). ChIP experiments using the Kaiso-specific monoclonal antibody 6F confirmed that Kaiso associated endogenously with the *cyclin D1*+69 KBS promoter region in MCF7 and HCT 116 cells (Figure 3B). More importantly,

A.

Probe Name	Oligonucleotide Sequence	# of CpGs	Binding
CpG1	G**CG**GGGGAGGGGG**CGCG**GGAGGAATTCACC	2	++
CpG2	**CG**TTCTTGGAAATG**CG**CCCATTCTGC**CG**GC	3	++
CpG3	TATGGGGTGT**CG**C**CGCG**CCCCAGTCACCCC	2	++
CpG4	GC**CG**CAGGGCAGG**CGCG**G**CG**CCTCAGGGAT	3	++
CpG5	CC**CG**G**CG**TTTGG**CG**CC**CGCG**CCCCCTCCCC	4	++++
CpG6	GCCCCCTCCCCCTG**CG**CC**CG**CCCC**CG**CCCC	3	+
CpG7	CAGAGGGCTGT**CG**G**CG**CAG***TAGCAG***CG**AGC	3	++
CpG8	GAGGGGCAGAAGAG**CGCG**AGGGAG**CGCG**GG	2	+++

B.

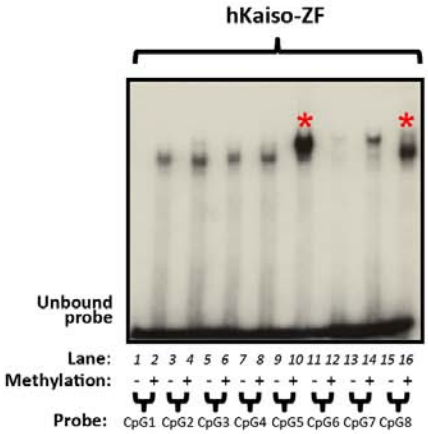

C.

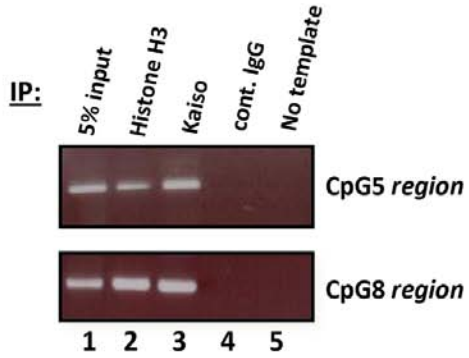

Figure 2. Kaiso binds specifically to methyl-CpG-dinucleotides in the *cyclin D1* promoter. (**A**) Summary of Kaiso binding to methyl-CpG sites in *cyclin D1* promoter-derived oligonucleotides. Eight CpG probes were synthesized from different regions of the *cyclin D1* promoter and used in EMSA experiments to elucidate Kaiso binding. The CpGs are bolded and underlined while the KBS is bolded and red. (**B**) EMSA revealed that Kaiso bound both single and consecutive CpG dinucleotides within *cyclin D1* promoter-derived oligonucleotides in a methylation-specific manner. Asterisks (*) denote very strong binding. (**C**) ChIP analysis of HCT 116 chromatin revealed that Kaiso specifically associated with the CpG5 and CpG8 sites in the *cyclin D1* promoter.
doi:10.1371/journal.pone.0050398.g002

treatment of MCF7 cells with 5′-azacytidine abolished Kaiso's endogenous association with the +69 KBS region as demonstrated using ChIP (Figure 3B). The specificity of Kaiso binding to the −1067, +69 KBS and CpG sites of the *cyclinD1* promoter in MCF7 cells was also confirmed using primers designed to amplify a region upstream of the KBS and CpG sites (Figure S2).

Since some Kaiso binding was retained with the +69 KBS mutant methylated probe, we created four additional mutated probes to determine which CpG dinucleotide sites were essential for the Kaiso-DNA interaction (Figure 4A). The +69 CMUT1 (mutated one 3′ CpG to GG but with intact KBS), +69 CMUT2 (mutated the two 5′ CpGs to GGs, with intact KBS and 3′ CG), +69 CMUT3 (mutated all three CpG sites to GGs but with intact KBS) and +69 ALLMUT (mutated all three CpGs and the KBS) methylated probes were incubated with GST-Kaiso-ΔPOZ fusion proteins. GST-Kaiso-ΔPOZ bound the methylated +69 KBS-mut probe similarly to that of the +69 CMUT1 probe, but with lower affinity than the wild type probe (Figure 4B, compare lanes 6 & 9 to 3). Since Kaiso did not bind the +69 CMUT2, +69 CMUT3 or +69 ALLMUT probes (Figure 4B, lanes 10–18), this suggests that the two CpG sites immediately upstream of the KBS are necessary for Kaiso binding to the *cyclin D1*-promoter-derived oligonucleotides and supports our 5′-azacytidine ChIP experiment (Figure 3B). Taken together, our data suggest that Kaiso's binding to the +69 KBS region is methyl-CpG-dependent and not KBS-specific. We further confirmed the specificity of Kaiso binding to the methylated +69 core KBS probe via cold competition assays with excess unlabelled probes (data not shown).

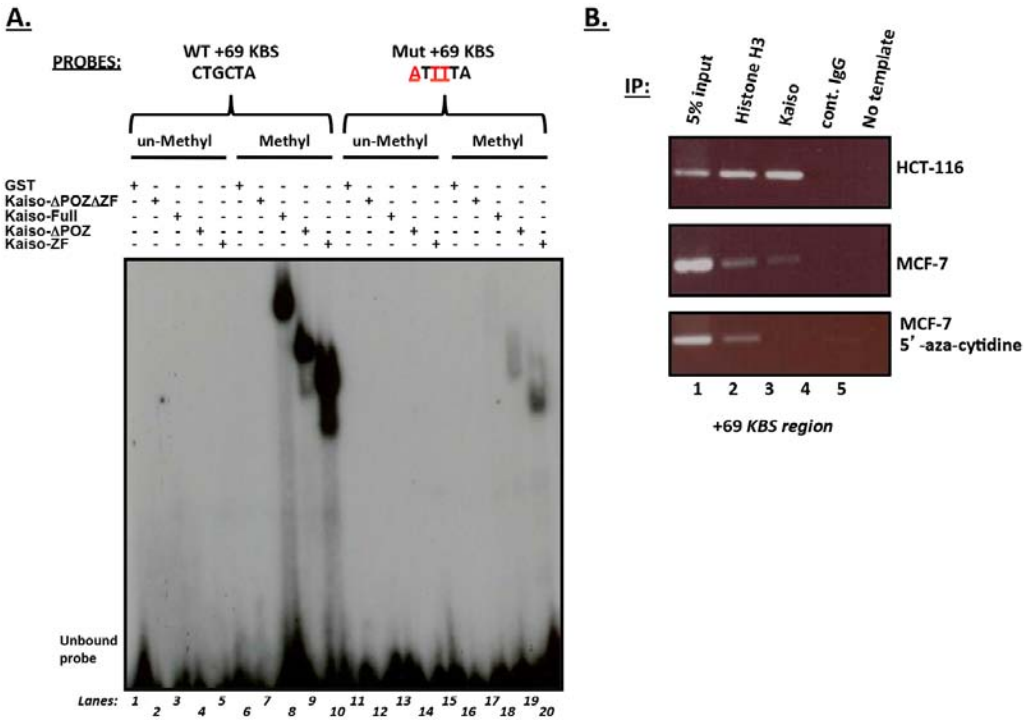

Figure 3. Kaiso binds the +69 core KBS region of the *cyclin D1* promoter *in vitro* and *in vivo*. (**A**) EMSA revealed that Kaiso bound the methylated *cyclin D1*+69 KBS promoter region but not the unmethylated +69 KBS probe. Kaiso also bound weakly to the methylated (but KBS mutated) +69 KBS probe compared to the wild type probe. (**B**) ChIP of the *cyclin D1* promoter in HCT 116 and MCF7 cells revealed that Kaiso specifically associated with the *cyclin D1* promoter +69 KBS region. 5′-azacytidine treatment of MCF7 cells abolished Kaiso's association with the *cyclin D1* promoter and suggests methyl-CpG-dependent binding of Kaiso to the promoter.
doi:10.1371/journal.pone.0050398.g003

A.

+69 Probe Name	Probe Sequence	Binding
WT KBS	CTGTCGGCGCAGTAGCAGCGAGCAGCAGAG	+++
KBS mut	CTGTCGGCGCAGTAAAATCGAGCAGCAGAG	+
CMUT1	CTGTCGGCGCAGTAGCAGGGAGCAGCAGAG	+
CMUT2	CTGTGGGGGCAGTAGCAGCGAGCAGCAGAG	-
CMUT3	CTGTGGGGGCAGTAGCAGGGAGCAGCAGAG	-
ALLMUT	CTGTGGGGGCAGTAAAATCGAGCAGCAGAG	-

B.

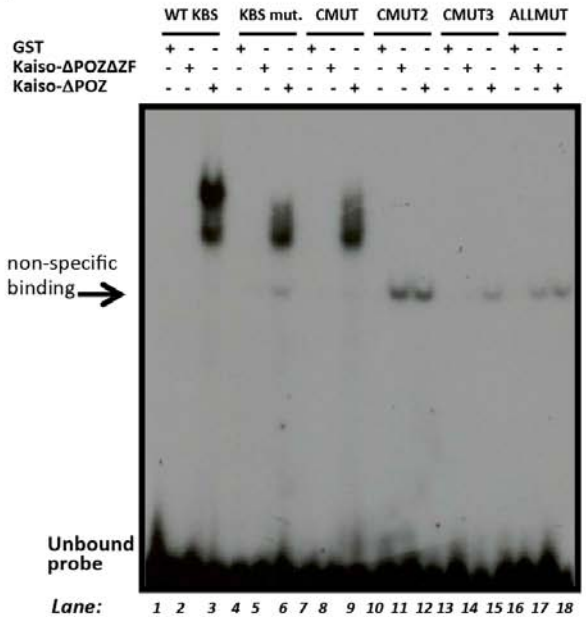

Figure 4. Kaiso binds the +69 core KBS region of the *cyclin D1* promoter in a methyl-CpG-specific manner. (**A**) Summary of Kaiso binding to wild type and mutated +69 core KBS *cyclin D1*-derived oligonucleotides. The CpGs (red) and KBS (blue) sites are highlighted and the mutations are underlined. (**B**) EMSA showed that Kaiso binding to the *cyclin D1*+69 KBS promoter region requires at least two intact methyl-CpG dinucleotides but not an intact KBS site.
doi:10.1371/journal.pone.0050398.g004

Kaiso Represses Transcription from the *cyclin D1* Minimal Promoter in a KBS-specific Manner

After determining that Kaiso bound the *cyclin D1* promoter region with dual-specificity (*i.e.* via the sequence-specific KBS and via methyl-CpG sites), we next assessed Kaiso's ability to regulate luciferase expression under control of a minimal *cyclin D1* promoter. Transfection of MCF7 cells with the unmethylated *cyclin D1* promoter-reporter (−1748 CD1), containing two KBSs and multiple CpG sites, resulted in an ~35-fold increase in luciferase reporter activity compared to the pGluc-Basic negative control vector lacking the *cyclin D1* promoter region (Figure 5A). Co-transfection of the −1748 CD1 promoter-reporter and a Kaiso expression plasmid abrogated this response and resulted in a dose-dependent decrease in luciferase activity (Figure 5A). A similar trend was observed in HCT 116 cells (data not shown). To confirm that transcriptional repression was attributed to Kaiso, we depleted endogenous Kaiso with Kaiso-specific siRNA. Increasing amounts of Kaiso-specific siRNA resulted in dose-dependent de-repression of the reporter gene (Figure 5B), and confirmed that Kaiso was negatively regulating the minimal *cyclin D1* promoter. Importantly, since the *cyclin D1* promoter-reporter plasmid was propagated in dam^{-}/dcm^{-} bacteria, the CpG sites were un-methylated. Thus it appears that Kaiso-mediated transcriptional repression of the *cyclinD1* promoter-reporter was occurring via the sequence-specific KBS sites and not the CpG sites.

Kaiso Represses Transcription from the Minimal *cyclin D1* Promoter in a Methyl-CpG-specific Manner

We next examined how a change in the methylation status of the promoter may affect Kaiso's ability to regulate expression of the minimal *cyclin D1* promoter-reporter. Thus, the −1748 CD1 promoter-reporter construct was *in vitro* methylated using *Sss1* methyltransferase prior to transfection. CpG methylation of the plasmid was confirmed by restriction digest with the methylation-resistant enzyme *HpaII* (Figure 6A*)*. Transfection of the unmethylated −1748*CD1* wild-type promoter-reporter construct resulted in more than 25-fold increase in luciferase activity compared to the control pGluc-Basic vector, while its methylated counterpart only exhibited an ~3.5-fold increase (Figure 6B). This is consistent with the notion that methylation of promoter regions is involved in gene silencing. However, when the methylated or unmethylated −1748 CD1 promoter-reporters were individually co-transfected with Kaiso, a similar two-fold decrease in luciferase activity was observed for both promoters tested (Figure 6B, compare 2.0 µg Kaiso for each reporter). This data suggests that Kaiso's ability to repress the *cyclin D1* promoter is via at least three distinct mechanisms: (1) via binding to the KBS, (2) via binding to methylated CpG sites, or (3) via combinatorial use of both KBS and CpG sites. To further delineate Kaiso's mechanism(s) of transcriptional repression of the *cyclin D1* promoter-reporter, we mutated the KBSs and assessed luciferase activity from the unmethylated and methylated mutant reporters. The methylated but KBS mutated promoter-reporter (Met+KBSmut) exhibited a dose-dependent decrease in luciferase activity upon ectopic Kaiso expression (Figure 6C) while its unmethylated and KBS mutated counterpart (Met-KBSmut) remained relatively unchanged (Figure 6D). Together our data suggests that Kaiso regulates *cyclin D1* via its dual-specificity DNA-binding.

Kaiso Depletion Increases HCT116 Cell Proliferation and cyclinD1 Protein Levels

As a first step toward examining Kaiso's potential role in cell cycle regulation we examined cyclin D1 protein levels by western blot analysis of Kaiso-depleted HCT 116 colon carcinoma cell lysates. Similar to Jiang *et al.* (2012), we found that Kaiso depletion resulted in increased cyclin D1 protein levels (Figure 7A). Conversely, transient overexpression of Kaiso in MCF7 cells resulted in decreased cyclinD1 protein levels (Figure S3). More importantly, the Kaiso-depleted cells displayed an ~2-fold increase in cell proliferation compared to the parental and control vector HCT 116 cells in three independent trials (Figure 7B). The increased cell proliferation observed in the HCT 116 Kaiso-depleted cells strengthens our hypothesis that *cyclin D1* is a *bona fide* Kaiso target gene.

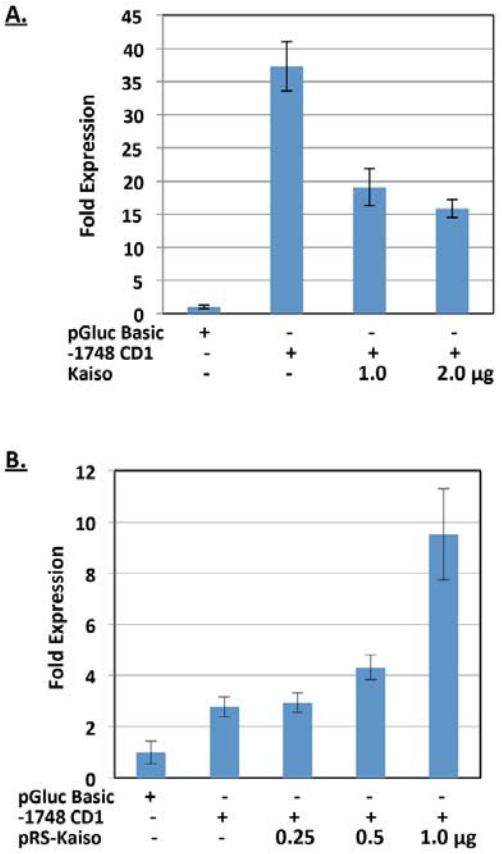

Figure 5. Kaiso represses expression of a minimal *cyclin D1* promoter-reporter. (**A**) Kaiso overexpression decreased luciferase expression from the minimal *cyclin D1* promoter-reporter in a dose-dependent manner in MCF7 cells. (**B**) Depletion of endogenous Kaiso caused de-repression of the minimal *cyclin D1* promoter-reporter in MCF7 cells.
doi:10.1371/journal.pone.0050398.g005

Discussion

Kaiso Binds and Represses the *cyclin D1* Promoter

Kaiso is a dual-specificity transcription factor with sequence- and methyl-CpG-specific transcriptional repression ability

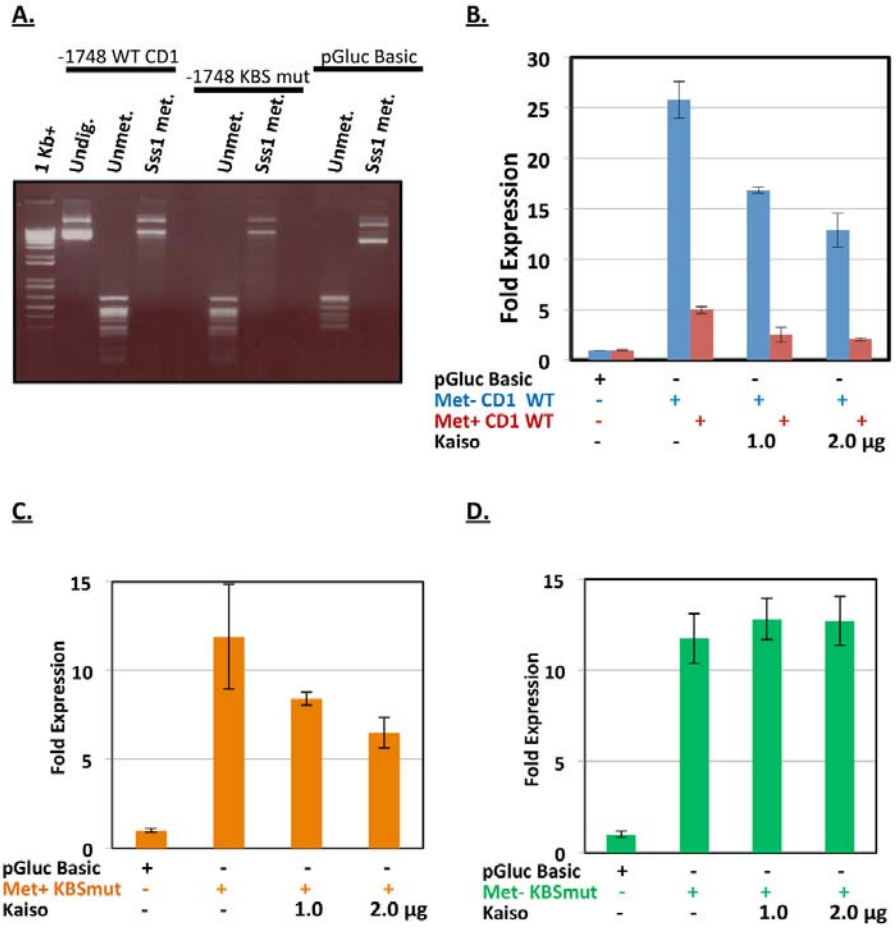

Figure 6. Kaiso represses expression of the minimal *cyclin D1* promoter-reporter in a KBS and methyl-CpG dependent manner. (**A**) Reporter plasmid methylation was confirmed by digesting the plasmid DNA with the CpG-methylation specific restriction enzyme *HpaII*. (**B**) Kaiso overexpression caused a dose-dependent decrease in luciferase gene expression from the minimal *cyclin D1* promoter reporter possessing active KBS but devoid of methyl-CpG sites (blue bars). Similarly, a dose-dependent decrease was observed when the KBS and CpG sites were both active (red bars). (**C**) Kaiso overexpression caused dose-dependent repression of luciferase activity in the presence of active methyl-CpG sites and mutated KBSs. (**D**) Ectopic Kaiso expression had little to no effect on the reporter construct when both the KBS and CpG sites were inactivated.
doi:10.1371/journal.pone.0050398.g006

[10,19,21]. In this study we showed that Kaiso exhibits dual-specificity DNA binding to the human *cyclin D1* promoter; Kaiso bound to the -1067 KBS region of the *cyclin D1* promoter in a sequence-specific manner and it bound multiple CpG rich sites within the *cyclin D1* promoter region in a methylation-dependent but KBS-independent manner (Figures 1, 2, 3). While the significance of Kaiso's sequence-specific versus methyl-CpG-specific DNA binding remains largely unknown, our data shows that both types of DNA-binding can occur independently at one gene promoter locus. Previously, Prokhortchouk *et al.*, [19] showed that the Kaiso zinc fingers preferentially associate with consecutive methylated CpG-dinucleotides, and that binding affinity decreases if there are one or more nucleotides between the consecutive CpG-dinucleotides. While our findings support those of Prokhortchouk *et al.*, we also showed that the presence of consecutive CpG-dinucleotides is not a strict requirement for Kaiso DNA binding (Figure 2A & B; CpG2 oligonucleotide). Furthermore, binding to methyl-CpG sites can also occur in the presence of a core KBS, as observed in this study.

The presence of a core KBS sequence in one of the CpG rich regions motivated us to examine Kaiso binding to this region using an oligonucleotide (CpG7) containing the KBS and CpGs. We found that Kaiso was able to bind this +69 core KBS region in a methyl-CpG-specific manner, and that binding required the presence of the two CpG-dinucleotides upstream of the core KBS (Figure 4). Mutation of this core KBS sequence decreased but did

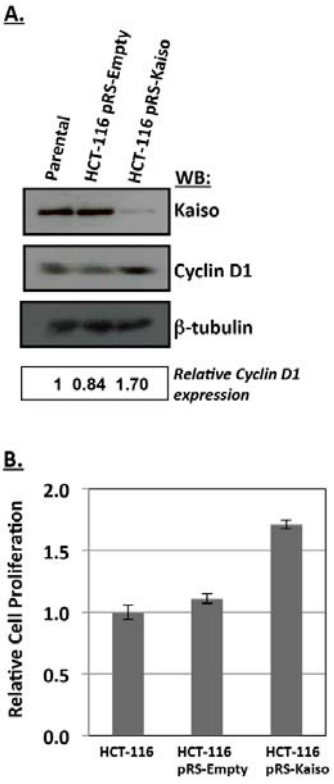

Figure 7. Kaiso depletion alters cyclin D1 expression and cell proliferation in HCT116 cells. (**A**) Depletion of endogenous Kaiso with Kaiso-specific siRNA resulted in an ~ 1.7-fold increase in cyclin D1 protein levels in HCT116 cells. (**B**) Kaiso depletion in HCT116 cells resulted in an ~ 2-fold increase in cell proliferation.
doi:10.1371/journal.pone.0050398.g007

not abolish Kaiso binding, suggesting that the role of this core KBS in close proximity to single CpGs is most likely to stabilize Kaiso DNA binding. Our data support those of Sasai *et al.,* [7], who demonstrated that Kaiso and the Kaiso-like zinc finger protein ZBTB4 bind single methylated-CpG sites with higher affinity if a core KBS was present [7]. However, it is possible that high affinity Kaiso binding requires two consecutive methylated-CpG sites in the absence of a core KBS. While previous studies have implicated *cyclin D1* as a Kaiso target gene [10,20], our study is the first to demonstrate Kaiso's dual-specificity (sequence- and methylation-specific) DNA-binding and transcriptional repression of the *cyclin D1* promoter in mammalian cells.

Importantly, we confirmed that Kaiso also associated with the −1067, +69 core KBS and CpG regions of the *cyclin D1* promoter *in vivo* in both MCF7 breast and HCT 116 colon carcinoma cells (Figures 1, 2, 3). However, since the +69 KBS, CpG5 and CpG8 sites are in close proximity to each other within the promoter, it is possible that Kaiso associates with one and or all 3 sites simultaneously; however it will be difficult to resolve these sites *in vivo* using ChIP assays. Nevertheless, our data indicates that Kaiso's binding to the *cyclin D1* promoter is not cell line specific and supports our hypothesis that *cyclin D1* is a *bona fide* Kaiso target gene. While we do not know if the Kaiso-*cyclin D1* promoter association is preserved in other cell types such as fibroblasts, we recognize the need to pursue such studies.

Our minimal promoter-reporter assays demonstrated that Kaiso overexpression resulted in dose-dependent repression of the *cyclin D1* promoter and further validated *cyclin D1* as a Kaiso target gene (Figure 5). This is consistent with the findings of Park *et al.* who previously reported that Kaiso was a negative regulator of *cyclin D1* expression in *Xenopus* [10], and the findings of Jiang *et al.* who recently demonstrated that Kaiso overexpression decreased cyclin D1 protein levels in lung cancer cells [20]. However, neither study determined Kaiso's mechanism of transcriptional repression of the *cyclin D1* promoter. Here we demonstrate that Kaiso-mediated transcriptional repression of *cyclin D1* occurred in a KBS sequence-specific and methyl-CpG-dependent manner (Figures 5 & 6). Our findings suggest that the KBS and methyl-CpG-dinucleotides are physiologically relevant for Kaiso-mediated transcriptional repression of *cyclin D1*. Interestingly, when both CpG and KBS sites were inactivated (due to demethylation and KBS mutations respectively), Kaiso overexpression had minimal effect on the *cyclin D1* promoter-reporter activity (Figure 6D). Collectively, our findings suggest that Kaiso binds and negatively regulates the *cyclin* D1 minimal promoter via two distinct mechanisms that involve the sequence-specific KBS or the methyl-CpG sites. Since mammalian DNA methylation is an essential epigenetic modification associated with transcriptional repression, our findings implicate Kaiso in both sequence-specific and methylation-dependent gene regulation of the *cyclin D1* promoter.

Finally, the increased cell proliferation observed in the HCT 116 Kaiso-depleted cells supports our hypothesis that *cyclin D1* is a *bona fide* Kaiso target gene. Since the Wnt pathway is constitutively active in HCT 116 cells and many other factors regulate *cyclin D1* expression and function, it is not surprising that we only observed an ~ 1.7-fold increase in cyclin D1 protein levels in HCT 116 depleted cells and a modest decrease in cyclin D1 protein levels upon Kaiso overexpression in MCF7 cells.

Whether Kaiso exhibits preferential binding to the KBS over the CpG sites in the *cyclin D1* promoter *in vivo* remains to be determined, and may be context dependent. Nevertheless, our data show a relationship between Kaiso and the cell cycle regulator *cyclin D1* in mammalian cells. Together our experiments demonstrate that the POZ-ZF transcription factor Kaiso associates with the *cyclin D1* promoter with dual-specificity and represses *cyclin D1* expression. However, the physiological relevance of this unique dual-specificity mechanism of transcriptional regulation of *cyclin D1* and other Kaiso target genes remains to be determined.

Supporting Information

Figure S1 GST-Kaiso fusion proteins. 5 μg of purified GST-Kaiso fusion proteins utilized in EMSA studies were resolved on an SDS-PAGE gel to confirm expression and integrity of proteins.
(TIFF)

Figure S2 Chromatin Immunoprecipitation negative control. Primers designed to amplify a region located at +326 to +526 bp of the *cyclinD1* promoter (which lacked KBS sites) were used as a negative control to confirm the specificity of Kaiso binding to the −1067, +69 and CpG sites of the *cyclinD1* promoter in MCF7 cells.
(TIFF)

Figure S3 Kaiso overexpression alters cyclinD1 expression in MCF7 cells. (**A**) Transient transfection of MCF7 cells with the Kaiso expression vector (pcDNA3.1-hKaiso) resulted in an ~ 1.7 fold decrease in cyclinD1 protein levels.
(TIFF)

Acknowledgments

The authors wish to thank Abena Otchere-Engmann and Simona Morone for experimental assistance.

Author Contributions

Conceived and designed the experiments: JMD NSD CCP. Performed the experiments: NSD CCP MIA SCR SW. Analyzed the data: JMD NSD CCP MIA SCR SW. Wrote the paper: JMD NSD CCP SCR.

References

1. Ndlovu MN, Denis H, Fuks F (2011) Exposing the DNA methylome iceberg. Trends Biochem Sci 36: 381–387.
2. Robertson KD (2005) DNA methylation and human disease. Nat Rev Genet 6: 597–610.
3. Ogoshi K, Hashimoto S, Nakatani Y, Qu W, Oshima K, et al. (2011) Genome-wide profiling of DNA methylation in human cancer cells. Genomics 98: 280–287.
4. Lan J, Hua S, He X, Zhang Y (2010) DNA methyltransferases and methyl-binding proteins of mammals. Acta Biochim Biophys Sin (Shanghai) 42: 243–252.
5. Lopes EC, Valls E, Figueroa ME, Mazur A, Meng F-G, et al. (2008) Kaiso contributes to DNA methylation-dependent silencing of tumor suppressor genes in colon cancer cell lines. Cancer Res 68: 7258–7263.
6. Filion GJ, Zhenilo S, Salozhin S, Yamada D, Prokhortchouk E, et al. (2006) A family of human zinc finger proteins that bind methylated DNA and repress transcription. Mol Cell Biol 26: 169–181.
7. Sasai N, Nakao M, Defossez PA (2010) Sequence-specific recognition of methylated DNA by human zinc-finger proteins. Nucleic Acids Res 38: 5015–5022.
8. Sasai N, Defossez PA (2009) Many paths to one goal? The proteins that recognize methylated DNA in eukaryotes. Int J Dev Biol 53: 323–334.
9. Kim SW, Park JI, Spring CM, Sater AK, Ji H, et al. (2004) Non-canonical Wnt signals are modulated by the Kaiso transcriptional repressor and p120-catenin. Nat Cell Biol 6: 1212–1220.
10. Park JI, Kim SW, Lyons JP, Ji H, Nguyen TT, et al. (2005) Kaiso/p120-catenin and TCF/beta-catenin complexes coordinately regulate canonical Wnt gene targets. Dev Cell 8: 843–854.
11. Ruzov A, Dunican DS, Prokhortchouk A, Pennings S, Stancheva I, et al. (2004) Kaiso is a genome-wide repressor of transcription that is essential for amphibian development. Development 131: 6185–6194.
12. Spring CM, Kelly KF, O'Kelly I, Graham M, Crawford HC, et al. (2005) The catenin p120ctn inhibits Kaiso-mediated transcriptional repression of the beta-catenin/TCF target gene matrilysin. Exp Cell Res 305: 253–265.
13. van Roy FM, McCrea PD (2005) A role for Kaiso-p120ctn complexes in cancer? Nat Rev Cancer 5: 956–964.
14. Yoon H-G, Chan DW, Reynolds AB, Qin J, Wong J (2003) N-CoR mediates DNA methylation-dependent repression through a methyl-CpG binding protein Kaiso. Molecular Cell 12: 723–734.
15. Daniel JM, Reynolds AB (1999) The catenin p120(ctn) interacts with Kaiso, a novel BTB/POZ domain zinc finger transcription factor. Mol Cell Biol 19: 3614–3623.
16. Kikuchi A, Yamamoto H, Sato A (2009) Selective activation mechanisms of Wnt signaling pathways. Trends Cell Biol 19: 119–129.
17. Willert K, Jones KA (2006) Wnt signaling: is the party in the nucleus? Genes Dev 20: 1394–1404.
18. Kelly KF, Daniel JM (2006) POZ for Effect- POZ-ZF Transcription Factors in Cancer and Development. Trends in Cell Biology 16: 578–587.
19. Prokhortchouk A, Hendrich B, Jorgensen H, Ruzov A, Wilm M, et al. (2001) The p120 catenin partner Kaiso is a DNA methylation-dependent transcriptional repressor. Genes Dev 15: 1613–1618.
20. Jiang G, Wang Y, Dai S, Liu Y, Stoecker M, et al. (2012) P120-catenin isoforms 1 and 3 regulate proliferation and cell cycle of lung cancer cells via beta-catenin and Kaiso respectively. PLoS One 7: e30303.
21. Daniel JM, Spring CM, Crawford HC, Reynolds AB, Baig A (2002) The p120(ctn)-binding partner Kaiso is a bi-modal DNA-binding protein that recognizes both a sequence-specific consensus and methylated CpG dinucleotides. Nucleic Acids Res 30: 2911–2919.
22. Daniel JM, Ireton RC, Reynolds AB (2001) Monoclonal antibodies to Kaiso: a novel transcription factor and p120ctn-binding protein. Hybridoma 20: 159–166.
23. Bardwell VJ, Treisman R (1994) The POZ domain: a conserved protein-protein interaction motif. Genes Dev 8: 1664–1677.

CHAPTER 6

Kaiso attenuates hypoxia inducible factor-1 alpha transcriptional autoregulation in chronic hypoxia.

Preface:

This chapter consists of the manuscript in preparation entitled: ***"Methylation-dependent regulation of hypoxia inducible factor-1 alpha gene expression by the transcription factor Kaiso"*** by Christina C. Pierre, Joseph Longo, Robin M. Hallett, Snezana Milosavljevic, Blessing I. Bassey, Laura Beatty, John A. Hassell and Juliet M. Daniel. Revisions were made to maintain formatting consistency with other chapters. Significant revisions include elimination of methods section (details in Chapter 2), removal of reference list (included in combined thesis list) and re-numbering of figures in order of appearance in the text.

This work was born out of an attempt to identify novel Kaiso target genes by gene expression profiling of HCT-116 colon carcinoma cells stably depleted of Kaiso. Differential expression analysis of genes altered in response to Kaiso depletion combined with Markov clustering and Pathway analysis revealed several pathways that were altered on depletion of Kaiso, one of which was hypoxic signaling. Indeed, Kaiso binds and represses the promoter of the master regulator of hypoxic signaling, HIF-1α thereby repressing its expression. Interestingly, Kaiso's regulation of HIF-1α occurred primarily in hypoxia, and this finding was attributed to an accumulation of Kaiso protein, which occurs from 4 to 8 hours of hypoxic incubation. These findings highlight a role for Kaiso in fine tuning HIF-1α expression in hypoxia.

Contributions:

Christina Pierre wrote the manuscript and performed the experiments in Figures 6.2, 6.3, 6.4B, and 6.5. Joseph Longo performed the experiments depicted in Figures 6.4A, 6.4C, 6.5A and assisted with the ChIP in Figure 6.2. Robin Hallet performed the bioinformatics analyses included in Tables 6.4 and 6.5. Snezena Milosavljevic and Blessing Bassey assisted with the ChIP experiment in Figure 6.2 and Blessing Bassey generated the MDA-MB-231 stable Kaiso depleted cell lines. Laura Beatty and Christina Pierre collaborated to perform the EMSA in Figure 6.1. Dr. Juliet Daniel provided significant intellectual input and guidance throughout the execution of this work and edited the manuscript.

ABSTRACT

Low oxygen tension (hypoxia) is a common characteristic of solid tumours that strongly correlates with poor prognosis and resistance to treatment. In response to hypoxia, cells initiate a cascade of transcriptional events regulated by the hypoxia inducible factor-1 (HIF-1) heterodimer. The oxygen-sensitive HIF-1α subunit is stabilized during hypoxia and functions as the regulatory subunit of the dimeric protein. While the mechanisms governing HIF-1α protein stabilization and function have been well studied, those governing *HIF1A* gene expression are not fully understood. However, recent studies have suggested that methylation of a HIF-1 binding site in the *HIF1A* promoter prevents its autoregulation. Here we report that the POZ-ZF transcription factor Kaiso modulates *HIF1A* gene expression by binding to the methylated *HIF1A* promoter in a region proximal to the autoregulatory HIF-1 binding site. Kaiso's regulation of *HIF1A* occurs primarily during hypoxia, which is consistent with the finding that Kaiso protein levels peak after 4 hours of hypoxic incubation and return to normoxic levels after 24 hours. Our data thus support a role for Kaiso in fine-tuning *HIF1A* gene expression after extended periods of hypoxia.

INTRODUCTION

A common characteristic of rapidly proliferating solid tumours are regions of hypoxia (reduced oxygen levels) that arise due to irregular, disorganized tumour vasculature (Goonewardene *et al.* 2002; Greijer and van der Wall 2004; Carroll and Ashcroft 2005). In response to hypoxia, tumour cells initiate a series of adaptive responses, the majority of which are orchestrated by the transcription factor hypoxia inducible factor-1 (HIF-1) (Wang and Semenza 1993). The hypoxic response enables tumour cell survival and selects for a more aggressive tumour phenotype (Harris 2002). Thus, it is not surprising that expression of the oxygen labile HIF-1 alpha subunit (HIF-1α) has been positively correlated with increased tumour grade and advanced pathologic stage (Costa *et al.* 2001).

The HIF-1 protein is a heterodimer comprised of the constitutively expressed HIF-1β subunit and the oxygen-sensitive regulatory HIF-1α subunit (Wang *et al.* 1995; Wang and Semenza 1995). In normoxia (21% O_2), HIF-1α is negatively regulated by hydroxylation of its oxygen-dependent degradation domain by prolyl hydroxylases (Huang *et al.* 1996). This enables HIF-1α to be bound by the von Hippel-Lindau (VHL) tumour suppressor protein that targets it for proteasomal degradation (Tanimoto *et al.* 2000). In hypoxia, reduced oxygen levels limit HIF-1α hydroxylation, which results in its stabilization and translocation to the nucleus where it dimerizes with HIF-1β to form a functional HIF-1 protein (Roberts and Ohh 2008). HIF-1 can then bind hypoxia response elements (HRE) in the promoter region of its target genes and activate their expression in conjunction with CREB binding protein (CBP) and p300 co-activators (Dames *et al.* 2002).

Regulation of HIF-1α has been largely attributed to post-translational mechanisms (Richard 1999; Mahon *et al.* 2001; Lando *et al.* 2002; Lando *et al.* 2002; Lee 2002). However, emerging evidence suggests that HIF-1α expression may also be epigenetically regulated (Lauzier *et al.* 2007; Walczak-Drzewiecka *et al.* 2010; Koslowski *et al.* 2011). A recent study suggested that demethylation of an HRE sequence in the *HIF1A* promoter augments *HIF1A* expression during hypoxia, since methylation hinders HIF-1 from binding to and activating this site (Koslowski *et al.* 2011). Indeed, treatment of cells with the demethylating agent 5-aza-2′-deoxycytidine enhances HIF-1 binding to its promoter during hypoxia and increases HIF-1α expression, and consequently HIF-1 target gene expression (Koslowski *et al.* 2011).

DNA methylation of cytosine residues in CpG dinucleotides is a heritable epigenetic mark that controls gene expression in mammals by promoting chromatin compaction, which hinders access of transcriptional machinery to DNA (Klose and Bird 2006; Fournier *et al.* 2012). Three families of proteins have been identified that repress gene expression by recognizing and binding methylated CpG dinucleotides; namely methyl-CpG binding domain (MBD), zinc finger (ZF), and SET and RING finger-associated (SRA) domain proteins (Buck-Koehntop and Defossez 2013). Kaiso was the first member of the ZF family of methyl-DNA binding proteins to be identified and characterized, and intriguingly Kaiso also binds and represses the non-methylated consensus sequence TC**CTGCnA** (where n is any nucleotide; core sequence is bolded), known as the Kaiso Binding Site (KBS) (Daniel and Reynolds 1999; Prokhortchouk *et al.* 2001; Daniel *et al.* 2002).

Kaiso was discovered and characterized over a decade ago, but only a few *bona fide* Kaiso target genes have been identified (Rodova *et al.* 2004; Spring *et al.* 2005; Donaldson *et al.* 2012; Jones *et al.* 2012). As a first step towards identifying *bona fide* genes and signaling pathways regulated by Kaiso, we analyzed gene expression changes following stable depletion of Kaiso in HCT-116 colorectal carcinoma cells. Here we report that in Kaiso depleted cells, *HIF1A* expression is significantly up-regulated and several hypoxia-related gene sets were enriched. Furthermore, Kaiso binds and represses the *HIF1A* promoter in a methylation-dependent manner in hypoxia, suggesting that Kaiso may fine-tune HIF-1α expression in hypoxia. Notably *Kaiso* expression negatively correlated with *HIF1A* expression in breast and colorectal cancer patient tissues, which further supports a role for Kaiso in repressing *HIF1A* expression.

RESULTS

Kaiso depletion results in increased HIF1A expression

In an attempt to identify *bona fide* Kaiso target genes and to gain insight into Kaiso's biological role, we examined RNA samples isolated from 3 biological replicates of HCT-116 cells stably depleted for Kaiso by microarray using the Agilent SurePrint G3 Human Exon 2x400K microarray. Overall, 759 genes exhibited significant differences in expression (Fold change >1.5, FDR<0.05), with 509 genes down-regulated and 250 genes up-regulated in response to Kaiso depletion. Kaiso has been characterized as both and activator and a repressor of transcription (Rodova *et al.* 2004; Ruzov *et al.* 2004; Defossez *et al.* 2005; Lopes *et al.* 2008; Donaldson *et al.* 2012; Koh *et al.* 2014). However, for this study, we focused most of our subsequent analysis on genes that were

significantly up-regulated, since the mechanism by Kaiso mediates gene repression is better characterized. Network analysis of up-regulated genes revealed that their protein products interacted in 9 distinct modules comprised of at least 3 genes each. Pathway analysis of each module suggested that multiple biological pathways were affected by Kaiso depletion, including hypoxia, metabolism, cell adhesion, and cell cycle (Table 6.1). Intriguingly, the hypoxia module (Module 2) included the master hypoxia regulator gene, *HIF1A*. Recent studies demonstrated that the *HIF1A* promoter is methylated in HCT-116 carcinoma cells, which results in attenuation of HIF-1 auto-activation and decreased HIF-1α expression (Walczak-Drzewiecka *et al.* 2010; Koslowski *et al.* 2011). Given our finding that *HIF1A* was up-regulated in response to Kaiso depletion and that Kaiso binds and represses methylated CpG dinucleotides (Prokhortchouk *et al.* 2001; Daniel *et al.* 2002) we focused on the hypoxia module, to determine whether Kaiso regulated hypoxic signaling by binding and repressing the methylated *HIF1A* promoter.

To confirm that regulation of *HIF1A* by Kaiso occurs in human tumours, and is not limited to HCT-116 cells, we examined the expression of *Kaiso* and *HIF1A* in relatively large cohorts of breast (GSE2034, n=286) and colon (GSE14333, n=290) cancer patients. Indeed, we found that *HIF1A* and *Kaiso* expression patterns are inversely correlated in colon and breast tumours, which raised the possibility that Kaiso regulates expression of *HIF1A* in colon and breast tumour cells (Table 6.2). Collectively these data suggest a role for Kaiso in mediating *HIF1A* transcription and downstream hypoxic signaling.

TABLE 6.1: Summary of genes and pathways enriched in Kaiso-depleted HCT-116 cells. Pathways enriched with a False Discovery Rate <0.05 are listed for each module.

Module	Genes	Pathways (FDR)
0	ASB9,DZIP3,KLHL13,NEDD4	Class I MHC mediated antigen processing & presentation (<1.00e-03)
1	CALML6,CAMK4,CDK8,PRKAA2	Organelle biogenesis and maintenance (2.70e-02); Long-term potentiation (1.60e-02); Amphetamine addiction (1.60e-02)
2	CAND1,CUL2,HIF1A	Hypoxic and oxygen homeostasis regulation of HIF-1-alpha (<1.00e-03); Regulation of Hypoxia-inducible Factor (HIF) by Oxygen (<3.33e-04); Cellular responses to stress (<3.33e-04)
3	MTM1,PLCB4,PLCE1	Inositol phosphate metabolism (<1.00e-03); Phosphatidyl inositol signaling system (<5.00e-04); Phospholipid metabolism (3.33e-04)
4	ACTN2,ADORA2A,LMO7	Adherens junction (2.60e-02)
5	ITGA2,LAMA3,LAMA4	Beta1 integrin cell surface interactions (<1.00e-03); Small cell lung cancer (<5.00e-04); ECM-receptor interaction (<3.33e-04)
6	ATR,ORC4,SMC3	Cell cycle (<1.00e-03); Meiosis (1.05e-02); Chromosome Maintenance (8.67E-03)
7	FANCM,MSH6,RECQL	-

Kaiso binds the HIF1A promoter in a methylation-dependent manner

The putative *HIF1A* promoter was retrieved from the Transcriptional Regulatory Element Database (Promoter ID 11879) and analyzed for the presence of CpG dinucleotides and CpG islands using the EMBOSS CpG plot program (http://www.ebi.ac.uk/Tools/emboss/cpgplot). We confirmed the presence of a CpG island spanning –302 to +138 bp relative to the transcription start site (Observed/Expected ratio > 0.60; Percent C + Percent G > 50.00; Length > 200), which was 73 bp larger than that identified by Koslowski *et al.* (Koslowski *et al.* 2011). We also confirmed the presence of the HRE that was previously shown to mediate HIF-1α autoregulation from -156 to -152 bp (Koslowski *et al.* 2011) (Figure 6.1A). Interestingly, we identified 3 core KBSs, one of which was located only 4 base pairs downstream of the HRE (from -147 to -142 bp), which we designated as KBS-3. The remaining two KBSs spanning -675 to -670 bp and -445 to -440 bp were designated as KBS-1 and KBS-2, respectively (Figure 6.1A). KBS-2 was flanked immediately and 6 nucleotides downstream by CpG dinucleotides, while KBS-3 was flanked immediately upstream and 2 base pairs downstream by CpG dinucleotides (Figure 6.1A).

We designed three *HIF1A* promoter-derived oligonucleotides (oligos) that encompassed each of the three KBSs identified, with the KBS-3 oligo encompassing the HRE site from -156 to -152 bp and an additional CpG dinucleotide located 14 bp upstream of the KBS. We also designed a CpG oligonucleotide that encompassed 7 CpG dinucleotides (+45 to +80 bp relative to the transcription start site). For these studies, we employed truncated GST-Kaiso fusion proteins lacking the POZ domain, since we have

TABLE 6.2: Correlation between *Kaiso (ZBTB33)* and *HIF1A* mRNA expression in colon and breast cancer gene expression data sets retrieved from (http://www.ncbi.nlm.nih.gov/geo/).

Type	**Gene Expression Omnibus ID**	**Correlation (*ZBTB33 vs HIF1A*)**	**p-value**
Colon (n=290)	GSE14333	-0.17	0.004
Breast (n=286)	GSE2034	-0.18	0.003

previously shown that full-length Kaiso associates very weakly with DNA *in vitro* (Donaldson *et al.* 2012). Both GST-KaisoΔPOZ (a deletion mutant lacking the POZ domain) and the GST-Kaiso-ZF (a deletion mutant comprised solely of the DNA-binding ZF domain) proteins bound to the methylated KSB-2 and KBS-3 probes (Figure 6.1B, lanes 8 & 9 and 13 & 14, respectively), but not to unmethylated KBS-2 and KBS-3 probes (Figure 6.1B, data not shown and lanes 23 & 24 respectively). Surprisingly, Kaiso bound to KBS-3 with significantly higher affinity than KBS-2 (Figure 6.1B, lanes 13 & 14 compared to lanes 8 & 9 respectively), which may be due to the presence of more CpG dinucleotides in this oligo. None of the Kaiso-GST fusion proteins associated with the methylated or unmethylated KBS-1 probe (Figure 6.1B, lanes 3 & 4 and data not shown, respectively), which supports our previous findings that the presence of a core KBS is not sufficient for Kaiso binding (Donaldson *et al.* 2012). Notably, GST-Kaiso-fusion proteins also bound the methylated CpG probe (Figure 6.1B, lanes 18 & 19), demonstrating that Kaiso binds the *HIF1A* promoter in a methylation-dependent manner in the absence of a core KBS.

Kaiso binds and represses the HIF1A promoter

To support our EMSA studies we performed ChIP assays to determine whether Kaiso interacts with the *HIF1A* promoter endogenously and whether this interaction is methylation-dependent. We focused on the region encompassing KBS-3, since Kaiso exhibited the highest affinity for this region in our EMSA studies. Kaiso precipitated the *HIF1A* promoter from both MCF-7 and HCT-116 cells in hypoxia, but surprisingly we observed little or no Kaiso binding to the *HIF1A* promoter in either cell line in normoxia

FIGURE 6.1: Kaiso binds to methylated CpG dinucleotides in the *HIF1A* promoter. **(A)** Schematic of the human *HIF1A* promoter showing core Kaiso binding sites, HRE and CpG dinucleotides. **(B)** EMSA using *HIF-1A* promoter-derived oligonucleotides and truncated GST-Kaiso fusion proteins revealed that Kaiso binds probes containing CpG dinucleotides in a methylation-dependent manner (Representative of 3 independent trials).

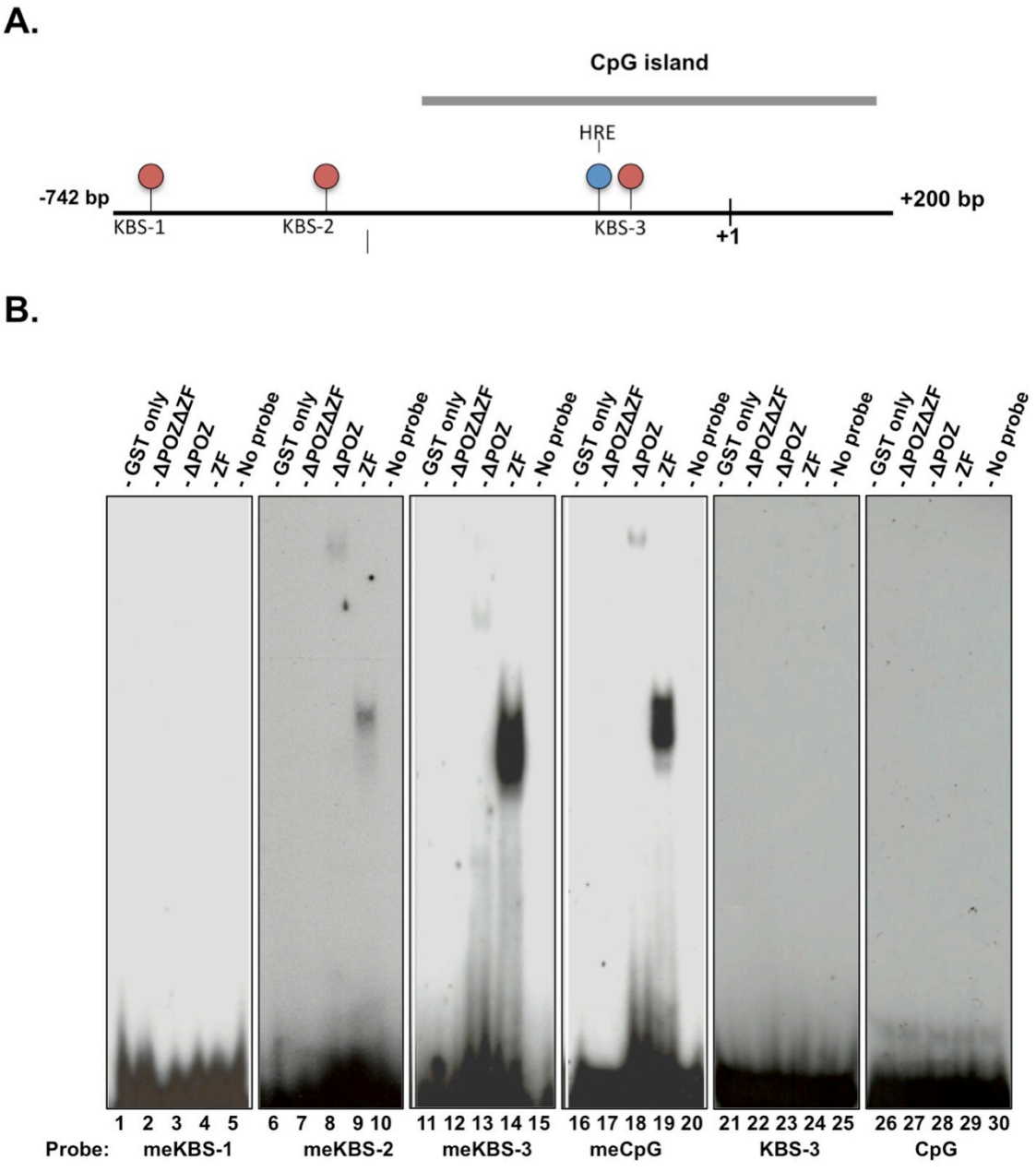
A.
CpG island
HRE
-742 bp
+200 bp
KBS-1
KBS-2
KBS-3
+1
B.
- GST only
- ΔPOZΔZF
- ΔPOZ
- ZF
- No probe
1 2 3 4 5
6 7 8 9 10
11 12 13 14 15
16 17 18 19 20
21 22 23 24 25
26 27 28 29 30
Probe:
meKBS-1
meKBS-2
meKBS-3
meCpG
KBS-3
CpG

(Figure 6.2). Since Koslowski *et al.* previously demonstrated that the *HIF1A* promoter is methylated in HCT-116 cells, we treated these cells with the demethylating agent 5-aza-2'-deoxycytidine (5-aza-dC) to determine whether Kaiso associates with the *HIF1A* promoter in a methylation-dependent manner. Consistent with our EMSA studies, 5-aza-dC treatment abolished Kaiso binding to the *HIF1A* promoter.

To ascertain whether Kaiso binding to the *HIF1A* promoter regulates its transcription, we generated a *HIF1A* promoter-reporter construct by cloning the ~1,000 bp putative regulatory region of the *HIF1A* promoter (Niu *et al.* 2008) into the pGLuc-basic luciferase vector (New England Biolabs). Ectopic expression of Kaiso repressed transactivation of the promoter construct in a dose-dependent manner in MCF-7 and HCT-116 cell lines (Figure 6.3A). Given that the reporter construct itself is not methylated, we reasoned that Kaiso's repressive effects might be attributed to repression of the endogenous *HIF1A* promoter, and consequently, a reduction in HIF-1α protein available to activate the reporter construct. Nevertheless, to confirm that the observed effects were not due to promoter squelching, we transfected cells with the *HIF1A* promoter-reporter construct and a *Kaiso* shRNA vector. Kaiso depletion resulted in increased *HIF1A* promoter activity compared to cells transfected with the reporter construct alone (Figure 6.3B). Furthermore, Kaiso depletion rescued the effects of ectopic Kaiso expression on the activity of the reporter construct (Figure 6.3B). Importantly, treatment of MCF-7 cells with 5-aza-dC abrogated Kaiso-mediated repression of the reporter construct (Figure 6.3C).

FIGURE 6.2: Kaiso binds the methylated *HIF1A* promoter. ChIP-qPCR analysis revealed that Kaiso binds to the *HIF-1A* promoter of MCF-7 and HCT-116 cells in hypoxia, but not in normoxia. Treatment of HCT-116 cells with the demethylating agent 5-aza-dC abolished Kaiso's association with the promoter. (* represents $p<0.05$; bars represent standard error of the mean and are representative of at least 2 independent trials).

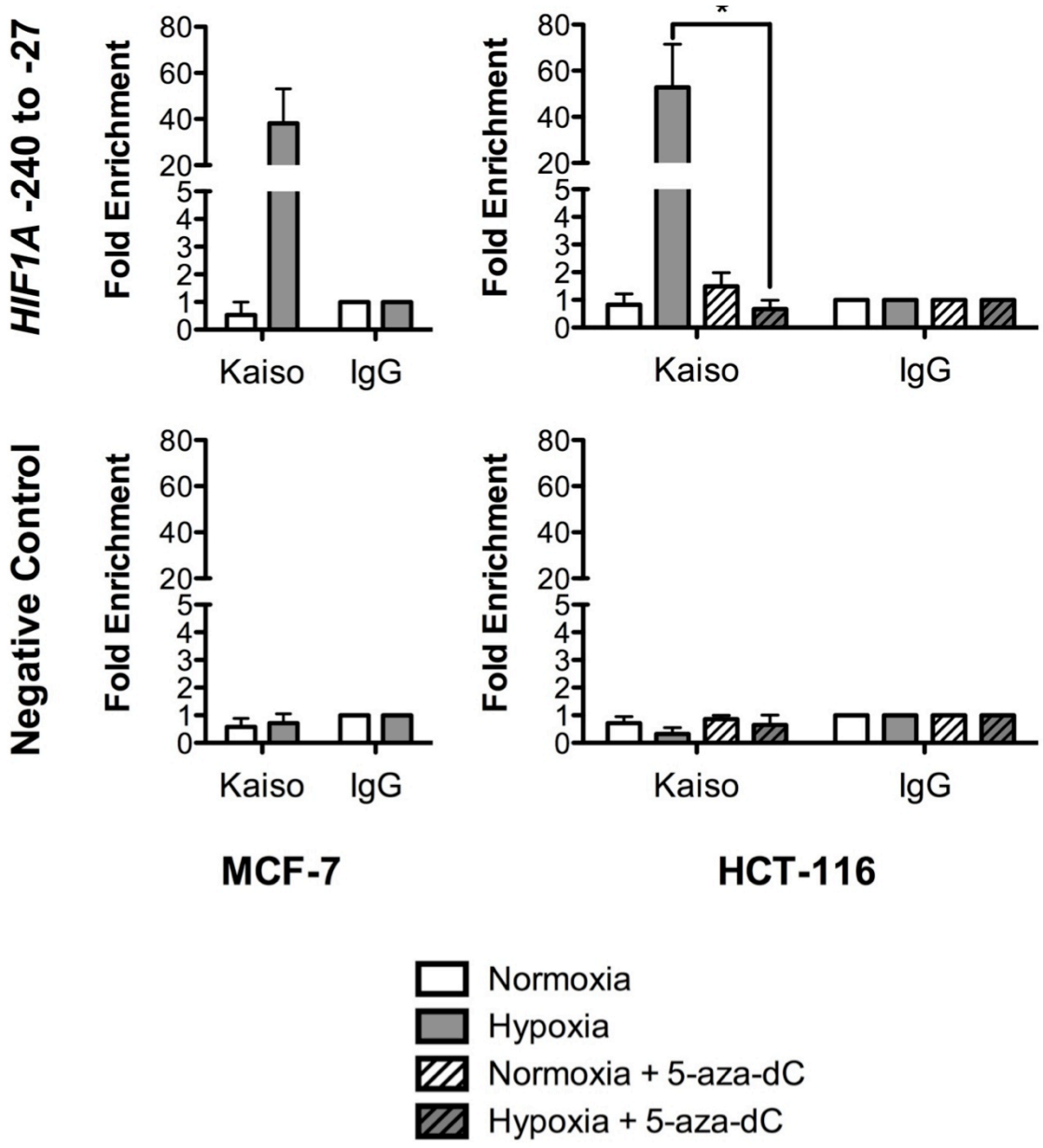
HIF1A -240 to -27
Negative Control
Fold Enrichment
80
60
40
20
5
4
3
2
1
0
Kaiso
IgG
*
MCF-7
HCT-116
Normoxia
Hypoxia
Normoxia + 5-aza-dC
Hypoxia + 5-aza-dC

FIGURE 6.3: Kaiso represses the *HIF1A* promoter in a methylation-dependent manner. (A) Ectopic Kaiso represses expression of a *HIF1A* promoter-luciferase construct in a dose-dependent manner. **(B)** Transfection of cells with a Kaiso shRNA vector results in activation of the *HIF1A* promoter. **(C)** Treatment of MCF-7 cells with 5-aza-dC abrogates Kaiso-mediated repression of the *HIF1A* promoter (* represents $p<0.05$; ** represents $p<0.01$; *** represents $p<0.001$; **** represents $p<0.0001$; representative of at least two independent trials; bars represent standard error of the mean).

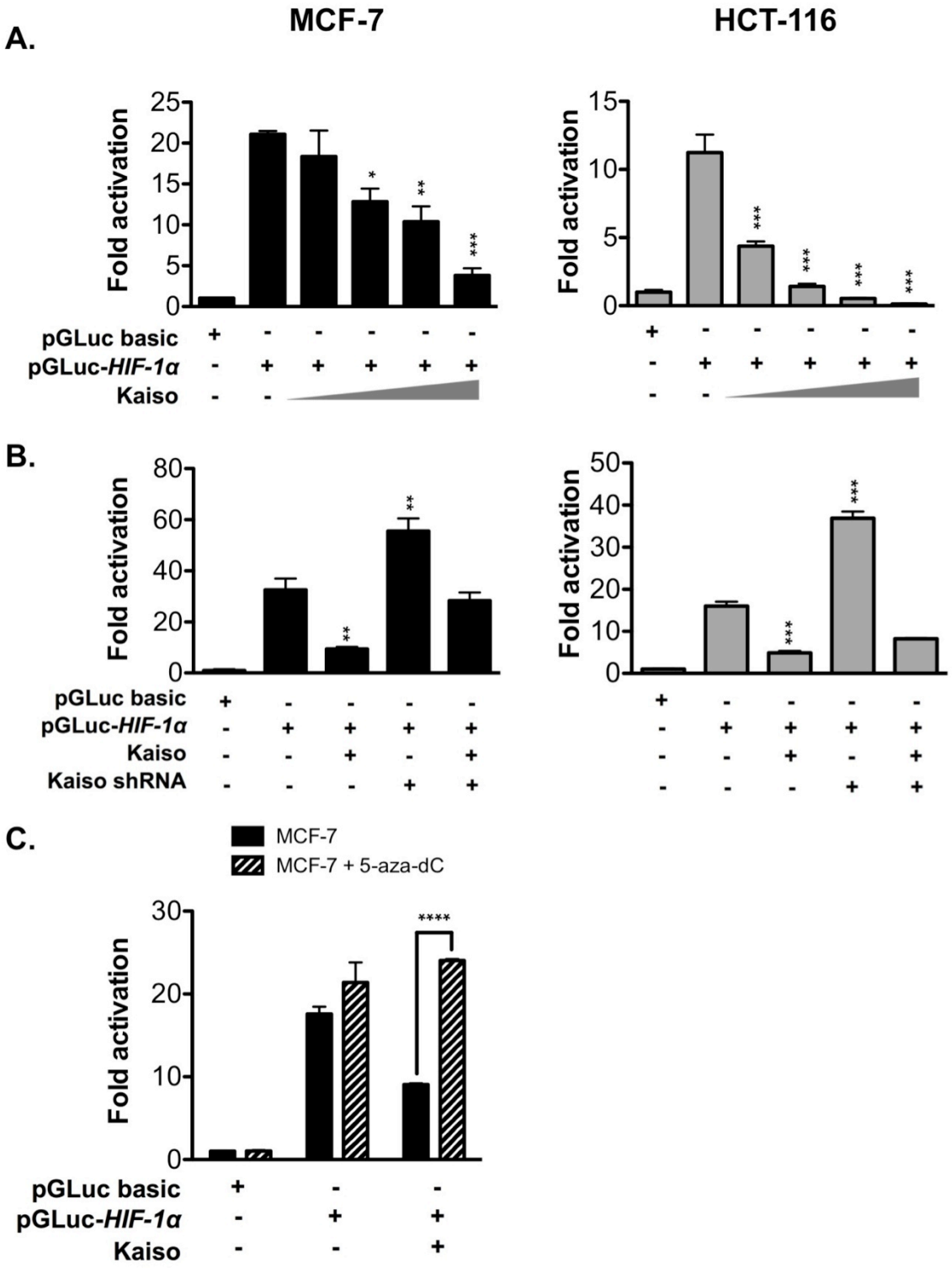
A.
MCF-7
HCT-116
Fold activation
pGLuc basic
pGLuc-HIF-1α
Kaiso
B.
Kaiso shRNA
C.
MCF-7
MCF-7 + 5-aza-dC

Kaiso depletion results in increased expression of HIF-1α and the HIF-1 target gene PDK-1

During hypoxia, cells undergo a metabolic switch from aerobic respiration to anaerobic glycolysis as a method of energy production (Kim *et al.* 2006; Semenza 2007). In the presence of oxygen, cells convert glucose to pyruvate, which is further converted to acetyl-Coenzyme A by pyruvate dehydrogenase (PDH) for entry into the tricarboxycylic acid (TCA) cycle (Kim *et al.* 2006). In hypoxia however, pyruvate dehydrogenase kinase isozyme 1 (PDK-1) is activated by HIF-1, which inhibits PDH activity and blocks the conversion of pyruvate to acetyl-Coenzyme A, thus preventing oxidative phosphorylation and energy production via the TCA cycle (Semenza 2007). Therefore, PDK-1 is one of several HIF-1 target genes that facilitate the switch from oxidative phosphorylation to glycolysis (Kim *et al.* 2006; Semenza 2007).

We examined the expression of HIF-1α and PDK1 in Kaiso-depleted cells to determine whether Kaiso's repressive effects on the *HIF1A* promoter alter HIF-1α expression and function (i.e. regulation of its target genes). Stable Kaiso-depleted HCT-116 and MDA-MB-231 cells exhibited an approximately 5-fold decrease in Kaiso transcripts, which was sustained during incubation of cells in hypoxia for 24 hours (Appendix Figure 1). In Kaiso-depleted HCT-116 cells, *HIF1A* transcripts were marginally increased in normoxia, whereas Kaiso-depleted MDA-MB-231 cells exhibited no change in *HIF1A* transcripts in normoxia. However, after 4 hours of hypoxic incubation, both HCT-116 and MDA-MB-231 Kaiso-depleted cell lines exhibited at least a 2-fold increase in *HIF1A* transcripts (Figure 6.4A). After 24 hours of hypoxic

incubation, *HIF1A* transcript levels decreased in both cell lines. While the decrease was still significant in hypoxia-treated MDA-MB-231 cells, it was not significant in hypoxia-treated HCT-116 cells (Figure 6.4A).

PDK-1 transcript levels were marginally increased upon Kaiso depletion in both cell lines in normoxia (Figure 6.4A). Significant increases in *PDK-1* transcripts were observed at 4 and 24 hours of hypoxic incubation in the MDA-MB-231 cell line, and after 4 hours of hypoxic incubation in the HCT-116 cell line (Figure 6.4A). Increased *PDK-1* transcript levels were also observed after 24 hours of hypoxic incubation in HCT-116 Kaiso-depleted cells, although this increase was not significant (Figure 6.4A). Kaiso depletion in MDA-MB-231 cell lines also resulted in increased HIF-1α protein expression after 4 hours of hypoxic incubation and increased PDK-1 protein expression in normoxia and after 4 and 24 hours of hypoxic incubation (Figure 6.4B). Increased HIF-1α protein expression was also detected in HCT-116 Kaiso-depleted cells after 4 and 24 hours of hypoxic incubation, while an increase in PDK-1 was only evident after 24 hours of hypoxic incubation (Figure 6.4B).

Finally, treatment of HCT-116 Kaiso-depleted cells with 5-aza-dC resulted in an even further increase in *HIF1A* expression (Figure 6.4C). These findings, combined with our ChIP data showing that Kaiso binds the *HIF1A* promoter preferentially during hypoxia, suggest that Kaiso's methylation-dependent regulation of *HIF1A* expression is enhanced during hypoxia.

FIGURE 6.4: Kaiso depletion increases HIF-1α expression. (A) *HIF1A* mRNA expression significantly increases in response to Kaiso depletion in HCT-116 and MDA-MB-231 cells. *PDK1* mRNA expression also increases in response to Kaiso depletion at all three time points, with the most significant change after 4 hours of hypoxic incubation in both cell lines **(B)** HIF-1α is increased in stable MDA-MB-231 and HCT-116 Kaiso depleted cells. **(C)** Treatment of cells with 5-aza-dC results in enhanced expression of *HIF1A* transcripts. (* represents $p<0.05$; ** represents $p<0.01$; *** represents $p<0.001$; **** represents $p<0.0001$. Bars represent standard error of the mean and are representative of at least 3 independent trials).

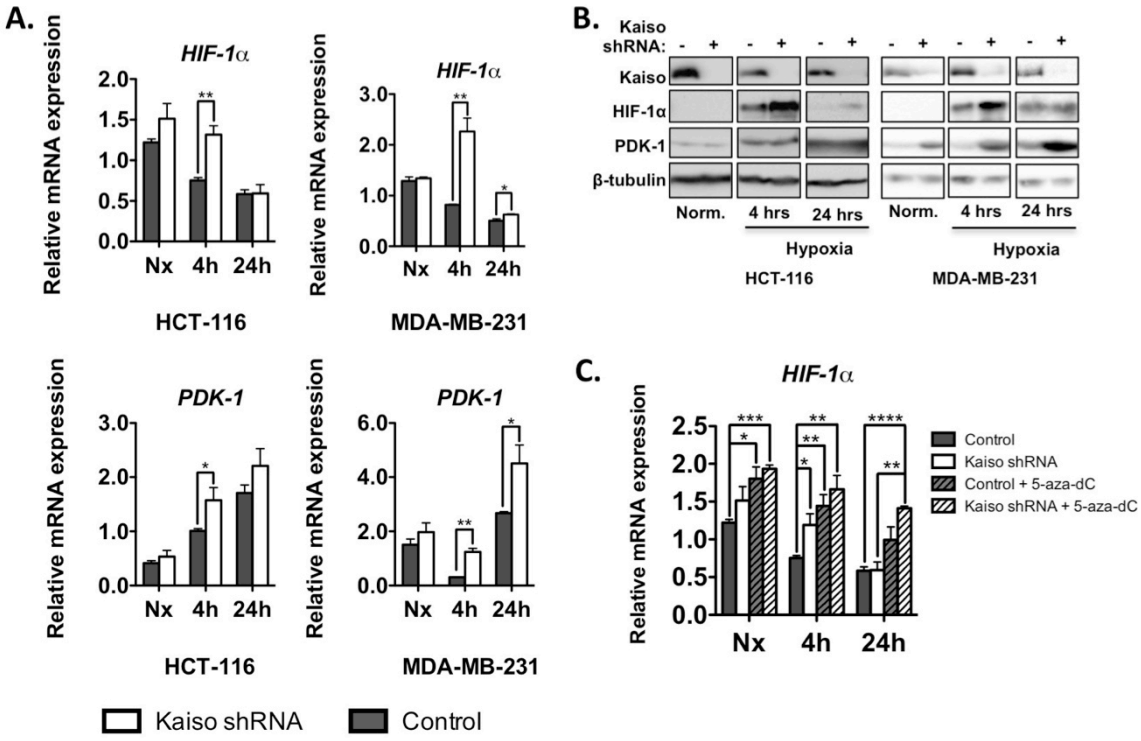
A.
HIF-1α
Relative mRNA expression
2.0
1.5
1.0
0.5
0.0
Nx 4h 24h
HCT-116
HIF-1α
Relative mRNA expression
3.0
2.0
1.0
0.0
Nx 4h 24h
MDA-MB-231
PDK-1
Relative mRNA expression
3.0
2.0
1.0
0.0
Nx 4h 24h
HCT-116
PDK-1
Relative mRNA expression
6.0
4.0
2.0
0.0
Nx 4h 24h
MDA-MB-231
Kaiso shRNA
Control
B.
Kaiso shRNA: - + - + - + - + - + - +
Kaiso
HIF-1α
PDK-1
β-tubulin
Norm. 4 hrs 24 hrs Norm. 4 hrs 24 hrs
Hypoxia Hypoxia
HCT-116 MDA-MB-231
C.
HIF-1α
Relative mRNA expression
2.5
2.0
1.5
1.0
0.5
0.0
Nx 4h 24h
Control
Kaiso shRNA
Control + 5-aza-dC
Kaiso shRNA + 5-aza-dC

Kaiso expression cycles during hypoxia

Our finding that Kaiso's binding and regulation of *HIF1A* occurred primarily in hypoxia was intriguing, since HIF-1α expression is typically induced during hypoxia. However, it has been previously shown that the hypoxia-induced stabilization of HIF-1α is transient and eventually dissipates under conditions of chronic hypoxia (24-48 hrs) (Stiehl *et al.* 2006; Ginouves *et al.* 2008; Bruning *et al.* 2011). Thus, we hypothesized that Kaiso functions to fine-tune the expression of HIF-1α in extended periods of hypoxia. If so, then Kaiso expression or function would also be altered in response to hypoxia.

To test our hypothesis, we incubated MDA-MB-231 and HCT-116 cells in hypoxic conditions and assayed Kaiso expression following 4, 8, 12 and 24 hours of incubation. There was no significant change in the expression of *Kaiso* mRNA over time in the MDA-MB-231 cell line (Figure 6.5A). However, similar to the oscillatory nature of HIF-1α protein expression during hypoxia (Stiehl *et al.* 2006; Ginouves *et al.* 2008; Bruning *et al.* 2011), Kaiso protein levels accumulated and peaked after 8 hours of hypoxic incubation, but subsequently declined back to normoxic levels by 24 hrs in hypoxia in MDA-MB-231 and HCT-116 cells (Figure 6.5B). These data suggest that Kaiso is stabilized at the protein level in early hypoxia, but subsequently returns to pre-hypoxic levels after extended periods in hypoxia.

DISCUSSION

To date, regulation of HIF-1α expression has been attributed to post-translational mechanisms, primarily stabilization of HIF-1α protein, which occurs at low oxygen levels (Wang *et al.* 1995). However, a recent study suggested that HIF-1α expression is also

FIGURE 6.5: **Hypoxia alters Kaiso protein expression**. (**A)** Kaiso transcript levels in MDA-MB-231 cells are unchanged by hypoxic incubation. (**B)** Kaiso protein increases up to 4 and 12 hours in hypoxia in MDA-MB-231 and HCT-116 cells and decline thereafter.

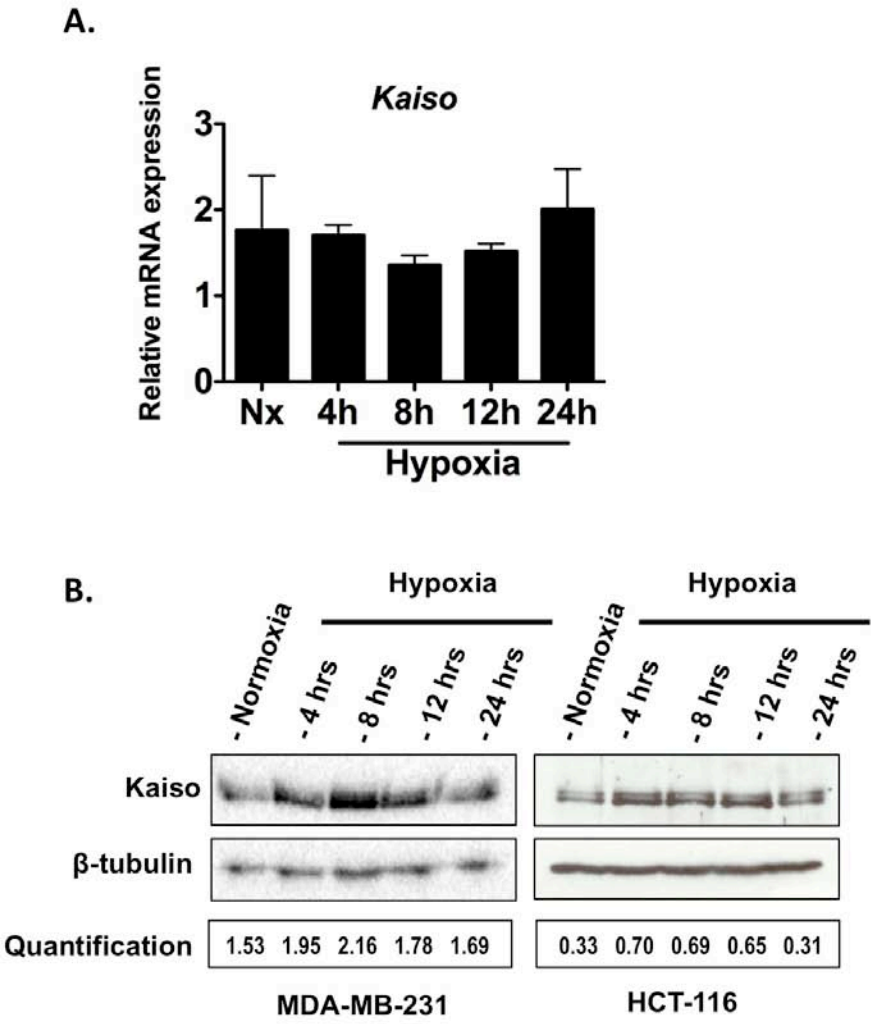
A.
Kaiso
Relative mRNA expression
3
2
1
0
Nx
4h
8h
12h
24h
Hypoxia
B.
Hypoxia
Hypoxia
- Normoxia
- 4 hrs
- 8 hrs
- 12 hrs
- 24 hrs
- Normoxia
- 4 hrs
- 8 hrs
- 12 hrs
- 24 hrs
Kaiso
β-tubulin
Quantification
1.53 1.95 2.16 1.78 1.69
0.33 0.70 0.69 0.65 0.31
MDA-MB-231
HCT-116

regulated at the transcriptional level through methylation of the CpG dinucleotide within an HRE in the *HIF1A* promoter, which prevents HIF-1 autoregulation during hypoxia (Koslowski *et al.* 2011). Intriguingly, this mechanism may also be relevant to HIF-1 target genes, since methylation of the CpG dinucleotide of an HRE in the promoter of the HIF-1 target gene, erythropoietin, was shown to abolish HIF-1 binding and transactivation of the promoter (Wenger *et al.* 1998; Yin and Blanchard 2000). Here we report that the transcription factor Kaiso, which binds methyl-CpG dinucleotides and represses transcription, regulates *HIF1A* gene expression by binding to its promoter in a methyl-CpG-dependent manner.

Kaiso is a unique dual-specificity transcription factor that binds methyl-CpG dinucleotides or the consensus Kaiso binding site (KBS) TCCTGCnA (Daniel and Reynolds 1999; Prokhortchouk *et al.* 2001; Daniel *et al.* 2002). We have previously shown that in the context of some gene promoters, methylation of CpG dinucleotides upstream of core KBS is necessary for Kaiso binding (Donaldson *et al.* 2012). However, Kaiso binds and regulates some promoters through the KBS or CpG dinucleotides alone (Spring *et al.* 2005; Lopes *et al.* 2008; Barrett *et al.* 2012; Jones *et al.* 2012; Jones *et al.* 2014). In the present study, Kaiso failed to bind non-methylated *HIF1A* promoter-derived oligos, in spite of the presence of core KBS sequences. Kaiso did however bind to methylated *HIF1A* promoter-derived oligos containing CpG dinucleotides, regardless of whether these oligonucleotides contained a core KBS. This suggests that the core KBS may not be sufficient for Kaiso binding to *HIF1A* promoter-derived DNA. It is intriguing that Kaiso bound to a methylated oligo encompassing a core KBS and 4 CpG

dinucleotides with higher affinity than a methylated oligo encompassing 7 CpG dinucleotides (Figure 6.1). This suggests that although the core KBS is dispensable for Kaiso binding to the *HIF1A* promoter, the presence of the KBS may strengthen Kaiso's association with the promoter.

While our finding that Kaiso expression increased during hypoxia was unexpected, it was consistent with our data showing that Kaiso binding to the *HIF1A* promoter occurs primarily in hypoxia. Surprisingly however, Kaiso accumulation did not appear to be due to enhanced transcription, as *Kaiso* mRNA levels remained relatively constant throughout hypoxic incubation. To date, few studies have identified factors that regulate Kaiso expression, however the fact that hypoxia-mediated regulation of Kaiso occurs post-transcriptionally suggests that hypoxia induces stabilization of Kaiso protein expression. The identification of pathways functioning upstream of Kaiso to modulate its expression and function are the topic of ongoing studies.

Surprisingly, PDK-1 protein expression increased in normoxia in MDA-MB-231 cells upon Kaiso depletion and, at high exposures, we also detected increased HIF-1α protein expression, although *HIF1A* mRNA remained unchanged (data not shown). These findings suggest that in addition to regulating *HIF1A* gene expression, Kaiso may also regulate HIF-1α via a post-transcriptional mechanism. Indeed, our pathway analysis revealed that phosphatidylinositol signaling was up-regulated in Kaiso-depleted cells (Table 6.1) suggesting that Kaiso may modulate HIF-1α protein stabilization via the PI3K pathway which is has been implicated in oxygen-independent stabilization of HIF-1α protein, by increasing HIF-1α protein synthesis (Zhong *et al.* 2000; Jiang *et al.* 2001;

Laughner *et al.* 2001; Pore *et al.* 2006; Maynard and Ohh 2007). However, additional studies need to be performed to determine whether this phenomenon occurs in other cell types, since we did not observe a similar trend in HCT-116 cells.

Collectively, our data suggest that Kaiso mediates methylation-dependent repression of the *HIF1A* promoter. Since the HIF-1α protein is stabilized during hypoxia, and HIF-1 activates transcription of *HIF1A* in a positive feedback autoregulatory loop, it is plausible that Kaiso protein accumulation in response to hypoxia functions to fine-tune *HIF1A* expression during the hypoxic response.

ACKNOWLEDGEMENTS

We would like to thank Dr. Nickett Donaldson for generating the pGLuc-*HIF1A* vector and Dr. Albert Reynolds (Vanderbilt University, Nashville, Tennessee) for the rabbit Kaiso polyclonal antibody.

CHAPTER 7

DISCUSSION

The identification of Kaiso as a nuclear binding partner for the Armadillo catenin p120^{ctn} over fifteen years ago (Daniel and Reynolds 1999; Daniel *et al.* 2002) was a significant discovery in the catenin-cadherin field, as it suggested that like β-catenin, p120^{ctn} modulated both cell adhesion and signaling events to effect changes in gene expression (Daniel 2007). Characterization of Kaiso led to its classification as a POZ-ZF protein and the founding member of a novel group of methylated DNA-binding proteins (Daniel and Reynolds 1999; Prokhortchouk *et al.* 2001; Daniel *et al.* 2002; Filion *et al.* 2006). Thus most initial Kaiso studies focused on elucidating Kaiso's transcriptional properties and mechanism of action. Since most POZ-ZF proteins were first identified in vertebrate development studies, early studies of Kaiso's role in *Xenopus* development provided critical insight into some of the molecular pathways and processes regulated by Kaiso, including apoptosis, the mid-blastula transition, non-canonical Wnt signaling and Wnt/β-catenin signaling (Kim *et al.* 2004; Ruzov *et al.* 2004; Park *et al.* 2005; Ruzov *et al.* 2009). However, contrary to findings in *Xenopus*, Kaiso is dispensable for murine development (Prokhortchouk *et al.* 2006). Nevertheless, Kaiso's regulation of apoptosis and canonical Wnt signaling appeared to be conserved in mammalian systems (Del Valle-Perez *et al.* 2011; Koh *et al.* 2014).

One glaring discrepancy exists between Kaiso's functions in modulating canonical Wnt signaling in *Xenopus* versus murine model systems; Kaiso represses Wnt signaling in *Xenopus* embryos, but Kaiso depletion delays polyp onset and prolongs lifespan in

Apc$^{Min/+}$ mice, which develop intestinal tumours due to the constitutive activation of Wnt signaling resulting from a loss of function mutation in *Apc* (Fodde *et al.* 2001; Prokhortchouk *et al.* 2006). While Kaiso has been found to promote tumorigenesis in several tissues including the intestines through mechanisms unrelated to Wnt signaling (Lopes *et al.* 2008; Zhang *et al.* 2011; Jones *et al.* 2012; Jones *et al.* 2014), it is not clear whether Kaiso's repressive effects on Wnt signaling are maintained in the murine intestines. Furthermore, how Kaiso contributes to tumorigenesis in intestines remains poorly understood. This thesis addressed these issues and provides valuable insight for future studies of Kaiso in carcinogenesis.

7.1. Characterization of phenotypes resulting from ectopic Kaiso expression in the intestine

7.1.1. Kaiso$^{Tg/+}$ *mice develop chronic intestinal inflammation*

Kaiso$^{Tg/+}$ mice exhibited several histological characteristics commonly associated with chronic intestinal inflammation, including enhanced immune cell infiltration of the lamina propria, villous blunting and fusion and crypt hyperplasia (Chapter 3, Figure 3). Although unexpected, this finding was intriguing in light of the findings that mosaic depletion of p120^{ctn} also results in chronic intestinal inflammation (Smalley-Freed *et al.* 2011). In humans, chronic intestinal inflammation underlies the etiology of the inflammatory bowel diseases (IBD), ulcerative colitis (UC) and Crohn's disease (CD) (Xavier and Podolsky 2007; Rubin *et al.* 2012). UC typically involves chronic inflammation of the rectum, which can progress proximally to affect the colon (Rubin *et*

al. 2012). In CD however, inflammation can occur along the entire gastrointestinal tract, with the ileum and colon most commonly affected (Rubin *et al.* 2012). Genome wide association studies have identified several genetic loci that can predispose individuals to UC and CD. However, it is now widely appreciated that IBD is a polygenic, complex disease, the pathology of which is heavily influenced by a number of environmental factors including altered immune responses to normal intestinal flora (Rubin *et al.* 2012).

A thorough examination of the underlying cause of inflammation in our *Kaiso*$^{Tg/+}$ model is beyond the scope of this thesis and is still under investigation (Chaudhary *et al.* manuscript in preparation). However given that p120^{ctn} has been found to regulate Kaiso function and localization, it is likely that the functions of p120^{ctn} and Kaiso in inflammation are related. In studies characterizing the inflammation resulting from p120^{ctn} knockout in various tissues, two recurring observations are that of RhoA-mediated activation of NFκB signaling and ectopic neutrophil recruitment (Perez-Moreno *et al.* 2006; Perez-Moreno *et al.* 2008; Smalley-Freed *et al.* 2010; Smalley-Freed *et al.* 2011; Stairs *et al.* 2011). To date, no study has examined whether Kaiso misexpression affects RhoA activity. However, we observed nuclear accumulation of p120^{ctn} in *Kaiso*$^{Tg/+}$ Line A and Line E mice (Chapter 3, Figure 4 & S2). Given that the cytoplasmic pool of p120^{ctn} inhibits RhoA activity, it is possible that the recruitment of p120^{ctn} to the nucleus when Kaiso is overexpressed in the intestine may phenocopy the effects of p120^{ctn} depletion, thus activating RhoA- NFκB signaling (Anastasiadis *et al.* 2000). Preliminary experiments also revealed increased neutrophil accumulation in the intestines of *Kaiso*$^{Tg/+}$

mice (Chaudhary *et al*., manuscript in preparation). Taken together, these data support the notion that the roles of Kaiso and p120^{ctn} in inflammatory signaling are related.

In the p120^{ctn} conditional knockout model, regions void of p120^{ctn} also exhibited significantly reduced E-cadherin expression resulting in a barrier defect as early as two months after p120^{ctn} loss was induced (Smalley-Freed *et al.* 2011). An intestinal barrier defect, which is described as the increased permeability of the intestinal epithelium, has been cited as both a cause and a consequence of IBD development (Antoni *et al.* 2014). This enhanced permeability enables food- and environmentally-derived microbes and antigens to come into contact with immune cells in the underlying lamina propria, which in turn mount an immune response resulting in inflammation (Antoni *et al.* 2014). Although Smalley-Freed *et al*. demonstrated that the inflammation resulting from p120^{ctn} loss was a cell autonomous phenomenon, the loss of E-cadherin and resultant barrier defect that occurred upon p120^{ctn} depletion likely exacerbated the inflammation in this model (Smalley-Freed *et al.* 2011). As previously mentioned, we noticed enhanced nuclear accumulation of p120^{ctn} in the intestines of *Kaiso*$^{Tg/+}$ mice. However we observed no change in E-cadherin expression (Roopali Chaudhary Doctoral Thesis, 2015). Nevertheless, we detected an intestinal barrier defect in 14-week-old Line E and 6 month-old Line A *Kaiso*$^{Tg/+}$ mice, which both exhibit extensive regions of inflammation-related dysplasia; however in 90-day old Line A and Line E mice, which exhibit detectable but less extensive dysplasia, we did not detect significant barrier defects (Chaudhary *et al.*, manuscript in preparation). Furthermore, in our preliminary analyses no consistent changes in the expression of tight junction proteins were detected in *Kaiso*$^{Tg/+}$ mice,

suggesting that the barrier defect is a consequence of, rather than a contributing factor to, inflammation in this model (Chaudhary *et al.*, manuscript in preparation).

Chronic inflammation is associated with malignancy in several different cancers including CRC (Xavier and Podolsky 2007; Rubin *et al.* 2012). Prolonged inflammation of the intestine results in a CRC subtype known as colitis-associated cancer (CAC), and IBD increases the risk of developing intestinal cancer by as much as 18% (Xavier and Podolsky 2007; Rubin *et al.* 2012). Not surprisingly, inflammation resulting from mosaic depletion of $p120^{ctn}$ resulted in adenoma formation in mice as early as 12 months of age (Smalley-Freed *et al.* 2011). This is another important distinguishing feature between the $p120^{ctn}$ conditional knockout model and our $Kaiso^{Tg/+}$ mice, since we have not observed adenomas in 12 month-old Line A $Kaiso^{Tg/+}$ mice. One potential explanation for this difference is that the onset of inflammation in mice conditionally depleted for $p120^{ctn}$ seems to occur earlier than in our $Kaiso^{Tg/+}$ model. Two months post-induction of $p120^{ctn}$ loss, mice exhibit enhanced neutrophil recruitment (Smalley-Freed *et al.* 2011), however the presence of activated neutrophils as indicated by myeloperoxidase assay is not detectable in 90 day old Line A $Kaiso^{Tg/+}$ mice (Appendix, Figure 2). Thus, it is possible that tumours develop later than 12 months of age in $Kaiso^{Tg/+}$ Line A mice and possibly earlier in other transgenic lines such as Line E, which have yet to be fully characterized. This possibility is supported by our observation of regionally advanced atypical hyperplasia in 8 month-old Kaiso Line A transgenic mice (Appendix, Figure 3). Thus, a more thorough histological analysis of Line A mice older than 12 months of age and other

transgenic lines with different transgene copy number is warranted to determine tumour development in this model.

7.1.2. Kaiso$^{Tg/+}$ mice exhibit an increased abundance of secretory cell populations in the intestines

Another striking feature that we observed in *Kaiso*$^{Tg/+}$ mice was the expansion of the secretory cell population i.e. goblet, Paneth and enteroendocrine cells in the small and large intestines (Chapter 3, Figure 5 & S3) accompanied by an overall decrease in cell proliferation (Chapter 3, Figure 6). This phenotype is reminiscent of that observed upon inhibition of the Notch signaling pathway in the intestine (Jensen *et al.* 2000; Fre *et al.* 2005; Ueo *et al.* 2012; van Es *et al.* 2012). Indeed, expression of the Notch pathway target gene *Hes1* was decreased in *Kaiso*$^{Tg/+}$ mice (Chapter 3, Figure 7), hinting at a novel role for Kaiso in regulating Notch signaling in the murine intestine.

The Notch signaling pathway is a cell-cell signaling pathway modulated by the binding of the transmembrane Delta-like (DLL1, DLL3, DLL4) and Serrate-like (JAGGED1 and JAGGED2) ligands to Notch receptors on neighbouring cells (Noah and Shroyer 2013). This binding event activates the Notch receptor, which subsequently undergoes two consecutive cleavages resulting in the release of the **N**otch **i**ntra**c**ellular **d**omain (NICD) into the cytoplasm. The NICD translocates to the nucleus, where it binds to the transcription factor recombining binding protein suppressor of hairless or RBP-J (Noah and Shroyer 2013). In unstimulated cells RBP-J associates with corepressors, which are displaced on NICD binding. NICD recruits coactivators to RPB-J to form an activator complex, the primary targets of which are members of the basic helix-loop-helix

hairy and **e**nhancer of **s**plit (HES) family of transcriptional repressors (Kageyama *et al.* 2007).

The Notch signaling pathway is essential in controlling the fate of intestinal stem cells (Noah and Shroyer 2013). HES proteins bind and repress the transcriptional activator **ato**nal **h**omolog **1** (ATOH1), also known as Math1 in mice and HATH1 in humans. In the intestine ATOH1 is responsible for intestinal secretory cell commitment and *Atoh1* depletion in mice elicits a secretory to absorptive fate switch in epithelial progenitors (Yang *et al.* 2001; Shroyer *et al.* 2007). Thus not surprisingly, inhibition of the Notch pathway by blocking cleavage of the Notch receptor, *Rbp-j* depletion or *Hes1* depletion results in a dramatic overproduction of goblet cells at the expense of absorptive enterocytes (Jensen *et al.* 2000; van Es *et al.* 2005). Complementary gain of function studies in mice expressing a transgene for the NICD yielded the opposite phenotype i.e. an expansion of immature progenitor cells and a block in the differentiation of goblet cells (Fre *et al.* 2005). Inhibition of Notch signaling by blocking cleavage of the Notch receptor or *Rbp-j* depletion has no effect on the numbers of enteroendocrine and Paneth cells (van Es *et al.* 2005); while *Hes1* depletion resulted in increased expression of enteroendocrine cells, but no change in Paneth cell numbers (Jensen *et al.* 2000). This discrepancy in phenotypes may be attributed to the expression of multiple redundantly functioning *Hes* genes (*Hes 1, 3, 5*) in the intestine (Jensen *et al.* 2000; van Es *et al.* 2005; Ueo *et al.* 2012). While the level at which Kaiso regulates the Notch pathway is currently under investigation in our lab, the fact that $Kaiso^{Tg/+}$ mice exhibit increased enteroendocrine and Paneth cell populations suggests that ectopic Kaiso expression

results in the loss of expression of multiple *Hes* genes. Future studies should focus on characterizing the expression of a wider scope of Notch-related proteins in *Kaiso*$^{Tg/+}$ mice, as the first step in delineating which level of the Notch pathway is modulated by Kaiso.

7.1.3. Summary of findings in Kaiso$^{Tg/+}$ *mice*

Assessment of the most prominent phenotypes resulting from ectopic expression of Kaiso in the intestines unearthed novel and exciting putative roles for Kaiso in regulating intestinal inflammation and Notch signaling in the intestine. Whether these phenotypes are related remains unknown; however, intestinal epithelial cell-specific depletion of Rbp-j results in spontaneous colitis, accompanied by decreased proliferation and an intestinal barrier defect (Obata *et al.* 2012). Thus the possibility exists that inflammation in *Kaiso*$^{Tg/+}$ mice may be secondary to inhibition of Notch signaling.

Our finding of atypical hyperplasia in *Kaiso*$^{Tg/+}$ mice suggests that Kaiso may promote intestinal malignancy. Based on previous studies, we assumed that Kaiso's role in intestinal tumorigenesis, if any, would be mediated through the Wnt pathway. However our findings in *Kaiso*$^{Tg/+}$ mice have hinted at alternate mechanisms by which Kaiso may participate in intestinal tumorigenesis.

7.2. Kaiso promotes intestinal tumorigenesis

7.2.1. Kaiso expression is increased in murine and human intestinal neoplasias

The expression of Kaiso has been positively correlated with malignancy in breast, lung and prostate cancer (Dai *et al.* 2009; Dai *et al.* 2010; Jones *et al.* 2012; Vermeulen *et al.* 2012; Jones *et al.* 2014). However prior to this study, a thorough analysis of Kaiso

expression in colon cancer tissue had not been performed. Our finding of increased Kaiso expression in human intestinal tumour tissue compared to normal tissues (Chapter 4, Figure 4.1) agrees with findings in both breast and prostate tissues where low Kaiso expression is found in healthy tissues but high Kaiso expression is found in high grade or metastatic tissues (Jones *et al.* 2012; Vermeulen *et al.* 2012; Jones *et al.* 2014). Notably, although Kaiso staining gradually increased from normal to metastatic tissue in human intestinal tissues, we did not notice a trend of increasing nuclear Kaiso staining with increasing malignancy. Instead Kaiso staining was localized to both the cytoplasm and the nucleus in most tissues, irrespective of stage (Chapter 4, Figure 4.1). In both studies examining Kaiso localization in breast and prostate cancer tissues, nuclear Kaiso was shown to repress E-cadherin expression. Thus the authors suggested that increased expression of Kaiso in poorly differentiated tumours and metastases may contribute to tumour metastasis (Jones *et al.* 2012; Jones *et al.* 2014). However, since we noted no change in E-cadherin expression between $Kaiso^{Tg/+}$:$Apc^{Min/+}$ and $Apc^{Min/+}$ tissues, Kaiso's repression of E-cadherin may not be maintained in the intestines (Appendix, Figure 4). These differences in Kaiso expression and function in diverse tumour types support the notion that Kaiso's roles in tumorigenesis are diverse and may be tissue- or context-specific.

Lastly, in contrast to human tissues, we noted increased nuclear expression of Kaiso in the polyps of $Apc^{Min/+}$ mice (Chapter 4, Figure 4.1). In adjacent normal murine intestinal tissue weak nuclear and cytoplasmic staining was observed and in tissues from age-matched non-transgenic mice staining for Kaiso was weak and mainly localized to

the cytoplasm. The difference in Kaiso localization between human and murine tissues may be attributed to differences in staining protocols utilized for the tissues. Human and murine tissue slides were fixed and prepared differently, and consequently protocols for staining these tissues were optimized individually and differed in many respects including the anti-Kaiso antibody used. Furthermore, the human tissue microarrays that we utilized in our analysis were largely comprised of tissues from the large intestine, while polyps in $Apc^{Min/+}$ mice develop primarily in the small intestine. Nevertheless, our studies demonstrate that the overall trend of increased Kaiso expression with increasing malignancy in the intestines is conserved between humans and mice.

7.2.2. Characterization of Kaiso$^{Tg/+}$: Apc$^{Min/+}$ mice

Similar to our studies in $Kaiso^{Tg/+}$ mice, we performed an unbiased analysis of the phenotypes resulting from ectopic expression of Kaiso in the intestines of $Apc^{Min/+}$ mice. From as early as 60 days of age, Line A $Kaiso^{Tg/+}$:$Apc^{Min/+}$ mice exhibited obvious signs of illness, including hunched posture, fecal occult blood and pale extremities, while age-matched $Apc^{Min/+}$ mice appeared relatively normal. Based on the early manifestation of these symptoms, we were not surprised that $Kaiso^{Tg/+}$:$Apc^{Min/+}$ mice exhibited endpoint symptoms and a dramatically increased polyp burden compared to $Apc^{Min/+}$ mice (Chapter 4, Figure 4.).

Unexpectedly, polyps in $Kaiso^{Tg/+}$:$Apc^{Min/+}$ mice were smaller than those observed in age-matched $Apc^{Min/+}$ mice. Furthermore, in spite of previous reports that Kaiso represses the cell cycle gene *cyclinD1* (Park *et al*. 2005; Donaldson *et al.* 2012; Jiang *et al.* 2012), there was no change in cell proliferation as measured by Ki67 staining in

Kaiso$^{Tg/+}$*:Apc*$^{Min/+}$ mice. Instead, we observed increased apoptosis in the polyps of *Kaiso*$^{Tg/+}$*:Apc*$^{Min/+}$ mice. These phenotypes, i.e. decreased polyp size, no change in proliferation and increased apoptosis are inconsistent with tumour formation, but may be partially attributed to Kaiso's role in promoting p53-mediated apoptosis (Koh *et al.* 2014). The tumour suppressor p53 becomes activated in response to cellular stresses such as ionizing radiation, hypoxia, carcinogens, and oxidative stress and mediates cell cycle arrest, DNA repair, senescence, and apoptosis (Pflaum *et al.* 2014). A recent report demonstrated that Kaiso is induced in response to the DNA-damaging agent etoposide and interacts with p300 to promote acetylation of p53 (Pflaum *et al.* 2014). Acetylation of p53 enhances its association with its target genes, and consequently Kaiso depletion results in decreased expression of cell cycle arrest gene *CDKN1A* and several pro-apoptotic genes including *PUMA*, *Bax*, *Caspase 3* and *Caspase 8*. Thus, in spite of the fact that ectopic Kaiso results in increased tumour incidence, Kaiso also promotes tumour cell apoptosis.

Based on Kaiso's seemingly contradictory roles in the intestines i.e. promoting polyp formation while inducing apoptosis, attempts to classify Kaiso as a *bona fide* tumour suppressor or an oncogene in the intestines may be overly simplistic. The overall effect that Kaiso elicits in a given tumour may be dependent on its interaction partners and the proteins functioning upstream of Kaiso to regulate its function and expression.

7.2.3. Wnt signaling is enhanced by Kaiso overexpression

Surprisingly, ectopic Kaiso expression increased expression of several Wnt target genes (*CD44*, *EphB2, Axin2*, *MMP7*), suggesting that Kaiso's regulation of Wnt signaling is complex and may be influenced by tissue- or organism-specific factors.

The majority of polyps in $Apc^{Min/+}$ mice have undergone a loss of heterozygosity at the *Apc* locus (Fodde and Smits 2001). Therefore, the increased Wnt target gene expression observed in $Kaiso^{Tg/+}$:$Apc^{Min/+}$ mice may be partially attributed to the significantly higher polyp burden. The mechanism underlying the increased Wnt target gene expression observed in $Kaiso^{Tg/+}$ mice is less obvious and while we were unable to determine precisely how Kaiso potentiates Wnt signaling, several mechanisms may contribute to this phenomenon. In the mammalian intestines, a Wnt signaling gradient exists whereby Wnt signaling is most active in the crypts and decreases in intensity further up the crypt-villus axis (Gregorieff and Clevers 2005). In Wnt-stimulated cells, the interaction between Kaiso and Tcf4 is reduced, alleviating Kaiso's repressive effects on Wnt target genes (Del Valle-Perez *et al.* 2011). This may explain why Kaiso's repression of Wnt target genes is not maintained in the intestine; however, it does not account for the enhanced Wnt target gene expression we observed. Promoter hypermethylation has been identified as a mechanism by which the expression of Wnt antagonists e.g. *Dkk1*, *Lect2* and *Sfrp5*, are downregulated in colorectal carcinogenesis (Sato *et al.* 2007; Phesse *et al.* 2008; Samuel *et al.* 2009; Zhang *et al.* 2014). Since Kaiso binds meCpG dinucleotides, it is possible that Kaiso mediates methylation-dependent silencing of Wnt antagonists in the intestines. In support of this notion, we found

decreased expression of the Wnt antagonist *Lect2* in *Kaiso*$^{Tg/+}$ mice. Lastly, since Kaiso functions as both a transcriptional activator and a repressor (Rodova *et al.* 2004; Daniel 2007; Koh *et al.* 2014), it is possible that Kaiso recruits co-activator rather than co-repressor complexes to the promoters of Wnt target genes in the intestines.

Although further studies are required to tease apart the mechanism by which Kaiso potentiates Wnt signaling in the intestine, ectopic expression of Kaiso alone was not sufficient to drive tumour formation in mice up to 12 months of age (Chapter 3). Thus multiple mechanisms may be responsible for Kaiso's role in promoting tumorigenesis in the intestine.

7.2.4. Kaiso$^{Tg/+}$:Apc$^{Min/+}$ mice exhibit accelerated intestinal inflammation

The inflammation that we observed in 12-month old *Kaiso*$^{Tg/+}$ mice combined with the increased tumour burden in *Kaiso*$^{Tg/+}$*:Apc*$^{Min/+}$, promted us to examine whether *Kaiso*$^{Tg/+}$*:Apc*$^{Min/+}$ exhibit intestinal inflammation. Polyposis in the *Apc*$^{Min/+}$ model is accompanied by increased inflammation and treatment of *Apc*$^{Min/+}$ mice with anti-inflammatory agents, such as sulindac and celecoxib, attenuates polyp formation (Swamy *et al.* 2006; McClellan *et al.* 2012; Lee *et al.* 2014). Thus not surprisingly, we observed increased inflammatory phenotypes in our 90-day old *Kaiso*$^{Tg/+}$*:Apc*$^{Min/+}$ mice, whereas only mild inflammation-associated histological features were observed in age-matched *Kaiso*$^{Tg/+}$ mice.

We did not observe nuclear accumulation of p120^{ctn} in 90-day old *Kaiso*$^{Tg/+}$*:Apc*$^{Min/+}$ mice (Appendix Figure 5), which suggests that the nuclear accumulation of p120^{ctn} may be not be a primary cause of inflammation in the intestine.

This finding does not however rule out the possibility that Kaiso's role in inflammation is linked to that of p120^{ctn}'s, since Kaiso may also influence p120^{ctn} activity or the expression different p120^{ctn} isoforms.

Whereas we observed increased expression of multiple pro-inflammatory cytokines in *Kaiso*$^{Tg/+}$*:Apc*$^{Min/+}$ intestinal homogenates, expression of IL-9 and IL-12(p70), cytokines associated with specific subsets of T-cells, were significantly decreased in *Kaiso*$^{Tg/+}$*:Apc*$^{Min/+}$ intestinal homogenates (Appendix, Figure 6). IL-9 is primarily secreted by a subset of T-helper cells (Goswami and Kaplan 2011), and IL-12 is secreted by activated antigen presenting cells and haematopoietic phagocytes to orchestrate immune responses by Th1 cells (Lasek *et al.* 2014). Cytokines that were increased in *Kaiso*$^{Tg/+}$*:Apc*$^{Min/+}$ intestinal homogenates include various cytokines involved in the differentiation and recruitment of granulocytes and macrophages. These data suggest that in intestinal epithelial cells, Kaiso may modulate the expression of cytokines that are essential for the proper recruitment of immune cells, which may in turn promote intestinal inflammation (Kunkel *et al.* 2003; Hart *et al.* 2010).

Regardless of the mechanism by which Kaiso promotes inflammation, inflammation may be a contributing factor to the increased polyp burden in *Kaiso*$^{Tg/+}$*:Apc*$^{Min/+}$. The products of immune cells, which infiltrate the intestine during inflammation, include pro-inflammatory cytokines and chemokines, as well as oxygen and nitrogen reactive species. These immune cell products can induce genomic mutations and DNA damage (Low *et al.* 2014). Indeed, mutations in *p53*, *Apc, Kras* and *β-catenin*

are found in colitis-associated cancer, although the incidence and timing of these mutations vary between sporadic CRC and CAC (Low *et al.* 2014; Rogler 2014).

7.2.5. Summary of findings in Kaiso$^{Tg/+}$:Apc$^{Min/+}$ mice

Our studies into Kaiso's role in intestinal tumorigenesis revealed previously uncharacterized mechanisms by which Kaiso may potentiate intestinal tumorigenesis and distinct contextual roles for Kaiso's regulation of the Wnt signaling pathway. The increased expression of Wnt target genes upon ectopic expression of Kaiso was surprising and may contribute to Kaiso's role in promoting tumorigenesis in the intestine. Kaiso-induced inflammation may also contribute to the enhanced polyp burden observed in *Kaiso$^{Tg/+}$:Apc$^{Min/+}$* mice. Given that inflammation can result in mutation of Wnt pathway components and consequently increase Wnt signaling activity in CAC, future studies should explore whether the increased Wnt signaling observed in *Kaiso$^{Tg/+}$* and *Kaiso$^{Tg/+}$:Apc$^{Min/+}$ mice* may be linked to Kaiso-induced inflammation.

7.3. Methylation and sequence-specific binding and regulation of the cell cycle gene *cyclinD1* by Kaiso

Crystal structures of the Kaiso zinc finger domain in complex with either the KBS or sequential meCpG dinucleotides revealed that the molecular interactions that mediate binding to these distinct DNA target sites are very similar (Buck-Koehntop *et al.* 2012) However, whether Kaiso discriminates between these two sites in binding and regulating a given locus has not been fully elucidated (Daniel and Reynolds 1999; Prokhortchouk *et al.* 2001; Daniel *et al.* 2002; Martin Caballero *et al.* 2009; Ruzov *et al.* 2009; Donaldson

et al. 2012). In this study, we utilized the *CCND1* promoter as the context to examine the relative contribution of Kaiso binding to these distinct sites within the promoter to regulate *cyclinD1* gene expression.

Prior to our study, two independent reports characterized *cyclinD1* as a Kaiso target gene in *Xenopus* embryos and mammalian cell lines (Park *et al.* 2005; Jiang *et al.* 2012). In our study, and that conducted by Jiang *et al.*, Kaiso was shown to interact with the *CCND1* promoter in a region containing a full KBS site located -1067 bp relative to the transcriptional start site (Jiang *et al.* 2012). We extended our characterization of Kaiso's interaction with the *CCND1* promoter to examine a region encompassing a core KBS at +69 bp, which is flanked 8 and 5 bp upstream and immediately downstream by CpG dinucleotides. Although the +69 core KBS was not necessary for Kaiso binding, mutation of this cite reduced Kaiso's affinity for the +69 EMSA oligonucleotide (Chapter 5, Figure 4). This finding suggests that the presence of the core KBS in close proximity to consecutive meCpG dinucleotides may serve to strengthen Kaiso's interaction with DNA, hinting that Kaiso binding to the KBS and proximal meCpG dinucleotides at a given locus may be cooperative. Indeed, xKaiso was shown to form homodimers or higher order oligomers (Kim *et al.* 2002), which may facilitate Kaiso binding to sites such as the +69 site.

Although our findings shed light on the mechanism by which Kaiso binds to and potentially regulates the *CCND1* promoter, the physiological circumstances under which Kaiso's repression of this locus results in a significant phenotypic change remain unknown. Kaiso is expressed at relatively high levels in MCF-7 and HCT-116 cells and

we detected Kaiso binding to the *cyclinD1* promoter in both cell lines; however Wnt-induced cyclin D1 expression is necessary for HCT-116 cell cycle progression (Tetsu and McCormick 1999) and cyclin D1 is overexpressed and drives proliferation of MCF-7 cells in response to estrogen stimulation (Sabbah *et al.* 1999). Thus, Kaiso may not be a major regulator of *cyclinD1* in these cell lines, which is supported by our findings of modestly increased cell proliferation and cyclin D1 protein expression in stable Kaiso-depleted HCT-116 cells (Chapter 5, Figure 7). Furthermore, to the best of our knowledge, promoter methylation has not been identified as mechanism by which *cyclinD1* gene expression is regulated.

Repression of *cyclinD1* is a hallmark of cell differentiation for certain cell lineages, and is also associated with the epithelial to mesenchymal transition and cellular quiescence (Klein and Assoian 2008). Examining a role for Kaiso in models such as these in which *cyclinD1* expression is repressed may be valuable in identifying a physiological context for the relationship between Kaiso and *cyclinD1*.

7.4. A role for Kaiso in the methylation-dependent regulation of HIF-1α expression during hypoxia

Hypoxia is a common characteristic of the tumour microenvironment that arises as a consequence of the highly abnormal and disorganized tumour microvasculature, which is incapable of meeting the metabolic demands of the rapidly growing tumour (Vaupel 2004). Cells experiencing hypoxia initiate a series of adaptive responses primarily orchestrated by the transcription factor HIF-1 that collectively enable them to adapt to the reduced oxygen concentrations (Wang and Semenza 1993). In most tumours, several

regulatory mechanisms are overridden, which results in uncontrolled cell proliferation, resistance to apoptosis and neovascularization and culminates in tumour cell migration, invasion and metastatic dissemination (Compagni 2000). In hypoxic tumours, HIF-1 and HIF-1 target genes, in addition to promoting overall survival, also mediate many of the aforementioned processes responsible for malignant progression. Thus HIF-1, and specifically the HIF-1α subunit has emerged as an important prognosticator and therapeutic target (Sullivan and Graham 2007).

The HIF-1 protein is a heterodimer comprised of the constitutively expressed HIF-1β subunit and the oxygen-sensitive HIF-1α subunit (Wang *et al.* 1995; Wang and Semenza 1995). The expression of the HIF-1α subunit is highly regulated, primarily by post-translational mechanisms affecting its protein synthesis, degradation and protein stability, and consequently it is this subunit that dictates HIF-1 function (Poon *et al.* 2009). Very few studies have explored the transcriptional mechanisms regulating HIF-1α expression. We sought to explore a role for Kaiso in modulating *HIF1A* gene expression in light of recent studies demonstrating that the *HIF1A* promoter is regulated by methylation (Koslowski *et al.* 2011) and our finding that *HIF1A* transcripts are increased in Kaiso-depleted cells.

Our studies demonstrated that Kaiso binds the *HIF1A* promoter in a methylation-dependent manner, in spite of the presence of 3 core KBS sites in the promoter. Kaiso depletion resulted in increased expression of HIF-1α mRNA transcripts and protein, as well as increased expression of the HIF-1 target PDK-1. Koslowski et al. demonstrated that methylation of an HRE within the *HIF1A* promoter prevents HIF-1 from binding to

this site, thereby impeding its transcriptional activation of the locus (Koslowski *et al.* 2011). It is unclear whether Kaiso represses *HIF1A* by recruiting co-repressor complexes to the promoter or by binding to the promoter at the autoregulatory HRE site, thereby sterically hindering HIF-1 from binding and activating the promoter.

Surprisingly, Kaiso's regulation of *HIF1A* expression occurs primarily in hypoxia, which is counterintuitive given that HIF-1α protein is stabilized in hypoxia. Multiple studies have reported that HIF-1α is transiently up-regulated in response to hypoxia, however this change is eventually resolved even while the cells are maintained in hypoxia (Stiehl *et al.* 2006; Ginouves *et al.* 2008; Bruning *et al.* 2011). Indeed, we noticed a similar oscillatory trend in HIF-1α protein expression in our own time course studies. Prolonged stabilization of HIF-1α was shown to induce necrosis in cells, highlighting the importance of HIF-1α down-regulation for cell survival during chronic hypoxia (Ginouves *et al.* 2008). While studies have attributed the resolution of HIF-1α expression after prolonged periods of hypoxia to an autoregulatory loop involving hypoxic induction of negative regulators HIF-1α, namely prolyl hydroxylases 2 and 3 and microRNA-155, it is possible that Kaiso may also function to mediate this process (Stiehl *et al.* 2006; Ginouves *et al.* 2008; Bruning *et al.* 2011).

In support of the involvement of Kaiso in a negative feedback loop with HIF-1α and/or hypoxia, Kaiso protein expression steadily increases within the first 8 hours of hypoxic incubation and gradually returns to pre-hypoxic levels by 24 hours of hypoxic incubation. We were unable to determine the precise mechanism responsible for these changes in Kaiso expression. However, we noted that Kaiso mRNA levels remained fairly

constant throughout hypoxic incubation, suggesting that hypoxia increases Kaiso expression via a post-transcriptional mechanism such as increased translation or protein stabilization. During hypoxia, tumour cells have been shown to reduce the overall level of mRNA translation to preserve energy while simultaneously increasing the translation of select proteins, including stress response proteins and proteins required for hypoxic adaptation (Leprivier *et al.* 2014). This is one possible explanation for the increased expression of Kaiso in hypoxia. However, the pathways functioning upstream of Kaiso to regulate its expression remain largely unknown and thus further studies are needed to determine how Kaiso protein expression is regulated during hypoxia.

Regulation of hypoxic gene expression through HRE methylation is not only limited to the of *HIF1A* promoter. Methylation of an HRE in the promoter of the HIF-1 target gene *erythropoietin* regulates its expression, enabling methylation-dependent, tissue-specific hypoxic induction of erythropoietin (Wenger *et al.* 1998; Yin and Blanchard 2000). Furthermore, methylation-dependent protein complexes in nuclear extracts from HeLa cervical carcinoma and Hep3B hepatocellular carcinoma cells bound *erythropoietin* promoter-derived oligonucleotides, although the identity of the proteins in these complexes was not confirmed (Yin and Blanchard 2000). Combined, these studies hint that HRE methylation and subsequent binding of methylated DNA binding proteins, such as Kaiso, may represent a novel mechanism of regulation of hypoxic response genes.

7.5. Outstanding Issues: The interplay of p120^{ctn} and Kaiso in inflammation

The studies described in this thesis have offered significant and unique insights into biological roles of Kaiso in the intestines, which may be conserved in other tissues and model systems. Many of our findings were interesting and novel, but perhaps the most pressing and unanswered question arising from this work is that of the mechanism by which Kaiso promotes intestinal inflammation. As previously described, Kaiso's role in inflammation may be linked to that of $p120^{ctn}$. The two most likely possibilities in this regard are: i.) Kaiso functions downstream of $p120^{ctn}$ to mediate inflammation and ii.) Kaiso modulates inflammation by altering $p120^{ctn}$'s function or expression. Rescue studies in which $p120^{ctn}$ and Kaiso are simultaneously depleted may help to resolve whether Kaiso functions downstream of Kaiso to modulate inflammation. Furthermore, most studies to date have focused on characterizing $p120^{ctn}$'s effect on Kaiso's and not *vice versa*, hence further experiments are required to determine whether Kaiso misexpression alters $p120^{ctn}$ function or expression. $p120^{ctn}$'s role in inflammation is incompletely understood, however multiple studies point to $p120^{ctn}$'s modulation of NF-κB signaling through its effects on RhoA as an explanation for the inflammation resulting from $p120^{ctn}$ depletion (Perez-Moreno *et al.* 2006; Perez-Moreno *et al.* 2008; Stairs *et al.* 2011). In spite of Kaiso's relationship with $p120^{ctn}$, no studies to date have investigated whether Kaiso modulates RhoA activity and consequently NF-κB signaling. Since ectopic expression of Kaiso results in inflammation, the effect of Kaiso on RhoA activity warrants investigation.

The physiological contexts in which Kaiso regulates inflammation also remain unclear. Preliminary studies of Kaiso expression in gene expression data sets from IBD

patient biopsies revealed no differences in Kaiso expression between IBD and normal tissue. The association between increased expression of Kaiso and malignant progression, coupled with the acceleration of inflammation in *Kaiso*$^{Tg/+}$:*Apc*$^{Min/+}$ mice, suggest that the pro-inflammatory function of Kaiso may be more relevant in the context of tumorigenesis.

7.6. Concluding remarks

Kaiso is a unique transcription factor with widespread and diverse functions. The findings of this thesis exemplify Kaiso's diversity and provide significant insight into the function of Kaiso in the intestines. Firstly, we identified novel roles for Kaiso in intestinal inflammation and in cell fate decisions through regulation of the Notch signaling pathway. Additionally, we determined two putative mechanisms by which Kaiso may contribute to intestinal tumorigenesis: i) through activation of Wnt target genes and ii) by promoting intestinal inflammation. Lastly, we identified roles for Kaiso in methylation-dependent regulation of the pro-oncogenic proteins cyclinD1 and HIF-1α. These exciting advancements have unearthed a plethora of new questions regarding Kaiso's function in tumorigenesis. As noted, of particular interest is the mechanism by which Kaiso promotes inflammation in the intestine. However, other pertinent questions include: i.) How does Kaiso modulate Notch signaling? ii.) In which context(s) does Kaiso repress *cyclinD1* expression? and iii.) How does hypoxia regulate Kaiso expression?

APPENDIX

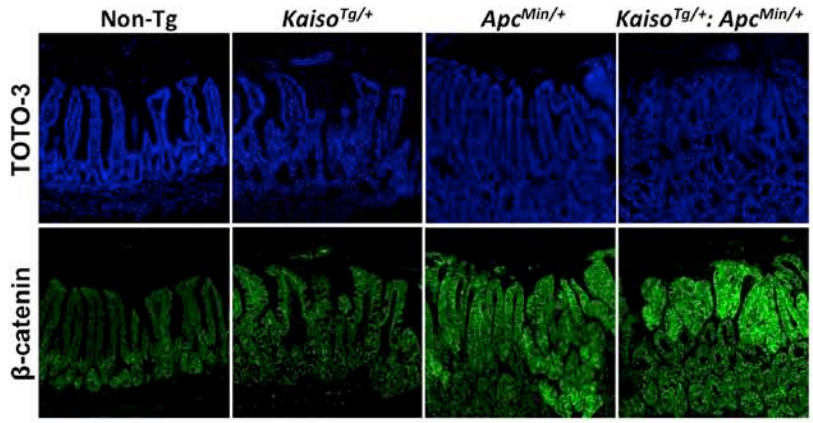

Figure A1: β-catenin staining in normal intestinal tissues of Non-Tg and *Kaiso*$^{Tg/+}$ mice and polyp tissue of *Apc*$^{Min/+}$ and *Kaiso*$^{Tg/+}$*:Apc*$^{Min/+}$ mice

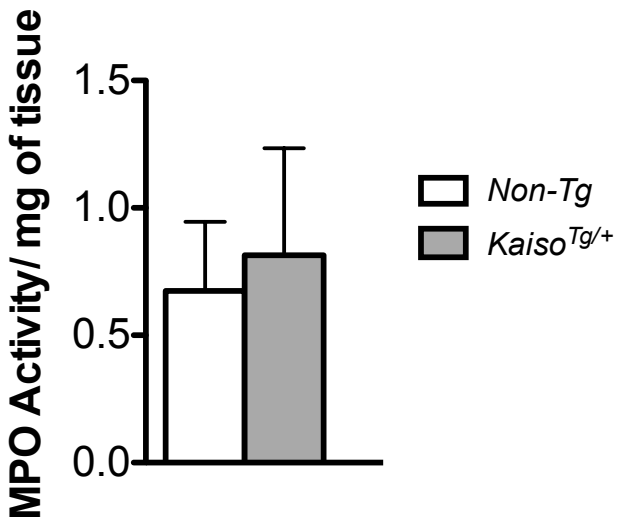

Figure A2: Myeloperoxidase activity in 90-day old Non-transgenic and *Kaiso*$^{Tg/+}$ mice

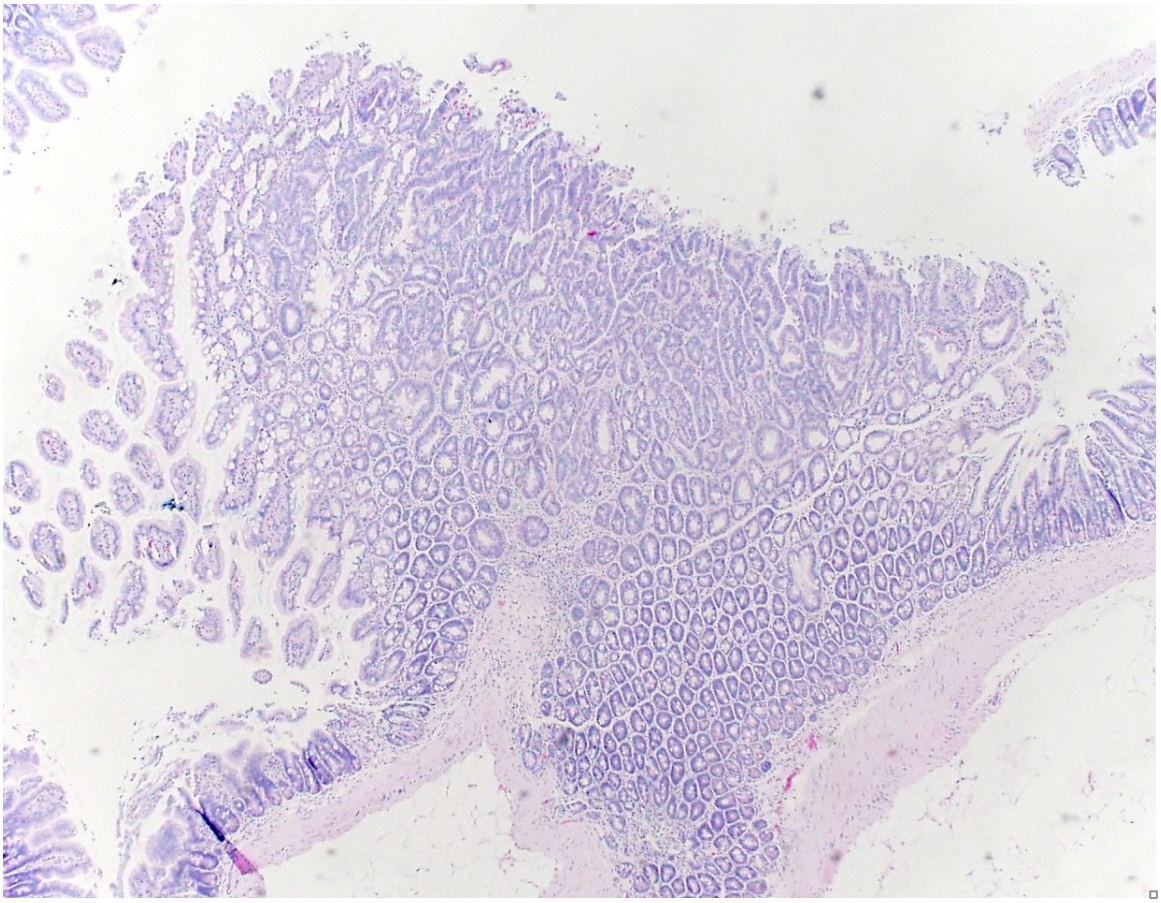

Figure A3: Regionally extensive focal atypical hyperplasia found in 8 month old *Kaiso*$^{Tg/+}$mouse

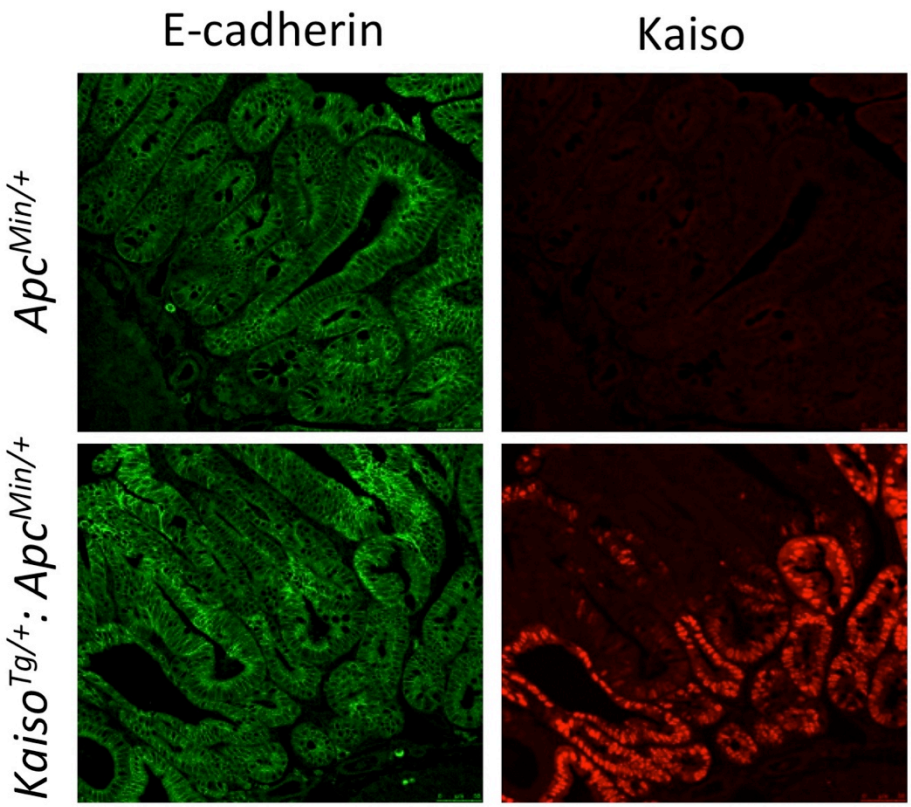

Figure A4: E-cadherin expression in $Apc^{Min/+}$ and $Kaiso^{Tg/+}$:$Apc^{Min/+}$ mice.

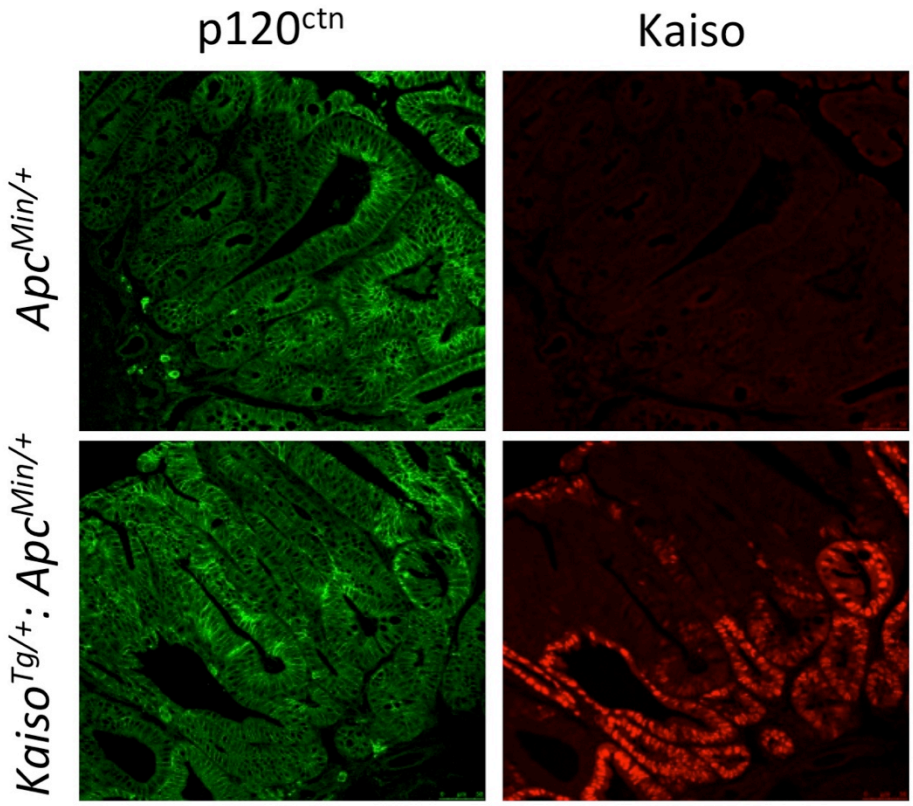

Figure A5: p120^{ctn} expression in *Apc*$^{Min/+}$ and *Kaiso*$^{Tg/+}$*:Apc*$^{Min/+}$ mice.

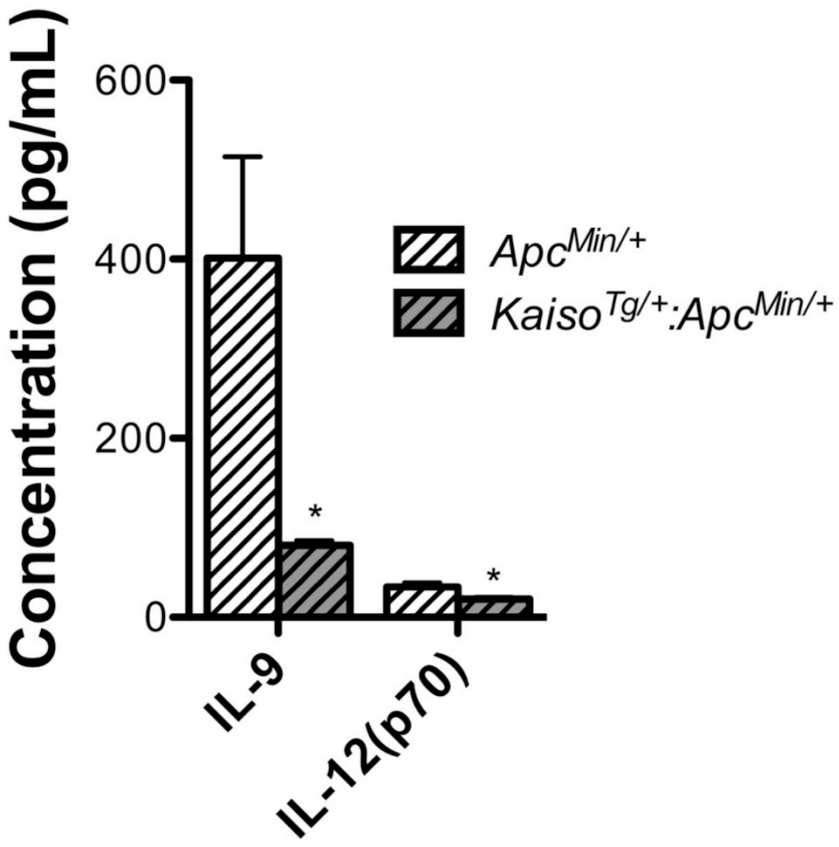

Figure A6: T-cell associated cytokines down-regulated in *Kaiso*$^{Tg/+}$*:Apc*$^{Min/+}$ mice

REFEENCES

Amit, S., A. Hatzubai, et al. (2002). "Axin-mediated CKI phosphorylation of beta-catenin at Ser 45: a molecular switch for the Wnt pathway." Genes Dev **16**(9): 1066-1076.

Anastasiadis, P. Z., S. Y. Moon, et al. (2000). "Inhibition of RhoA by p120 catenin." Nat Cell Biol **2**(9): 637-644.

Anastasiadis, P. Z. and A. B. Reynolds (2001). "Regulation of Rho GTPases by p120-catenin." Curr Opin Cell Biol **13**(5): 604-610.

Antoni, L., S. Nuding, et al. (2014). "Intestinal barrier in inflammatory bowel disease." World J Gastroenterol **20**(5): 1165-1179.

Aono, S., S. Nakagawa, et al. (1999). "p120(ctn) acts as an inhibitory regulator of cadherin function in colon carcinoma cells." J Cell Biol **145**(3): 551-562.

Barrett, C. W., J. J. Smith, et al. (2012). "Kaiso directs the transcriptional corepressor MTG16 to the Kaiso binding site in target promoters." PLoS One **7**(12): e51205.

Bates, S. and G. Peters (1995). "Cyclin D1 as a cellular proto-oncogene." Semin Cancer Biol **6**(2): 73-82.

Batlle, E., J. T. Henderson, et al. (2002). "Beta-catenin and TCF mediate cell positioning in the intestinal epithelium by controlling the expression of EphB/ephrinB." Cell **111**(2): 251-263.

Behrens, J., J. P. von Kries, et al. (1996). "Functional interaction of beta-catenin with the transcription factor LEF-1." Nature **382**(6592): 638-642.

Benjamini, Y., D. Drai, et al. (2001). "Controlling the false discovery rate in behavior genetics research." Behav Brain Res **125**(1-2): 279-284.

Bhanot, P., M. Brink, et al. (1996). "A new member of the frizzled family from Drosophila functions as a Wingless receptor." Nature **382**(6588): 225-230.

Bilchik, A. J., M. DiNome, et al. (2006). "Prospective multicenter trial of staging adequacy in colon cancer: preliminary results." Arch Surg **141**(6): 527-533; discussion 533-524.

Bray, F., J. S. Ren, et al. (2013). "Global estimates of cancer prevalence for 27 sites in the adult population in 2008." Int J Cancer **132**(5): 1133-1145.

Bruning, U., L. Cerone, et al. (2011). "MicroRNA-155 promotes resolution of hypoxia-inducible factor 1alpha activity during prolonged hypoxia." Mol Cell Biol **31**(19): 4087-4096.

Buck-Koehntop, B. A. and P. A. Defossez (2013). "On how mammalian transcription factors recognize methylated DNA." Epigenetics **8**(2): 131-137.

Buck-Koehntop, B. A., R. L. Stanfield, et al. (2012). "Molecular basis for recognition of methylated and specific DNA sequences by the zinc finger protein Kaiso." Proc Natl Acad Sci U S A **109**(38): 15229-15234.

Canavan, C., K. R. Abrams, et al. (2006). "Meta-analysis: colorectal and small bowel cancer risk in patients with Crohn's disease." Aliment Pharmacol Ther **23**(8): 1097-1104.

Cancer Genome Atlas, N. (2012). "Comprehensive molecular characterization of human colon and rectal cancer." Nature **487**(7407): 330-337.

Carroll, V. A. and M. Ashcroft (2005). "Targeting the molecular basis for tumour hypoxia." Expert Rev Mol Med **7**(6): 1-16.

Chaudhary, R., C. C. Pierre, et al. (2013). "The POZ-ZF transcription factor Kaiso (ZBTB33) induces inflammation and progenitor cell differentiation in the murine intestine." PLoS One **8**(9): e74160.

Clarke, A. R. (2006). "Wnt signalling in the mouse intestine." Oncogene **25**(57): 7512-7521.

Cofre, J., J. R. Menezes, et al. (2012). "Knock-down of Kaiso induces proliferation and blocks granulocytic differentiation in blast crisis of chronic myeloid leukemia." Cancer Cell Int **12**(1): 28.

Compagni, A. (2000). "Recent advances in research on multistage tumorigenesis." British Journal of Cancer **83**(1): 1-5.

Costa, A., D. Coradini, et al. (2001). "Re: Levels of hypoxia-inducible factor-1alpha during breast carcinogenesis." J Natl Cancer Inst **93**(15): 1175-1177.

Dai, S. D., Y. Wang, et al. (2010). "Kaiso is expressed in lung cancer: its expression and localization is affected by p120ctn." Lung Cancer **67**(2): 205-215.

Dai, S. D., Y. Wang, et al. (2009). "Cytoplasmic Kaiso is associated with poor prognosis in non-small cell lung cancer." BMC Cancer **9**: 178.

Dames, S. A., M. Martinez-Yamout, et al. (2002). "Structural basis for Hif-1 alpha /CBP recognition in the cellular hypoxic response." Proc Natl Acad Sci U S A **99**(8): 5271-5276.

Daniel, J. M. (2007). "Dancing in and out of the nucleus: p120(ctn) and the transcription factor Kaiso." Biochim Biophys Acta **1773**(1): 59-68.

Daniel, J. M. and A. B. Reynolds (1999). "The catenin p120(ctn) interacts with Kaiso, a novel BTB/POZ domain zinc finger transcription factor." Mol Cell Biol **19**(5): 3614-3623.

Daniel, J. M., C. M. Spring, et al. (2002). "The p120(ctn)-binding partner Kaiso is a bi-modal DNA-binding protein that recognizes both a sequence-specific consensus and methylated CpG dinucleotides." Nucleic Acids Res **30**(13): 2911-2919.

Das, P. M. and R. Singal (2004). "DNA methylation and cancer." J Clin Oncol **22**(22): 4632-4642.

Davis, J. N., L. McGhee, et al. (2003). "The ETO (MTG8) gene family." Gene **303**: 1-10.

Davis, M. A., R. C. Ireton, et al. (2003). "A core function for p120-catenin in cadherin turnover." J Cell Biol **163**(3): 525-534.

Davis, M. A. and A. B. Reynolds (2006). "Blocked acinar development, E-cadherin reduction, and intraepithelial neoplasia upon ablation of p120-catenin in the mouse salivary gland." Dev Cell **10**(1): 21-31.

de Lau, W., P. Kujala, et al. (2012). "Peyer's patch M cells derived from Lgr5(+) stem cells require SpiB and are induced by RankL in cultured "miniguts"." Mol Cell Biol **32**(18): 3639-3647.

Defossez, P. A., K. F. Kelly, et al. (2005). "The human enhancer blocker CTC-binding factor interacts with the transcription factor Kaiso." J Biol Chem **280**(52): 43017-43023.

Del Valle-Perez, B., D. Casagolda, et al. (2011). "Wnt controls the transcriptional activity of Kaiso through CK1epsilon-dependent phosphorylation of p120-catenin." J Cell Sci **124**(Pt 13): 2298-2309.

Donaldson, N. S., C. L. Nordgaard, et al. (2010). "Kaiso regulates Znf131-mediated transcriptional activation." Exp Cell Res **316**(10): 1692-1705.

Donaldson, N. S., C. C. Pierre, et al. (2012). "Kaiso Represses the Cell Cycle Gene cyclin D1 via Sequence-Specific and Methyl-CpG-Dependent Mechanisms." PLoS One **7**(11): e50398.

Downing, J. R. and A. B. Reynolds (1991). "PDGF, CSF-1, and EGF induce tyrosine phosphorylation of p120, a pp60src transformation-associated substrate." Oncogene **6**(4): 607-613.

Eaden, J. A., K. R. Abrams, et al. (2001). "The risk of colorectal cancer in ulcerative colitis: a meta-analysis." Gut **48**(4): 526-535.

Feagins, L. A., R. F. Souza, et al. (2009). "Carcinogenesis in IBD: potential targets for the prevention of colorectal cancer." Nat Rev Gastroenterol Hepatol **6**(5): 297-305.

Fevr, T., S. Robine, et al. (2007). "Wnt/beta-catenin is essential for intestinal homeostasis and maintenance of intestinal stem cells." Mol Cell Biol **27**(21): 7551-7559.

Filion, G. J., S. Zhenilo, et al. (2006). "A family of human zinc finger proteins that bind methylated DNA and repress transcription." Mol Cell Biol **26**(1): 169-181.

Fodde, R., W. Edelmann, et al. (1994). "A targeted chain-termination mutation in the mouse Apc gene results in multiple intestinal tumors." Proc Natl Acad Sci U S A **91**(19): 8969-8973.

Fodde, R., J. Kuipers, et al. (2001). "Mutations in the APC tumour suppressor gene cause chromosomal instability." Nat Cell Biol **3**(4): 433-438.

Fodde, R. and R. Smits (2001). "Disease model: familial adenomatous polyposis." Trends Mol Med **7**(8): 369-373.

Fodde, R., R. Smits, et al. (2001). "APC, signal transduction and genetic instability in colorectal cancer." Nat Rev Cancer **1**(1): 55-67.

Fournier, A., N. Sasai, et al. (2012). "The role of methyl-binding proteins in chromatin organization and epigenome maintenance." Brief Funct Genomics **11**(3): 251-264.

Fre, S., M. Huyghe, et al. (2005). "Notch signals control the fate of immature progenitor cells in the intestine." Nature **435**(7044): 964-968.

Gall, T. M. and A. E. Frampton (2013). "Gene of the month: E-cadherin (CDH1)." J Clin Pathol **66**(11): 928-932.

Gerbe, F., J. H. van Es, et al. (2011). "Distinct ATOH1 and Neurog3 requirements define tuft cells as a new secretory cell type in the intestinal epithelium." J Cell Biol **192**(5): 767-780.

Ginouves, A., K. Ilc, et al. (2008). "PHDs overactivation during chronic hypoxia "desensitizes" HIFalpha and protects cells from necrosis." Proc Natl Acad Sci U S A **105**(12): 4745-4750.

Goonewardene, T. I., H. M. Sowter, et al. (2002). "Hypoxia-induced pathways in breast cancer." Microsc Res Tech **59**(1): 41-48.

Goss, K. H. and J. Groden (2000). "Biology of the adenomatous polyposis coli tumor suppressor." J Clin Oncol **18**(9): 1967-1979.

Goswami, R. and M. H. Kaplan (2011). "A brief history of IL-9." J Immunol **186**(6): 3283-3288.

Gottardi, C. J., E. Wong, et al. (2001). "E-cadherin suppresses cellular transformation by inhibiting beta-catenin signaling in an adhesion-independent manner." J Cell Biol **153**(5): 1049-1060.

Gregorieff, A. and H. Clevers (2005). "Wnt signaling in the intestinal epithelium: from endoderm to cancer." Genes Dev **19**(8): 877-890.

Greijer, A. E. and E. van der Wall (2004). "The role of hypoxia inducible factor 1 (HIF-1) in hypoxia induced apoptosis." J Clin Pathol **57**(10): 1009-1014.

Grivennikov, S. I. (2013). "Inflammation and colorectal cancer: colitis-associated neoplasia." Semin Immunopathol **35**(2): 229-244.

Grosheva, I., M. Shtutman, et al. (2001). "p120 catenin affects cell motility via modulation of activity of Rho-family GTPases: a link between cell-cell contact formation and regulation of cell locomotion." J Cell Sci **114**(Pt 4): 695-707.

Gunther, C., H. Neumann, et al. (2013). "Apoptosis, necrosis and necroptosis: cell death regulation in the intestinal epithelium." Gut **62**(7): 1062-1071.

Half, E., D. Bercovich, et al. (2009). "Familial adenomatous polyposis." Orphanet J Rare Dis **4**: 22.

Hall, P. A., P. J. Coates, et al. (1994). "Regulation of cell number in the mammalian gastrointestinal tract: the importance of apoptosis." J Cell Sci **107 (Pt 12)**: 3569-3577.

Hanahan, D. and R. A. Weinberg (2011). "Hallmarks of cancer: the next generation." Cell **144**(5): 646-674.

Harris, A. L. (2002). "Hypoxia--a key regulatory factor in tumour growth." Nat Rev Cancer **2**(1): 38-47.

Hart, A. L., S. C. Ng, et al. (2010). "Homing of immune cells: role in homeostasis and intestinal inflammation." Inflamm Bowel Dis **16**(11): 1969-1977.

Hart, M. J., R. de los Santos, et al. (1998). "Downregulation of beta-catenin by human Axin and its association with the APC tumor suppressor, beta-catenin and GSK3 beta." Curr Biol **8**(10): 573-581.

Higgins, J. P., R. Shinghal, et al. (2003). "Gene expression patterns in renal cell carcinoma assessed by complementary DNA microarray." Am J Pathol **162**(3): 925-932.

Hiroki, O. (2012). "Evolution of the cadherin-catenin complex." Subcell Biochem **60**: 9-35.

Hong, J. Y., J. I. Park, et al. (2010). "Shared molecular mechanisms regulate multiple catenin proteins: canonical Wnt signals and components modulate p120-catenin isoform-1 and additional p120 subfamily members." J Cell Sci **123**(Pt 24): 4351-4365.

Hu, G. (2012). "p120-Catenin: a novel regulator of innate immunity and inflammation." Crit Rev Immunol **32**(2): 127-138.

Huang, L. E., Z. Arany, et al. (1996). "Activation of hypoxia-inducible transcription factor depends primarily upon redox-sensitive stabilization of its alpha subunit." J Biol Chem **271**(50): 32253-32259.

Iioka, H., S. K. Doerner, et al. (2009). "Kaiso is a bimodal modulator for Wnt/beta-catenin signaling." FEBS Lett **583**(4): 627-632.

Ireton, R. C., M. A. Davis, et al. (2002). "A novel role for p120 catenin in E-cadherin function." J Cell Biol **159**(3): 465-476.

Irizarry, R. A., B. Hobbs, et al. (2003). "Exploration, normalization, and summaries of high density oligonucleotide array probe level data." Biostatistics **4**(2): 249-264.

Ivanov, D. B., M. P. Philippova, et al. (2001). "Structure and functions of classical cadherins." Biochemistry (Mosc) **66**(10): 1174-1186.

Jensen, J., E. E. Pedersen, et al. (2000). "Control of endodermal endocrine development by Hes-1." Nat Genet **24**(1): 36-44.

Jess, T., C. Rungoe, et al. (2012). "Risk of colorectal cancer in patients with ulcerative colitis: a meta-analysis of population-based cohort studies." Clin Gastroenterol Hepatol **10**(6): 639-645.

Jiang, B. H., G. Jiang, et al. (2001). "Phosphatidylinositol 3-kinase signaling controls levels of hypoxia-inducible factor 1." Cell Growth Differ **12**(7): 363-369.

Jiang, G., Y. Wang, et al. (2012). "P120-catenin isoforms 1 and 3 regulate proliferation and cell cycle of lung cancer cells via beta-catenin and Kaiso respectively." PLoS One **7**(1): e30303.

Jones, J., H. Wang, et al. (2014). "Nuclear localization of Kaiso promotes the poorly differentiated phenotype and EMT in infiltrating ductal carcinomas." Clin Exp Metastasis **31**(5): 497-510.

Jones, J., H. Wang, et al. (2012). "Nuclear Kaiso indicates aggressive prostate cancers and promotes migration and invasiveness of prostate cancer cells." Am J Pathol **181**(5): 1836-1846.

Kageyama, R., T. Ohtsuka, et al. (2007). "The Hes gene family: repressors and oscillators that orchestrate embryogenesis." Development **134**(7): 1243-1251.

Kanner, S. B., A. B. Reynolds, et al. (1991). "Tyrosine phosphorylation of a 120-kilodalton pp60src substrate upon epidermal growth factor and platelet-derived growth factor receptor stimulation and in polyomavirus middle-T-antigen-transformed cells." Mol Cell Biol **11**(2): 713-720.

Kaplan, J. and K. Calame (1997). "The ZiN/POZ domain of ZF5 is required for both transcriptional activation and repression." Nucleic Acids Res **25**(6): 1108-1116.

Kelly, K. F. and J. M. Daniel (2006). "POZ for effect--POZ-ZF transcription factors in cancer and development." Trends Cell Biol **16**(11): 578-587.

Kelly, K. F., A. A. Otchere, et al. (2004). "Nuclear import of the BTB/POZ transcriptional regulator Kaiso." J Cell Sci **117**(Pt 25): 6143-6152.

Kelly, K. F., C. M. Spring, et al. (2004). "NLS-dependent nuclear localization of p120ctn is necessary to relieve Kaiso-mediated transcriptional repression." J Cell Sci **117**(Pt 13): 2675-2686.

Kim, J. W., I. Tchernyshyov, et al. (2006). "HIF-1-mediated expression of pyruvate dehydrogenase kinase: a metabolic switch required for cellular adaptation to hypoxia." Cell Metab **3**(3): 177-185.

Kim, K. A., M. Kakitani, et al. (2005). "Mitogenic influence of human R-spondin1 on the intestinal epithelium." Science **309**(5738): 1256-1259.

Kim, S. W., X. Fang, et al. (2002). "Isolation and characterization of XKaiso, a transcriptional repressor that associates with the catenin Xp120(ctn) in Xenopus laevis." J Biol Chem **277**(10): 8202-8208.

Kim, S. W., J. I. Park, et al. (2004). "Non-canonical Wnt signals are modulated by the Kaiso transcriptional repressor and p120-catenin." Nat Cell Biol **6**(12): 1212-1220.

Kitagawa, M., S. Hatakeyama, et al. (1999). "An F-box protein, FWD1, mediates ubiquitin-dependent proteolysis of beta-catenin." EMBO J **18**(9): 2401-2410.

Klaus, A. and W. Birchmeier (2008). "Wnt signalling and its impact on development and cancer." Nat Rev Cancer **8**(5): 387-398.

Klein, E. A. and R. K. Assoian (2008). "Transcriptional regulation of the cyclin D1 gene at a glance." J Cell Sci **121**(Pt 23): 3853-3857.

Klose, R. J. and A. P. Bird (2006). "Genomic DNA methylation: the mark and its mediators." Trends Biochem Sci **31**(2): 89-97.

Koh, D. I., D. Han, et al. (2014). "KAISO, a critical regulator of p53-mediated transcription of CDKN1A and apoptotic genes." Proc Natl Acad Sci U S A **111**(42): 15078-15083.

Korinek, V., N. Barker, et al. (1998). "Depletion of epithelial stem-cell compartments in the small intestine of mice lacking Tcf-4." Nat Genet **19**(4): 379-383.

Koslowski, M., U. Luxemburger, et al. (2011). "Tumor-associated CpG demethylation augments hypoxia-induced effects by positive autoregulation of HIF-1alpha." Oncogene **30**(7): 876-882.

Kowalczyk, A. P. and A. B. Reynolds (2004). "Protecting your tail: regulation of cadherin degradation by p120-catenin." Curr Opin Cell Biol **16**(5): 522-527.

Krausova, M. and V. Korinek (2014). "Wnt signaling in adult intestinal stem cells and cancer." Cell Signal **26**(3): 570-579.

Kuhnert, F., C. R. Davis, et al. (2004). "Essential requirement for Wnt signaling in proliferation of adult small intestine and colon revealed by adenoviral expression of Dickkopf-1." Proc Natl Acad Sci U S A **101**(1): 266-271.

Kulis, M., A. C. Queiros, et al. (2013). "Intragenic DNA methylation in transcriptional regulation, normal differentiation and cancer." Biochim Biophys Acta **1829**(11): 1161-1174.

Kunkel, E. J., D. J. Campbell, et al. (2003). "Chemokines in lymphocyte trafficking and intestinal immunity." Microcirculation **10**(3-4): 313-323.

Lamlum, H., M. Ilyas, et al. (1999). "The type of somatic mutation at APC in familial adenomatous polyposis is determined by the site of the germline mutation: a new facet to Knudson's 'two-hit' hypothesis." Nat Med **5**(9): 1071-1075.

Lando, D., D. J. Peet, et al. (2002). "FIH-1 is an asparaginyl hydroxylase enzyme that regulates the transcriptional activity of hypoxia-inducible factor." Genes Dev **16**(12): 1466-1471.

Lando, D., D. J. Peet, et al. (2002). "Asparagine hydroxylation of the HIF transactivation domain a hypoxic switch." Science **295**(5556): 858-861.

Langan, R. C., J. E. Mullinax, et al. (2013). "Colorectal cancer biomarkers and the potential role of cancer stem cells." J Cancer **4**(3): 241-250.

Lasek, W., R. Zagozdzon, et al. (2014). "Interleukin 12: still a promising candidate for tumor immunotherapy?" Cancer Immunol Immunother **63**(5): 419-435.

Laughner, E., P. Taghavi, et al. (2001). "HER2 (neu) signaling increases the rate of hypoxia-inducible factor 1alpha (HIF-1alpha) synthesis: novel mechanism for HIF-1-mediated vascular endothelial growth factor expression." Mol Cell Biol **21**(12): 3995-4004.

Lauzier, M. C., E. L. Page, et al. (2007). "Differential regulation of hypoxia-inducible factor-1 through receptor tyrosine kinase transactivation in vascular smooth muscle cells." Endocrinology **148**(8): 4023-4031.

Lee, E., Sujin Yim, Seung-Ki Lee, and Hyunsung Park (2002). "Two Transactivation Domains of Hypoxia-inducible Factor-1α Regulated by the MEK-1/p42/p44 MAPK Pathway." Molecules and Cells **14**: 9-15.

Lee, M., H. Ji, et al. (2014). "P120-catenin regulates REST/CoREST, and modulates mouse embryonic stem cell differentiation." J Cell Sci.

Lee, Y. S., D. Choi, et al. (2014). "CXCR2 inhibition enhances sulindac-mediated suppression of colon cancer development." Int J Cancer **135**(1): 232-237.

Leprivier, G., B. Rotblat, et al. (2014). "Stress-mediated translational control in cancer cells." Biochim Biophys Acta.

Li, V. S., S. S. Ng, et al. (2012). "Wnt signaling through inhibition of beta-catenin degradation in an intact Axin1 complex." Cell **149**(6): 1245-1256.

Li, W. and B. F. Chen (2013). "Aberrant DNA methylation in human cancers." J Huazhong Univ Sci Technolog Med Sci **33**(6): 798-804.

Liu, Y., Q. Z. Dong, et al. (2014). "Kaiso interacts with p120-catenin to regulate beta-catenin expression at the transcriptional level." PLoS One **9**(2): e87537.

Lopes, E. C., E. Valls, et al. (2008). "Kaiso contributes to DNA methylation-dependent silencing of tumor suppressor genes in colon cancer cell lines." Cancer Res **68**(18): 7258-7263.

Low, D., M. Mino-Kenudson, et al. (2014). "Recent advancement in understanding colitis-associated tumorigenesis." Inflamm Bowel Dis **20**(11): 2115-2123.

Lustig, B., B. Jerchow, et al. (2002). "Negative feedback loop of Wnt signaling through upregulation of conductin/axin2 in colorectal and liver tumors." Mol Cell Biol **22**(4): 1184-1193.

Mahon, P. C., K. Hirota, et al. (2001). "FIH-1: a novel protein that interacts with HIF-1alpha and VHL to mediate repression of HIF-1 transcriptional activity." Genes Dev **15**(20): 2675-2686.

Makrilia, N., A. Kollias, et al. (2009). "Cell adhesion molecules: role and clinical significance in cancer." Cancer Invest **27**(10): 1023-1037.

Manfredi, S., A. M. Bouvier, et al. (2006). "Incidence and patterns of recurrence after resection for cure of colonic cancer in a well defined population." Br J Surg **93**(9): 1115-1122.

Martin Caballero, I., J. Hansen, et al. (2009). "The methyl-CpG binding proteins Mecp2, Mbd2 and Kaiso are dispensable for mouse embryogenesis, but play a redundant function in neural differentiation." PLoS One **4**(1): e4315.

Maynard, M. A. and M. Ohh (2007). "The role of hypoxia-inducible factors in cancer." Cell Mol Life Sci **64**(16): 2170-2180.

McCart, A. E., N. K. Vickaryous, et al. (2008). "Apc mice: models, modifiers and mutants." Pathol Res Pract **204**(7): 479-490.

McClellan, J. L., J. M. Davis, et al. (2012). "Intestinal inflammatory cytokine response in relation to tumorigenesis in the ApcMin/+ mouse." Cytokine **57**(1): 113-119.

McCrea, P. D. and D. Gu (2010). "The catenin family at a glance." J Cell Sci **123**(Pt 5): 637-642.

Melcher, K. (2000). "The strength of acidic activation domains correlates with their affinity for both transcriptional and non-transcriptional proteins." J Mol Biol **301**(5): 1097-1112.

Miyashita, Y. and M. Ozawa (2007). "Increased internalization of p120-uncoupled E-cadherin and a requirement for a dileucine motif in the cytoplasmic domain for endocytosis of the protein." J Biol Chem **282**(15): 11540-11548.

Moser, A. R., H. C. Pitot, et al. (1990). "A dominant mutation that predisposes to multiple intestinal neoplasia in the mouse." Science **247**(4940): 322-324.

Nagafuchi, A. and M. Takeichi (1988). "Cell binding function of E-cadherin is regulated by the cytoplasmic domain." EMBO J **7**(12): 3679-3684.

Niu, G., J. Briggs, et al. (2008). "Signal transducer and activator of transcription 3 is required for hypoxia-inducible factor-1alpha RNA expression in both tumor cells and tumor-associated myeloid cells." Mol Cancer Res **6**(7): 1099-1105.

Noah, T. K. and N. F. Shroyer (2013). "Notch in the intestine: regulation of homeostasis and pathogenesis." Annu Rev Physiol **75**: 263-288.

Obata, Y., D. Takahashi, et al. (2012). "Epithelial cell-intrinsic Notch signaling plays an essential role in the maintenance of gut immune homeostasis." J Immunol **188**(5): 2427-2436.

Ozawa, M., H. Baribault, et al. (1989). "The cytoplasmic domain of the cell adhesion molecule uvomorulin associates with three independent proteins structurally related in different species." EMBO J **8**(6): 1711-1717.

Park, J. I., S. W. Kim, et al. (2005). "Kaiso/p120-catenin and TCF/beta-catenin complexes coordinately regulate canonical Wnt gene targets." Dev Cell **8**(6): 843-854.

Peglion, F. and S. Etienne-Manneville (2013). "p120catenin alteration in cancer and its role in tumour invasion." Philos Trans R Soc Lond B Biol Sci **368**(1629): 20130015.

Perez-Moreno, M., M. A. Davis, et al. (2006). "p120-catenin mediates inflammatory responses in the skin." Cell **124**(3): 631-644.

Perez-Moreno, M., W. Song, et al. (2008). "Loss of p120 catenin and links to mitotic alterations, inflammation, and skin cancer." Proc Natl Acad Sci U S A **105**(40): 15399-15404.

Pflaum, J., S. Schlosser, et al. (2014). "p53 Family and Cellular Stress Responses in Cancer." Front Oncol **4**: 285.

Phesse, T. J., L. Parry, et al. (2008). "Deficiency of Mbd2 attenuates Wnt signaling." Mol Cell Biol **28**(19): 6094-6103.

Pieters, T., F. van Roy, et al. (2012). "Functions of p120ctn isoforms in cell-cell adhesion and intracellular signaling." Front Biosci (Landmark Ed) **17**: 1669-1694.

Pinson, K. I., J. Brennan, et al. (2000). "An LDL-receptor-related protein mediates Wnt signalling in mice." Nature **407**(6803): 535-538.

Pinto, D., A. Gregorieff, et al. (2003). "Canonical Wnt signals are essential for homeostasis of the intestinal epithelium." Genes Dev **17**(14): 1709-1713.

Poon, E., A. L. Harris, et al. (2009). "Targeting the hypoxia-inducible factor (HIF) pathway in cancer." Expert Rev Mol Med **11**: e26.

Pore, N., Z. Jiang, et al. (2006). "Akt1 activation can augment hypoxia-inducible factor-1alpha expression by increasing protein translation through a mammalian target of rapamycin-independent pathway." Mol Cancer Res **4**(7): 471-479.

Potten, C. S. and M. Loeffler (1990). "Stem cells: attributes, cycles, spirals, pitfalls and uncertainties. Lessons for and from the crypt." Development **110**(4): 1001-1020.

Powell, S. M., N. Zilz, et al. (1992). "APC mutations occur early during colorectal tumorigenesis." Nature **359**(6392): 235-237.

Prokhortchouk, A., B. Hendrich, et al. (2001). "The p120 catenin partner Kaiso is a DNA methylation-dependent transcriptional repressor." Genes Dev **15**(13): 1613-1618.

Prokhortchouk, A., O. Sansom, et al. (2006). "Kaiso-deficient mice show resistance to intestinal cancer." Mol Cell Biol **26**(1): 199-208.

Prokhortchouk, E. and B. Hendrich (2002). "Methyl-CpG binding proteins and cancer: are MeCpGs more important than MBDs?" Oncogene **21**(35): 5394-5399.

Raghav, S. K., S. M. Waszak, et al. (2012). "Integrative genomics identifies the corepressor SMRT as a gatekeeper of adipogenesis through the transcription factors C/EBPbeta and KAISO." Mol Cell **46**(3): 335-350.

Reynolds, A. B., J. Daniel, et al. (1994). "Identification of a new catenin: the tyrosine kinase substrate p120cas associates with E-cadherin complexes." Mol Cell Biol **14**(12): 8333-8342.

Reynolds, A. B., D. J. Roesel, et al. (1989). "Transformation-specific tyrosine phosphorylation of a novel cellular protein in chicken cells expressing oncogenic variants of the avian cellular src gene." Mol Cell Biol **9**(2): 629-638.

Richard, D. E. R., Edurne Berra, Emmanuel Gothie´ , Danie` le Roux, and Jacques Pouysse´gur (1999). "p42/p44 Mitogen-activated Protein Kinases Phosphorylate Hypoxia-inducible Factor 1a (HIF-1a) and Enhance the Transcriptional Activity of HIF-1." The Journal of Biological Chemistry **274**(November 12): 32632-32627.

Roberts, A. M. and M. Ohh (2008). "Beyond the hypoxia-inducible factor-centric tumour suppressor model of von Hippel-Lindau." Curr Opin Oncol **20**(1): 83-89.

Roczniak-Ferguson, A. and A. B. Reynolds (2003). "Regulation of p120-catenin nucleocytoplasmic shuttling activity." J Cell Sci **116**(Pt 20): 4201-4212.

Rodova, M., K. F. Kelly, et al. (2004). "Regulation of the rapsyn promoter by kaiso and delta-catenin." Mol Cell Biol **24**(16): 7188-7196.

Rogler, G. (2014). "Chronic ulcerative colitis and colorectal cancer." Cancer Lett **345**(2): 235-241.

Rosenbluh, J., X. Wang, et al. (2014). "Genomic insights into WNT/beta-catenin signaling." Trends Pharmacol Sci **35**(2): 103-109.

Rubin, D. C., A. Shaker, et al. (2012). "Chronic intestinal inflammation: inflammatory bowel disease and colitis-associated colon cancer." Front Immunol **3**: 107.

Ruzov, A., D. S. Dunican, et al. (2004). "Kaiso is a genome-wide repressor of transcription that is essential for amphibian development." Development **131**(24): 6185-6194.

Ruzov, A., J. A. Hackett, et al. (2009). "The interaction of xKaiso with xTcf3: a revised model for integration of epigenetic and Wnt signalling pathways." Development **136**(5): 723-727.

Ruzov, A., E. Savitskaya, et al. (2009). "The non-methylated DNA-binding function of Kaiso is not required in early Xenopus laevis development." Development **136**(5): 729-738.

Sabbah, M., D. Courilleau, et al. (1999). "Estrogen induction of the cyclin D1 promoter: involvement of a cAMP response-like element." Proc Natl Acad Sci U S A **96**(20): 11217-11222.

Saeed, A. I., N. K. Bhagabati, et al. (2006). "TM4 microarray software suite." Methods Enzymol **411**: 134-193.

Saeed, A. I., V. Sharov, et al. (2003). "TM4: a free, open-source system for microarray data management and analysis." Biotechniques **34**(2): 374-378.

Saleh, M. and G. Trinchieri (2011). "Innate immune mechanisms of colitis and colitis-associated colorectal cancer." Nat Rev Immunol **11**(1): 9-20.

Samuel, M. S., H. Suzuki, et al. (2009). "Elevated Dnmt3a activity promotes polyposis in Apc(Min) mice by relaxing extracellular restraints on Wnt signaling." Gastroenterology **137**(3): 902-913, 913 e901-911.

Sasai, N., M. Nakao, et al. (2010). "Sequence-specific recognition of methylated DNA by human zinc-finger proteins." Nucleic Acids Res **38**(15): 5015-5022.

Sato, H., H. Suzuki, et al. (2007). "Frequent epigenetic inactivation of DICKKOPF family genes in human gastrointestinal tumors." Carcinogenesis **28**(12): 2459-2466.

Schepers, A. and H. Clevers (2012). "Wnt signaling, stem cells, and cancer of the gastrointestinal tract." Cold Spring Harb Perspect Biol **4**(4): a007989.

Semenza, G. L. (2007). "Oxygen-dependent regulation of mitochondrial respiration by hypoxia-inducible factor 1." Biochem J **405**(1): 1-9.

Shibahara, T., N. Sato, et al. (1995). "The fate of effete epithelial cells at the villus tips of the human small intestine." Arch Histol Cytol **58**(2): 205-219.

Shroyer, N. F., M. A. Helmrath, et al. (2007). "Intestine-specific ablation of mouse atonal homolog 1 (Math1) reveals a role in cellular homeostasis." Gastroenterology **132**(7): 2478-2488.

Smalley-Freed, W. G., A. Efimov, et al. (2010). "p120-catenin is essential for maintenance of barrier function and intestinal homeostasis in mice." J Clin Invest **120**(6): 1824-1835.

Smalley-Freed, W. G., A. Efimov, et al. (2011). "Adenoma formation following limited ablation of p120-catenin in the mouse intestine." PLoS One **6**(5): e19880.

Sotomayor, M., R. Gaudet, et al. (2014). "Sorting out a promiscuous superfamily: towards cadherin connectomics." Trends Cell Biol.

Soubry, A., J. van Hengel, et al. (2005). "Expression and nuclear location of the transcriptional repressor Kaiso is regulated by the tumor microenvironment." Cancer Res **65**(6): 2224-2233.

Spring, C. M., K. F. Kelly, et al. (2005). "The catenin p120ctn inhibits Kaiso-mediated transcriptional repression of the beta-catenin/TCF target gene matrilysin." Exp Cell Res **305**(2): 253-265.

Stairs, D. B., L. J. Bayne, et al. (2011). "Deletion of p120-catenin results in a tumor microenvironment with inflammation and cancer that establishes it as a tumor suppressor gene." Cancer Cell **19**(4): 470-483.

Staller, P., K. Peukert, et al. (2001). "Repression of p15INK4b expression by Myc through association with Miz-1." Nat Cell Biol **3**(4): 392-399.

Stiehl, D. P., R. Wirthner, et al. (2006). "Increased prolyl 4-hydroxylase domain proteins compensate for decreased oxygen levels. Evidence for an autoregulatory oxygen-sensing system." J Biol Chem **281**(33): 23482-23491.

Su, L. K., K. W. Kinzler, et al. (1992). "Multiple intestinal neoplasia caused by a mutation in the murine homolog of the APC gene." Science **256**(5057): 668-670.

Subramanian, A., P. Tamayo, et al. (2005). "Gene set enrichment analysis: a knowledge-based approach for interpreting genome-wide expression profiles." Proc Natl Acad Sci U S A **102**(43): 15545-15550.

Sullivan, R. and C. H. Graham (2007). "Hypoxia-driven selection of the metastatic phenotype." Cancer Metastasis Rev **26**(2): 319-331.

Swamy, M. V., J. M. Patlolla, et al. (2006). "Chemoprevention of familial adenomatous polyposis by low doses of atorvastatin and celecoxib given individually and in combination to APCMin mice." Cancer Res **66**(14): 7370-7377.

Tamai, K., M. Semenov, et al. (2000). "LDL-receptor-related proteins in Wnt signal transduction." Nature **407**(6803): 530-535.

Tamai, K., X. Zeng, et al. (2004). "A mechanism for Wnt coreceptor activation." Mol Cell **13**(1): 149-156.

Tanimoto, K., Y. Makino, et al. (2000). "Mechanism of regulation of the hypoxia-inducible factor-1 alpha by the von Hippel-Lindau tumor suppressor protein." EMBO J **19**(16): 4298-4309.

Tetsu, O. and F. McCormick (1999). "Beta-catenin regulates expression of cyclin D1 in colon carcinoma cells." Nature **398**(6726): 422-426.

Ueo, T., I. Imayoshi, et al. (2012). "The role of Hes genes in intestinal development, homeostasis and tumor formation." Development **139**(6): 1071-1082.

van de Wetering, M., E. Sancho, et al. (2002). "The beta-catenin/TCF-4 complex imposes a crypt progenitor phenotype on colorectal cancer cells." Cell **111**(2): 241-250.

van Es, J. H., A. Haegebarth, et al. (2012). "A critical role for the Wnt effector Tcf4 in adult intestinal homeostatic self-renewal." Mol Cell Biol **32**(10): 1918-1927.

van Es, J. H., M. E. van Gijn, et al. (2005). "Notch/gamma-secretase inhibition turns proliferative cells in intestinal crypts and adenomas into goblet cells." Nature **435**(7044): 959-963.

van Hengel, J., P. Vanhoenacker, et al. (1999). "Nuclear localization of the p120(ctn) Armadillo-like catenin is counteracted by a nuclear export signal and by E-cadherin expression." Proc Natl Acad Sci U S A **96**(14): 7980-7985.

van Roy, F. M. and P. D. McCrea (2005). "A role for Kaiso-p120ctn complexes in cancer?" Nat Rev Cancer **5**(12): 956-964.

Vaupel, P. (2004). "Tumor microenvironmental physiology and its implications for radiation oncology." Semin Radiat Oncol **14**(3): 198-206.

Vermeulen, J. F., R. A. van de Ven, et al. (2012). "Nuclear Kaiso expression is associated with high grade and triple-negative invasive breast cancer." PLoS One **7**(5): e37864.

Vestweber, D. and R. Kemler (1984). "Some structural and functional aspects of the cell adhesion molecule uvomorulin." Cell Differ **15**(2-4): 269-273.

Walczak-Drzewiecka, A., M. Ratajewski, et al. (2010). "DNA methylation-dependent suppression of HIF1A in an immature hematopoietic cell line HMC-1." Biochem Biophys Res Commun **391**(1): 1028-1032.

Wang, G. L., B. H. Jiang, et al. (1995). "Hypoxia-inducible factor 1 is a basic-helix-loop-helix-PAS heterodimer regulated by cellular O2 tension." Proc Natl Acad Sci U S A **92**(12): 5510-5514.

Wang, G. L. and G. L. Semenza (1993). "Characterization of hypoxia-inducible factor 1 and regulation of DNA binding activity by hypoxia." J Biol Chem **268**(29): 21513-21518.

Wang, G. L. and G. L. Semenza (1993). "General involvement of hypoxia-inducible factor 1 in transcriptional response to hypoxia." Proc Natl Acad Sci U S A **90**(9): 4304-4308.

Wang, G. L. and G. L. Semenza (1995). "Purification and characterization of hypoxia-inducible factor 1." J Biol Chem **270**(3): 1230-1237.

Waterman, M. L. (2004). "Lymphoid enhancer factor/T cell factor expression in colorectal cancer." Cancer Metastasis Rev **23**(1-2): 41-52.

Wehrli, M., S. T. Dougan, et al. (2000). "arrow encodes an LDL-receptor-related protein essential for Wingless signalling." Nature **407**(6803): 527-530.

Wenger, R. H., I. Kvietikova, et al. (1998). "Oxygen-regulated erythropoietin gene expression is dependent on a CpG methylation-free hypoxia-inducible factor-1 DNA-binding site." Eur J Biochem **253**(3): 771-777.

Wu, G., X. Feng, et al. (2010). "A human functional protein interaction network and its application to cancer data analysis." Genome Biol **11**(5): R53.

Xavier, R. J. and D. K. Podolsky (2007). "Unravelling the pathogenesis of inflammatory bowel disease." Nature **448**(7152): 427-434.

Yanagisawa, M., D. Huveldt, et al. (2008). "A p120 catenin isoform switch affects Rho activity, induces tumor cell invasion, and predicts metastatic disease." J Biol Chem **283**(26): 18344-18354.

Yang, Q., N. A. Bermingham, et al. (2001). "Requirement of Math1 for secretory cell lineage commitment in the mouse intestine." Science **294**(5549): 2155-2158.

Yap, A. S., C. M. Niessen, et al. (1998). "The juxtamembrane region of the cadherin cytoplasmic tail supports lateral clustering, adhesive strengthening, and interaction with p120ctn." J Cell Biol **141**(3): 779-789.

Yin, H. and K. L. Blanchard (2000). "DNA methylation represses the expression of the human erythropoietin gene by two different mechanisms." Blood **95**(1): 111-119.

Yoon, H. G., D. W. Chan, et al. (2003). "N-CoR mediates DNA methylation-dependent repression through a methyl CpG binding protein Kaiso." Mol Cell **12**(3): 723-734.

Zeineldin, M. and K. L. Neufeld (2013). "Understanding phenotypic variation in rodent models with germline Apc mutations." Cancer Res **73**(8): 2389-2399.

Zhang, H., Y. Q. Zhu, et al. (2014). "Detection of promoter hypermethylation of Wnt antagonist genes in fecal samples for diagnosis of early colorectal cancer." World J Gastroenterol **20**(20): 6329-6335.

Zhang, P. X., Y. Wang, et al. (2011). "p120-catenin isoform 3 regulates subcellular localization of Kaiso and promotes invasion in lung cancer cells via a phosphorylation-dependent mechanism." Int J Oncol **38**(6): 1625-1635.

Zhong, H., K. Chiles, et al. (2000). "Modulation of hypoxia-inducible factor 1alpha expression by the epidermal growth factor/phosphatidylinositol 3-kinase/PTEN/AKT/FRAP pathway in human prostate cancer cells: implications for tumor angiogenesis and therapeutics." Cancer Res **60**(6): 1541-1545.